Iron production in the state of Qin during the Warring States period

Yaxiong Liu

Thesis submitted to

University College London

for the Degree of

Doctor of Philosophy

UCL Institute of Archaeology

2/9/2021

I, Yaxiong Liu, confirm that the work presented in this thesis is my own. Where information has been derived from other sources, I confirm that this has been indicated in the thesis.

Date: 2/9/2021

Signature:

Abstract

This thesis focuses on the Qin State during the Warring States period as a political entity, and sets out to explore its iron production industry, aiming to model and understand the technological system adopted for iron production, tracing changes through time as well as exploring the interaction between the technology and its social context.

Through the scientific study of archaeological iron unearthed from Qin civilian cemeteries and workshop across the Guanzhong Plain, it has been demonstrated that the iron production in the Qin state was predominantly based on cast iron smelting from the later stage of the middle Warring States period, with multiple technical pathways developed to cost-effectively produce various types of iron products. The mould casting process was adopted for producing most of the daily use artefacts and farming implements, with controlled cooling and annealing process applied to improve the mechanical strength of cast iron. Annealing and *chaogang*/fining techniques were used to convert cast iron into soft iron/steel, then further manufacture into tools and weapons through the forging process. Through the comparison between different technological choices, it has been demonstrated that the whole technological system was developed based on the aim to achieve optimum cost-effectiveness with the available techniques, while the technological tradition and cultural preferences also played key roles for the adoption of such an iron production system.

Based on a synthesis of current research results, it has been argued that the State of Qin made the transition from bloomery iron smelting to cast iron smelting during the middle stage of the Warring States period, then quickly developed a functional and efficient technological system by the end of the Warring States period. This iron

production system greatly promoted the development of the Qin state, mainly in the field of agricultural production, while weapon production for the Qin army also benefited from such an iron industry, which laid the foundations for the success of the unification war.

Impact statement

The contribution of this research can be divided into three parts.

To begin with, through the systematic investigation into the iron production industry in the State of Qin during Warring States period, this research has contributed to the understanding toward the iron production technologies in Guanzhong Plain, where past research has not been focusing on, yet are of great significance in the history of China. The thesis also provided the earliest evidence of systematic production of grey/mottled cast iron as well as the liquid state decarburisation techniques of cast iron in human history.

In addition to the new insights into the iron production technologies in the Qin state, this research also contributed to methodological developments, provided new approaches to the characterisation and differentiation of early iron materials, the reconstruction of their production techniques as well as evaluating the engineering parameters, which could be useful for future research. Through the comparison between technological choices based on a holistic consideration including both technical and social factors, this thesis also offered new comprehensions to the developments and technological changes of iron production techniques in early China.

Furthermore, this thesis summarised and presented the current research results regarding the iron production in early China, along with the new finding from this research. These knowledge will be shared to non-Chinese speaking audience and facilitates the archaeometallurgical research from a global perspective.

The results of this research have been written into three papers published on peer-reviewed journals, including *Archaeological and Anthropological Science*, *Journal of*

Cultural Heritage and a Chinese journal *Kaogu (Archaeology)*, in which I am the first author. I have also contributed and co-authored several other journal articles. In the meantime, I have also presented my findings at several conferences and lectures, I believe such will have an impact on fellow researchers as well as a more general audience.

Table of contents

List of Figures

List of tables

Acknowledgements

This research cannot be done without the help from many people and organisations.

To begin with, I would like to thank my supervisors, Marcos Martinón-Torres, Yijie Zhuang and Kunlong Chen, for offering me such a once in a lifetime opportunity, and for their guidance, support and unswerving trust in my research capability, which I always had doubt with.

I would also like to thank the Chinese government and the China Scholarship Council (CSC), for paying my overpriced tuition fee as well as the living cost. Without their financial support, I would never even consider taking on this adventure.

Archaeological science is a highly dependent research subject, where we heavily rely on archaeological materials which we do not have to dig up, therefore I would like to express my gratitude toward those wonderful archaeologists who took part in the excavation work, mostly staff from the Shaanxi Provincial Institute of Archaeology, including Weigang Sun, Anding Shao, Yaqi Tian, Lizheng Zhangyang, Weihong Xu, Qinggang Geng, Lianjian Yue, Zhouyong Sun and many others to whom I feel sorry for not listing here. It is their selfless help that made my research much smoother and more painless.

I would like to thank the wonderful staff and colleagues in the UCL Institute of Archaeology, who have helped me in many ways throughout these four years, especially to Lisa Daniel, Rui Pang, Shan Huang, Janice Xiuzhen Li, Michael Charlton, Tom Gregory, Agnese Benzonelli and Patrick Quinn. Thanks to you, I was able to accommodate to the drastic change of environment and quickly get used to the new routine.

Special thanks have to be given to my basement family in B53 and B11, with whom I had the pleasure to share this journey with. Thanks to Jonathan Wood, Ole Nordland, Hayley Simon, David Larreina-Garcia, for countless inspiring talks and encouragements, to Ana Franjic, Veronica Occari, Antanas Melinis, Umberto Veronessi, Cristina Ichim, Yunxiao Liu, Zhehao Zhao, Zhiming Chen etc., for their companionship. Without them, I would not have been able to overcome the loneliness, anxiety, stress, depression and extremely cold winters.

I would also like to thank those people who helped me during my master's degree, when I started my research career in archaeological science. To professor Jianjun Mei, who was my supervisor and my idol, it is his recognition and support that brought me where I am today, and I can never repay that debt. To professor Rubin Han and professor Jianli Chen, with whom I had to pleasure to share a common research interest, and received many guidance, support and love from them. And to many others who have made me a better person.

Finally, I would like to thank my parents, whom, although did not have the opportunity to receive education, had always insisted me staying in school as long as I can. Thanks to my three older sisters, for being incredible daughters, so I do not have to be a good son.

1. Introduction

Of all the metal materials that has been utilised in early human history, iron is arguably the most influential one to the development of early civilisation (Childe 1944; Engels 1972: 88; Fleming and Schenck 1989). Compared to other metals used in the preindustrial world, iron is much more abundant, constituting up to 5.63% of all elements of the Earth's crust (Lide 2005); its physical and mechanical properties, such as melting temperature and hardness, can be tailored to fit different functional purposes through alloying with carbon and other technical processes. More importantly, metallic iron and its alloys have a greyish colour which is not aesthetically pleasing in most cultures, hence they were less likely being monopolised as symbolisation for power or wealth. While other types of metals such as gold, silver and bronze also played key roles in different cultures, their limited ore deposit available for direct exploitation, relatively poor mechanical strength have largely confined the application of such materials to a small range of non-utilitarian social activities such as rituals, ceremonial use and trade.

In early China, in spite of the numerous findings of extravagant bronze vessels and weaponry from the Bronze Age, both historical and archaeological evidence suggest that bronze production was largely monopolised by the ruling class, primarily used in ritual activities and warfare, and very few bronze items were actually available to those common people who were key participants of any social development (Chang 2013). For instance, it has long been argued that early agricultural production in Bronze Age China rarely benefited from the development of bronze production, and the main materials used for making agricultural tools remained wood and stone, despite the

ready availability of bronze material and production techniques (Yu 1957; Rostoker et al. 1983; Bai 1985; Bai 1989; Han and Chen 2013).

The emergence of iron metallurgy gradually changed the situation. During the early Iron Age, iron in most cultures was considered as a rare and valuable material due to its limited availability (Forbes 1964). An old Assyrian text suggests iron was 40 times more valuable than silver by weight (Wertime and Muhly 1980:36). Additionally, findings of early iron across the Old World very often show it was used in conjunction with other precious materials such as gold and jade, suggesting it was highly valued and only available to a small group of social elites (Erb-Satullo 2018). With the development and spread of the smelting technique, iron started to be mass produced across the Old World, and such a material soon became “utilitarian” and fundamentally transformed the society for its broad applications in many socioeconomic spheres (Childe 1944; Engels 1972:88; Gordon and Killick 1993).

Recent studies show that the earliest iron smelting practice emerged around the early to middle 2nd millennium BC in Anatolia (Erb-Satullo 2018). The smelting technique used is known as the bloomery iron smelting process, or the direct process. In this process, iron ore was reduced by charcoal at a temperature around 1200˚C, much lower than the melting point of pure iron, which is 1538˚C, hence iron did not melt. As a result, instead of separating the metal and slag in a liquid state based on their density, this process creates a fayalitic slag that can be melted or softened, and a solid iron bloom forms through the slag by the coalescence of small, reduced particles of metallic iron. Inevitably, some slag will also remain entrapped inside the iron bloom. Several steps of hammering are thus required to consolidate the bloom and expel the slag, eventually to be shaped into final products (Tylecote et al. 1971; Tylecote 1992; Pleiner 2000: 131-133). Notwithstanding the variation of several engineering

parameters during the practice, this technique was widely used and remained the only method to extract iron from the ore in western countries until at least the 13th century AD (Rostoker and Bronson 1990; Craddock 1995; Jockenhövel et al. 1997).

At the same time, in central China (Figure 1.1), a unique approach to extract iron from the ore appears to have been widely adopted around the 6th century BC, namely the cast iron smelting process, or the indirect process (Nanjing Museum 1974; Li 1975, Han 1998; Han and Ko 2007; Chen 2014). This process was carried out in a blast furnace, which through a stronger blast of air, can operate at a temperature around 1400˚C or higher, and possibly more reducing atmospheres (higher CO/CO_2 ratio) than a bloomery furnace. Consequently, the iron ore will be reduced and still have the time and suitable environment to be alloyed with carbon during the smelting process. According to the iron-carbon phase diagram, the melting point of such an iron-carbon alloy can drop to 1148 ˚C with a carbon content around 4.3 wt.% (Figure 1.2), hence the final separation of metal and slag will be in the liquid state. As the slag and metal can be tapped out separately from the bottom of the furnace, ore and charcoal can be recharged from the top, so that cast iron production can continue without stop for a long period until the furnace needs to be repaired (Wagner 2008: 14-15).

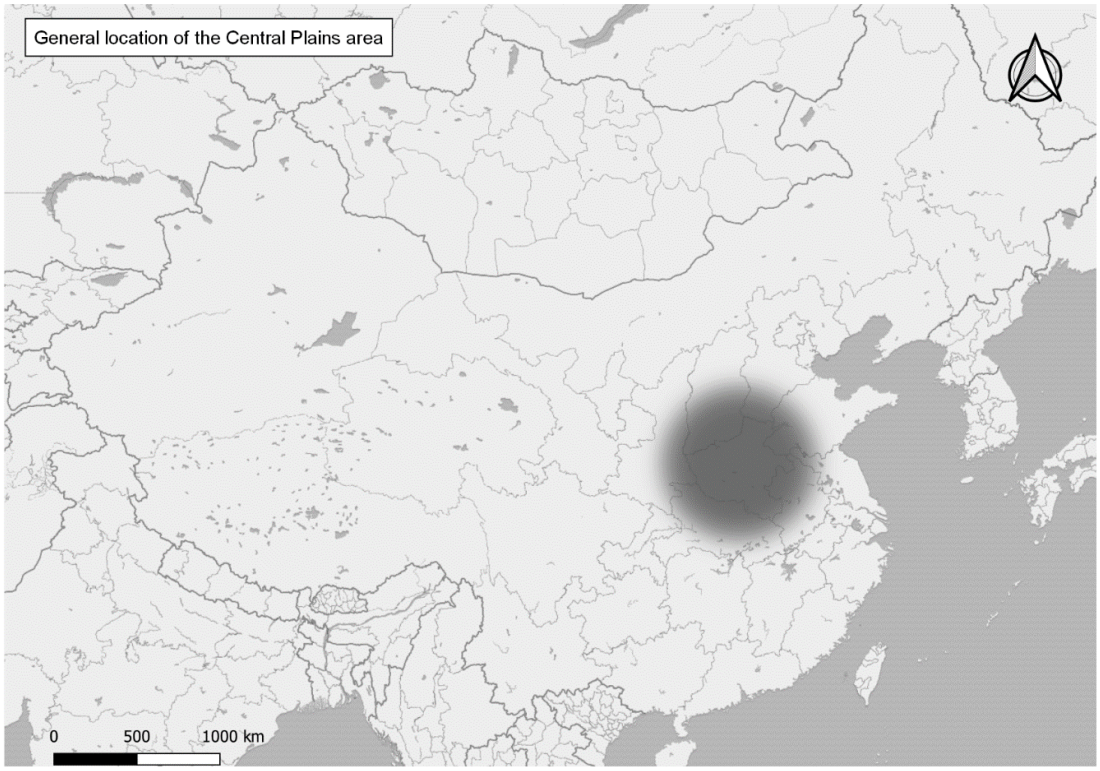

Figure 1.1 Map showing a general location of the Central Plain area in China[1], base map: Wikipedia unlabelled (https://maps.wikimedia.org/osm/)

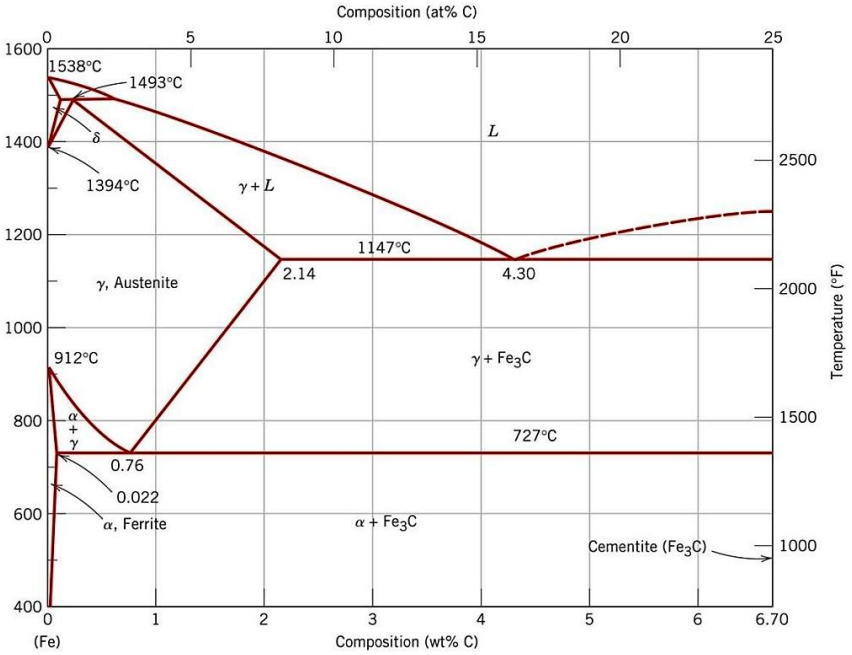

Figure 1.2 Iron-carbon phase diagram, source: www.tf.uni-kiel.de

[1] All maps were created by author using QGIS (version 3.4) unless otherwise indicated.

The metallic product of the indirect smelting process is normally white cast iron, in which the carbon mainly presents in the form of cementite (or iron carbide), or grey cast iron, where carbon mainly presents in the form of flake/lamellar graphite. While cast iron is suitable for mould casting due to its low melting temperature and high fluidity, such alloys are also relatively hard and brittle, hence not ideal when making tools or weapons for which better mechanical strength will be necessary. In these cases, additional processes to reduce the hardness or decarburise the metal to convert the cast iron into malleable soft iron or steel will be necessary.

Outside China, where the manufacture of iron products was mainly based on the forging (smithing) technique, cast iron occasionally produced from imperfect bloomery smelting was typically deemed as a waste due to its high hardness, which rendered such a material unusable in the forging based technological system (Pleiner 2000: 139-140; Crew et al. 2004; Navasaitis and Selskienė 2007). However, in early China, following the mould casting technological tradition established during the Bronze Age, craftspeople may have adapted the bronze casting technology to cast iron production soon after the innovation of this technique, and started using this new material to cast several types of artefacts such as tripods (*Ding* vessels), cooking pots and farming implements by the end of 6th century BC (Li 1975; Chen 2014:221-228). While it was still necessary to make cast iron malleable for certain functional purposes, one of the critical technological procedures, the decarburisation process, did not take very long to be developed – making its first appearance almost at the same time as the spread of cast iron smelting in central China around the 6th - 5th century BC (Li 1975; Chen 2014:221-228).

Embracing the cast iron smelting technique early, iron production in early China developed into a unique and complicated system, with various types of techniques,

materials, as well as highly diversified product categories. It is widely believed that such an iron production system provided sufficient amount of affordable metal products during the Warring States period (475 BC - 221 BC), which further became an essential part of people's daily life and had a fundamental impact on the development of social economies (Lei 1980; Yang 1980; Lei 1986; Taylor and Shell 1986; Taylor 1988; Bronson 1999; Wang 2004; Li 2005b; Han and Chen 2013).

Rising from the western frontier of the central China, the Qin state, initially considered by the Central Plains regime a political and cultural outsider, become a superpower during the Warring States period and finally unified the "Seven States" into the first empire in the history of China. The achievement of the Qin state has been studied by historians and philosophisers for two millennia. Its success has traditionally been related to a series of factors including the highly centralised political system, successful military mobilisation strategy and state endeavour to facilitate agricultural production. Some of these factors can be directly or indirectly related to a booming iron production industry and its pioneering application of this technology into agricultural and military uses as well as other social production activities (Han and Ko 2007: 440-444; Wagner 2008: 146). However, most of such research work were strictly historical, with very little material evidence supporting such an argument.

Indeed, the unprecedented socioeconomic changes in the Qin State coincided with the rapid development of the iron production industry. Such close and concurrent socioeconomic and technological developments make it an ideal case to examine how technology transformed, and was transformed by, social evolution. Against this background, this thesis will focus on the State of Qin during the Warring States period (475 BC - 221 BC) as a political entity and sets out to explore the iron production industry through a range of analytical methods, tracing changes both in technology

and scale of production through time as well as exploring the interaction between the technology and its social context.

1.1 Spatial and temporal settings

This research will be mainly focusing on the Guanzhong Plain, which is located mainly in the southern part of the modern Shaanxi Province. The Guanzhong Plain is a vast alluvial plain along the Jing and Wei rivers. It is within a temperate zone with freezing winter temperatures (but little snow) and warm to hot summers; the average temperature in modern days is around 12˚C - 13.6˚C, with annual precipitation around 550 - 660 mm (Li 1984). The whole Guanzhong plain and its surrounding area is covered by loess laid down by sandstorms, with a thickness up to 150 meters. With fertile and easily workable loess, the Guanzhong Plain is very well suited for agricultural production, especially for millet farming before the onset of large-scale irrigation agriculture (Marks 2011: 29; Zhuang 2016). During the Neolithic period, this area was one of the centres for the Yangshao Culture (around 5000 BC - 3000 BC) and Longshan Culture (around 2500 BC - 2000 BC), and it continued to be a centre stage for social and political developments during the following early dynastic and imperial periods in the Bronze and Iron Ages. During the Warring States period, the state of Qin spanned mainly the Guanzhong Plain and its surrounding area (Figure 1.4).

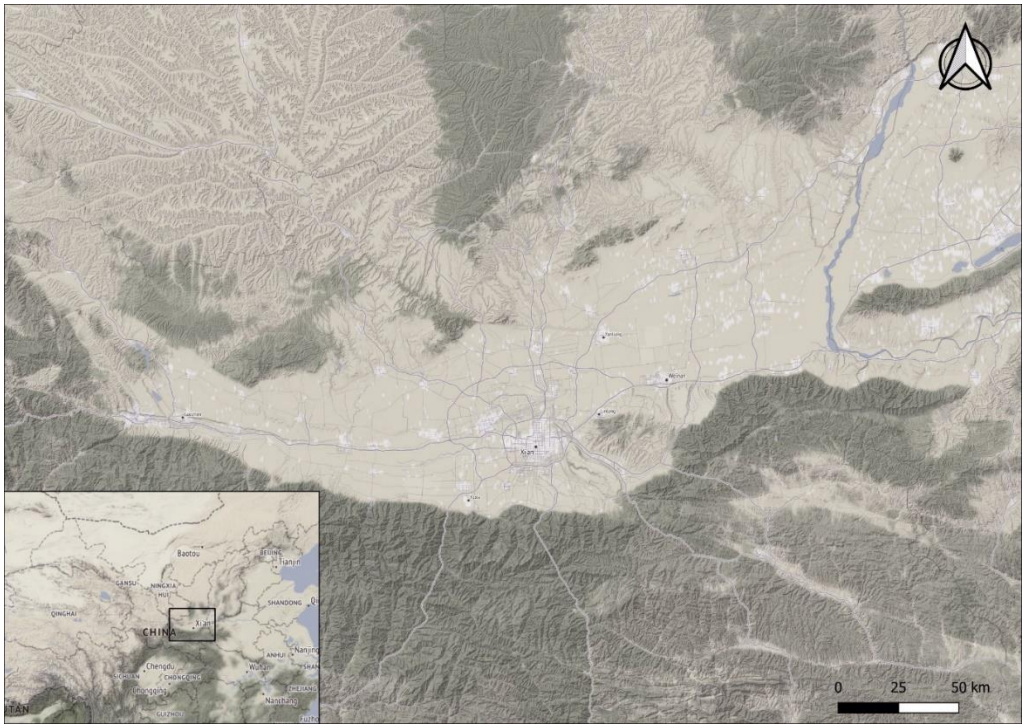

Figure 1.3 Map showing the location and terrains of the Guanzhong Plain, base map: ESRI World Terrain Base (http://tile.stamen.com/terrain)

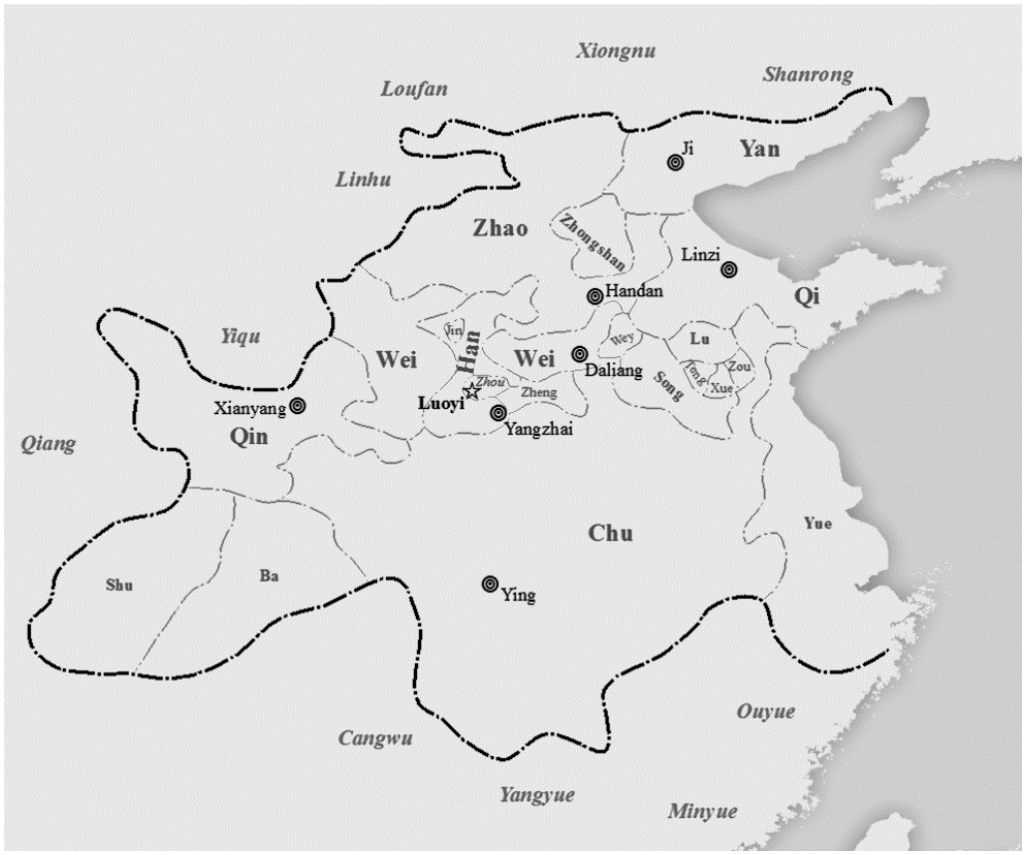

Figure 1.4 Map showing the location of the Vassal States in the beginning of the Warring States period (5th c. BC). Source: Wikipedia. https://en.wikipedia.org/wiki/Warring_States_period

Another area which will be frequently referred to in this research is central China. While the “Central Plains China” is generally used to refer to the region that covers modern-day Henan province, the southern part of Hebei province, the southern part of Shanxi province, and the western part of Shandong province (Figure 1.1), in this research, we have extended this area and used the “central China” to refer to the expanse occupied by the vassal states of Zhou royalty during Warring States period. Geographically, this area spans large Plains and Hills including the Guanzhong Plain, North China Plain, and the lower and middle part of the Yangtze Plain. With suitable soil and abundant precipitation, these areas were mostly exploited for agricultural production since the Neolithic Age and have continued to be key sources for food production throughout history (Figure 1.5). Culturally, early societies in central China shared a similar economic livelihood, featuring sedentary agricultural practice, as well as broadly similar cultural traditions and ideology that passed down from the Zhou dynasty and earlier Shang dynasty (around 1600 BC - 1046 BC).

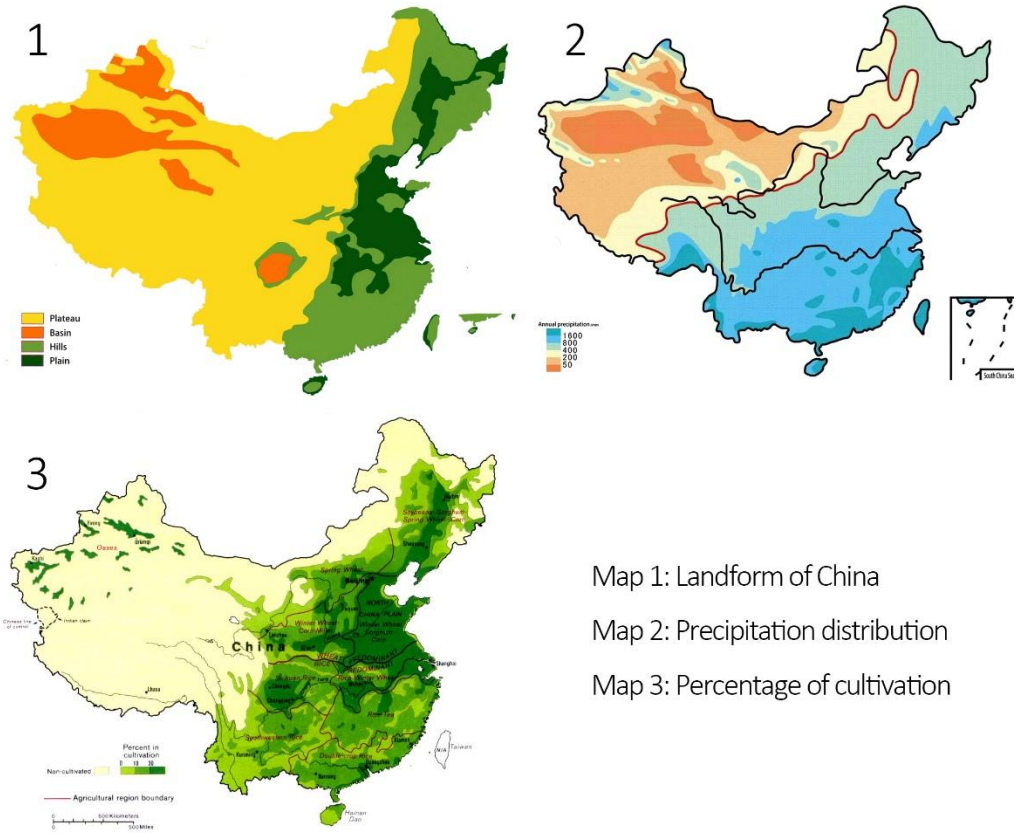

Figure 1.5 Map showing the landforms, precipitation and percentage of cultivation of modern China. Source: https://baike.baidu.com/item/中国地形/2061598?fr=aladdin; https://en.wikipedia.org/wiki/Geography_of_China

The time span this research focuses on will be the Warring States period, starting from 475 BC to the establishment of the Qin empire in 221 BC. The exact beginning date of the Warring States period is still under debate, but 475 BC is widely accepted in academic circles, following the writings of Sima Qian, a historian from the early Han dynasty (206 BC - 220 AD). During the Warring States period, central China was divided and occupied by vassal states of the Zhou royalty, seven of which, including Qin, Qi, Chu, Yan, Han, Zhao and Wei were considered as the dominant superpowers (Figure 1.4). The collapse of the Zhou royalty triggered a fierce competition for power and orthodoxy between regional states. This period is characterised as being fraught with turmoil and warfare, while also notable are political reforms and developments that led to the development of the economy, population increase, territorial expansion as well as improvements in the efficiency of governance. The Warring States period

ended when the State of Qin completed the conquest and unification of the seven states in 221 BC and established the first empire in Chinese history. The short-lived Qin dynasty, which only lasted for 15 years (221 BC - 207 BC), is also included in this research.

1.2 Aims and objectives

The focus of this thesis is to investigate three main research questions:

- How was iron produced in the State of Qin during the Warring States period?
- How did the production system develop throughout this period?
- To what extent was the iron production industry connected to broader social developments in the Qin state?

In the first part, this research is set out to model the history of iron production industry in the State of Qin during the Warring States period. Through the scientific analysis of archaeological iron samples dated to this period, their production technologies, including the iron smelting and manufacturing techniques will be explored, with particular attention paid to a variety of engineering parameters, including temperature, time and operational details that led to different iron products. By combining the study of materials and their associated production techniques with the typology and function of the final objects, the thesis seeks to model the iron production technological system. In the meantime, by applying a range of scientific analyses and data processing techniques, this research also contributes to new methodologies for identifying iron production techniques, including material characterisation, differentiation of manufacturing techniques as well as evaluating the engineering parameters.

In the second part, by combining the broader archaeological and historical evidence with the technological reconstruction, this thesis also aims to provide a chronological

framework for iron production in the Qin state, and to understand the underlying contextual reasons explaining how the production system developed and evolved over time. In this part, both the technical and social factors will be considered as the fundamental elements that affect the long-term trajectory of technological developments. By qualitatively evaluating the cost-efficiency of different technological choices considering factors such as the ore and fuel consumption, time and labour investment, the transportation cost, etc., an initial understanding from a technical perspective will be reached. These data will be further cross-examined with social factors such as the technological tradition, social organisation and natural resource limitations, and used altogether to further comprehend how such a production system was shaped from a social perspective.

Finally, this thesis also intends to provide a fresh overview on the possible social impact of the iron production industry on the development of the Qin state during the Warring States period. Previous research has focused on this topic from a historical perspective, but the archaeological and technological studies have been limited and hence could only offer assumptions and hypotheses. While it would be unrealistic to expect to address this issue comprehensively, it is hoped that the high-resolution analytical work and discussion presented and contextualised in this thesis will provide a fundamental contribution to this subject.

Some particular objectives this thesis intends to deliver include:

1. Analytical study of contextualised iron artefacts from nine archaeological sites located within the Qin state dated to the Warring States period and Qin dynasty.

2. Characterising the materials of the analysed samples and further reveal their production techniques as well as evaluating the engineering parameters applied during production.
3. Modelling the technological system for iron production in the Qin state during the Warring States period.
4. Discussion of the properties of iron alloys and decarburisation techniques with reference to materials science and historical evidence, and further evaluate the cost-benefit of each technological choices.
5. Summarise the current knowledge on iron production in the Qin state and provide a chronological framework of the development history.
6. Discussion of the social impact of iron production on the agricultural development and weapon production in the Qin state.

1.3 Thesis structure

This Chapter has presented a general introduction to the importance of iron in early human history, the development of iron smelting techniques, and the uniqueness as well as complexity of iron production technologies in central China, along with the importance of the Qin state in Chinese history. This was necessary as a starting point to outline the key questions and research topics to be addressed in this thesis.

Chapter 2 presents more detailed background for this research, in the form of a critical and synthetic review of the literature. This chapter is divided into four parts. Section 2.1 provided a metallurgical framework, including the technicalities of the two iron smelting systems, with particular emphasis on their commonalities and differences, along with current metallurgical theory of cast iron crystallisation and decarburisation.

Section 2.2 discusses current knowledge of iron artefacts in early China dated before the 5th century BC, including meteoritic iron, bloomery iron and cast iron, along with their implications regarding the early development of iron production in central China. Section 2.3 begins with a synthesis of current research results regarding the development of iron production technologies based on cast iron smelting from the 5th century BC to the beginning of the Han dynasty, around the 2nd century BC, followed by discussion of the regional technological differences within central China. Section 2.4 summarises key research gaps in the study of iron production technologies in early China.

Chapter 3 presents an overview of the workflow and analytical methodologies engaged in this research, followed by an introduction to the archaeological background of the sites, sampling strategy, samples selected for analysis and analytical protocol.

In Chapter 4, the analytical results obtained in this research are presented. In particular, section 4.1 provides the results of metallographic study; section 4.2 presents the compositional data of slag inclusions along with an initial data treatment process. An independent section providing the visual comparison between the slag inclusion data obtained in this research and the reference data from published work is given in section 4.3, with brief summarisation given in section 4.4.

Based on the analytical results, chapter 5 concentrates on the first research question, namely the iron production techniques in the Qin state. In section 5.1 and 5.2, a reconstruction of production technologies and the evaluation of associated engineering parameters is presented based on the analytical results in combination with relative metallurgical theories.

Building on chapter 5, the technological system is modelled in section 6.1. Section 6.2 takes further the discussion on the different technological choices adopted by the craftsmen in the Qin state, with both technological and social factors taken into account.

In Chapter 7, the overall development trajectory of iron production in the Qin state is summarised. By considering the broader context, the possible impact of iron production industry on social developments, mainly the agricultural economy and weapon production of the State of Qin are discussed.

Conclusions are presented in Chapter 8, where the main finding of this thesis is summarised. In addition, the limitations of this research were acknowledged, which further points to the potential further research work to address the remaining questions.

In the appendix, a chrono table of the early Iron Age China, a list of detailed information of the samples collected in this thesis, the metallograph of the analysed samples, the compositional data of CRMs and slag inclusions were provided.

2. Background

2.1 Metallurgical theories

In this chapter, I present the metallurgical theories of the two iron smelting systems, namely direct and indirect system, followed by a brief introduction to the crystallisation process of different types of cast iron and the current methods to decarburise or malleablise cast iron.

2.1.1 The two smelting systems

Due to its high chemical activity, iron rarely appears in Nature in metallic state. However, its compounds, mostly iron oxides or sulphides, are very common on the Earth's crust (Plainer 2000: 87-89; Rapp 2009). Minerals containing sufficient amount of iron that can be economically extracted through the available metallurgical technologies during the period concerned can be considered as iron ore (Killick 2014, Martinón-Torres 2018).

The most common form of iron ore exploited in early human history are mainly composed of iron oxides, such as hematite (Fe_2O_3) and magnetite (Fe_3O_4), or other forms of compounds, such as goethite [FeO(OH)] or siderite ($FeCO_3$), which can be transformed into iron oxides through a roasting process (Pleiner 2000: 107).

$$2FeO(OH) \triangleq Fe_2O_3 + H_2O$$

$$2FeCO_3 \triangleq Fe_2O_3 + 2CO_2$$

To extract metallic iron from its oxides, a reducing agent that can break the chemical bond of Fe-O and form a new, stronger bond with oxygen will be necessary. The most common form of such a reducing agent in both early and modern metallurgical industry

is carbon monoxide (CO). Carbon monoxide can be generated through an incomplete combustion of charcoal or mineral coal, following the chemical reaction:

$$C + O_2 = CO_2$$

$$CO_2 + C = CO$$

During reduction of iron oxides, chemical reactions will take place in the following sequence until the iron oxides are reduced to metallic iron:

$$3Fe_2O_3 + CO \triangleq 2Fe_3O_4 + CO_2$$

$$Fe_3O_4 + CO \triangleq 3FeO + CO_2$$

$$FeO + CO \triangleq Fe + CO_2$$

As the intermediate product, FeO, also known as wüstite, is unstable under a temperature lower than 570˚C and can automatically decompose into Fe_3O_4 and α-Fe; therefore, to make these reactions go on in the right direction, a temperature higher than 570˚C will be necessary (Wang 1991: 77). In early metallurgical practices, such a high temperature could be achieved in an enclosed environment, i.e., the smelting furnace, through the combustion of charcoal, which will also provide the reducing agent - CO gas - for the reduction reaction. The CO/CO_2 ratio and temperature in the furnace are the key factors affecting the reaction rate, which can be adjusted by changing the flow rate of the air going into the furnace. In theory, a higher CO/CO_2 rate ($CO/CO_2>3$) and temperature will facilitate the reduction process (Van Der Merwe and Avery 1982).

In addition to the reduction of iron oxides, the separation of metal from the impurities is essential for a successful smelt. Iron ores are often associated with other non-metallic minerals from the parent rock, such as quartz, feldspar or limestone, known

as gangue (Pleiner 2000: 106). During smelting, these minerals along with any iron oxides not reduced to metal and certain amount of the melted furnace linings and fuel ash will form a mixture known as slag. Given that pure metallic iron has a melting temperature as high as 1538 ˚C, well above the temperature early smelting furnaces can attain, separating metal and slag posed a great challenge to early metallurgists. To resolve this, two technological approaches, namely the direct and indirect smelting process, were adopted in different parts of the world, which created an initial divergence on the technological trajectory of iron smelting as well as the associated artefact manufacturing techniques.

As mentioned in the introduction part, the direct process produces metallic iron in a single step. A key requirement of this process is the production of fayalitic slag. When the chemical composition of such slag was properly controlled, it could be melted around 1200˚C, which is easily achievable in the early furnaces (Figure 2.1) (Rehren et al. 2007; Charlton et al. 2010). The reduced iron particles, with little to no carbon content, remain largely solid but can coalesce through the melted or softened slag and form an iron bloom. Such a hot spongy bloom will be further hammered to consolidate the iron and expel the entrapped slag, thus completing the metal/slag separation process.

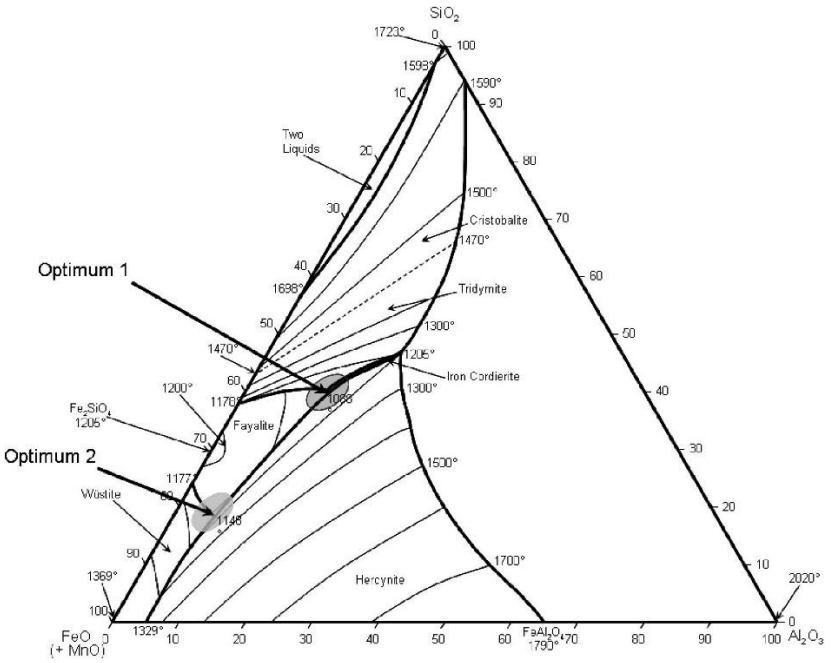

Figure 2.1 Ternary diagram of FeO–SiO_2–Al_2O_3, from Charlton et al. (2010), showing two optimum points of slag composition where they can reach a lower melting point.

In the indirect process, the smelting will be carried out in a blast furnace. By applying a strong air blast, the blast furnace can achieve a much higher operating temperature compared with the bloomery furnace, easily around 1300 - 1400 ˚C, and a more reducing atmosphere. Under this environment, iron oxides can be reduced earlier on, at a higher position inside the furnace. As the reduced iron particles drip down through the furnace, they will be alloyed with carbon via the contact with charcoal and gradually increase the carbon content. The resulting iron-carbon alloy, known as cast iron, has a melting temperature as low as 1148 ˚C with carbon content around 4.3 wt.%, hence will be melted and sink to the bottom of the furnace, forming a pool of liquid cast iron with melted slag floating on top. The separation of these two components will be greatly simplified compared to the direct process, as both liquids can be tapped out separately by opening a tapping hole in the bottom of the blast furnace.

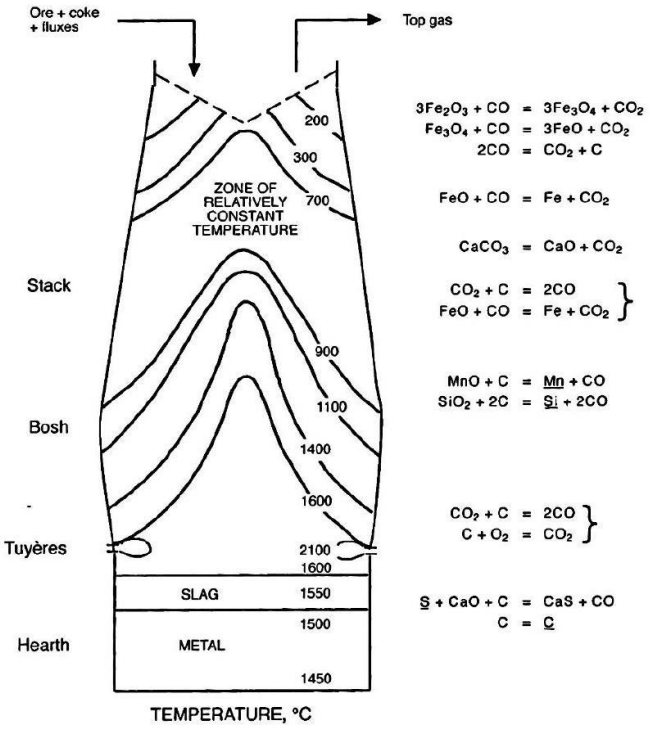

Figure 2.2 Diagram of a modern blast furnace, reactions indicated on the right (Wagner 2008: 14)

The different solutions adopted to separate the metal from the slag, and the resulting primary smelting products - bloomery iron with little to no carbon content and cast iron with around 3 - 5 wt.% carbon content - constituted the fundamental technical differences between these two smelting systems.

In bloomery smelting, since the reduced iron usually contains little to no carbon, it is very soft (hardness around HB80) and directly workable. After the primary smithing process to expel the entrapped slag, the bloom will normally be transformed into a billet/bar and further manufactured into final products by blacksmiths. Conversely, for cast iron, due to the high hardness and brittleness of the metal, further post-smelting treatments are necessary to reduce the hardness and/or to convert the cast iron into low carbon soft iron/steel. In addition, given its low melting temperature, cast iron is more susceptible of being directly cast into its final shape using moulds. The extra step

needed in the indirect smelting process to obtain soft iron, and the available technological choice for mould casting, have fundamentally affected the production model for these two smelting systems.

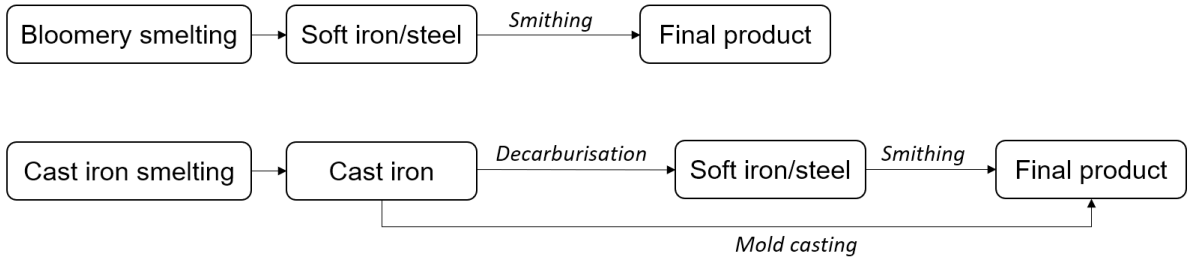

Figure 2.3 Flowchart of processes needed to obtain final products through the direct and indirect process

On the other hand, since the direct process creates a solid bloom inside the furnace, in most cases, the smelting process has to come to a full stop and the furnace needs to be opened each time to retrieve the iron bloom. After that, the furnace has to be repaired before getting ready for the next smelting cycle. Occasionally the furnace needs to be fully destroyed and potentially abandoned depending on the furnace type or other practical conditions. This has determined that the bloomery smelting is inherently an intermittent and relatively small-scale production system, where production scale reaches a maximum threshold that can only be increased by multiplying the number of furnaces. For the indirect process, as the slag and metal can be tapped out separately at the bottom of the furnace, charcoal and ore can be continuously charged from the top, and the smelting process can go on for a long period without stopping until the furnace needs to be repaired (Figure 2.4). In this sense, it will be more cost-efficient that the furnace runs as long as possible and produce as much cast iron as it can in each smelting cycle, hence the cast iron smelting is more suitable for large scale production in nature.

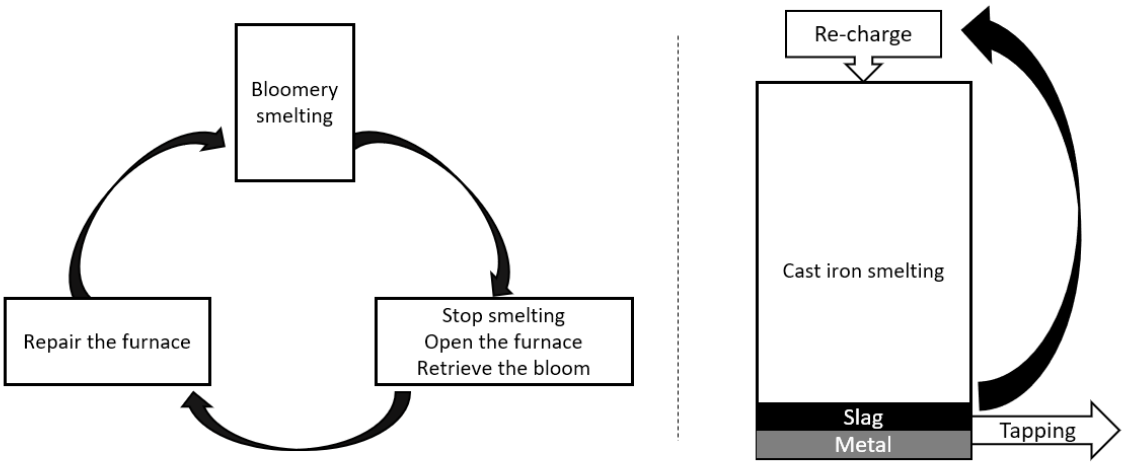

Figure 2.4 Diagram of the production cycles of direct and indirect system

Analytical studies show that cast iron smelting/melting slag in early China typically contains a significant amount of calcium oxide (usually above 20 wt.%), which, along with findings of limestone at metallurgical sites and unreacted limestone in the slag, together suggests that a calcium-rich flux (limestone, $CaCO_3$) was used for cast iron smelting and melting (Chen and Zhang 2016; Du et al. 2011; Zhang 2015a; Lam et al. 2018). By adding such a flux into the smelting system, it was possible to reduce the amount of iron lost into the slag, by forming a SiO_2-Al_2O_3-CaO slag as opposed to the SiO_2-Al_2O_3-FeO slag that is typical of bloomery smelting. In fact, cast iron smelting slag from early China has been shown to contains little to no FeO (Du 2011; Chen and Zhang 2016; Huang et al. 2016), indicating a high utilisation rate of the iron ore. This enabled smelters to efficiently exploit poor grade iron ores. In comparison, in bloomery iron smelting, most of the smelting slags are dominated by fayalite, containing around 50 wt.% of FeO or higher, therefore only high-grade ores can be used to successfully extract iron. Sometimes bloomery iron slag may also contain relatively high percentages of CaO or MnO (Veldhuijzen and Rehren 2007; Iles 2014; Iles and

Martinón-Torres 2009), but in most cases these oxides came with the ore itself rather than being an indication of intentional fluxing.

Despite all these differences between the direct and indirect smelting systems, it is necessary to point out that there is essentially no knowledge or technological barrier between these two techniques. Both systems use the same raw materials and runs under the same metallurgical principles, even if with different operation parameters. Findings of cast iron lumps have been reported from multiple bloomery smelting sites in Northern Italy, Germany, Lithuania and Britain, where they are believed to constitute accidental products resulting from an imperfect control of the bloomery smelting condition. Due to the lack of technologies to process such a material, most of them were deemed as a waste (Birch 2006; Navasaitis and Selskienė 2007), but their very presence shows that their production was within the reach of bloomery furnaces. In addition, experimental smelting work carried out by Crew et al. (2011) has also proven that it is technically feasible for bloomery furnace to produce highly alloyed cast iron. In this sense, it appears that the technological choice on which smelting technique to adopt will not be solely based on the availability of knowledge and expertise, but also other factors including the technological tradition, cultural preferences, limitations of natural resources, or broader parameters affecting production organisation and consumption. These two smelting systems therefore represent not only some technical differences, but more importantly other factors that are deeply rooted in their social background.

2.1.2 Post smelting treatments of cast iron

One of the most challenging part for adopting the cast iron smelting technique lies in the post-smelting treatment of the primary smelting product, namely cast iron. As

aforementioned, cast iron is an iron-carbon alloy in which the carbon content is greater than 2.1 wt.%. When such an alloy solidifies, depending on the cooling rate and the alloying elements of the cast iron, the solidification will either follow the iron-cementite system or the iron-graphite system (Figure 2.5)(Cui and Tan 2000: 388).

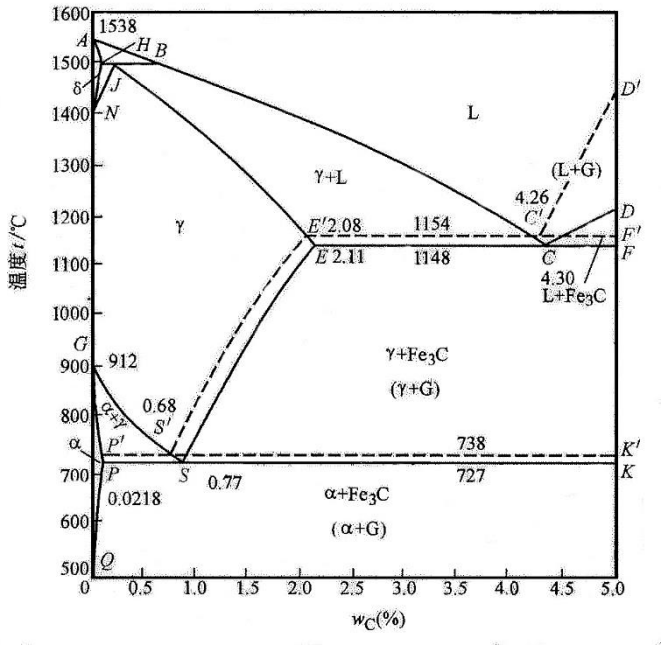

Figure 2.5. Iron-cementite and iron-graphite phase diagram, with the dashed line representing the iron-graphite system and the solid line representing the iron-cementite system (Cui and Tan 2000: 364)

Cementite has a carbon content of 6.69 wt.%, which is closer to that of liquid cast iron (usually between 3 - 5 wt.%) and austenite (0.77 - 2.11 wt.%), in contrast to graphite, which has a carbon content of 100 wt.%. In addition, the crystal structure of cementite is also closer to austenite, hence when liquid cast iron solidifies quickly, i.e., the latent heat of crystallisation cannot be released promptly, the crystallisation process will follow the iron-cementite system. In this system, when the temperature of liquid cast iron (L_c) drops to 1148 ˚C, the eutectic reaction will take place where the liquid metal will crystallise into two solid phases, the austenite (γFe) and cementite (Fe_3C, eutectic cementite).

$$L_c \overset{1148\,℃}{\Longleftrightarrow} \gamma Fe + Fe_3C$$

Austenite at this temperature has a carbon content around 2.11 wt.%, and the solubility of carbon is positively related to the temperature. When temperature continues to drop after the eutectic reaction, more cementite, namely secondary cementite, will be precipitated from the austenite. The secondary cementite is closely combined with eutectic cementite and cannot be separated. When the temperature drops down to 727 ˚C, the solubility of austenite drops to the lowest 0.77 wt.%, and the eutectoid reaction will take place where austenite transforms into ferrite (αFe) and cementite (eutectoid cementite), namely pearlite.

$$\gamma Fe \overset{727\,℃}{\Longleftrightarrow} \alpha Fe + Fe_3C$$

After the eutectoid reaction, no more crystallisation or phase transformation will take place, hence the solidification of cast iron is complete. During the period when the solidified cast iron cools down to room temperature, a small amount of tertiary cementite will be precipitated from the ferrite as its solubility of carbon drops from 0.02 wt.% at 727 ºC to 0.0008 wt.% at room temperature, yet the quantity is extremely small and can hardly be recognised. As a result, cast iron solidified through this system is primarily composed cementite and pearlite.

However, cementite is a metastable phase, it contains higher free energy compared to graphite. Hence for cast iron with the same chemical composition, if a slow cooling rate was applied during solidification, then the latent heat of crystallisation can be emitted promptly and the crystallisation process will follow the iron-graphite system, where graphite instead of cementite will form. As shown in Figure 2.5, the eutectic temperature of the iron-graphite system (1154 ˚C) is slightly higher than that of the

iron-cementite (1148 ˚C), hence when liquid cast iron is cooled down to between 1148 - 1154 ˚C, flake graphite will form in the eutectic reaction where liquid cast iron crystallises into austenite and graphite. After the eutectic reaction, as the temperature continues to drop, more carbon atoms will be released from the cementite to grow on the existing graphite flakes. When the temperature falls between 727 - 738˚C, eutectoid reaction will take place, where austenite transforms into ferrite and graphite. Depending on the actual control of the cooling rate, the resulting cast iron can either have a pearlite or a ferrite matrix. When the slow solidification is stopped before reaching the eutectoid point (738 ˚C), the matrix will be composed of pearlite. Otherwise, the matrix will be ferrite.

Depending on the form in which the carbon presents in the solidified cast iron, modern metallurgical science categorises cast iron into three different type of materials, namely white cast iron, grey cast iron and mottled cast iron. In white cast iron, carbon mainly appears in the form of cementite (iron carbide, Fe_3C), and in grey cast iron as graphite (crystalline carbon). When a mixture of both forms is present, the material is further categorised as mottled cast iron (corresponding micrograph can be seen in section 4.1.1) (Wagner 1989; Craddock et al. 2003; Cui and Tan 2000:363). White cast iron with 4% of carbon consists of 54% of cementite (hardness HBW=800) and 46% of pearlite (hardness between 180-280 HBS), hence the material itself is extremely hard. A higher hardness often corresponds to a higher brittleness, which means the material is more resistant to plastic deformation and more prone to fracture (Zhang et al. 2011), therefore when the cementite is interconnected and forms the matrix, the metal will be unmalleable. As for grey cast iron, while the presence of graphite instead of cementite may reduce the overall hardness compared to white cast iron, such graphite, mostly in the shape of lamellar or flakes, will act as internal cracks

and voids, hence diminishing the overall strength of the metal, making the grey cast iron also prone to break under physical pressure (Wagner 1989). In terms of mottled cast iron, its physical properties will be largely between white and grey cast iron. In this sense, all types of cast iron are unable to undergo any deformation work such as smithing or forging, which is essential to make metal products with high strength and toughness, therefore, methods to reduce the hardness and brittleness of cast iron will be essential to fully utilise the cast iron smelting technique.

In theory, the mechanical properties of iron are primarily related to its carbon content. Higher carbon content often corresponds to a higher percentage of cementite in the metal, which will increase the overall hardness. Conversely, to reduce the hardness, carbon content will have to be reduced to diminish the presence of cementite. This can be achieved theoretically through two technical pathways, either by directly removing the cementite through decarburisation, or by transforming the cementite into low hardness phases through malleablisation.

Cementite, in the formula of Fe_3C, is a metastable phase and contains high free energy. In nature cementite tends to slowly decompose into iron and carbon and such a process can be greatly accelerated under a high temperature (Hua 1982). When there is an oxidising agent present during the decomposition of cementite, decomposed carbon atoms will be oxidised and removed; this will be known as the decarburisation process. When there are no oxidising agents present during decomposition, decomposed carbon atoms will combine with each other and form into graphite, namely temper carbon. Unlike flake graphite, temper carbon can be smaller and roundish when properly controlled, therefore less likely to separate the metal matrix, and hence it can reduce the overall hardness of cast iron, and such a process is known as the malleablisation process (Yan and Wu 1985: 228; Wagner 1989).

The temperature under which the cast iron is heated for decarburisation or malleablisation is the key factor for determining the corresponding technique. When the temperature is under the melting point of cast iron, decarburisation or malleablisation will take place in solid state, such a process will be referred as the annealing process; if the temperature is above the melting point of cast iron, only decarburisation will take place, and such as process will be further known as the fining or puddling technique.

In modern metallurgical industry, most of the cast iron is decarburised in liquid state, namely through fining or puddling. Such a process is fairly straightforward despite the many engineering variances: oxygen or air was pumped into liquid cast iron in a converter, where carbon atoms in cast iron will be burnt away as carbon dioxide, leaving the cast iron decarburised into soft iron or steel. As for comparison, the annealing process is much more complicated, with many variables including temperature, atmosphere and duration affecting the type of the techniques as well as the final products.

During the annealing process, white cast iron will be heated up to a high temperature, typically around 950˚C in modern practice, and maintained for a duration ranging from hours to days (Yan and Wu 1985: 27). At this temperature, the basic components of the cast iron will be austenite (γ-Fe) and cementite. As aforementioned, cementite is a metastable phase, hence it will decompose into austenite (γ-Fe) and carbon atoms under this temperature. Due to the limited solubility of carbon, austenite at this temperature will be oversaturated, hence the extra carbon atoms decomposed from cementite will be in a free state. In the following stage, when the cooling begins, the solubility of the austinite for carbon will also drop, hence more free carbon atoms will be released. At around 727 ˚C (eutectoid temperature), the solubility of austenite is at

its lowest point (0.77 wt.%), and the eutectoid reaction takes place, whereby austenite transforms into layered microstructure of ferrite (α-Fe) and cementite, namely pearlite. By continuing to heat the cast iron, cementite in the pearlite structure will also decompose into α-Fe and carbon.

To decarburise the cast iron, the annealing atmosphere will be set to be oxidising, hence the free state carbon atoms at the surface of cast iron will be oxidised. In modern practice, the oxidising agents used can be either solid, such as iron ores or oxidised iron crusts, or gaseous, mostly CO_2 mixed with other components (CO, H_2, H_2O and N_2) (Yang and Wu 1985: 250-251). For gaseous oxidant such as CO_2, the following reaction will take place

$$C + CO_2 \triangleq 2CO$$

By removing the free carbon atoms, the surface of the white cast iron will be decarburised, creating a gradient of carbon concentration from surface to the core, hence carbon atoms will diffuse towards the surface and continue to be removed, leaving the whole white cast iron decarburised. Depending on the annealing temperature and the following cooling process, this process can decarburise white cast iron into a wide range iron-carbon alloys with various carbon contents, and such materials were named as white-heart malleable cast iron. An example of one of the annealing settings adopted in modern practice to obtain white-heart malleable cast iron with a mixed matrix of ferrite and pearlite (with possible ferrite layers on the surface) is shown in Figure 2.6.

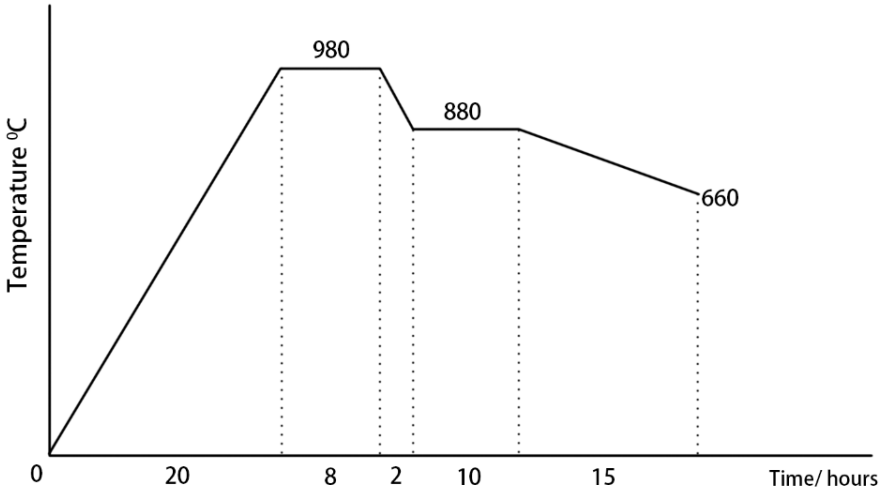

Figure 2.6 Annealing settings to decarburise white cast iron into a mixed structure of ferrite and pearlite. This practice begins with heating up to 980 ˚C, maintain this temperature for a period, then cool down to 880 ˚C, maintain for a period, then slowly cool down to 660 ˚C (Yan and Wu 1985: 251)

The annealing temperature is the one of the main factors that affects the decarburisation process. Higher temperatures will not only accelerate the decomposition of the cementite, but also raise the diffusion rate of the carbon atoms. Carbon atoms diffuse much faster in the austenite (γ-Fe), which has a face centred cubic (FCC) crystal structure, compared to ferrite (α-Fe), which has a body centred cubic (BCC) structure (Figure 2.7). In this sense, the decarburisation will be much faster when the temperature is maintained above 727 ˚C, whereas to achieve a ferritic matrix, a much longer annealing duration will be needed at below 727 ˚C, where carbon atoms will diffuse slowly through the α-Fe.

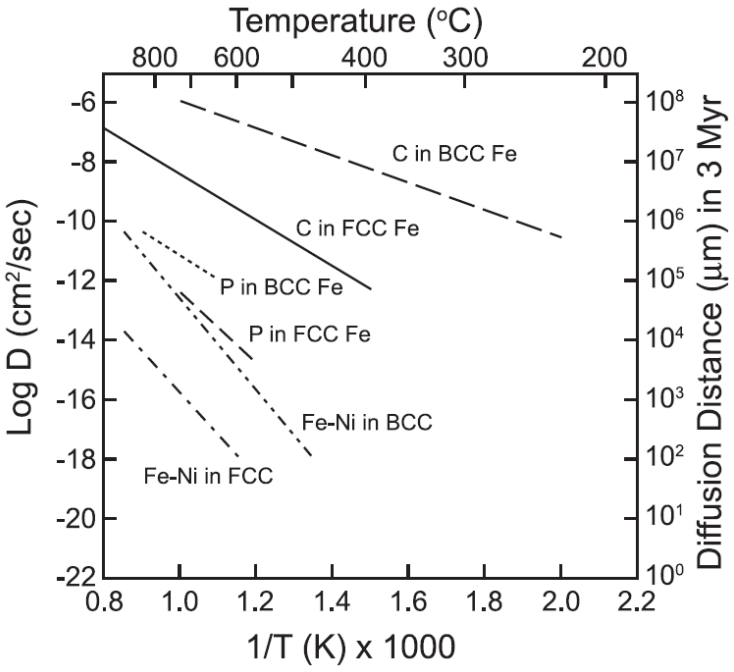

Figure 2.7 Diffusion rate of different elements in iron (Goldstein et al. 2017)

For malleablisation purpose, the annealing atmosphere should be maintained neutral or reducing. Under this condition, instead being oxidised, the former decomposed carbon atoms will crystallise into graphite crystals. Such a process includes two consecutive stages: the nucleation period and the growth of graphite.

The mechanism of the nucleation process is still poorly understood; it is generally believed to be related to sub-microscopic discontinuities such as voids or cracks, which are often located around the grain boundaries between austenite and cementite (Yan and Wu 1985: 228, Wagner 1989) (Figure 2.8). In modern annealing practice, an incubation process where the white cast iron is preheated to 350-450 ˚C and kept for 3-4 hours is applied to facilitate the nucleation (Yan and Wu 1985: 34-36). The more nuclei formed in this process; the shorter time will be needed for the whole graphitisation process. Certain elements such as silicon will also promote the nucleation process, yet the underlying principles are not well understood.

After the nucleation process, graphite will grow on the nuclei. The growth of graphite is related to both the temperature and the alloying elements, which determines the final shape and size of the graphite. In simple terms, a higher temperature will increase the decomposition rate of cementite as well as the diffusion rate of carbon atoms, which will facilitate the growth process. However, when the annealing temperature rises above 1050 ˚C, the graphite will tend to grow in one direction instead of isotropically, hence the flake graphite will start to form, therefore the temperature for malleablisation should be maintained below this threshold (Li et al. 1983; Qian and Li 1985).

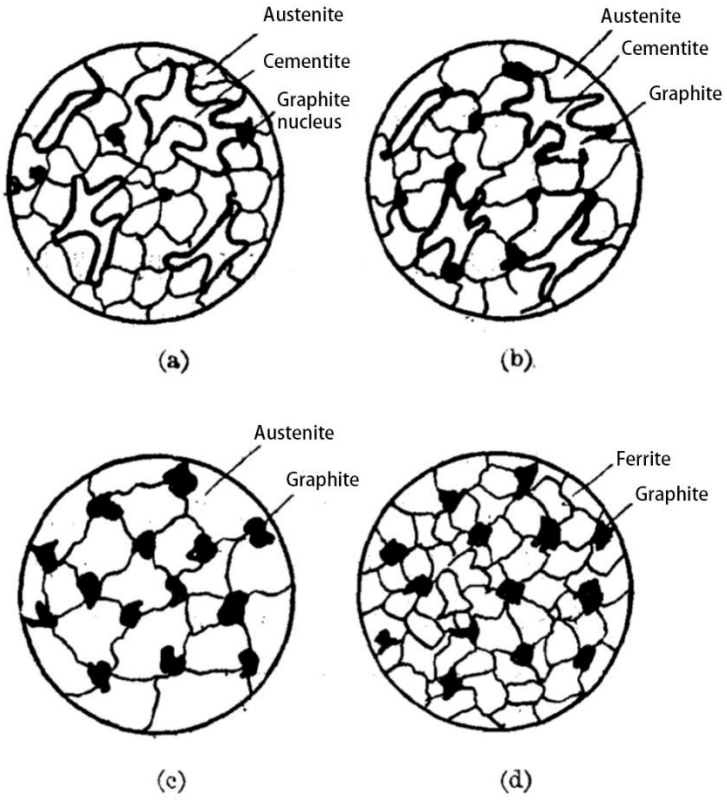

Figure 2.8 Diagram of the growth of graphite in malleable cast iron. (a) nucleus of graphite starts to form in the grain boundaries between austenite and cementite; (b) cementite starts to dissolve into austenite, carbon atoms start to grow on the nucleus; (c) cementite is dissolved, carbon atoms crystallised into graphite; (d) austenite transforms into ferrite, precipitated carbon atoms grow on the existing graphite (Yan and Wu 1985: 38).

In terms of the morphology of the resulting graphite, since the growth takes place in the solid state, there is an equal chance for the growth of graphite crystals in each

direction, hence such graphite usually occurs in the shape of spheres or as a mass of flocculant or vermicular (see Figure 4.11 in section 4.1.2). In a series of experimental work carried out by Li et al. (1983), it has been demonstrated that the shape of graphite is related to weight percentage ratio of Mn/S and the annealing temperature. When the Mn/S ratio is around one, the graphite is often spherical. When the Mn/S ratio rises, the shape of graphite starts to transit to flocculant. When the ratio is around four to five, the flocculant graphite will be loose, and when the Mn/S ratio is around two to three, the flocculant graphite will be more compact.

With the carbon atoms crystallising into graphite, the remaining cast iron will have a much lower carbon content, hence the matrix, in which the graphite is embedded in, can be either pearlitic or ferritic or a mixture of both. To achieve a pearlitic matrix, the annealing temperature is usually maintained above 910˚C followed by a fast cooling process (Figure 2.9). To achieve a ferritic matrix, two methods are available, either by slowly cooling down (3-5 degrees per hour) so the austenite will directly transform into ferrite and graphite in the eutectoid reaction (Figure 2.10), or decompose the eutectoid cementite after the eutectoid reaction where the austenite transforms into pearlite at 727˚C. To achieve a matrix of mixed structure, an example is given in Figure 2.11, which involves annealing between 800-950 ˚C to allow some amount of ferrite to precipitate from austenite. Correspondingly, these types of materials were named as black-heart malleable cast iron.

Figure 2.9 Annealing settings for the production of malleable cast iron with pearlite matrix (Yan and Wu 1985: 252)

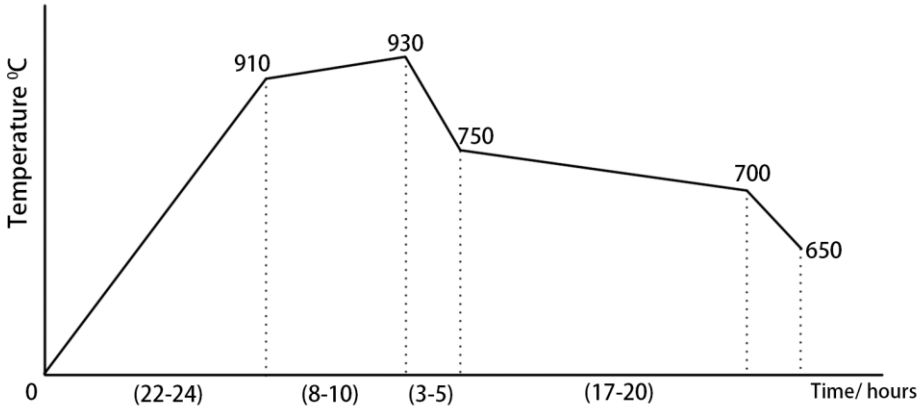

Figure 2.10 Annealing settings for the production of malleable cast iron with ferrite matrix (Yan and Wu 1985: 248)

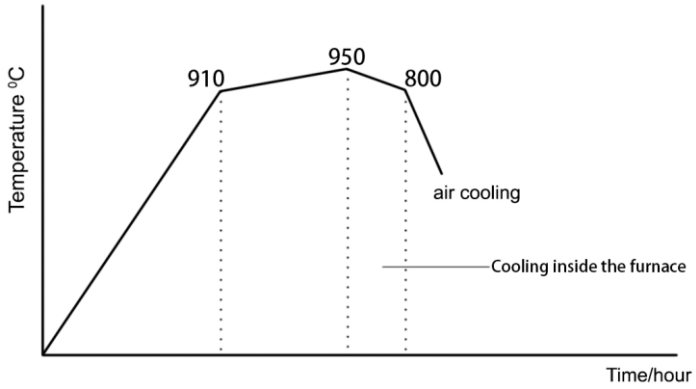

Figure 2.11 Annealing settings for the production of malleable cast iron with mixed matrix of ferrite and pearlite (Yan and Wu 1985: 253)

2.2 Iron in early China

In this chapter, I outline recent archaeometallurgical research work carried out on iron production in early China prior to the 5th century BC, with the aim of providing an overview of technological developments of the iron production industry during the Warring States period.

2.2.1 Meteoritic iron in early China

Meteoritic iron, a type of native iron mostly found in meteorites, provided the earliest access to this material before the inception of iron smelting technique. It is believed that through the manipulation of meteoritic iron, humans became acquainted with iron as a useful and desirable material and later mastered essential techniques to process iron and its alloys, which further laid the foundation for the invention of the iron smelting technique (Van Der Merwe and Avery 1982).

Due to its unique formation process (fusion of light elements in space with an extremely slow cooling rate), meteoritic iron has certain characteristic features that make it different from smelted iron, which can be recognised through scientific analysis. Among these features, the most important one is the nickel content, usually between 6 wt.% - 20 wt.%, compared to smelted iron, which only rarely shows nickel at detectable levels (Yalçin 1999; Rehren et al. 2013; Jambon 2017). Other clues, such as the presence of germanium, characteristic Ni/Co ratio and Widmannstätten structure have also been used to identify meteoritic iron in antiquity (Comelli et al. 2016; Chen et al. 2017; Jambon 2017). Most of the early meteoritic iron findings, including nine Egyptian iron beads from Gerzeh in northern Egypt dated to 3200 BC (Rehren et al. 2013), the Tutankhamun dagger dated to the 14th century BC (Comelli et al. 2016) were confirmed based on such evidence.

In early China, the journey of iron exploitation also started with meteoritic iron. According to current research, seven bimetallic artefacts excavated from four different locations were confirmed to be manufactured using meteoritic iron in association with bronze (Table 2.1, Figure 2.5). The earliest meteoritic iron product in China so far, was found in *Taixi* village, Gaocheng, Hebei province. The artefact, a battle-axe (*Yue*), made of bronze with a piece of iron embedded as the blade, was dated to the 14th century BC, corresponding to middle Shang Dynasty (around 1600 BC - 1046 BC). Scientific analysis of the iron part has shown the estimated nickel content before corrosion is between 12% - 30%, which strongly suggest the iron blade is made from meteoritic iron (Li 1976a). The same type of artefact, a battle-axe with bronze body and an iron blade, was found in another Shang burial in *Pinggu* county, Beijing, which was also dated to middle Shang dynasty (around the 14th century BC). Analysis carried out on the corrosion products of the iron revealed a significant amount of nickel (4.7 wt.%), indicating a much higher nickel content before corrosion, hence was identified as meteoritic iron. In the collection of Freer Gallery of Art in United States, another two unique bimetallic weaponry, a broad-axe with a bronze tang and iron blade, a dagger-axe with a bronze blade and the remains of an iron tip, were reported to be originally found in *Xin* village, *Jun* county, Henan province. These two artefacts were dated to early Zhou dynasty, around the 10th century BC. Analysis carried out on these two artefacts has also identified the iron part were made from meteoritic iron (Gettens et al. 1971). In addition, in the royal cemetery of the *Guo* state during the Western Zhou period, which was dated to 8th century BC, large numbers of early iron products were unearthed. Among those findings, three bimetallic artefacts, a bronze dagger-axe (*Ge*) with an iron blade, an iron adze with bronze handle hole, and an iron knife with bronze handle were also identified to be made of bronze and meteoritic iron through scientific

analysis (Han et al. 1999; Chen et al. 2018). A list of meteoritic iron findings from early China is provided in Table 2.1, and the map showing locations of these findings is given in Figure 2.12.

Table 2.1 List of meteoritic iron findings in early China

Dating	Description	Region	Province
14c. BC	Bronze Battle-axe(*yue*) with an iron blade	*Taixi* village	Hebei
14c. BC	Bronze battle-axe(*yue*) with an iron blade	*Pinggu*	Beijing
10c. BC	Bronze broad-axe(*yue*) with an iron blade	*Xin* village	Henan
10c. BC	Bronze battle-axe(*yue*) with an iron blade		
8c. BC	Bronze dagger-axe (*Ge*) with iron blade	*Sanmanxia* city	Henan
8c. BC	Iron adze with bronze handle hole		
8c. BC	Iron knife with bronze handle		

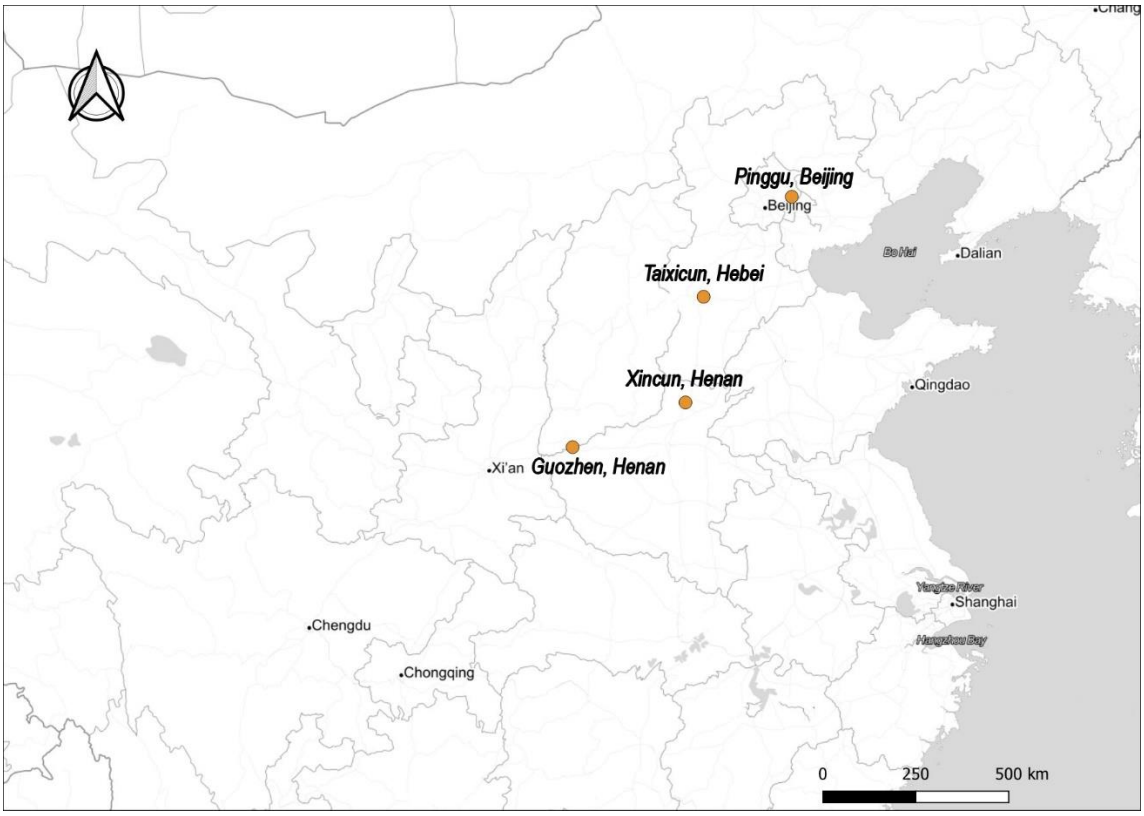

Figure 2.12 Map showing the locations of meteoritic iron findings in early China. Base map: Stamen Toner Lite/OSM (http://tile.stamen.com/toner-lite)

Based on the current research, some common features can be observed among these meteoritic iron findings. To begin with, all seven artefacts were bimetallic products, combining meteoritic iron with bronze and sometimes decorated with malachite or jade (Figure 2.13). Based upon the design of such artefacts and their archaeological context, it is safe to assume all these artefacts were made for ritual use instead of for practical functions. Combined with the overall scarcity of such findings, all evidence suggests meteoritic iron was a rare and valuable material in early China during the 14th – 8th century BC.

Figure 2.13 Photos of meteoritic iron artefacts from Taixi Village, Hebei (left, from the website of National Museum of China) and Sanmenxia Guo-State cemetery in Henan (right, from Chen et al. 2017)

2.2.2 Bloomery iron in early China

The origins of bloomery production in China remains an active and contested field of research. On the one hand, north and northwest China show different development stages compared to central China. It is generally believed that the Xinjiang region entered the Iron Age around the 10th century BC (Chen 1990; Han 2018), with large quantities of iron artefacts found in local burials. Outside Xinjiang, most of the

bloomery iron findings in central China and its periphery area are dated later than the 8th century BC (Table 2.2, Figure 2.7), hence it has been argued that the iron smelting technique was possibly introduced to central China from Xinjiang around the 9th century BC (Guo 2009). On the other hand, some scholars argue that those early iron artefacts were possibly introduced into Xinjiang through the migration of nomadic people from the Eurasia Steppe. Indigenous iron production did not start until around the 5th century BC, when the occurrence of iron arrowheads, which are considered as consumables used in war activities, indicates iron smelting was practiced locally and provided sufficient amounts of iron steadily (Wei 2017). In 2012, an iron bar unearthed from a burial at Mogou, Gansu province, was scientifically examined and identified as smelted iron produced through the bloomery smelting process. Compositional analysis showed no traces of nickel content in the metal matrix, and the slag inclusions are predominantly fayalitic with wüstite crystals. Radiocarbon dating on the human bones and charcoal samples are in line with the typological study, both suggesting that the burial could be dated to around the 14th century BC (Chen et al. 2012). This finding has provided yet another challenge for the already complex situation on the origin and possible technological transmission route of early bloomery iron smelting technique, which is beyond the scope of this dissertation.

In central China, the earliest finding of bloomery iron products overlaps with meteoritic iron both in time and space, namely at the *Guo* state cemetery in Sanmenxia city, Henan province. In this cemetery, in addition to the three meteoritic iron artefacts introduced in the last chapter, another three iron weapons, a sword with an iron handle, a dagger-axe with an iron blade and an iron spear with a bronze handle were also sampled and analysed (Han et al. 1999). Compositional analysis of the iron parts showed no traces of nickel in the metal or corrosion products, while typical bloomery

iron slag inclusions, i.e., wüstite crystals on an fayalitic matrix, were observed, suggesting the iron was possibly obtained through the bloomery smelting process.

From the 8th century BC onwards, more bloomery iron products are found in multiple locations across central China as well as the surrounding area (Table 2.2, Figure 2.14). The majority of such findings are still bimetallic products, mostly unearthed from burials located in Gansu, Ningxia and Shaanxi provinces, which are located to the north and north-west of central China. For instance, in the tomb No.2 in *Yimencun*, Shaanxi province, a total of 24 iron swords and knives with gold handles were unearthed (Baoji Municipal Institute of Archaeology 2016). The burial itself was dated to the 5th century BC, with a mixture of both the Qin and nomadic cultural elements (Zhang 1993; Zhao 1997). Analysis carried out on one of the swords showed a ferritic matrix with typical bloomery slag inclusions embedded, while no nickel content was detected in the iron, indicating the iron was smelted through the bloomery process (Bai 1994). Similar results were obtained from the analysis of other iron findings, including four iron swords with bronze handles unearthed from different locations in Ningxia (Han 1998), one iron sword with bronze handle unearthed from tomb No.1 in *Lingtai*, Gansu province (Liu and Zhu 1981), one bronze knife with iron blade and a bronze dagger-axe with iron blade unearthed from tomb No.27 in *Liangdaicun*, Shaanxi province (Chen et al. 2009). In addition to the bimetallic feature, the archaeological context of such findings has also shown some similarities. For instance, the tomb No.1 in *Lingtai*, Gansu, tomb No.2 in Yimencun and tomb No.27 in *Liangdaicun* are all large scale burials belonging to social elites. Furthermore, all these burials contain certain cultural elements related to the nomadic civilisation (Liu and Zhu 1981; Zhao 1997; Chen et al. 2009).

In comparison, bloomery iron findings in the eastern part of central China, including Shanxi, Jiangsu and Shandong province are more variable and scattered (Figure 2.14). To begin with, all these bloomery iron findings are not bimetallic products, nor do they have any decorative characteristic of the bloomery iron products found in the western part. The typology of these artefacts is also more diversified, with no clear patterns to suggest a common way of using such a material (Table 2.2).

Table 2.2 Findings of bloomery iron dated before 5th century BC (excluding Xinjiang area)

Dating	Description	Region	Province	Source
14th c. BC	Iron bar	Mogou	Gansu	(Chen et al. 2012)
8th c. BC	Iron sword with a jade handle	Sanmenxia	Henan	(Han 1999)
8th c. BC	Bronze dagger-axe with iron blade			
8th c. BC	Iron spear with bronze handle			
7th c. BC	Iron sword with bronze handle	Lingtai	Gansu	(Liu and Zhu 1981)
8-6th c. BC	Bronze knife with iron blade	Liangdaicun	Shaanxi	(Chen et al. 2009)
8-6th c. BC	Bronze dagger-axe with iron blade			
7-6th c. BC	Iron bar	Qucun	Shanxi	(Zou 2000)
6th c. BC	Iron shovel	Wu xian	Jiangsu	(Han 1998)
6th c. BC	Iron sword with gold handle	Yimen	Shaanxi	(Bai 1994)
5th c. BC	Iron sword with bronze handle	Guyuan	Ningxia	(Han 1998)
5th c. BC	Iron sword with bronze handle			
5th c. BC	Iron sword with bronze handle	Xiji	Ningxia	
5th c. BC	Iron sword with bronze handle	Pengyang	Ningxia	
5th c. BC	Iron bar	Liuhe	Jiangsu	(Nanjing Museum 1974)
5th c. BC	Iron knife	Linzi	Shandong	(Shandong Museum 1977)

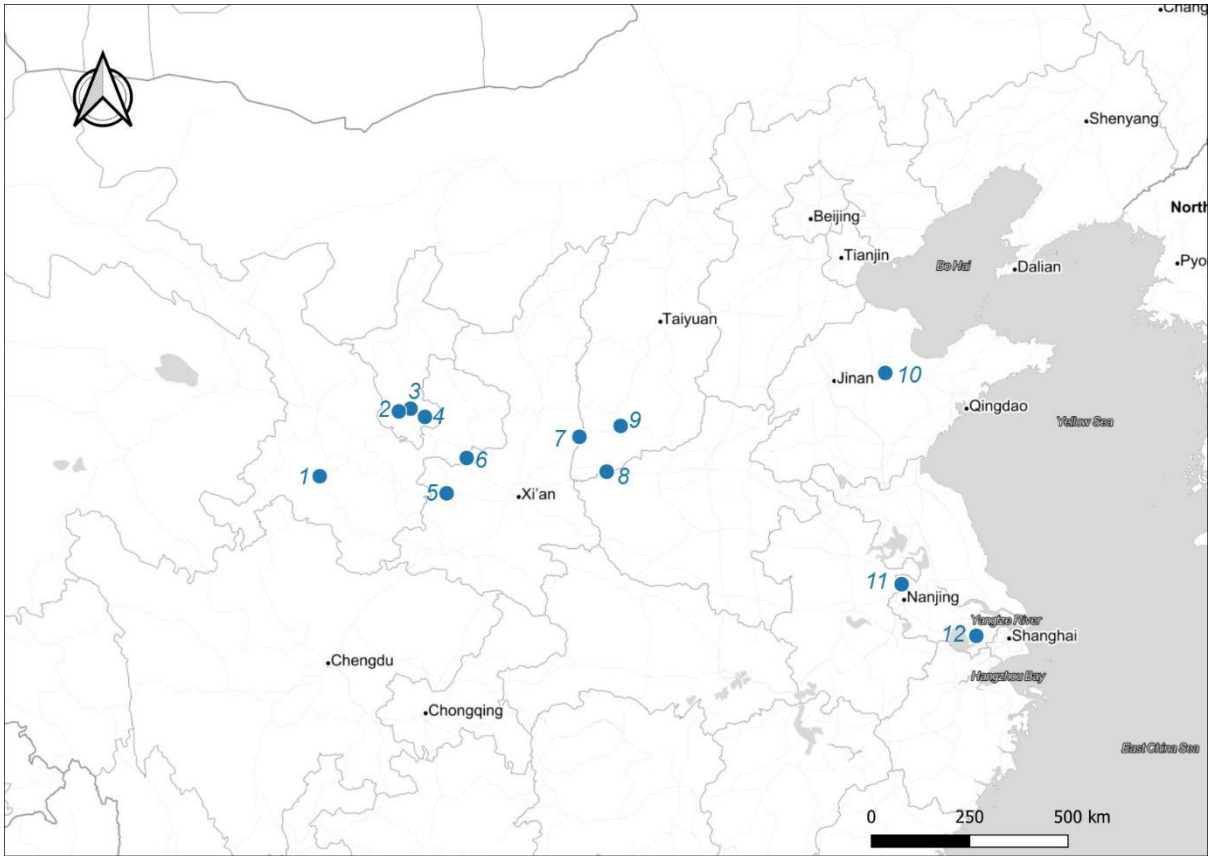

Figure 2.14 Map showing the location of sites where bloomery iron dated to before the 5th century BC were found (excluding Xinjiang). Base map: Stamen Toner Lite/OSM (http://tile.stamen.com/toner-lite)

1.Mogou, Gansu; 2. Xiji, Ningxia; 3. Guyuan, Ningxia; 4. Pengyang, Ningxia; 5. Yimen, Shaanxi; 6. Lingtai, Gansu; 7, Liangdaicun, Shaanxi; 8, Sanmenxia, Henan; 9, Qucun, Shanxi; 10. Linzi, Shandong; 11, Liuhe, Jiangsu; 12, Wuxian, Jiangsu

In general, bloomery iron findings in central China and its periphery area are still scarce before the 5th century BC, considering the huge area coverage. Despite the controversy on the origin of the bloomery smelting technique in early China, the overall scarcity of such products, its high social value indicated by the archaeological context, along with the absence of smelting sites, all suggest the scale of bloomery production in central China and its periphery area was limited.

2.2.3 Cast iron in early China

Contrary to the uncertainty on whether bloomery iron smelting was developed indigenously or not, the cast iron smelting technique, with no doubt, was independently developed in central China. The earliest evidence of cast iron consists of two

fragments, unearthed from a *Jin* state cemetery, separately dated to around the 8th and 7th century BC, corresponding to early and middle Spring and Autumn period (Zou 2000: 1178-1180). Metallographic examination has shown both of them were white cast iron, with carbon contents at 4.1 wt.% and 4.5 wt.%, respectively (Han and Ko 2007: 385). While the typology of these two artefacts was not recognisable due to the heavy corrosion, rendering such a finding less convincing to serve as the evidence of an intentional technological choice of cast iron smelting, the presence of such a material nonetheless points to an important fact that the technical conditions to produce cast iron were already accomplished in the early iron smelting practices in this area. In a burial dated to Eastern Zhou period, around the 6th century BC, an iron ball was unearthed, which was also confirmed to be made of white cast iron through metallographic study (Nanjing Museum 1974; Han 1998). From the 6th century BC onwards, large quantities of iron products with practical functions are found in multiple archaeological sites and burials. In the *Yangying* site from Laohekou city, Hubei province, 42 iron tools dated to late Spring and Autumn period (around the 6th - 5th century BC) were unearthed (Hubei Provincial Institute of Cultural Relics and Archaeology and Laohekou Municipal Museum 2003), eight of them were scientifically examined and identified as cast iron (Chen 2014:221 - 228). Another archaeological site dated to a slightly later period was found in Luoyang, Henan province, yielding large quantities of cast iron tools and farming implements (Li 1975). An iron foundry site was also found in Dengfeng, Henan province, yielding furnace fragments, casting moulds as well 12 farming implements dated to the 5th century BC (Henan Provincial Institute of Cultural Heritage 1992). Six of those implements were subjected to metallographic examination and recognised to be made of white cast iron and further subjected to a decarburisation process (Han 1998). Other occasional findings,

including an iron axe from Jiangling city, Hubei province, an axe from Changzhi city, Shanxi province were also subjected to scientific study and identified as cast iron products (Han 1998). Altogether, these evidence suggests that by the 5th century BC, iron production based on cast iron smelting has been widely established in central China. A list of such findings is given in Table 2.3, and the locations of such findings is given in Figure 2.15.

Table 2.3 List of cast iron findings in central China dated before the 5th century BC

Date	Typology	Region	Province	Material	Source
8th c. BC	Fragment	Qucun	Shanxi	White cast iron	(Zou 2000)
7th c. BC	Iron bar			White cast iron	
6th c. BC	Iron ball	Liuhe	Jiangsu	White cast iron	(Nanjing Museum 1974)
6th -5th c. BC	Shovel (Chan)	Yangying	Hubei	Decarburised cast iron	(Chen 2014: 221-229)
	Adze (Ben)			White cast iron	
	Sickle			Decarburised cast iron	
	Adze (Ben)			Decarburised steel	
	Adze (Ben)			Decarburised cast iron	
	Fragment			White cast iron	
	Fragment			Decarburised steel	
	Fragment			Mottled cast iron	
5th c. BC	Axe	Jiangling	Hubei	Decarburised cast iron	(Han and Ko 2007: 388)
5th c. BC	Fragment	Xinzheng	Henan	White cast iron	(Ko et al. 1993)
5th c. BC	Adze (Ben)	Luoyang	Henan	Decarburised cast iron	(Li 1975)
5th c. BC	Shovel (Chan)			Malleable cast iron	
5th c. BC	Hoe (Jue)	Dengfeng	Henan	Decarburised cast iron	(HICH and NM 1992)
	Hoe (Jue)				
	Hoe (Jue)				
	Hoe (Jue)				
	Hoe (Jue)				
	Hoe (Chu)				
5th c. BC	Axe	Changzhi	Shanxi	Decarburised cast iron	(Bian 1972)

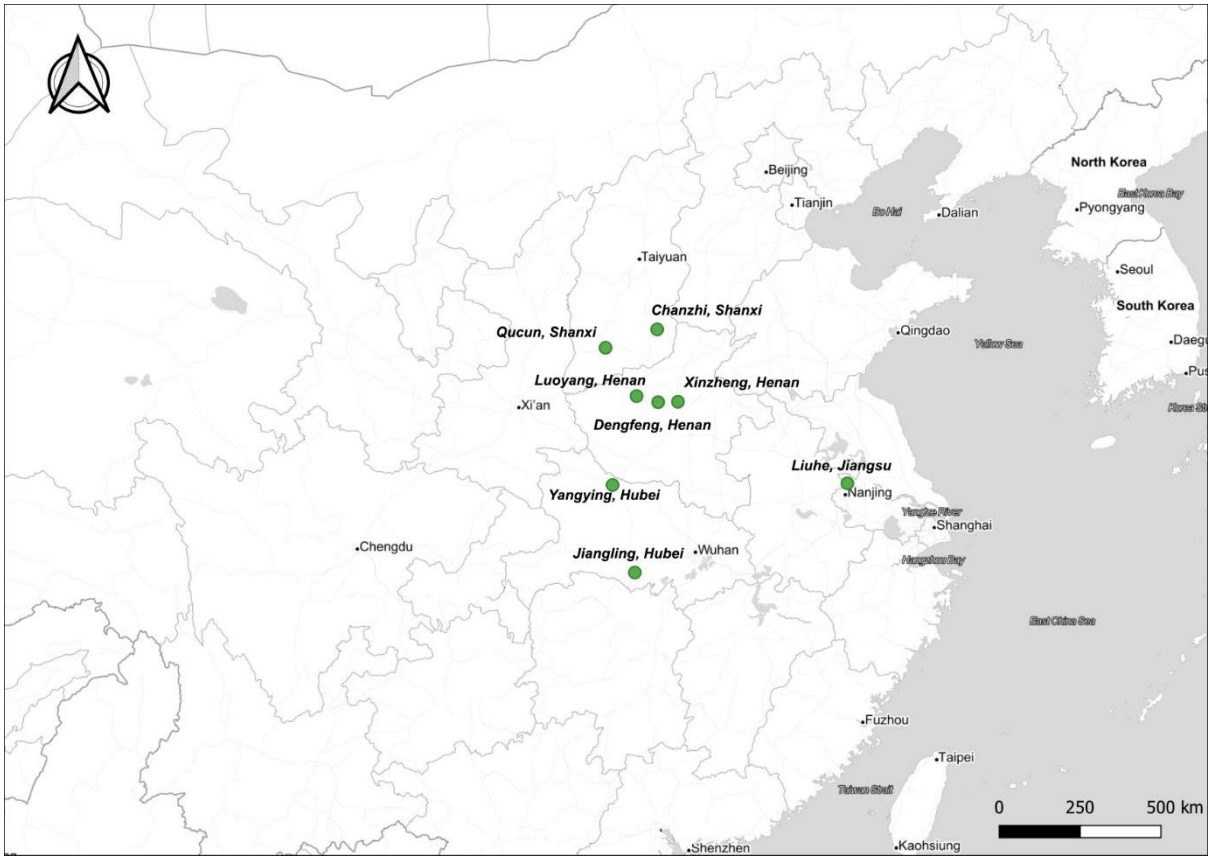

Figure 2.15 Map showing the locations of early cast iron finds in central China predating the 5th century BC. Base map: Stamen Toner Lite/OSM (http://tile.stamen.com/toner-lite)

Based on the findings of early cast iron products, an apparent shift in how iron was being perceived and used in early central China can be observed. To begin with, these cast iron products are no longer used in association with precious materials. The main product from the 5th century BC onwards are implements designed to work the soil, which is highly utilitarian. The sites yielding such findings are also no longer associated with high social hierarchy elites. Overall, this evidence suggests that, by the 5th century BC, cast iron production was sufficiently developed to provide large quantities of iron products at relatively low cost, rendering such a material less scarce and available for utilitarian social activities.

2.2.4 Summary

Based on the current archaeological and archaeometallurgical study on early iron products found in central China and its periphery dated to before the 5th century BC, it can be observed that the use of iron has gone through three different phases. From around the 14th century BC to the 8th century BC, the use of iron was limited to a small amount of meteoritic iron, suggesting iron smelting was not practiced in this area; From the 8th century BC to the 6th century BC, a small number of bloomery iron products are found in multiple sites across central China, indicating bloomery smelting was practiced on a small scale at different locations. Between the 6th and the 5th century BC, relatively large quantities of cast iron objects are found across central China, indicating the cast iron smelting technique has been developed and widely adopted as an alternative method to smelt iron.

Along with the transition in the source and production techniques of iron, the quantities of such findings, and the purpose and function of the iron objects have also changed. Early meteoritic and bloomery iron were predominantly used for ornamental or ritual purposes, while early cast iron was used in a more practical and utilitarian way, mostly for making craft tools and farming implements. Such a transition also indicates the social and economic value of iron has changed, where iron was no longer a rare and valuable material that was exclusive to a small number of social elite individuals following the innovation and adoption of the cast iron smelting technique. This further suggests the scale of cast iron production was also relatively large, where mass production had been achieved to make iron products at a much lower unit cost compared to the bloomery iron production.

However, it is worth noting that the current understanding of iron production in early China is based on archaeological findings as well as analytical work carried out on a limited amount of finished objects. With ongoing archaeological and archaeometallurgical research work, more evidence may come up in the future which might change our current understanding. In the meantime, questions were also raised regarding the characterisation of bloomery iron and the differentiation from indirect products in these early analytical work (Wagner 2008: 137-140). In most of the cases, only very few analytical data have been provided in the published work, and there is no way to verify if such conclusions are valid. In this thesis, such conclusions will be temporarily accepted, and in the following chapters, a more detailed discussion on the method to recognise production techniques based on analytical data will be provided.

2.3 The development of iron production in central China

In this chapter, past and current research work on the iron production in central China between the 5th century BC - 2nd century BC, roughly covering the Warring States period to early Han dynasty, is summarised and discussed. Along with the technological development involving the use of cast iron, special attention is paid to different technological choices in different areas.

2.3.1 Technological development based on cast iron smelting

From the 5th century onwards, iron objects unearthed from central China subjected to scientific analysis have been shown to be predominantly made from cast iron, indicating such a smelting method was widely adopted throughout this region. Along with this technological transition, a complicated technological system aiming to utilise this material was also developed in the following centuries, and further consolidated its dominant position in iron production industry in central China.

As demonstrated in section 2.1.2, while cast iron cannot be deformed through hot or cold working due to its high hardness and brittleness, the relatively low melting temperature which is achievable in early smelting/melting furnaces made this material ideal for the mould casting process. Scientific examination of early cast iron objects dated before the 5th century BC confirmed these products, mostly farming implements, were invariably shaped through this process (Table 2.3). In the following Warring State period, large quantities of daily use objects such as cooking pots (*Fu*), tripods (*Ding* vessels), lamps and belt-hooks etc. were also produced using the same technique (Bai 2004: 97-108).

In addition, early iron production sites in central China have yielded large quantities of casting moulds and kilns for making such moulds. In the *Yangcheng* casting site in Dengfeng, Henan province, casting moulds with multiple cavities were also found, which were designed to produce several objects in one single cast (Henan Provincial Institute of Cultural Heritage and National Museum 1992:256-336) (Figure 2.16). While the majority of early casting moulds were made of low-fired clay, iron casting moulds have also been found dated to the Warring States period. In the excavation of an iron production site in *Xinglong* county, Hebei province, 40 pairs of casting moulds made of cast iron, mostly designed for craft tools and farming implements were unearthed (Zheng 1956) (Figure 2.10). Metallographic study carried out on one of them showed it was made of white cast iron (Yang 1960). Casting moulds made of cast iron can be used for multiples times, therefore can reduce the unit cost of mould casting as well as raising the degree of standardisation of the casting products. In addition, using iron moulds can also provide a higher solidification rate, as metal moulds have a much lower heat capacity comparing to sand or clay moulds, therefore such moulds will be ideal to be used for making white cast iron products.

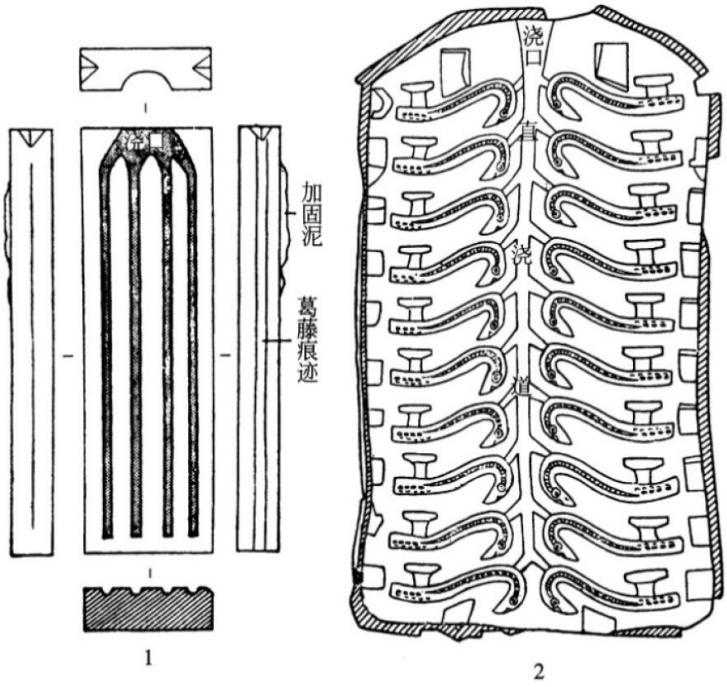

Figure 2.16 Diagram of casting moulds with multiple cavities from Yangcheng casting site in Dengfeng, Henan province (Bai 2004). 1: casting mould for iron bars; 2: casting mould with multiple cavities for belt hooks.

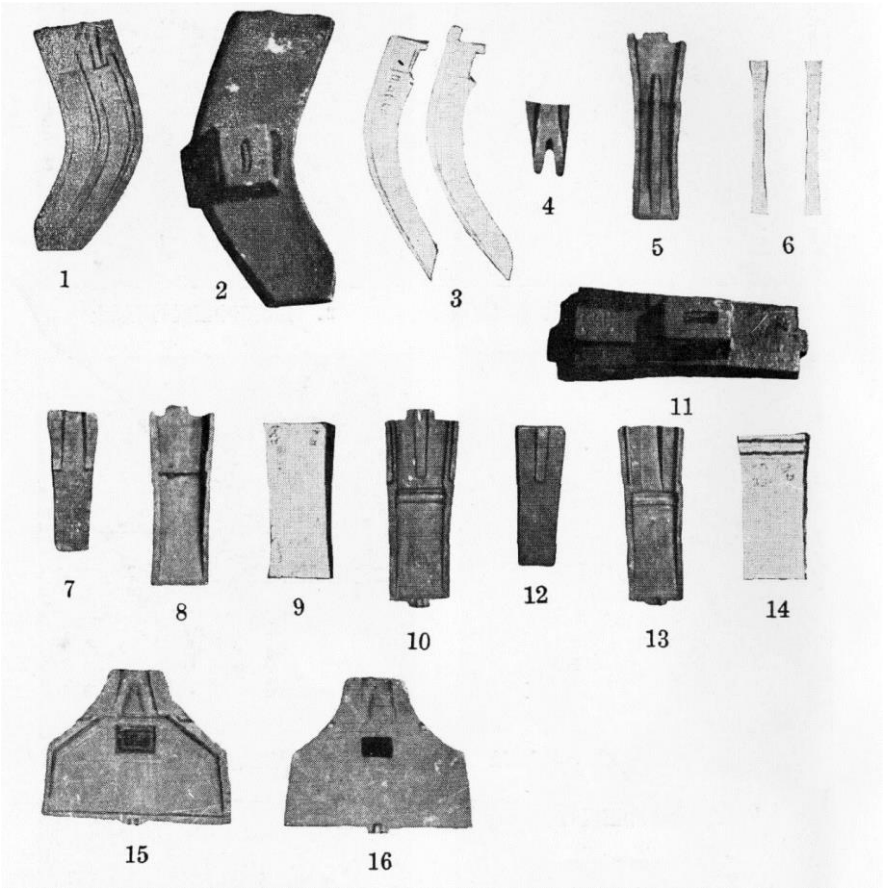

Figure 2.17 Selected iron moulds excavated in Xinglong County, Hebei province (Zheng 1956)

The most common material resulting from the mould casting process is white cast iron. Previous studies carried out on cast iron products from central China have shown the majority of them were made of such material. However, a small number of grey or mottled cast iron objects have also been found in multiple sites (Beijing University of Iron and Steel Technology 1976; Hua et al. 1960; Ko et al. 1993; Li 1982; Rong et al. 2013; Yang 1960; Zhao et al. 1985; Ye 1975; Duan 2001; Chen 2014). In the following Han dynasty, grey and mottled cast iron become increasingly common among the archaeological findings, indicating the production of such materials has become a standing technological choice (Table 2.4).

Table 2.4 Examples of grey/mottled cast iron products in central China dated before 2nd c. AD

Site/Cemetery	Province	Arch No.	Date	Typology	Material
Daye	Hubei		WS[1]	Hammer	Mottled cast iron
Yangying	Hubei		SA-WS	Fragment	Mottled cast iron
Siqi	Shanxi	M2189	WS	Pot	Mottled cast iron
Changzhi	Shanxi	TM78	WS	Belt-hook	Mottled cast iron
Yuci	Shanxi	M7	WS	Hoe (*Jue*)	Mottled cast iron
Yuci	Shanxi	M134	WS	Adze (*Ben*)	Mottled cast iron
Yuci	Shanxi	M144	WS	Adze (*Ben*)	Mottled cast iron
Tieshenggou	Henan	T5:42	Han	Fragment	Mottled cast iron
Tieshenggou	Henan	T13:7	Han	Fragment	Grey cast iron
Tieshenggou	Henan	T5:28	Han	Fragment	Grey cast iron
Tieshenggou	Henan	T11:10	Han	Plate	Grey cast iron
Tieshenggou	Henan	T13:7	Han	Plate	Grey cast iron
Tieshenggou	Henan	T18:4	Han	Plate	Grey cast iron
Tieshenggou	Henan	T18:15	Han	Mould	Grey cast iron
Tieshenggou	Henan	T19:1	Han	Plate	Grey cast iron
Tieshenggou	Henan		Han	Plate	Grey cast iron
Guxing	Henan		Han	Jiaokoutie[2]	Mottled cast iron
Guxing	Henan		Han	Jiaokoutie	Grey cast iron
Zhenping	Henan	H1:18	Han	Mould	Grey cast iron
Nanzhao	Henan		Han	Ploughshare	Mottled cast iron
Xinzheng	Henan		Han	Ploughshare	Mottled cast iron
Lushan	Henan		Han	Weight standard	Mottled cast iron

Mixian	Henan		Han	Ploughshare	Mottled cast iron
Lushan	Henan		Han	Mould	Mottled cast iron
Shenmingpu	Henan	M28	Han	Mou[3]	Mottled cast iron
Shenmingpu	Henan	M146	Han	Ring	Grey cast iron
Shenmingpu	Henan	M158	Han	Mou	Mottled cast iron

1. Warring States period; 2. Refers to the leftovers of cast iron on the mould after casting process; 3. A specific type of cooking pot in Qin state

Based on these analytical work, it has been argued that grey/mottled cast iron may have been intentionally produced for certain types of objects since the Warring States period (Li 1975). The reason for adopting such a technological choice is believed to be that grey/mottled cast iron offered superior material properties compared to those of white cast iron. For instance, among these finds, iron moulds made of grey/mottled cast iron have been recovered at different sites dated to the Han dynasty. It was argued that moulds made of such materials would be more stable under the thermal shock created when liquid cast iron was poured into them (Li 1982). As for other types of products, it is established that grey or mottled cast iron have lower hardness and less prone to break during collision due to the graphite flakes inside acting as shock absorbents, therefore can provide longer service life compared to white cast iron. Regarding the production technique for grey/mottled cast iron, it has been suggested that a slower cooling rate could have been applied during the casting process to facilitate the formation of graphite. This could be achieved by using a thicker casting mould to slow down the heat loss during solidification, or by pre-heating the casting mould before casting (Ko et al. 1993; Craddock et al. 2003; Wagner 2008:162).

While most daily use artefacts do not require exceptional toughness, which is the material's ability to plastically deform without fracturing and often negatively related to hardness, hence the white cast iron and grey/mottled cast iron can suffice, for craft tools or farming implements that will be used against other materials such as wood or

soil, a lower hardness and higher toughness will be necessary to guarantee an acceptable quality as well as a long service life. In this case, a technical process capable of reducing the hardness of cast iron will be necessary for the effective utilisation of the cast iron. Based on the metallographic study carried out on early cast iron findings from the *Yangying* site in Hubei province and the *Dengfeng* site in Henan province (Chen 2014: 221-228; Henan Institute of Cultural Heritage and National Museum 1992), it has been demonstrated that during late Spring and Autumn period and early Warring States period (around the 6th - 5th centuries BC), the annealing process was adopted to decarburise or malleablise cast iron products.

The adoption of such a technique is believed to originate from the pottery making knowledge dating back to Neolithic age, where both the firing temperature and redox conditions were finely controlled (Hua 1982; Chen 2014: 232-233). Archaeological excavation of an iron production site in *Tieshenggou*, Henan province shows the process was carried out in an annealing kiln as shown in Figure 2.18. The kiln has an independent chamber to contain the finished casts, and a separate fire pit where heat will be generated and transmitted into the chamber. By properly controlling the annealing temperature, atmosphere and duration, cast iron products can be partially or fully decarburised or malleablised through this process. The corresponding materials, *malleable cast iron* (可锻铸铁), *decarburised cast iron* (脱碳铸铁) and *decarburised soft iron/steel* (铸铁脱碳熟铁/钢) were frequently found among the early cast iron farming implements in central China from the 6th century BC onward, indicating that by then the annealing technique had been widely adopted for improving the mechanical properties of cast iron (Li 1975, Wagner 1989).

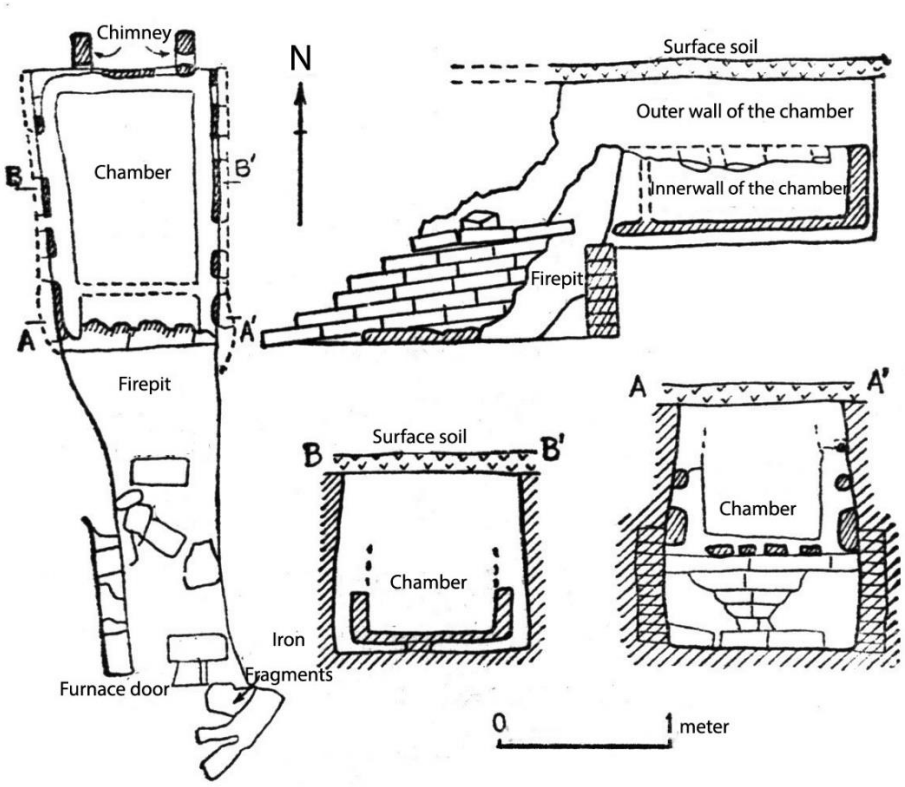

Figure 2.18 Diagram of the annealing kiln from Tieshenggou Site in Henan province (Zhao, Li et al. 1985)

With the annealing technique being developed and adopted, the iron production technological system based on cast iron smelting was theoretically completed. Combining cast iron smelting, casting, and the annealing techniques, iron with different levels of carbon content and various material properties can be produced depending on the cost-efficiency requirements.

During early Han dynasty, around the 2nd century BC, it is believed that another major technological innovation regarding cast iron decarburisation took place, namely the method to decarburise cast iron in liquid state. This method is known as the *chaogang* technique, directly translated as stir-fry steel, which runs under the same metallurgical principle of fining or puddling as introduced in section 2.1.2. Several English translations has been used to describe such this primitive technical process, including “fining”, “refining” or “puddling”, despite the many differences in how such techniques

was practiced. In this research, following Wagner (2008: 16), “fining” is used along with Chinese pinyin *chaogang* as designated terms for this process.

The *chaogang* (fining) process is believed to be first mentioned in an early compilation of Daoist literature know as *Tai Ping Jing* (Scriptures of the Great Peace), which was assembled in the Eastern Han period, around the 2nd century AD (Wang 1960). The text reads: “to produce iron weapons, craftsmen should first find the proper ore, smelt it to get liquid iron, then have skilled craftsmen hammer it multiple times until a sword comes out of it”. The sentence only described a production process where liquid iron, presumably cast iron, was forged into weapons, without providing any exact description on how the metal was decarburised, hence scholars have deemed this as an indirect evidence of liquid state decarburisation of cast iron (Han and Ko 2007: 612). A more detailed description of such a process was provided in a much later technological treatise entitled *Tiangong Kaiwu* (The Exploitation of the Works of Nature), compiled by Song Yingxing (1587-1666 AD) around the 17th century AD. In this treatise, along with text description, a diagram was also provided depicting the scene of the *chaogang* process (Figure 2.19). The process as described includes smelting/melting the cast iron, directing the liquid metal into a large rectangular pond, then stirring it with wooden rods so air will be introduced into the cast iron to facilitate the oxidisation. In addition, additives described as “*Chaonihui”* (*潮泥灰*, allegedly certain type of mud) were also used while stirring. By the end of the whole process, decarburised iron was left to solidify, then cut into pieces and ready for sale (Song 1997: 98). As described by Han and Ko (2007: 612), and subsequently repeated by many scholars, a standard *chaogang* process starts with the re-melting of cast iron lumps in an open hearth. A strong blast will be applied to create high temperature as well as an oxidising atmosphere to remove the carbon; when the cast iron starts to

melt, a stirring process will be applied to promote oxidation; at the end of the process, a red-hot iron bloom will be retrieved from the hearth and further hammered to expel the slag before shaping into final products.

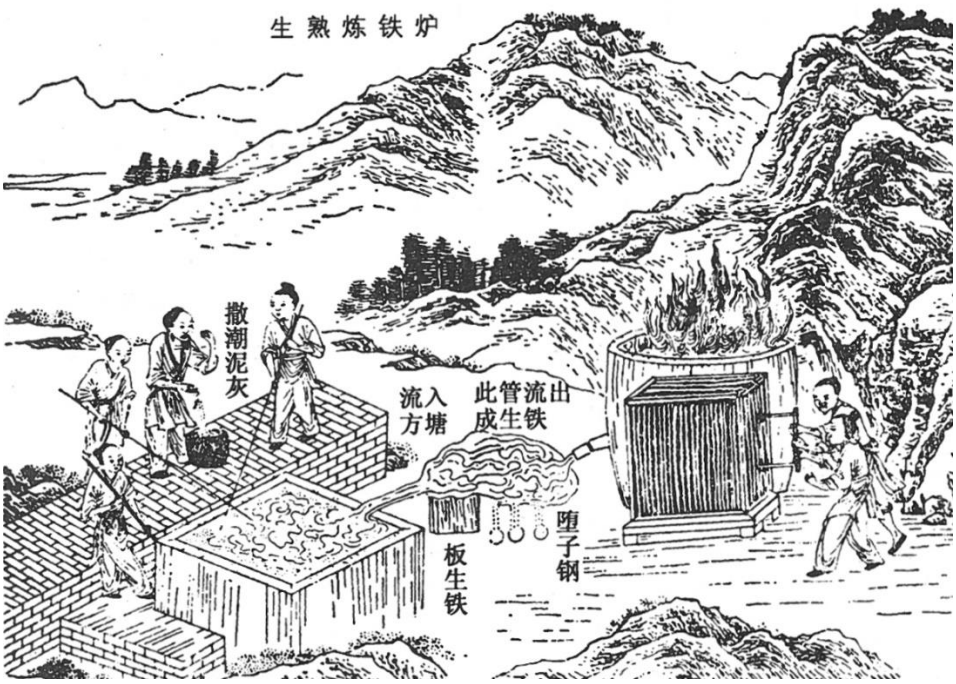

Figure 2.19 Diagram of the chaogang process in Tiangong Kaiwu, showing how melted cast iron was directed into a rectangular pond, with two craftsmen standing next to it while stirring, while another man throws additives into the pond.

Despite the uncertainties of the technical details owing to the lack of direct archaeological evidence, the main feature of the *chaogang* technique, and the fundamental difference compared to the annealing process, is that the *chaogang* decarburisation is an exothermic reaction with a liquid-gas reaction interface, while the annealing process has a solid-gas reaction interface and needs continuous heating for the reaction to go on. Depending on the amount of cast iron to be decarburised, the *chaogang* process can take from minutes to a few hours (Yang 1960; Wagner 1985: 60; 1989, 2008: 30); which is less time-consuming and theoretically saves more fuel compared to the annealing process.

The earliest archaeological evidence confirming the existence of such a technique are five iron objects unearthed from a royal Han tomb in *Shizishan*, Xuzhou, Jiangsu province, belonging to the Marquis Chu of the Han royalty, dated to the 2nd century BC. Scientific examination including metallographic study and slag inclusions analysis was carried out on 21 iron objects from this burial. Among these, five of them were interpreted as made through the *chaogang* process based on the distinctive chemical composition of the slag inclusions, such as the high CaO and P_2O_5 content and low FeO content (Chen and Han 1999), indicating such a technique was already in use during the early Han dynasty.

With cast iron smelting widely adopted, along with a series of post-smelting treatments being developed, a highly diversified iron production technological system had been fully established in central China by the end of the Warring States periods. It is against this technical background that iron production reached a substantial scale. Large industrial complexes were reportedly be found on multiple locations, where the ore was reduced to metal, and foundries where objects for daily use, craft tools and farming implement as well as weaponry were mass-produced (Hua 1983; Li 1997). Production at this scale had undoubtedly reached industrial level, requiring both highly specialised expertise and substantial investment including material supplies and labour force. Historical documents record that such smelting foundries may mobilise a labour force up to thousands of persons during Warring States period, with profits so high that the state considered them as a threat to the central government (Sima 2010: 7615-7616). In this context, the replacement of bronze with iron starts to take place in earnest, and iron gradually became an important material in many social spheres. Such technological developments would be inevitably tied to broader social developments, which will be further discussed in chapter 7. This iron production

system was later inherited and further improved in the following Han Dynasty. In the year 117 BC, the Han central government set out to monopolise the production of iron and ultimately transformed the iron industry into a state-owned business (Wagner 2001). Despite the controversy surrounding this policy, the state control of iron production continued in the following dynasties due to its great potential for the government revenue and the social economy (Larreina-Garcia et al. 2018).

2.3.2 Regional variance

While the central China, where was dominated by the vassal states of the Zhou royalty, developed the iron production system based on cast iron smelting from the beginning of the Warring States period, current research reveals interesting regional variances in terms of scale of production and technological choices. Part of this apparent variability may be the result of biased archaeological and archaeometallurgical work, while other differences could be the result of divergent regional technological trajectories as well as intentional technological choices based on contextual technical and social conditions.

To begin with, extensive archaeometallurgical research carried out in modern day Henan province has shown this area was one of the centres for cast iron production and related technological innovation during Warring States period. As a matter of fact, most of the early cast iron production sites excavated and dated to Warring States period are located in this area (Figure 2.20). Important ones include the *Cangcheng* casting site located in *Xinzheng*, Henan province, dated to late Warring States period (Liu 1962); the *Yangcheng* casting site in *Dengfeng*, dated from early Warring States period to Han dynasty (Henan Provincial Institute of Cultural Heritage and National Museum 1992:256-336); the *Jiudian* smelting site located in *Xiping*, dated to late

Warring States period (Henan Provincial Institute of Cultural Heritage and Archaeology 1998); and the *Gugongcheng* casting site located in *Huixian,* dated from middle to late Warring States period (Xinxiang Municipal Institute of Cultural Heritage 1996).

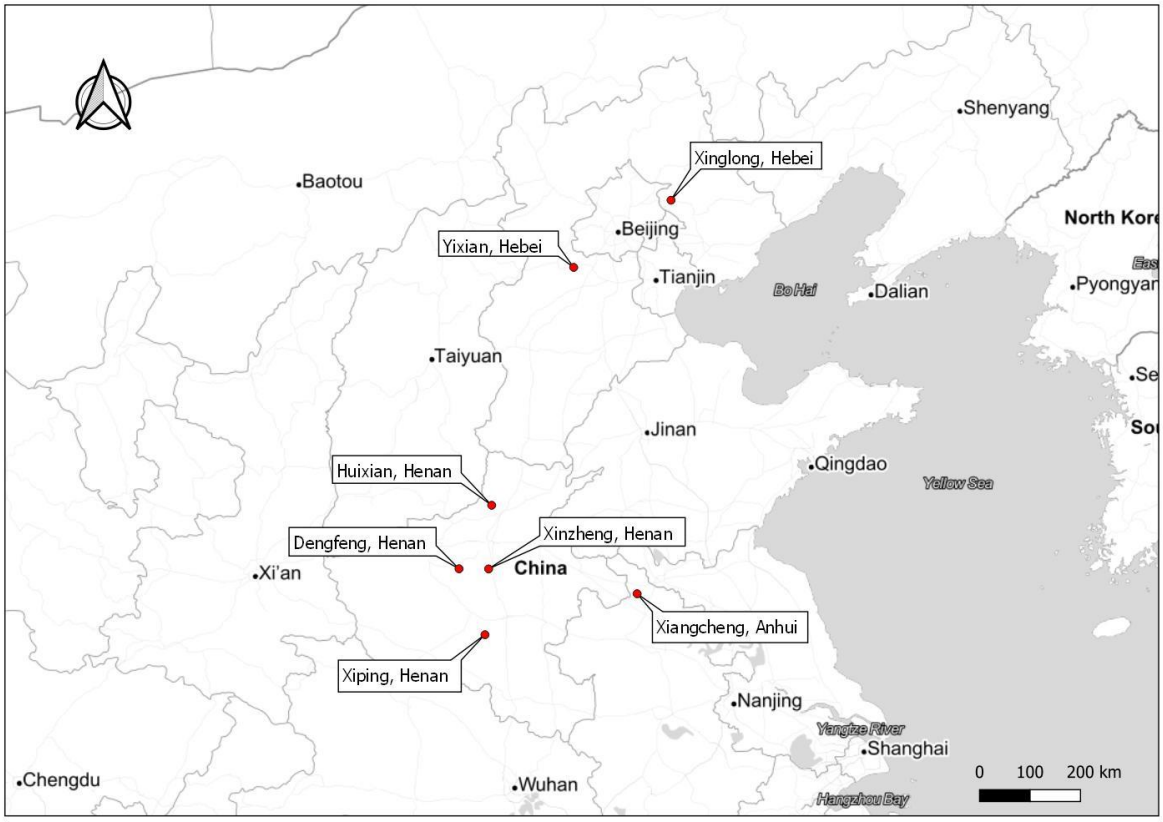

Figure 2.20 Locations of iron production sites in central China dated to Warring States period. Base map: Stamen Toner Lite/OSM (http://tile.stamen.com/toner-lite)

These sites have yielded large quantities of furnace remains, tuyeres, kilns for firing casting moulds, and fragments of casting moulds, along with various types of finished iron objects. Overall, the evidence suggests the iron production in this area was predominantly based on cast iron smelting and casting from the beginning of the Warring States period. Analytical work carried out on the finished iron products suggests the annealing technique was widely applied for decarburisation and malleablisation in the early Warring States period (Han 1998). In addition, thin cast iron sheets and bars were also found at the *Yangcheng* and *Gugongcheng* casting sites, which are believed to have been used for producing soft iron/steel through the

annealing process for further manufacture, hence suggesting that soft iron/steel production in this area was also based on cast iron decarburisation.

In comparison, archaeometallurgical study in other areas has been based on the study of burial goods and iron hoards due to the lack of findings related to production activities. Duan (2001) carried out systematic research into the iron production techniques in the *Jin* state (later divided into *Han, Zhao* and *Wei* state, see Figure 1.4) during the Warring States period, which is mostly located in the modern day Shanxi province. In this research, a total number of 130 iron objects unearthed from several burial complexes were subjected to scientific analysis. Altogether, the evidence showed that from the beginning of the Warring States period, the cast iron smelting technique was developed and adopted for iron production in this area. From middle to late Warring States period, iron production in this area was predominantly based on cast iron smelting and casting, with the annealing technique later adopted to decarburise/malleablise cast iron. In addition, four swords analysed in this research revealed a clean metal matrix with graphite residues, indicating a production process where cast iron was first decarburised into soft iron through the annealing process, then subjected to further forging process was adopted to make weapons.

Apart from Henan and Shanxi province, no systemic research has been conducted to investigate the iron production during the Warring States period covering a large area. However, isolated case studies on archaeological remains can still provide information on the general technological traits in certain areas.

The *Chu* state in the southern part of central China (modern day Hunan and Hubei province) is also believed to be a centre for iron production and technological innovation in early China. Based on the study of finished objects from the *Yangying*

site in *Laohekou* city, Hubei province, it has been demonstrated that by the end of the Spring and Autumn period, cast iron smelting and annealing had been adopted for iron production in this area (Chen 2014: 221-228). In the mining site at *Tonglüshan*, Daye city, Hubei province, iron mining tools dated to between middle to late Warring States period were also found. Analysis carried out on five of them shows both bloomery iron and cast iron were used to make such tools (Ye 1975). In addition, during the excavation of the *Chu* cemetery in Changsha, Hunan province, large quantities of iron objects dated from late Spring and Autumn period to late Warring States period were also found, yet no scientific study has been carried out. Overall, it appears that cast iron smelting was developed relatively early in the *Chu* state compared to other regions, while bloomery iron smelting was also practiced in the following Warring States period.

In the Hebei province located in the northern part of central China, two iron production sites dated to Warring States period have been excavated. In the Xinglong county, a total of 87 casting moulds made of cast iron were unearthed, along with large quantities of iron ores, charcoal and pottery fragments in the surrounding area. Researchers believe this site was used for casting during the Warring States period (Zheng 1956). In the capital city of the *Yan* state, an iron foundry site dated to middle to late Warring States period was also excavated, yielding large quantities iron lumps, slags as well as 861 finished iron objects (Hebei Provincial Institute of Cultural Heritage 1996). Scientific study carried out on some of these iron objects has shown the majority of them were made from cast iron, with the annealing technique adopted to improve mechanical properties. In addition to the foundry site, a fallen soldiers' burial (M44) dated to late Warring States period was also excavated, yielding 79 iron objects, including 51 weapons, along with coins and farming implements etc. (Liu

1975). Scientific study carried out on the weapons, including three swords, one halberd and one spear, has shown that they were made of bloomery iron, while the farming implements from the same burial were made of cast iron with annealing process applied for decarburisation (Beijing University of Iron and Steel Technology 1975). Overall, the evidence suggests in the Yan state in the northern part of central China, cast iron smelting has been adopted and well developed for iron production at least since the middle stage of the Warring States period, with the annealing technique developed at the same time for decarburisation and malleablisation. However, the weapons unearthed from the fallen soldiers' tomb suggest that despite the availability of cast iron smelting and decarburisation technique, bloomery iron was still in use for weapon production, indicating the direct and indirect smelting system could have coexisted in this area during the late Warring States period.

Overall, based on the analytical work carried out on early iron products unearthed from central China, it appears that cast iron smelting, casting and annealing techniques were subsequently adopted among the vassal states since the late Spring and Autumn period. While the majority of the iron products such as daily use artefacts and farming implements found in this area shared the same production technique, namely mould casting and annealing process, in terms of producing soft iron/steel for making tools and weapons, different areas seem to have made different technological choices. In the Henan and Shanxi province, soft iron/steel was mostly produced through decarburising cast iron sheets or rods in solid state, with no evidence of bloomery iron smelting being used. In contrast, based on the analytical work carried out on the weapons from the fallen soldiers' burial in the Yan state and the mining tools from the *Tonglüshan* mining site, bloomery iron production was still practiced in certain areas in the northern and southern part of central China.

2.4 Research Gap

Archaeometallurgical research regarding iron production technologies in early China has been going on for decades, and it has contributed greatly to an extensive understanding of the technological system employed in central China. However, due to the different research interests and the limitations of archaeological materials available for study, there are still research areas that remain unexplored, and research question that have not been answered. It is a core aim of this thesis to shed more light on our understanding of early iron production technologies in a new geographic area as well as contributing to remaining research questions and the development of research methodologies.

To begin with, previous research was mostly based on the study of archaeological materials unearthed from the Henan, Shanxi, Hebei and Hubei Province, whereas for the Guanzhong Plain, which is mostly located in the Shaanxi Province, very little is known so far about the overall iron production industry during the Warring States period. The State of Qin, located in the Guanzhong plain, is an important area which not only geographically bridges central China to the western world, but is also a cultural, political as well as technological frontier between the agricultural and nomadic civilisations. However, prior to this research, only one iron sword unearthed from the western part of the Guanzhong Plain with solid archaeological background had been subjected to scientific study, which is far from adequate. Meanwhile, in recent years, with the on-going large-scale infrastructure construction, the Shaanxi Provincial Institute of Archaeology along with other institutions has carried out a series of extensive excavations on multiple sites across the Guanzhong Plain. These sites, mostly civilian cemeteries belonging to the State of Qin during the Warring States period, have yielded substantial numbers of early iron products designed for all kinds

of social activities, which offered an excellent opportunity to systematically study the iron production industry in the Qin state (Shaanxi Provincial Institute of Archaeology 2018b).

In addition, the archaeometallurgical research in China, which systematically begun during the 1970s when the editorial team for “History of Ancient Chinese Metallurgy” was first organised, was rather narrowly focused on the revealing of the technological parameters, rather than studying metal production from an archaeological approach. In is not until the 21st century that archaeologists and archaeometallurgists started to work together closely to systematically study early metal production as an inherent part of the early society, which can be of great significance to understand the development of human civilisation. Having said that, due to the enormous amount of early archaeological findings awaiting and limited trained personnel to carry out such work, archaeometallurgical research in China is still largely focusing on sample analysis and material characterisation, while the research methodology to study the of technology within social construction remains underdeveloped (Mei et al. 2015). Against this background, this research sets out to focus on the Qin state during the Warring States period as a political entity, to systematically investigate the iron production industry through scientific study of archaeological materials, as well as contextualising this trajectory of technological development within a wider socio-economic and political framework.

While it has been raised by many scholars that the study of finished objects unearthed from archaeological sites is not enough for revealing the whole production *chaîne opératoire*, early iron production sites are not always available for study, either due to their limited numbers, or remote locations where archaeological investigation has not reached. Conversely, large quantities of finished objects excavated from burials or

deposits, when properly studied, can provide solid evidence which can be further used to model the general technological system. In this sense, developing an analytical methodology that can extract information not only regarding the material and production technology, but also can reveal particulars of the engineering parameters, will be essential. Despite many years of ongoing research, the methodology developed to analyse archaeological iron remains vague and largely depends on personal experience. Some key methods such as differentiating soft iron products from direct and indirect process, or criteria for inferring the engineering parameters of the annealed cast iron products, remain deficient. It is in this sense, this thesis intends to further develop the analytical methodology, to provide a more reliable, repeatable analytical protocol for the future study of early iron production techniques.

3. Methods and Materials

This chapter aims to provide an overview of the methods and materials employed in this research. The first section introduces the broader workflow of this research and theoretical concepts and frameworks that were found useful to both inspire and investigate the research questions. The second section provides a detailed introduction to the archaeological sites, including their location, dating, cultural background and additional information, along with the sampling strategy as well as discussion of the representativeness of the final sample collection. The last section introduces the analytical methods and protocols used in this thesis for material characterisation and technological reconstruction.

3.1 Research framework

3.1.1 Revealing the materials and production technologies

The basic foundation of this thesis is the characterisation of the material constituents of the analysed samples, as a starting point to further investigate the production techniques involved in the making of the object, including the smelting of the iron, the shaping, and possible heat-treatment techniques. In the meantime, the engineering parameters, which refers to the operational settings of the technical process, such as temperature, redox condition and duration will also be evaluated based on such information. In order to do so, scientific analysis will be applied to extract technical information from the samples.

Since metallic materials, including iron and its alloys, are primarily composed of numerous crystals, the microstructure of such crystals conveys key information including the alloying elements, solidification condition, and fabrication methods. To

obtain such technical information, the most common method is metallographic study (Han et al. 2015).

Metallography is the study of microstructures of metal materials. When a metal solidifies, its crystal structure largely depends on two main factors: the chemical components (alloying elements) and the cooling rate. After solidification, any further work undertaken, such as deformation or heat treatments, will also affect the microstructure, leaving recognisable traces that can be identified under the microscope. By examining and interpreting the microstructure, it will be possible to retrieve the aforementioned parameters and further recognise the technical processes applied during the making of a metal product (Scott 1992: 5-10).

For iron and iron-carbon alloys, metallographic study is particularly straightforward and useful. As summarised in the phase diagram, iron-carbon alloys at room temperature are composed of several types of microstructures or phases such as ferrite, cementite, pearlite, ledeburite or a mixture of them (Figure 3.1). Each type of microstructure corresponds to a relatively fixed amount of carbon content, hence by examining the type and proportion of these phases, the original carbon content can be deduced. When the solidifying condition has been altered, specific microstructures will also form. For instance, when the solidification of liquid cast iron has been slowed down, crystalline carbon, also known as graphite, will form; if iron/steel was quenched, martensite or bainite will occur (Han 1998). Through the study of such phases or microstructures, most of the engineering parameters applied in the production process can be retrieved, hence the metallographic study is usually the first step to initiate a scientific study of iron samples.

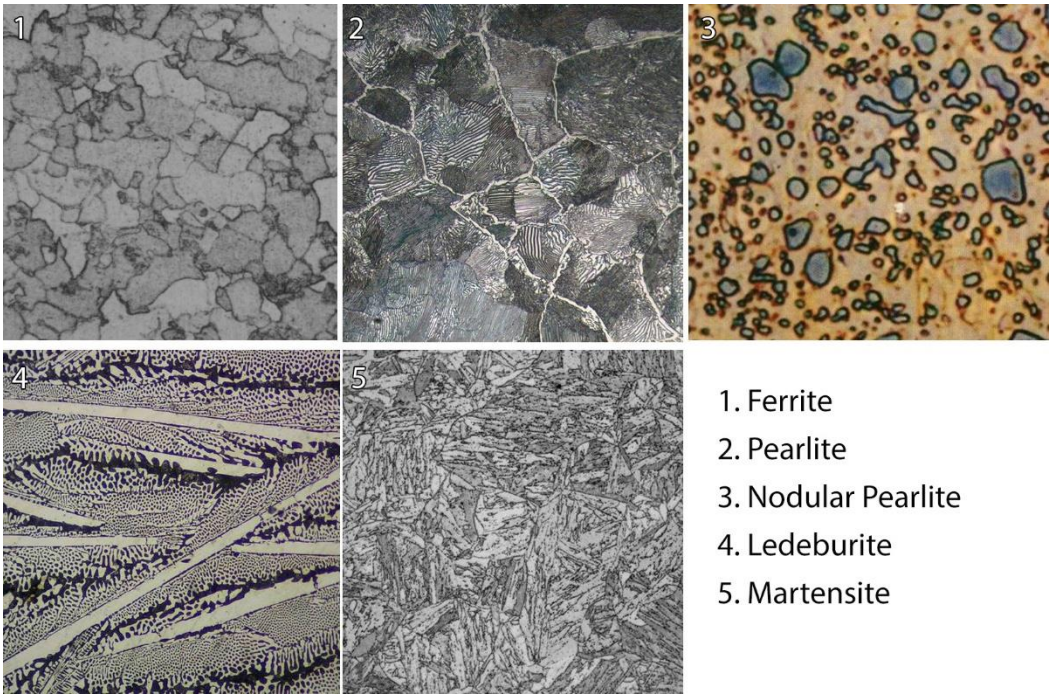

Figure 3.1 Typical microstructures in iron-carbon alloys. Source: baike.baidu.com

While metallographic study is useful for differentiating certain types of iron materials, the production technique, and specifically the smelting technique, is not always directly related and recognisable, as the same type of material can be produced through different technological pathways. For instance, both the direct and indirect process can create soft iron or steel products with similar microstructures. Metallographic examination alone will be insufficient to tell them apart. In this sense, more technical information which can indicate the manufacturing processes needs to be extracted from the sample. For early iron products, the most common approach is the study of slag inclusions.

Slag inclusions are combinations of non-metallic compounds entrapped in the metal matrix. During early iron smelting and refining practices, the separation of metal and slag was never perfect, hence certain amount of the smelting slag may remain entrapped in the metal. Such slag is essentially a mixture of the materials involved in the iron making process, including the impurities from the ore (gangue), the melted

furnace linings, the fuel ash and the possible fluxing agents. In this sense, the slag inclusions in the metal matrix retain a material signature from the original smelting system. In the following stages of the manufacturing process, such as smithing, fining, welding, new slag inclusions may also be generated or introduced, while the original ones could also be chemically altered. The slag inclusions generated in different stages usually have different materials sources, hence may have characteristic chemical components, which can be recognised through compositional analysis. By interpreting the results with reference to our understanding of the technical processes, the analysis of slag inclusions can reveal further key information regarding the material source as well as the techniques involved in the smelting and manufacturing process (Piaskowski 1976, 1992; Gordon 1997; Starley 1999; Dillmann and L'Héritier 2007; Blakelock et al. 2009; Charlton et al. 2012; Disser et al. 2014; Dillmann et al. 2017). In the meantime, it has to be acknowledged that such a method is still under development, slag inclusions have a lot of mixed signatures and separating them are not always straightforward. Some key questions, such as the formation mechanism of the inclusions, their materials source is still poorly understood, therefore extra attention needs to be paid while applying such a method.

3.1.2 Modelling the technological system

After obtaining the information regarding the materials and production techniques for each sample, the next step will be the modelling of the technological system based on such information and associated contextual data.

Before the inception and adoption of cast iron smelting, the production of iron objects followed a single technological pathway, namely bloomery smelting, followed by smithing and forging into the final product. Of course, there are multiple variants within

this overall pathway, but the core elements remain the same. However, under the cast iron smelting technological system, the same type of iron product can be produced through multiple technical pathways as different technological choices become available at different stages. For raw material smelting, both bloomery and cast iron smelting can be used to extract metallic iron from the ore. Following the cast iron smelting technological trajectory, more technological choices will need to be made at each production stage, including casting vs forging, fast cooling vs slow cooling, decarburisation vs malleablisation, and many other post-smelting techniques. At the same time, with a complicated technological system, a more diversified product category will also become available, where products that were not possible to be made become attainable with new technical solutions.

In this sense, the study of iron production based on cast iron smelting should not only be focusing on the production technique of the individual artefact, but also aim more broadly to understand the overall *technological system*, which is a combination of series of technological pathways that are consciously established and repeated.

To model the technological system, this research will begin with investigating the individual production technique of each sample through scientific analysis, to gather the necessary technical information from the raw material smelting to the manufacturing of the final product. After this, samples sharing the same typology and function, and materials produced from the same technical pathway will be grouped and analysed to reveal the patterns of repeated technological choices and hence further link materials, production techniques and final products.

In this thesis, the collected samples were divided typologically into four general categories. These include objects for daily use, farming implements, craft tools, and

weapons (Table 3.1). Each category has a specific functional purpose, usage environment and user expectation, which will lead to specific requirements in terms of material properties and performance characteristics. For instance, artefacts for daily use include iron objects used in household activities rather than productive, economic activities, which means the material properties of such artefacts will be rarely tested other than some extreme conditions such as collision and fall, therefore it can be assumed that a lower production cost would be prioritised even if this meant compromises in material properties. The farming implements were products especially designed to work against soil in farming activities, which arguably could also be used in construction activities. In this sense, the hardness, toughness and abrasive resistance of such objects will be constantly tested, hence will require a better mechanical strength comparing to those daily use artefacts. Craft tools, on the other hand, are mostly designed to work on materials with harder surfaces, such as wood, bones and metals, therefore will need a better toughness than farming implements. Both the farming implements and craft tools are designed to supply the peasants and craftspeople, while the scale of demand will also be quite substantial, therefore an affordable price and the option to be mass produced will also become key factors when selecting the corresponding production technologies. In contrast, weapons, especially swords and spears etc., are mostly designed for war activities, their quality, including sharpness, hardness as well as toughness will be most important, whereas the price will be less relevant. Comparatively, arrowheads, which are considered as consumable and often produced in large scale, will be less cost sensitive. Overall, the required mechanical strength rises from daily use artefacts to weapons, while the production cost become lesser important. Through a relatively large sample collection covering all types of iron products, patterns of preferred materials and production

techniques for each category can be observed. By linking the raw material production to the end product through different technological pathways, the general technological system can be modelled.

Table 3.1 Sample categories classified in this thesis

	Examples	Usage environment
Artefacts for daily use	Pot, tripod, lamp, belt-hook, etc.	Household activities
Farming implements	Shovel, adze, ploughshare, etc.	Farming, construction activities
Craft tools	Knife, chisel,	Craft production activities
Weapons	Sword, spear, arrowhead	War activities

3.1.3 Understanding technological choices

Technological choices, which is the selection of a specific technological solution among the many available alternatives (Lemonnier 1993: 3; Sillar and Tite 2000), are essentially the fundamental cause and impetus of the establishment of the technological system, and key to understand the long-term technological changes. Specific technological choices, whether individual or collective, conscious or unconscious, utilitarian or symbolic, are typically affected by a series of factors, including technical ones such as cost-benefit assessments or the limitations in natural resources, as well as broader social factors such as the market size and demand, the technological tradition, cultural and ideological preferences or political interventions that may also affect final decisions. It is difficult to determine which of these factors played a key role in the process of decision making, but it is possible all of them were involved in the shaping of the final technological system (Tylecote 1981; Hua 1983; Wagner 1996; Schiffer 2004).

To study technological choices, first we need to understand what technical solutions were available to choose, the performance characteristics among the various

alternatives, and the constraints that may have affected the final decision-making process. In this thesis, after revealing all possible technical pathways which can achieve the same objective, the cost-benefit analysis between different techniques, which is one of the fundamental elements that affects the decision-making process, will be qualitatively evaluated and compared to understand the technological choices in a technical perspective. In addition, other social factors mentioned above which might have contributed to the decision-making process or affect the long-term technological trajectory will also be taken into account in the discussion in order to get a holistic perspective. Following the discussion, these factors will be further integrated into a performance matrix following Schiffer (2004), which visualises the technical, social and economic performance characteristics may have affected the decision-making process .

Meanwhile, it needs to be mentioned that most of these factors that affect the technological choices will be subjected to changes throughout history, with technological transmission, social-economy development, political change, population growth or decline as well as the depletion of natural resources. In this sense, the long-term technological change will be the result of the dynamic interaction between the technology and the ever-changing social context. Such changes are most likely to be gradual rather than sudden and drastic, therefore they need to be reviewed along with long-term social developments.

3.1.4 Exploring of the social impact of the iron industry

This thesis is based on the premise that iron production was an important social activity with the potential to transform society at a fundamental level and promote social developments that would otherwise be unattainable. With the cast iron smelting and

associated post-smelting treatments being widely applied for iron production, iron products with various functional purposes could be mass-produced at reasonable cost, which would undoubtedly affect many social spheres in direct and indirect ways.

For instance, among the early cast iron production sites as well as burials dating to the Warring States period, farming implements are always the main types of iron objects, indicating the earliest large-scale use of iron was in agricultural production. The use of iron farming tools, in comparison to the earlier stone and wood one, can greatly improve the productivity of peasants and boost agricultural production by expanding the cultivated area, and increasing the yield per unit area by renovating traditional farming techniques with the use of iron implements for deep ploughing and the building of irrigation system. The expansion of the agricultural economy will further provide the necessary food surplus for a larger population, which can increase the labour pool to be engaged in farming as well as other professions such as infrastructure construction and military.

In the meantime, constant wars between vassal states would be fought with iron weapons. With the availability of new iron production technologies, iron gradually replaced bronze as the main material for weapon production. While the old types of bronze weapons started to be replaced by the iron ones, newly designed weapons that could fully utilise the mechanical properties of iron, such as the long handle iron sword, iron rods as well as several types of armours were also developed and equipped, which might change the way wars were fight during the Warring States period. In the past research, the use of iron weapons in the Qin army has been discussed, with conflicting point of views on whether iron weapons were used in the Qin army, yet without any solid conclusion (Keightley 1976; Trousdale 1977; Yu and Qian 2010; Han and Chen 2013). In this thesis, in the light of new archaeological

evidence and archaeometallurgical study, renewed discussion on the iron weapon usage in the Qin army during the Warring States period will be presented.

A useful approach to study the social impact of the iron industry is to find proxies for certain social spheres, such as food production, population and military power, whose development can be quantified through comparative study. However, due to the lack of reliable and fine-grained archaeological and historical data, the study of such social changes will largely remain qualitative and theoretical for the time being. This thesis will be focusing on two main areas which have the most abundant archaeological and historical data to explore, including agricultural production along with associated developments, and the use of iron weapons in the Qin military during the Warring States period.

3.2 Materials

In order to obtain a representative dataset to study the iron production in the state of Qin during the Warring States period, iron objects unearthed from the Qin people's burials as well as other sites in the Qin state dated to the period concerned were selected for analysis. With the permission and assistance from the Shaanxi Provincial Institute of Archaeology, two fieldwork seasons was carried out in 2017 and 2018 to obtain samples for analysis as well as the archaeological context information. The first trip was focused on archaeological sites located around Xi'an city, including the Xinfeng and Xiekou cemeteries, both dated to late Warring States period. The second trip placed more focus on the archaeological sites around the Xianyang city and Baoji city towards the west and revisited those sites in Xi'an. Overall, the archaeological sites included in this thesis were distributed across the Guanzhong Plain, mostly around the early Qin capitals cities including Xianyang (Qin capital city from 350 BC

to 205 BC, in modern day Xianyang city), Yueyang (Qin capital city from 383 BC to 350 BC, in modern day north-eastern Xi'an city) and Yong (Qin capital city from 667 BC- 383 BC, near modern day Baoji city), where were the mostly populated area. The general location of these sites were given in Figure 3.2.

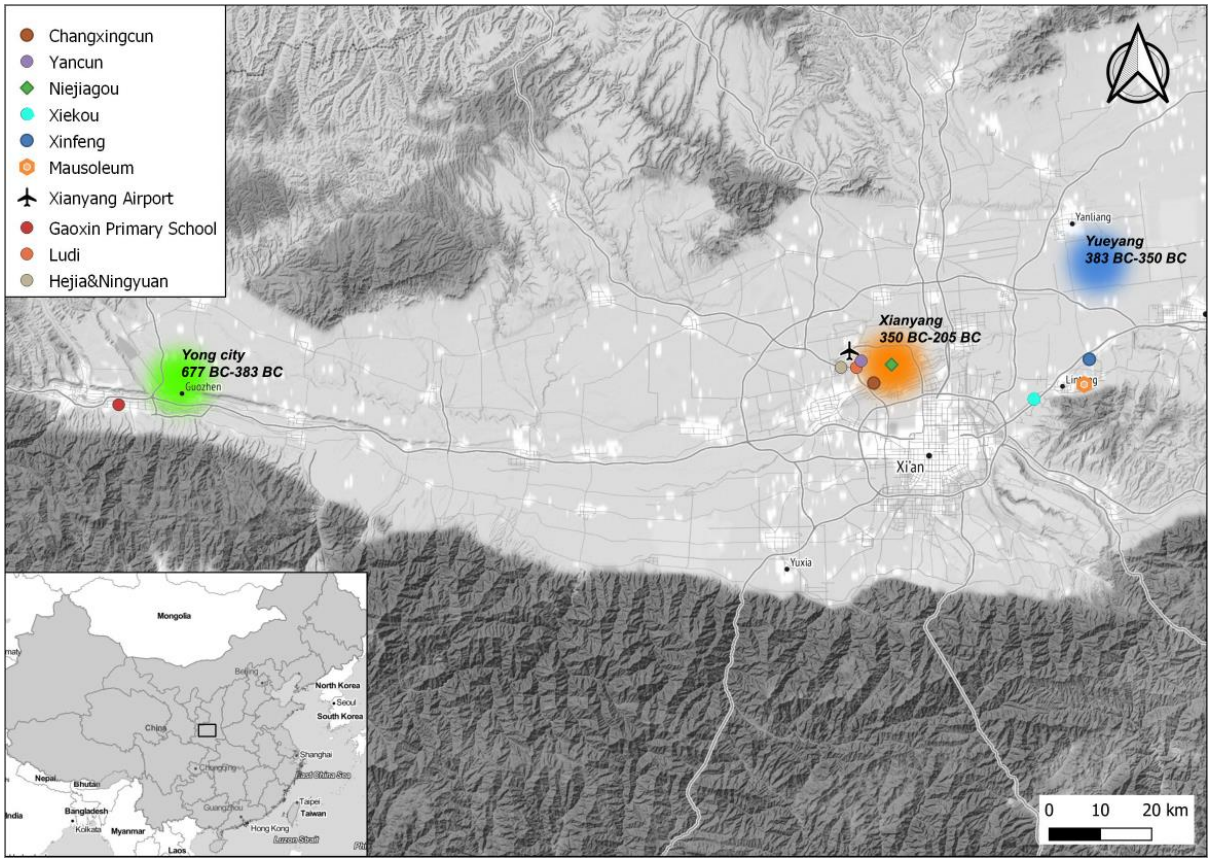

Figure 3.2 Map showing the location of the selected archaeological sites from this research, with the three Qin capital cities Yong city (green), Xianyang (orange), Yueyang (blue) and the Mausoleum of Qinshihuang labelled

3.2.1 Site introduction

The archaeological sites included in this research are mostly cemeteries and small scattered burials, with the exception of the Niejiagou site, which is a workshop for making bone products and were believed to be attached to the Qin palace in Xianyang city. A detailed introduction including their location, dating as well as relevant contextual information are given below.

Xinfeng (XF) Cemetery 新丰

The Xinfeng cemetery is located in the north-eastern part of the Xi'an City, Shaanxi Province, around 6 km to the north of the Mausoleum of the First Qin Emperor. The excavation was carried out by the Shaanxi Provincial Institute of Archaeology during 2007-2009. During the excavation, 729 tombs in total were excavated, 596 of which were dated to late Warring States period and Qin dynasty. The Xinfeng cemetery is the first finding of large-scale Qin cemetery in the eastern part of Guanzhong Plain.

The whole cemetery was highly organised, and intrusion between individual tombs are rare, indicating that this was the local civilian cemetery for a long period. Based on the pottery typology, burial style and inscriptions on pottery, referencing with other similar Qin cemeteries, these Qin tombs were divided into four consecutive stages, namely stage one: later stage of middle Warring States period; stage two: late Warring States period; stage three: between the end of the late Warring State period and the Qin dynasty; stage four: between the end of Qin and beginning of Han dynasty (221 BC-202 BC). The burials of the first two stages show a dominance of Qin material culture, while new cultural elements including *Rong* culture from the north and Jin culture from the west can be observed in the burials dated to latter two stages.

Due to the special location of this cemetery, the excavator believes this cemetery belong to the civilians living in the "*Xi* (戏)" county, who may have been workers in the construction of the Mausoleum of the first Qin emperor (Shaanxi Provincial Institute of Archaeology 2017: 1479).

For the Xinfeng cemetery, a total number of 95 iron objects (including unrecognisable fragments) were unearthed, 52 of which were sampled for analysis. For some types of objects, including tripods (ding vessel), cooking pots and *Mou* (a specific Qin type

cooking vessel), multiple samples were taken from different parts. After preliminary analysis, 50 samples from 36 iron objects were deemed to contain technical information and were retained for analysis.

Xiekou (XK) Cemetery 斜口

The Xiekou cemetery is located in the *Lintong* district, Xi'an city, Shaanxi province, adjacent to the Xinfeng cemetery mentioned above. The excavation was carried out during April to July 2014 by the Shaanxi Provincial Institute of Archaeology and the local cultural heritage committee. A total number of 67 tombs were excavated, 16 of which were categorised as Qin style burials and dated to late Warring States period. Based on the inscriptions on the pottery, the excavators believe this cemetery belong to the citizens of the *Zhiyang* (芷阳) City of the Qin state.

Currently there is no published material regarding this cemetery, and all information was provided by Shaanxi Provincial Institute of Archaeology. A total of 24 objects were sampled from this site, 14 of them containing technical information that could be retained.

Niejiagou (NJG) workshop 聂家沟

The Niejiagou site is located in *Yaodian* (窑店) County, Xianyang city, Shaanxi province, 582 meters to the east of the first, second and third Palace building of the Qin Xianyang city. The site is a deposit pit mainly for bone remains. It was first found during a field survey in November 2014, followed by an excavation by Shaanxi Provincial Institute of Archaeology. In the deposit pit K1, 52 iron objects along with other remains were found. Based on stratigraphy, typology of potteries and bronze coins, the K1 pit was dated to the end of the Qin dynasty (221 BC - 206 BC). In

reference to the surrounding environment, the excavator believes this site is the secondary deposit area of the bone artefact manufacturing workshop serving the Qin palace in Xianyang city (Shaanxi Provincial Institute of Archaeology 2019). According to the published report, 52 iron objects were unearthed from the site. For this thesis, 37 of them were sampled for analysis, 27 of which were sufficiently preserved.

Yancun (YC) cemetery 岩村

The Yancun site is a Qin people's public cemetery located in the southern part of the Yan Village, Dizhang County, Xianyang City, Shaanxi Province, excavated by Shaanxi Provincial Institute of Archaeology during June to December 2017. A total number of 48 tombs dated between late Warring States period and Qin dynasty were excavated. Currently there are no published materials regarding this cemetery available, hence all information was provided by Shaanxi Provincial Institute of Archaeology. Seven iron objects unearthed from this site were sampled for analysis, five of which were retained.

Changxingcun (CXC) 长兴村

The Changxingcun site locates in the northern part of the *Yaodian* County, Xianyang city, Shaanxi province. This site was believed to be part of the state owned workshops inside the Qin capital city-Xianyang city. Excavation was carried out between March to September 2017 by the Shaanxi Provincial Institute of Archaeology. A total surface area of 2900 square meters were excavated, and different types of remains including wells, firepit, houses and tombs etc. were found, mostly dated between late Warring States period to the Qin dynasty. Currently there is no published excavation reports regarding this cemetery, and all information was provided by Shaanxi Provincial Institute of Archaeology. Four iron objects unearthed from the burials in this site were sampled for analysis, but only one of them contains information that can be retrieved.

Xianyang Airport (JC) 咸阳机场

During the construction of the Xianyang Airport, occasional excavation of tombs found inside the construction site were carried out, and some of these tombs were dated to the late Warring States period. There are no published excavation reports, but relevant information was provided by Shaanxi Provincial Institute of Archaeology. Six iron objects unearthed from this site were sampled for analysis, five of them containing technical information.

Lüdi (LD) 绿地

The Lüdi site is located in the southwest part of the *Yanjiazhai* Village, Dizhang County, Xianyang city, Shaanxi Province. The site was excavated between January-July 2014 by the Shaanxi Provincial Institute of Archaeology. In this site, sacrificial pit, tombs, houses and other structures were found. Based on the typology of pottery vessels and inscriptions as well as other information, the site was dated to later stage of the middle Warring States period (Shaanxi Provincial Institute of Archaeology 2018a). The tombs found in this site shows relatively higher social status comparing to other civilian cemeteries mentioned above. Four iron objects unearthed from the tomb M8 and M48 at this site were sampled for analysis, all containing relevant information.

Hejia (HJ) & *Ningyuan*(NY) 贺家&凝远

Both the Hejia and Ningyuan sites are believed to be Qin peoples' public cemeteries; they are located in the northern part of the Hejia Village, Weicheng district, Xianyang city. These two sites were only around 500 m away from each other and share common features in terms of their burial style and associated material culture, hence they are believed to be the same cemetery. A total number of 153 Qin tombs were

excavated between September 2012 and February 2013. The excavation was carried out by the Shaanxi Provincial Institute of Archaeology. Based on the burial style, typology of the pottery and other evidence, this cemetery was dated to late Warring States period. Currently there is no publication regarding the excavation, all information was provided by the Shaanxi Provincial Institute of Archaeology. 12 iron objects unearthed from the Hejia site were sampled for analysis, 10 of them contains technical information. A further nine iron objects unearthed from the Ningyuan site were sampled for analysis, 7 of them were sufficiently preserved.

Gaoxin Primary School (GX) 高新小学

The Gaoxin primary school is located in the South Gaoxin avenue, *Weibin* district, Baoji city, Shaanxi province. Before the construction of this school, a survey and excavation were carried out by the Shaanxi Provincial Institute of Archaeology, yielding 41 tombs, 37 of which were dated to late Warring States period. In the absence of published reports, all information was provided by Shaanxi Provincial Institute of Archaeology. Four iron objects unearthed from this site were sampled for analysis, two of them containing information that could be retrieved.

A list of these sites is given in Table 3.2. In total, the sample collection of this thesis includes 125 samples from 114 individual objects, including all types of iron products such as cooking vessels, craft tools, farming implements, weapons and several other types of artefacts designed for daily use. The earliest dated samples were from Lüdi site, which is dated to later stage of the middle Warring States period, the rest of the samples were generally dated from late Warring States period to the Qin dynasty. Overall, this sample collection covers roughly from 300 BC to 205 BC. Detailed information of these samples is given in the appendix-2.

Table 3.2 List archaeological sites and sample quantities in this research

Site	Location	Dating	Number of samples
Xinfeng cemetery	Xi'an city	Later stage of middle Warring States period to the beginning of Han dynasty	50
Xiekou cemetery	Xi'an city	Late Warring States period	14
Niejiagou workshop	Xianyang city	Late Qin dynasty	27
Yancun cemetery	Xianyang city	From late Warring States period to Qin dynasty	5
Changxingcun site	Xianyang city	Late Warring States period to Qin dynasty	1
Xianyang airport	Xianyang city	Late Warring States period	5
Lüdi site	Xianyang city	Later stage of the middle Warring States period	4
Hejia & Ningyuan cemetery	Xianyang city	Late Warring States period	17
Gaoxin Primary School	Baoji city	Late Warring States period	2

3.2.2 Sampling strategy

Owing to the high chemical activity of iron, most of the archaeological iron artefacts appear heavily corroded on the surface, and it is hard to tell if there is still metallic iron left based on appearance only. Meanwhile, some of the corroded iron may contain ghost microstructure or uncorroded slag inclusions, from which the technical information could still be extracted. Based on these considerations, this research has adopted a unique sampling strategy: To begin with, an initial selection process was carried out by attaching a small magnet to the object to test its magnetism. If the object is magnetic, this could possibly because there is still metallic iron left in the object. Another possibility is the corrosion products contains a large amount of Fe_3O_4, which is also magnetic. In either case, a sample will be taken for further analysis. However,

if the object is no longer magnetic, this means the corrosion has gone thorough where most of iron has been oxidised into F_2O_3 or other mineral compounds, which means no information can be extracted under this condition, hence sampling on such objects will not be carried out. Photos of some of the selected samples is given in Figure 3.3.

Figure 3.3 Photograph of selected iron objects analysed in this research

Due to the possibility of heterogeneous microstructure in different locations of an individual object, for bladed tools or weapons, the sampling position was consistently at the edge unless otherwise indicated. For other types of daily use objects, as past experience suggests they tend to be more homogeneous as most of them were

directly cast without further treatment, hence the sampling position was chosen at the most convenient cutting point. For large vessels such as tripods and cooking pots, the solidification rate could be more variable in different positions; hence, in order to evaluate the homogeneity of such types of objects, multiple samples from different positions were taken where possible (Figure 3.4).

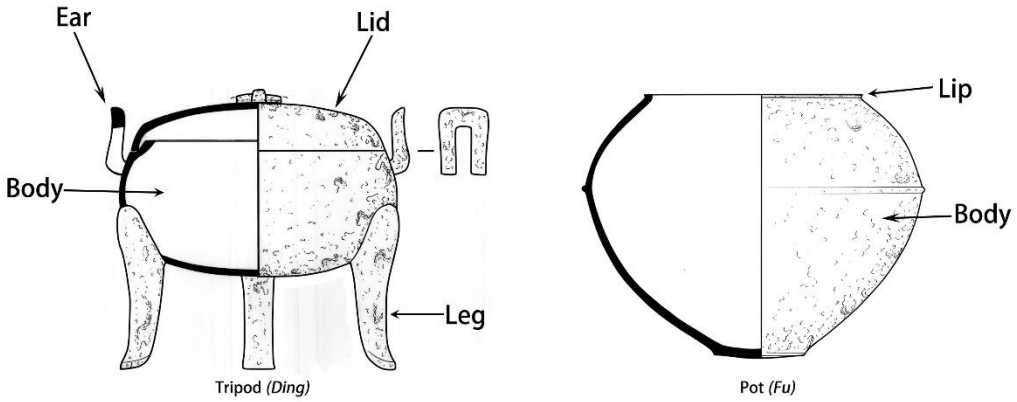

Figure 3.4 Sampling position of tripods and cooking pots indicated

After cutting, the samples were taken to the lab for preparation. In this step, all corroded samples were mounted and examined using optical microscope and scanning electron microscope to look for possible traces of ghost microstructure or slag inclusions. Samples that failed to show any of those were then excluded from the final sample collection.

3.2.3 Sample collection and its representativeness

Acquiring a representative sample collection for scientific study is a major challenge for archaeometallurgical study. Potentially, this is especially challenging when studying finished artefacts recovered from burial contexts, as these might have been specifically selected or even manufactured to be buried with the deceased following particular cultural norms, and hence not be representative of the typical metallurgy of

the period. In this thesis, apart from the samples from the Niejiagou site, which were recovered in a secondary deposit pit, the rest of the samples were all unearthed from Qin tombs, therefore whether these artefacts represent the production technologies in real life or not needs to be validated. Additionally, due to unforeseeable corrosion status of the iron objects, the final sample collection for scientific study is also highly selective, which might also lead to a biased result, hence the representativeness of the final sample collection also needs to be discussed.

It is believed that, during the Warring States period, “funerary wares” (*Ming Qi, 明器*) were used in burial practices. These were certain types of objects that are specifically designed to be buried with the deceased. The main purpose of using such products was to avoid using real artefacts which were considerably more expensive, while still conducting the funeral in conformity with the traditions. Zhang (2002) has summarised the main characteristics of funerary wares during the Warring States period, including to-scale miniaturised, non-functional and/or poorly made artefacts. In this sense, such objects should be easily recognisable based on their appearance and texture. As for metal products, it has been pointed out that bronze products with an unpolished rough surface, or remains of airholes left from the casting process, strongly indicate such objects were not made for practical use (Gao 2010; Yue et al. 2017). While currently there is no discussion regarding the production of “funerary wares” using iron during the Warring States period, but the same principle can also be applied for recognising potential iron objects specifically designed for a burial purpose. It may be assumed that iron funerary wares would not be likely to be subjected to post-production treatments such as annealing, decarburising/carburising, which were mainly aimed to improve mechanical properties rather than appearance, hence evidence of such treatments can serve as the indicator that the object were designed for actual use. The

challenging part for iron objects is that most of them were severely corroded on the surface when unearthed, hence whether the object has been polished or has any signs of usage cannot be told by judging its surface. In this sense, the size, shape and microstructure should be main characteristics for distinguishing functional from purely ritual artefacts.

During sampling, it was observed that most of the iron objects from the selected sites are consistent in terms of their size and shape. For instance, the farming implements including shovels, adzes and spades showed a high degree of standardisation across the Guanzhong Plain (Figure 3.5). While the large cooking vessels were mostly broken, based on the fragments and the restoration, it appears they were originally designed with practical purposes with uniform shape and size. As for other products such as craft tools or weaponries, the analytical results have also shown that these products were properly made through technical processes which were aimed to improve their mechanical properties, which are unlikely to be applied on funerary wares. In this sense, it is safe to assume that the iron objects sampled for analysis in this thesis should be considered as functioning products designed for daily use and represent the real technologies for iron production in this area.

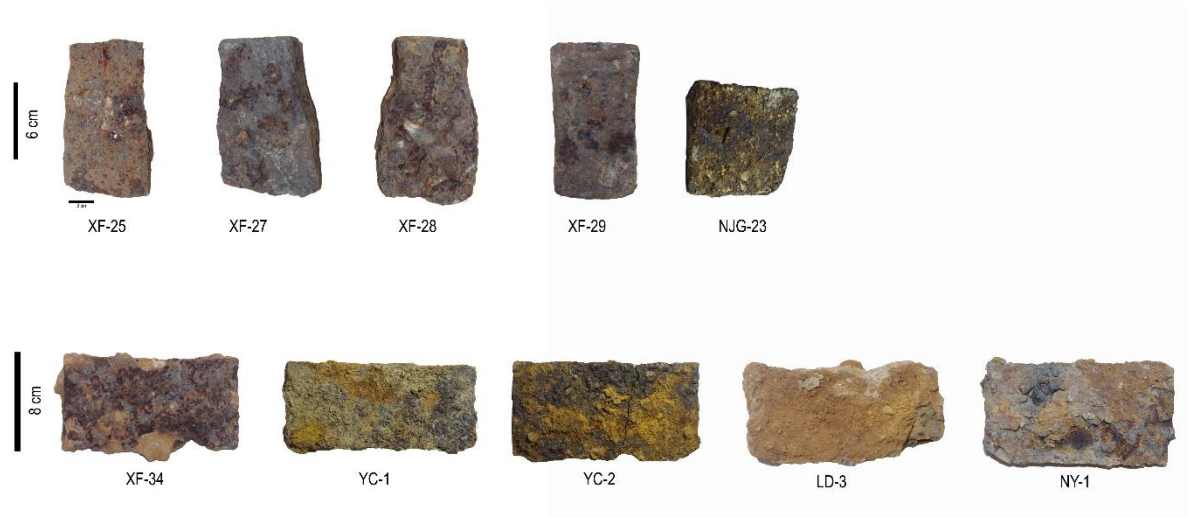

Figure 3.5 Photos of selected iron farming implements in this research

3.3 Analytical method and protocol

Invasive sampling of the artefacts selected for analysis was carried out in the storage room of the archaeological assemblages using a small abrasive saw. A small section was taken from the object while trying to preserve the overall shape. After this procedure, samples were taken back to the lab for mounting and preparation. In this research, all samples were mounted in epoxy resin with a 4:1 mixing ratio between epoxy resin and resin hardener. Such resin blocks were first ground with abrasive paper from coarse (P320) to fine (P4000), then polished with diamond paste of 3 μm and 1 μm grades, to expose a polished cross-section of the metal. After polishing, metallographic study was first carried out. The samples were first etched with 2 wt.% nital to reveal its microstructure. Metallography pictures were taken in the optical microscope lab, using a Leica DM 4500 P LED microscope equipped with a Leica DFC 290 HD camera, and the results along with a brief description of the microstructure is provided in appendix-3.

After the metallographic study, all samples were polished again to remove the etched layer, then carbon coated for further microstructural and compositional analysis using scanning electron microscope (SEM) equipped with energy-dispersive spectroscopy (EDS). This part of analysis was carried out in two separate stages in Wolfson Archaeological Science Lab. In the first stage, samples taken from the first field campaign (including XF-F17, XF-F19, XF-F29, XK-Sw14, XK-Kn10 and XK-Sp1) were analysed using a Philips XL30 ESEM with an Oxford Instruments EDS detector equipped with INCA software. The accelerating voltage was set at 20kV with a working distance of 10 mm. A live time of 100 seconds and 35-40% of deadtime was applied with cobalt calibration every 1 hour.

During this process, the lab went through an upgrade process, and a new SEM-EDS instrument was installed, hence samples taken from the second field season were analysed using the new Carl-Zeiss EVO scanning electron microscope equipped with an Oxford X-Man 80 EDS detector. The accelerating voltage remained at 20kV while working distance was changed to 8.5 mm, following manufacturer's recommendations. The EDS signal collection process was no longer time based; instead, a signal count of 750,000 for each analysis was applied. To ensure the compositional data from these two instruments was comparable as well as to monitor the precision and accuracy of the compositional data, certified reference materials (CRM) similar to the composition of slag inclusions were repeatedly analysed while using both instruments, and the results were subsequently compared (see appendix-4). For all the compositional analyses, the results were presented in stoichiometric oxides and normalised to 100%. Detailed analytical results are included in appendix-5, and only brief summaries are provided in the text.

During the analysis, as many slag inclusions as possible from each sample were analysed to obtain a statistically meaningful dataset. To avoid localised concentration effects, only those inclusions larger than 10 μm in diameter were chosen (Dillmann and L'Héritier 2007). The INCA software attached to the Philips SEM-EDS offers an auto-selection tool to choose the analysis area, which is based on the colour difference between slag inclusion and the metal matrix, hence for the glassy silicate inclusions with only one phase, such a method was employed. For slag inclusions with more than one phase, analysis was carried out by manually drawing a polygon covering most parts of the inclusion. The Aztec software from the Oxford SEM-EDS does not include the auto-selection tool, therefore all analysis area was manually selected.

4. Analytical results

In this chapter, the analytical results obtained through metallographic study and SEM-EDS analysis are presented, along with an initial assessment of the material type of the samples. To begin with, samples made of cast iron or with recognisable microstructures that can be confirmed to be made from the indirect process through metallographic study are presented in section 4.1. Samples with a soft iron or steel microstructure and slag inclusions embedded in the metal matrix may have been obtained from either the direct or the indirect process, hence a slag inclusion analysis was carried out to confirm their material and technological origin, and the results are presented in section 4.2. In section 4.3, the compositional data of slag inclusions from this research is further compared with reference data collected from published research work. Additionally, a brief summary of the analytical results is provided in section 4.4.

4.1 Metallography

4.1.1 Cast iron

White cast iron is one of the most common materials among the analysed samples as well as early iron products in China. Its microstructure is mainly ledeburite, which is a mixture of cementite and pearlite formed through the eutectic and eutectoid reaction during the solidification of cast iron (Figure 4.1).

Based on the carbon content, white cast iron can be further divided into three sub-categories as hypereutectic cast iron, eutectic cast iron and hypoeutectic cast iron. Hypereutectic cast iron has a carbon content higher than 4.3 wt.%, hence during solidification large cementite crystals (primary cementite) will form before the liquid cast iron reaches the eutectic point where ledeburite forms. The microstructure, as a

result, will be large primary cementite crystals on a ledeburite matrix (Figure 4.2). Hypoeutectic cast iron, on the other hand, has a carbon content between 2.1 wt.% to 4.3 wt.%, hence primary austenite will form before the liquid cast iron reaches the eutectic point, which then transforms into pearlite and cementite through eutectoid reaction. As a result, hypoeutectoid cast iron displays a microstructure mainly composed of primary pearlite on the ledeburite matrix (Figure 4.3). Eutectic cast iron has a carbon content right around 4.3 wt.% and its microstructure is mainly ledeburite. It is worth noting that during the casting and solidification process, carbon content and solidification rate may vary in different parts of the mould. As a result, heterogeneous microstructures resulting from the fluctuation of carbon content may be observed in the same object, but such gradients cannot be necessarily taken as suggestive of the use of different materials or technological choices applied.

Despite the variance in carbon content and its resulted microstructure, all white cast iron are extremely hard and brittle. It is therefore not surprising that most of the white cast iron products found in this research are objects made for daily use or ceremonial purposes, which does not require exceptional toughness or strength. Such products include tripods (XF-2, XF-4), cooking pots (XF-17, XK-Pot8), and belt-hooks (XF-22, YC-4, HJ-1,5, 6, 9, 10). A list of the samples identified as white cast iron samples is given in Table 4.1.

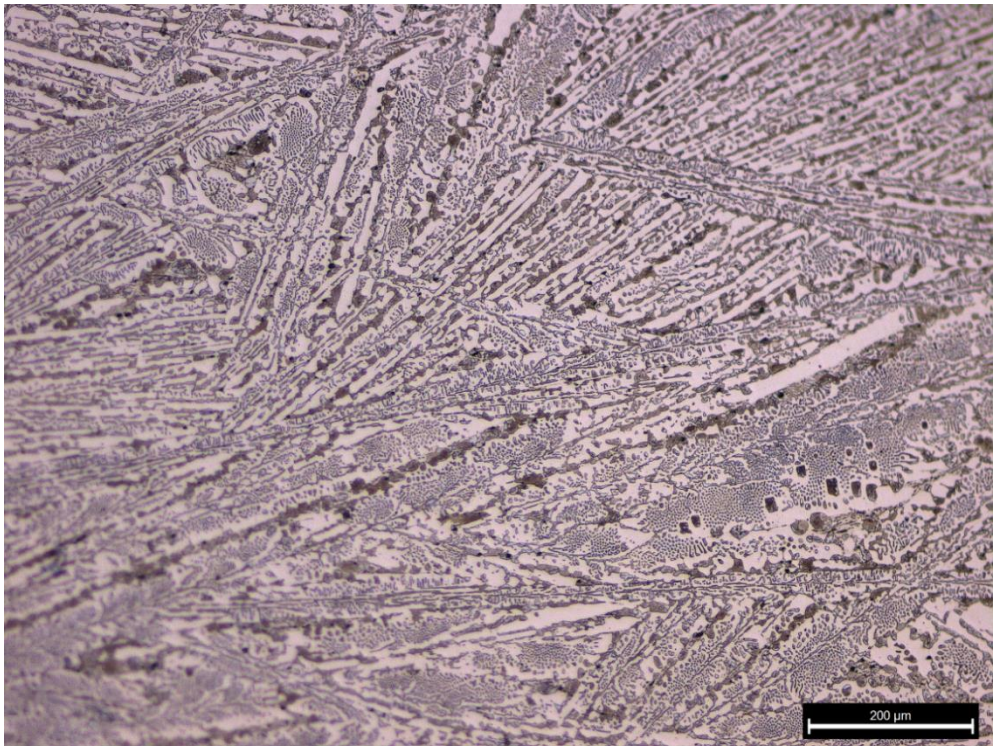

Figure 4.1 Metallography of sample XF-2, tripod, ledeburite structure[2].

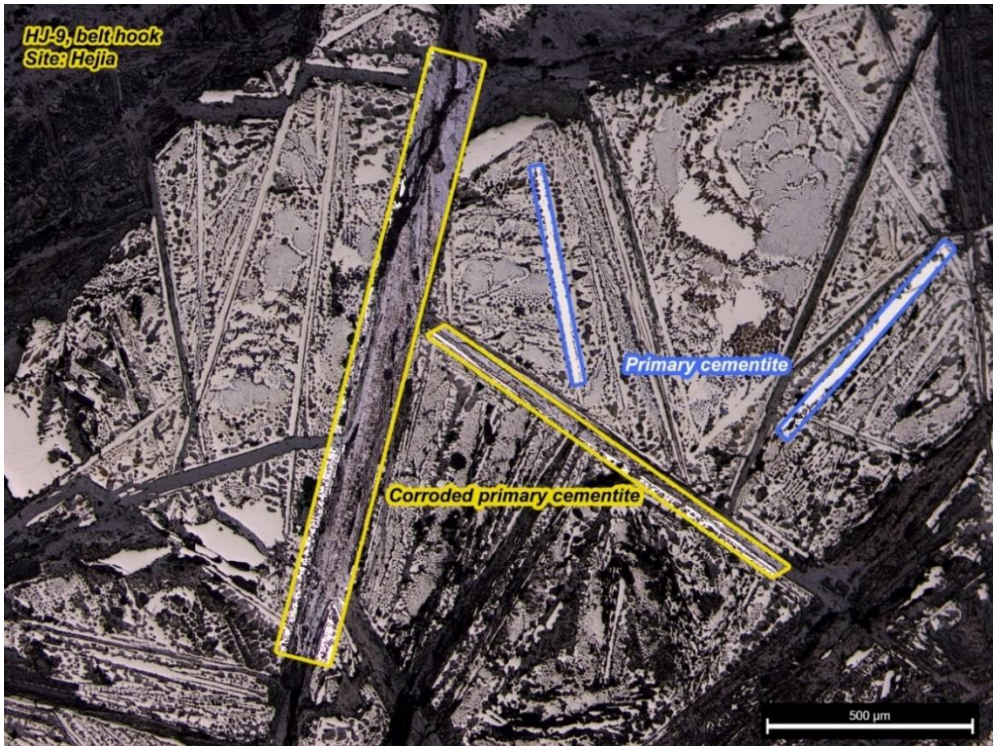

Figure 4.2 Metallography of sample HJ-9, belt-hook, hypereutectic cast iron, primary cementite on a ledeburite matrix

[2] All metallography pictures presented in this thesis were after etching unless otherwise indicated.

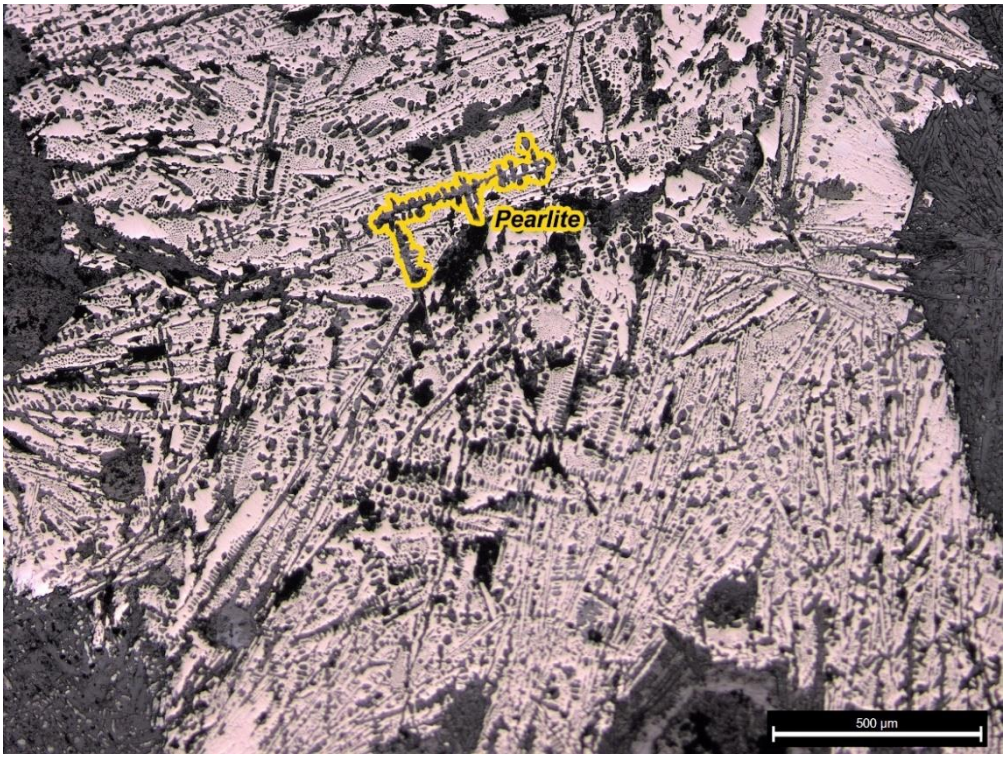

Figure 4.3 Metallography of sample YC-4, belt hook, hypoeutectic cast iron, pearlite on a ledeburite matrix

Table 4.1 List of samples with white cast iron microstructure

Lab No.	Site	Typology	Sampling Position
XF-2	Xinfeng	Tripod	Lip
			Body
			Leg
XF-4	Xinfeng	Tripod	Body
XF-17	Xinfeng	Pot	Lip
			Body
XF-22	Xinfeng	Belt-hook	
XK-Pot8	Xiekou	Pot	Body
NJG-22	Niejiagou	Shovel (Chan)	Blade
NJG-33	Niejiagou	Fragment	
YC-4	Yancun	Belt-hook	
HJ-1	Hejia	Belt-hook	
HJ-5	Hejia	Belt-hook	
HJ-6	Hejia	Belt-hook	
HJ-9	Hejia	Belt-hook	
HJ-10	Hejia	Belt-hook	

Grey and mottled cast iron are also very common materials among the samples analysed in this research. Their major difference compared to white cast iron is the presence of flake/lamellar graphite, which can be observed under the optical microscope before and after etching. In grey cast iron, carbon is mostly present in the form of graphite (Figure 4.4), whereas for mottled cast iron, depending on the level of graphitisation, it may appear as white cast iron with small amounts of flake graphite precipitated, or as predominantly grey iron with very few cementite patches left in the matrix (Figure 4.5).

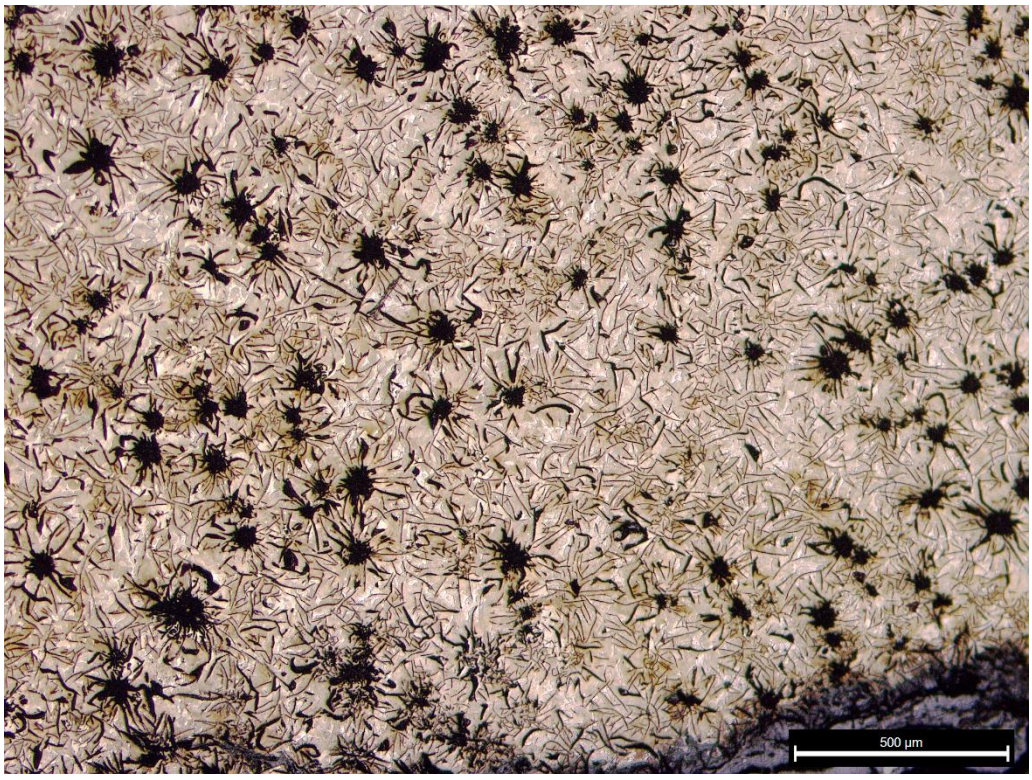

Figure 4.4 Metallography of sample XF-3 (lip), tripod, grey cast iron, graphite flakes (black) on pearlite matrix.

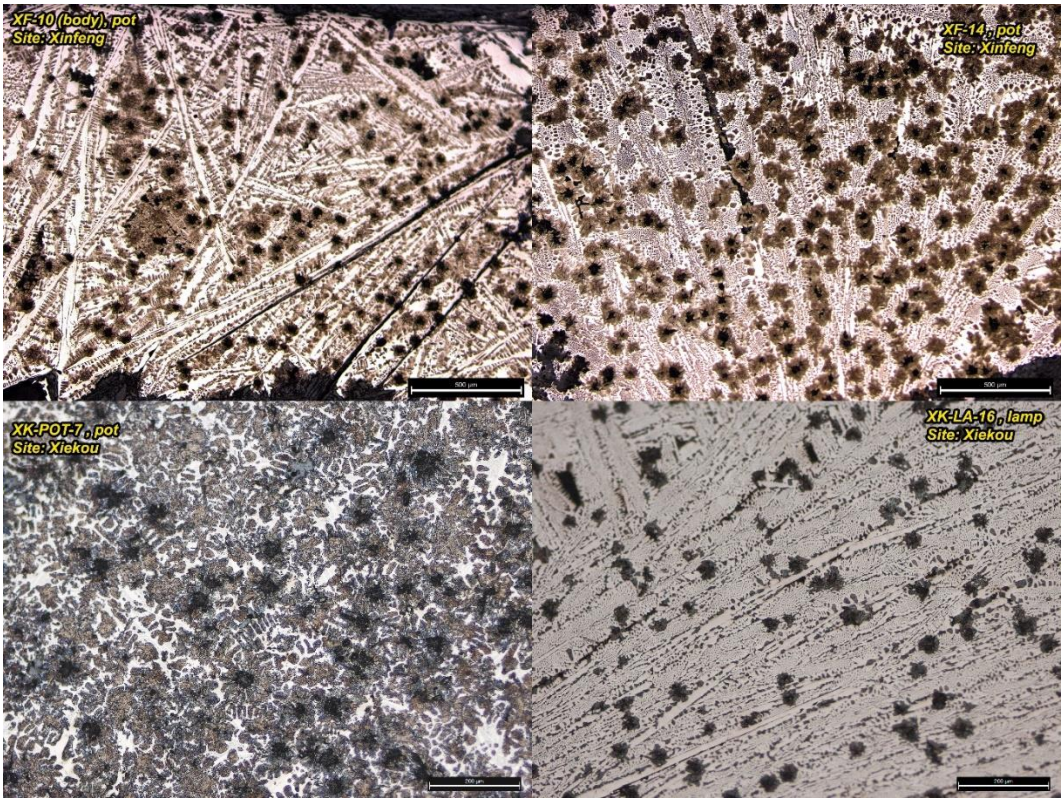

Figure 4.5 Metallography showing different levels of graphitisation. In sample XF-10, XF-14 and XK-La16, the ledeburite can still be observed, with various amount of flake graphite precipitated. In sample XK-Pot7, ledeburite can no longer be observed, the matrix is pearlite with flake graphite and cementite (white) on it.

It is worth noting that during the mould casting process, solidification rate on the surface, where liquid cast iron will be in direct contact with the casting mould, is typically higher than the core, which solidifies last. Due to the difference in solidification rate, variance of graphitisation levels can be observed, whereby more cementite will be crystallised on the surface, with more graphite crystallising towards the centre (Figure 4.6). Similarly, results of multiple samples taken from different positions of the same object also indicate that the cooling rate can be heterogeneous inside the casting mould, resulting in different levels of graphitisation in one object (Figure 4.7). More importantly, this observation also indicates that, in essence, grey and mottled cast iron are same type of material with only different levels of graphitisation that may simply result from heterogeneous cooling conditions. A list of grey and mottled cast iron samples in this research is given in Table 4.2.

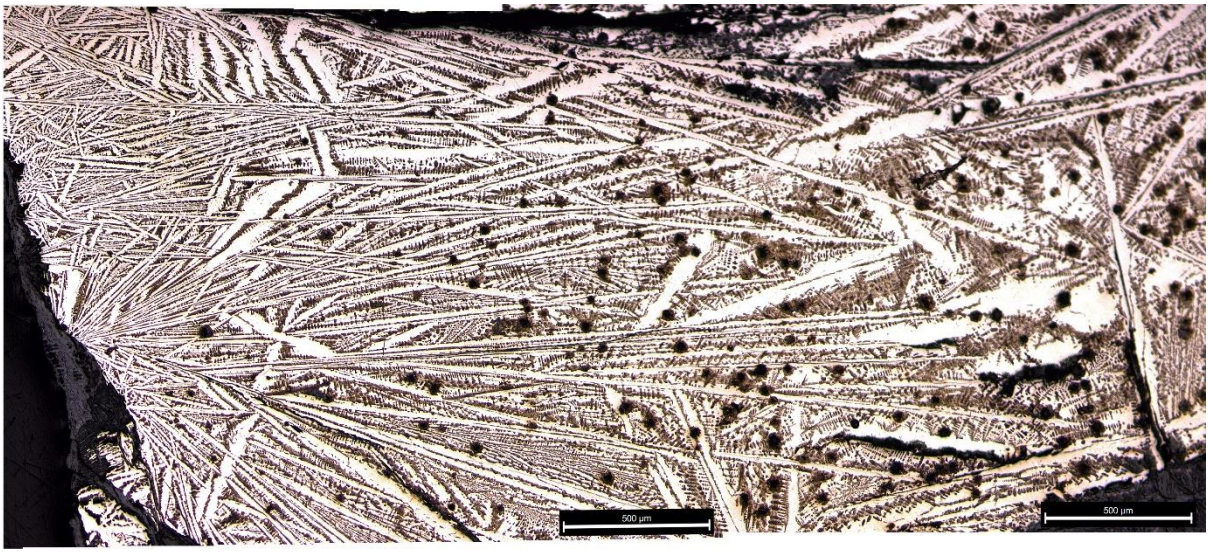

Figure 4.6 Metallography showing different levels of graphitisation from surface toward inside, sample XF-10 (body).

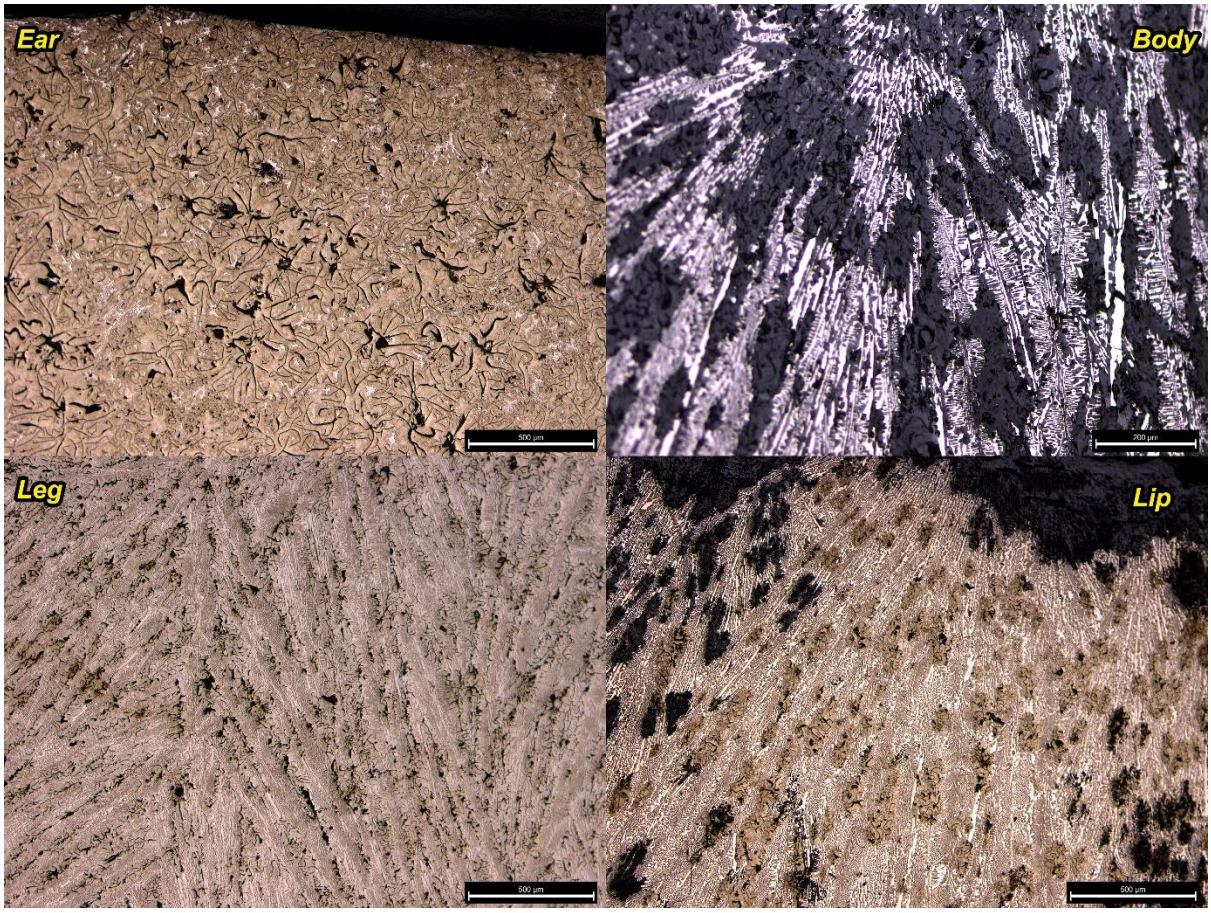

Figure 4.7 Metallography of samples taken from different positions on XF-1, tripod, showing different levels of graphitisation. In the ear part of the object, the cast iron is essentially grey, with very small amount on cementite left, while in other parts of object, large amount of ledeburite crystals can be observed.

Table 4.2 List of samples with grey or mottled cast iron microstructure

Lab No.	Site	Typology	Sampling Position	Material
XF-1	Xinfeng	Tripod	Lip	MCI
			Body	MCI
			Ear	GCI
			Leg	MCI
XF-3	Xinfeng	Tripod	Lip	GCI
			Lid	MCI
XF-5	Xinfeng	Mou	Lip	MCI
			Body	MCI
XF-7	Xinfeng	Pot	Body	GCI
XF-8	Xinfeng	Pot	Lip	GCI
			Body	MCI
XF-9	Xinfeng	Pot	Lip	GCI
			Body	MCI
XF-10	Xinfeng	Pot	Lip	MCI
			Body	MCI
XF-11	Xinfeng	Pot	Body	GCI
XF-12	Xinfeng	Pot	Body	MCI
XF-14	Xinfeng	Pot	Lip	MCI
			Body	GCI
XF-15	Xinfeng	Pot	Lip	GCI
			Body	GCI
XF-16	Xinfeng	Pot	Lip	MCI
			Body	GCI
XF-18	Xinfeng	Pot	Body	MCI
XF-24	Xinfeng	Lamp		MCI
XF-F27	Xinfeng	Lamp		GCI
XK-Pot7	Xiekou	Pot	Body	MCI
XK-Pot9	Xiekou	Pot	Body	MCI
XK-La13	Xiekou	Lamp		MCI
XK-La14	Xiekou	Lamp		GCI
XK-La15	Xiekou	Lamp		MCI
XK-La16	Xiekou	Lamp		MCI
XK-La17	Xiekou	Lamp		MCI
NJG-36	Niejiagou	Fragment		GCI
YC-5	Yancun	Belt-hook		MCI
JC-5	Airport	Unknown Vessel		MCI

NY-8	Ningyuan	Fragment		MCI
NY-9	Ningyuan	Pot	Body	MCI
HJ-2	Hejia	Belt-hook		MCI
HJ-4	Hejia	Belt-hook		MCI

In addition, the distribution pattern of the flake graphite in mottled or grey cast iron may also vary depending on the carbon content, cooling rate and other alloying elements. In order to visualise such differences more clearly, high magnification metallographic images of two typical microstructures are provided in Figure 4.8, and the images were subsequently compared to the international standards for graphite classification, as illustrated in Figure 4.9 (International Standard Organization 2008). Most of the grey or mottled cast analysed in this research contains flake/lamellar graphite that, according to this classification, is type-I based on its physical shape, and can be further categorized as type-C′ based on its distribution pattern, with the exception of sample XF-1, in which the graphite presents in the pattern of type-A.

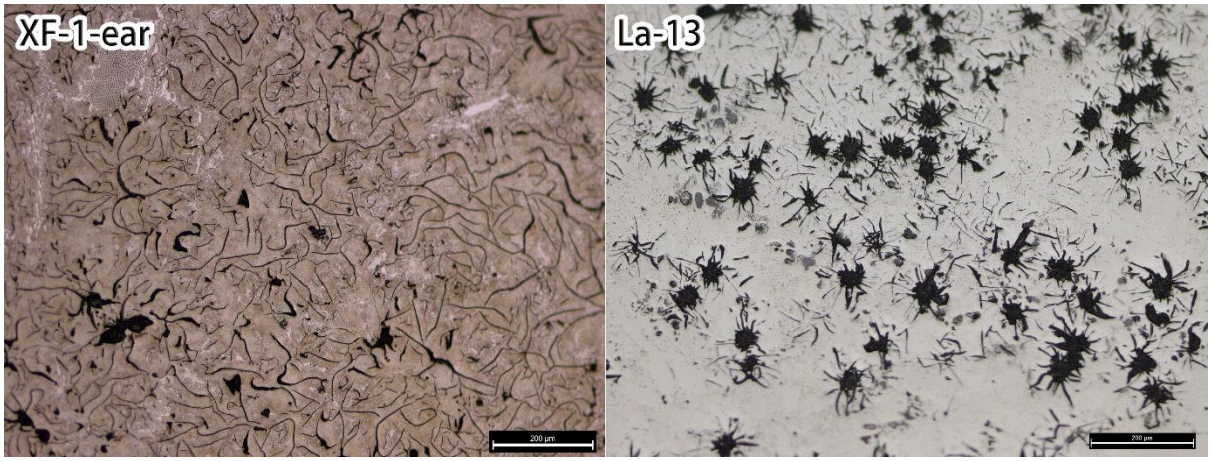

Figure 4.8 Metallography of Sample XF-1 (ear, after etching) and XK-La13 (before etching)

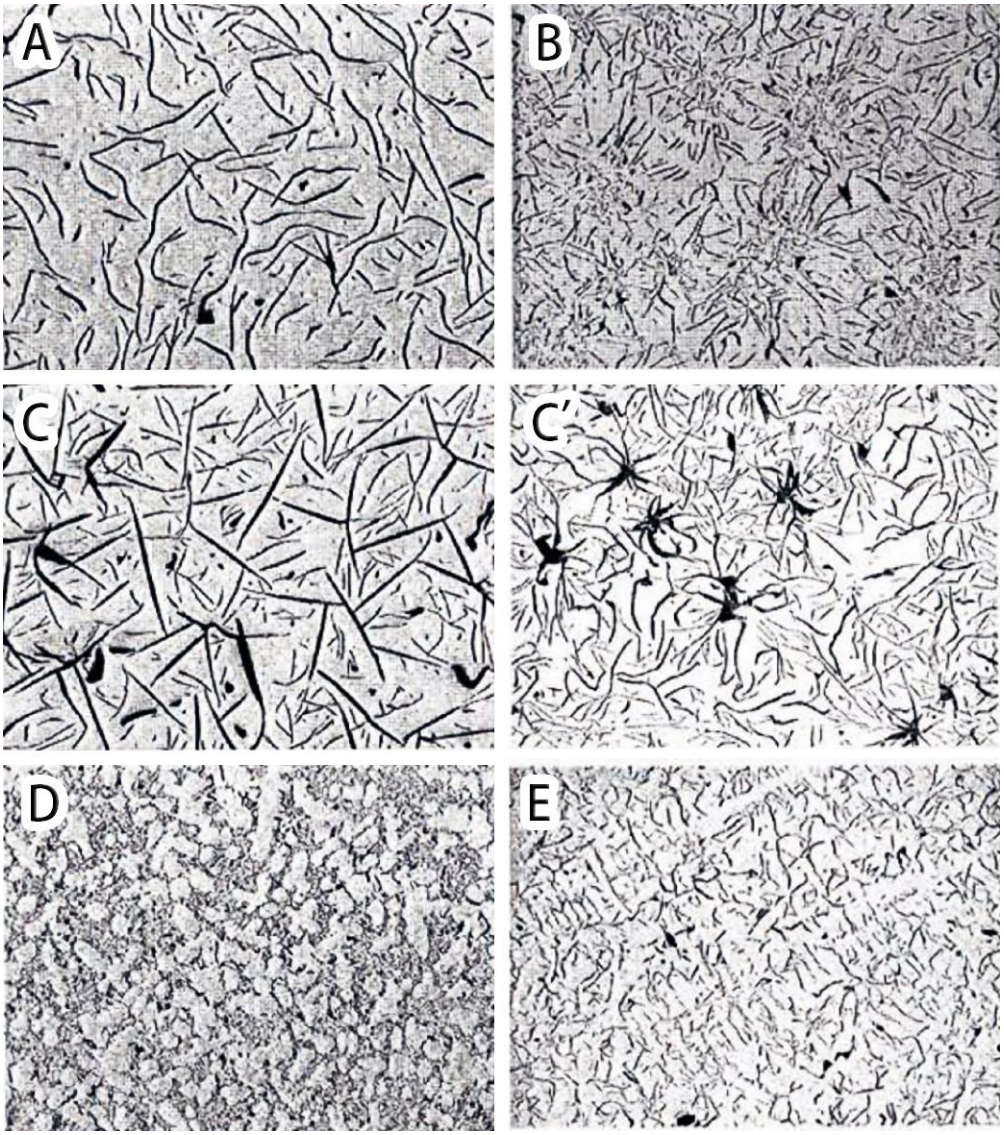

Figure 4.9 Distribution patterns of flake graphite examples provided in ISO-945-1 (International Standard Organization 2017).

4.1.2 Annealed cast iron

White cast iron subjected to an annealing process will be either decarburised or malleablised depending on the annealing atmosphere, leaving characteristic microstructures that can be recognised under optical microscope. As introduced in section 2.1.2, in modern metallurgy, annealed cast iron is termed as malleable cast iron, and further divided into white heart malleable cast iron and black heat malleable cast iron, depending on whether the process is aiming for decarburisation or malleablisation, respectively (Yan and Wu 1985). However, such a categorisation

method can lead to confusion as early metallurgical processes were often carried out under imperfect conditions, resulting in material types that cannot be precisely categorised. In this sense, this research used the categorisation system established by early Chinese archaeometallurgists (Figure 4.10) (Li 1975). This system is mainly based on the microstructure and the resulting mechanical properties, which divided annealed cast iron into three types of materials: *malleable cast iron* (可锻铸铁), *decarburised cast iron* (脱碳铸铁) and *decarburised soft iron/steel* (铸铁脱碳熟铁/钢).

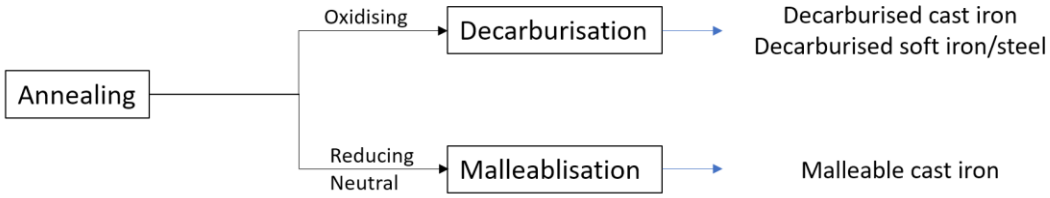

Figure 4.10 Categorisation of technical pathways of the annealing process and resulted material types

Malleable cast iron refers to cast iron that has gone through an annealing process where cementite was fully decomposed and formed into graphite (temper carbon). Morphologically, such graphite can either be flocculant (sample XF-34 in Figure 4.11), vermicular (sample XK-Pl1 in Figure 4.11) or spheroidal (sample LD-3 and NJG-35 in Figure 4.11), depending on multiple factors including the annealing temperature and alloying elements. The matrix, depending on the annealing settings, can either be pearlite or ferrite, or a mixture of both. Due to the imperfect control of the annealing atmosphere, certain amount of oxidants will always be presented in the annealing kiln, therefore most of the malleable cast iron samples have a decarburisation layer that can observed on the surface (Figure 4.12). A list of the malleable cast iron samples identified in this research is given in Table 4.3.

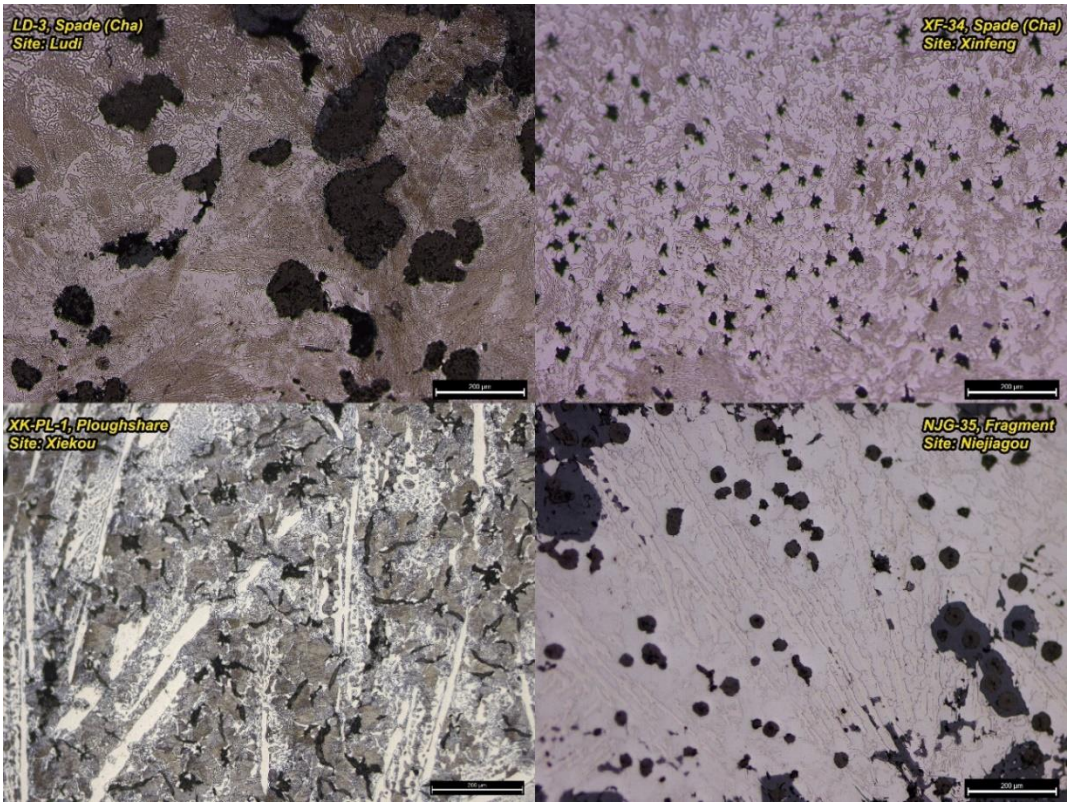

Figure 4.11 Metallography of samples LD-3, XF-34, XK-PL1 and NJG-35, showing different types of malleable cast iron with graphite in various size, shape in different matrix. Sample XK-Pl1 was incompletely malleablised, with cementite crystals left in the matrix.

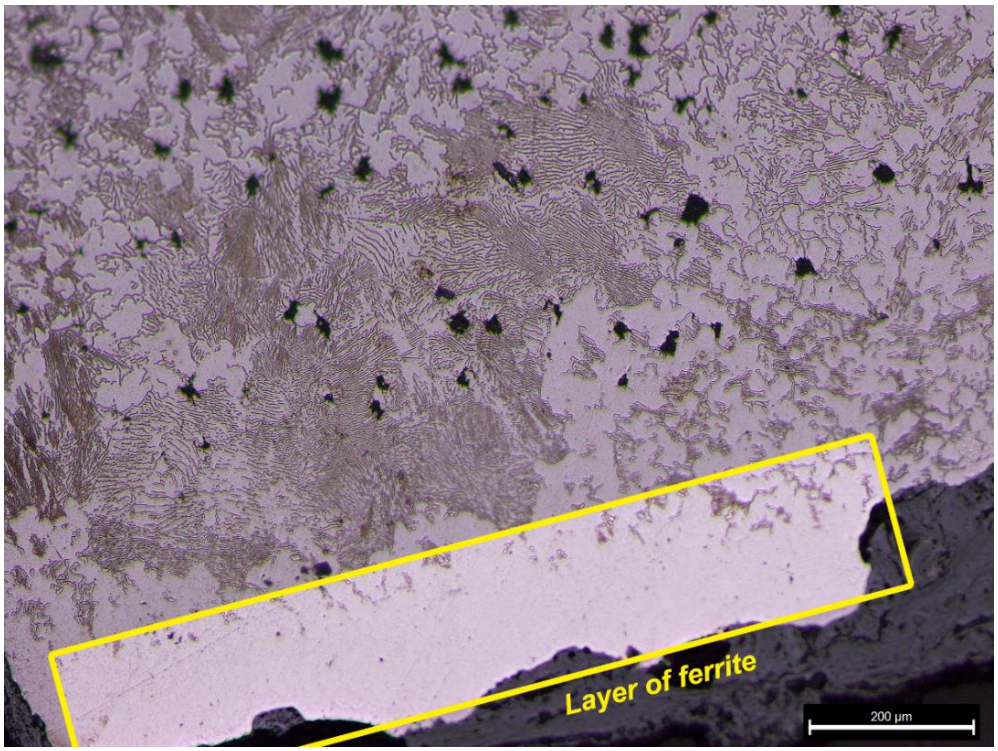

Figure 4.12 Metallography of sample XF-34, Spade (Cha), malleable cast iron, with a decarburisation layer on the surface primarily of ferrite.

Table 4.3 List of malleable cast iron samples in this research and their microstructure

Lab No.	Site	Typology	Graphite morphology	Matrix
XF-20	Xinfeng	Belt-hook	Flocculant	Pearlite and ferrite
XF-21	Xinfeng	Belt-hook	Flocculant	Corroded
XF-34	Xinfeng	Spade (Cha)	Flocculant	Pearlite and ferrite
XK-Pl1	Xiekou	Ploughshare	Vermicular	Pearlite, with cementite remains
NJG-24	Niejiagou	Bar	Flocculant	Pearlite and ferrite
NJG-35	Niejiagou	Fragment	Spheroidal	Ferrite
YC-1	Yancun	Spade (Cha)	Flocculant	Ferrite
LD-3	Lüdi	Spade (Cha)	Spheroidal	Pearlite
NY-1	Ningyuan	Spade (Cha)	Flocculant	Pearlite and ferrite
NY-3	Ningyuan	Adze (Ben)	Flocculant	Pearlite
NY-4	Ningyuan	Belt-hook	Flocculant (close to flake)	Pearlite and ferrite
NY-6	Ningyuan	Knife	Flocculant (large size)	Pearlite
HJ-7	Hejia	Belt-hook	Flocculant	Pearlite
HJ-8	Hejia	Belt-hook	Flocculant	Pearlite and ferrite
HJ-11	Hejia	Ring	Spheroidal	Pearlite and ferrite

Decarburised cast iron refers to white cast iron that has been partially decarburised through an annealing process, with typical white cast iron microstructure remaining in the core, and decarburised layer (pearlite and/or ferrite) on the surface. The decarburisation depth varies depending on the annealing duration and temperature settings. Some of the samples in this research were only slightly decarburised on the surface with most of the core maintained as white cast iron, while some samples were mostly decarburised with only a small part of cast iron left in the centre (Figure 4.13). It is worth noting that as most of the samples were heavily corroded, it is hard to evaluate the actual decarburisation depth owing to the microstructure on the outer surface being lost to corrosion. A list of decarburised cast iron samples identified in this research is given in Table 4.4.

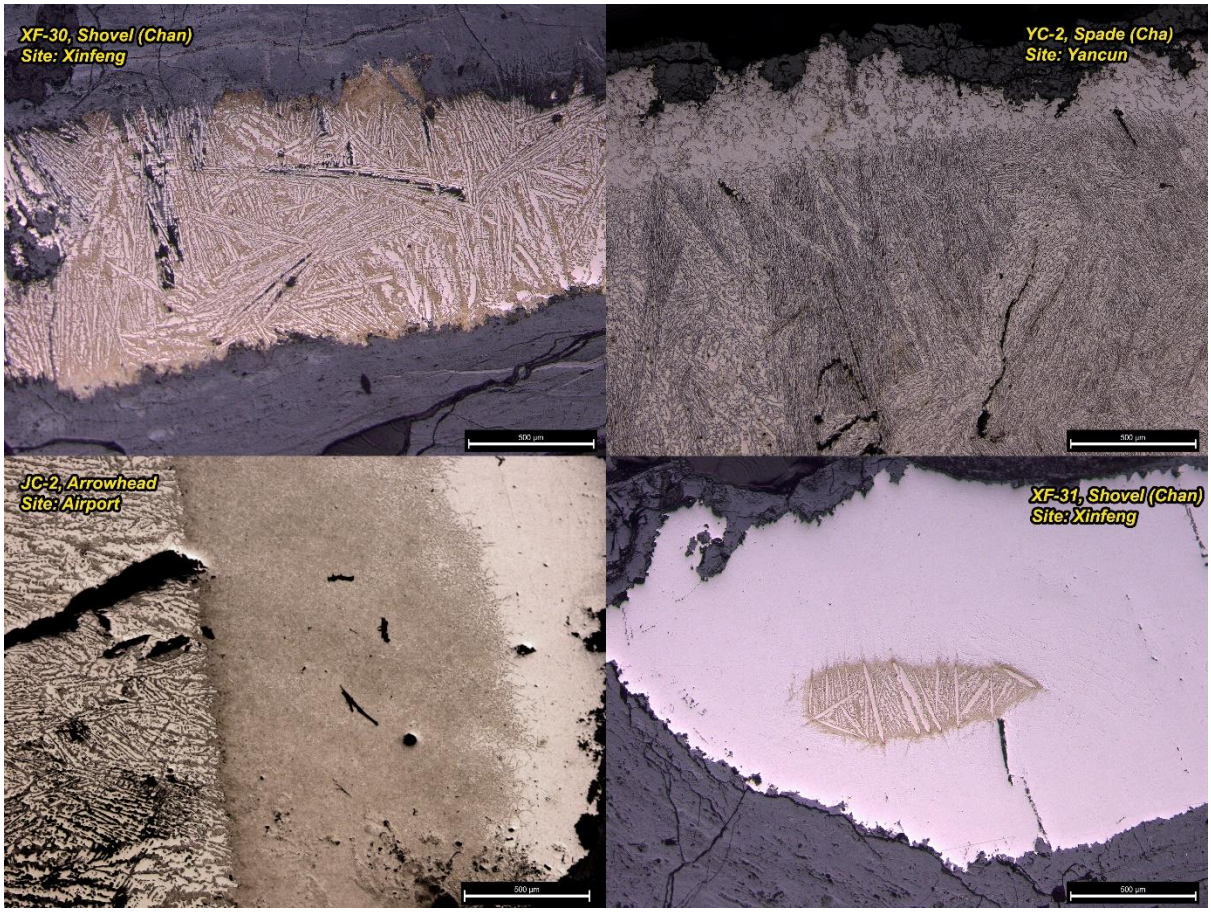

Figure 4.13 Metallography of sample XF-30, YC-2, JC-2 and XF-31, showing different levels of decarburisation depth

Table 4.4 List of decarburised cast iron samples in this research

Lab No.	Site	Typology
XF-30	Xinfeng	Shovel (Chan)
XF-31	Xinfeng	Shovel (Chan)
XF-33	Xinfeng	Spade (Cha)
XF-35	Xinfeng	Spade (Cha)
YC-2	Yancun	Spade (Cha)
YC-3	Yancun	Spade (Cha)
JC-2	Airport	Arrowhead
JC-4	Airport	Arrowhead
GX-3	Gaoxin Primary School	Spade (Cha)

Decarburised soft iron or steel refers to cast iron that has been thoroughly decarburised through the annealing process, with no cast iron microstructures left. Compared to their counterparts derived from the bloomery smelting or fining process

etc., soft iron or steel made through the annealing process contains little to no slag inclusions. This is because its raw material, white cast iron, has gone through a thorough metal/slag separation process, hence typically no slag inclusions are left in the metal. The subsequent annealing process is carried out in solid state, hence no slag inclusions will be formed or introduced either, therefore soft iron/steel samples having a clean metal matrix will be considered as made through the annealing decarburisation process. Among such samples analysed in this research, different levels of carbon content were observed, ranging from pure ferritic iron with little to no carbon content, to eutectoid steel with around 0.77 wt.% carbon (Figure 4.14). Occasionally, graphite nodules can be observed in the decarburised matrix, indicating that decarburisation and graphitisation were going on at the same time, when the decomposed carbon atoms were not only oxidised, but also formed into graphite at the same time (Figure 4.15). A list of decarburised soft iron or steel samples identified in this thesis is given in Table 4.5.

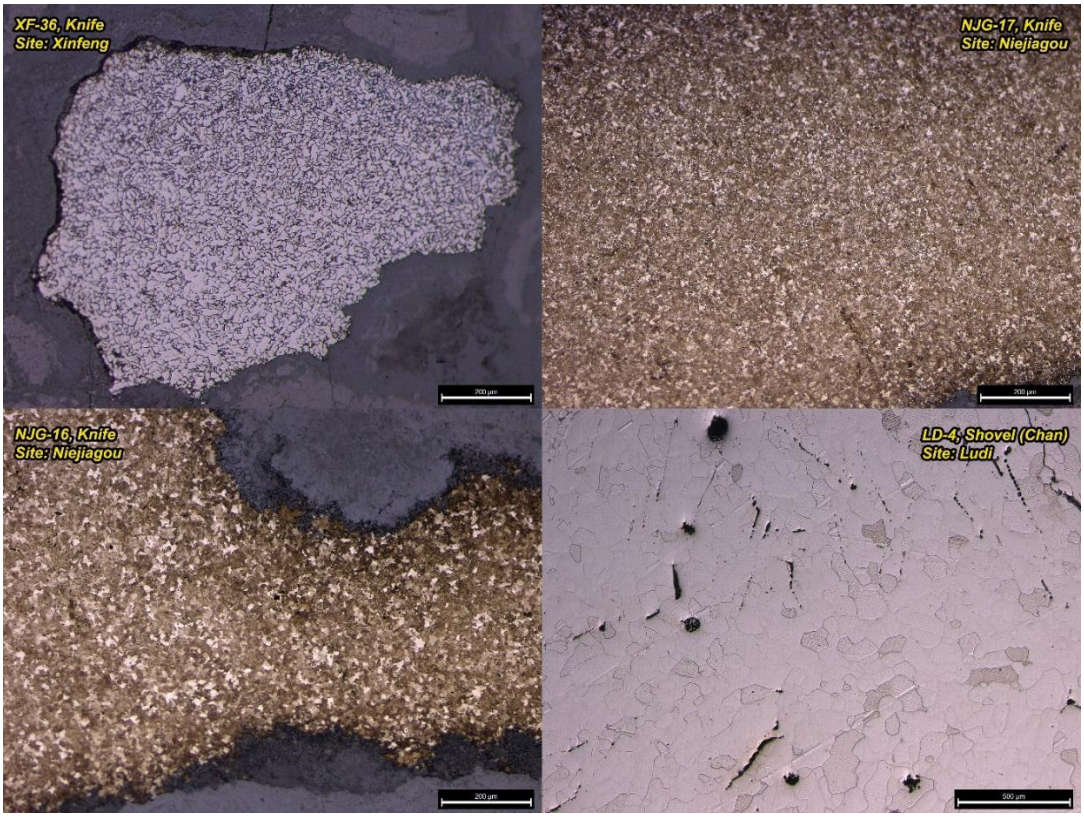

Figure 4.14 Metallography of sample XF-36, NJG-17, NJG-16 and LD-4. XF-36 is primarily composed of ferrite grains, with small amount on pearlite between the grains; NKG-17 and NJG-16 is composed on ferrite and pearlite grains; LD-4 is mainly ferritic, with corrosion stringers (identified under SEM) in the matrix. .

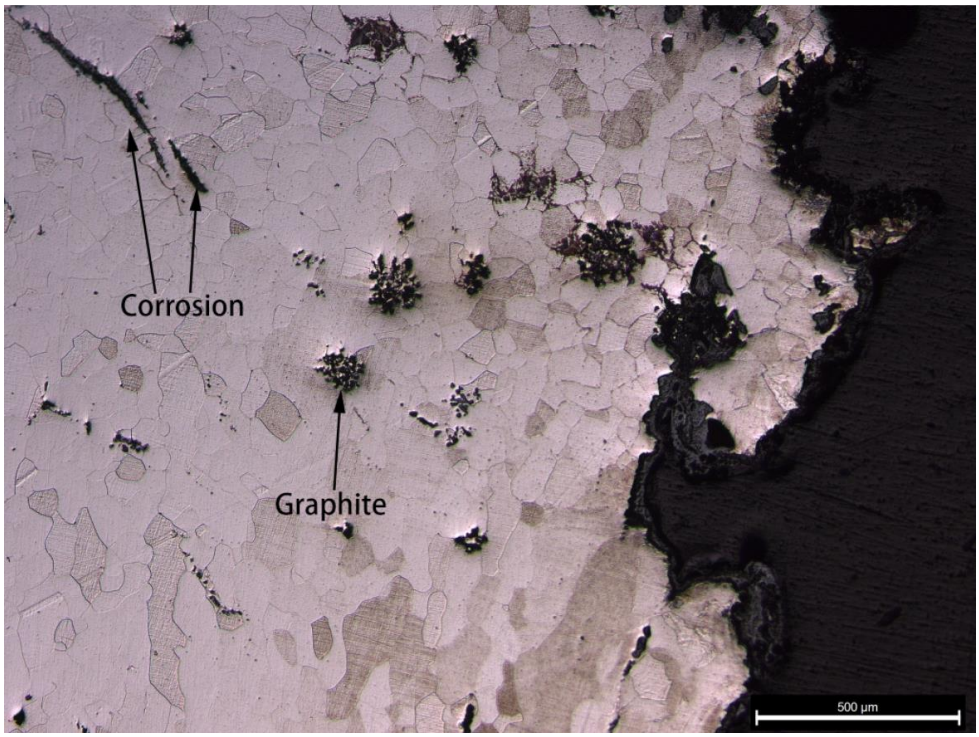

Figure 4.15 Metallography of sample LD-4, temper graphite (flocculant) remains in one corner with ferrite grains as the matrix.

Table 4.5 List of decarburised soft iron/steel samples

Lab No.	Site	Typology	Material
XF-29	Xinfeng	Adze (Ben)	Decarburised soft iron
XF-36	Xinfeng	Knife	Decarburised steel
XK-Saw1	Xiekou	Saw	Decarburised soft iron
XK-Kn11	Xiekou	Knife	Decarburised steel
NJG-1	Niejiagou	Chisel	Decarburised steel
NJG-2	Niejiagou	Chisel	Decarburised steel
NJG-3	Niejiagou	Chisel	Decarburised steel
NJG-4	Niejiagou	Chisel	Decarburised steel
NJG-5	Niejiagou	Chisel	Decarburised steel
NJG-8	Niejiagou	Chisel	Decarburised steel
NJG-9	Niejiagou	Chisel	Decarburised steel
NJG-12	Niejiagou	Chisel	Decarburised steel
NJG-14	Niejiagou	Knife	Decarburised steel
NJG-16	Niejiagou	Knife	Decarburised steel
NJG-17	Niejiagou	Knife	Decarburised steel
NJG-18	Niejiagou	Knife	Decarburised steel
NJG-19	Niejiagou	Knife	Decarburised steel
NJG-21	Niejiagou	Shovel (Chan)	Decarburised steel
NJG-23	Niejiagou	Adze (Ben)	Decarburised steel
NJG-31	Niejiagou	Fragment	Decarburised steel
NJG-32	Niejiagou	Fragment	Decarburised steel
JC-3	Airport	Arrowhead	Decarburised soft iron
LD-4	Lüdi	Adze (Ben)	Decarburised soft iron

4.1.3 Soft iron and steel

The rest of the samples are predominantly soft iron or steel with inhomogeneous microstructures and slag inclusions embedded in the metal matrix. Based on current research, such materials can be either derived from the bloomery smelting process, or the fining process which converts cast iron into low carbon soft iron or steel in liquid state. Additionally, the possibility remains when decarburised soft iron/steel went through a smithing/forging process in which smithing slag was introduced, therefore a

further slag inclusion analysis will be necessary to differentiate the technological origin of such materials.

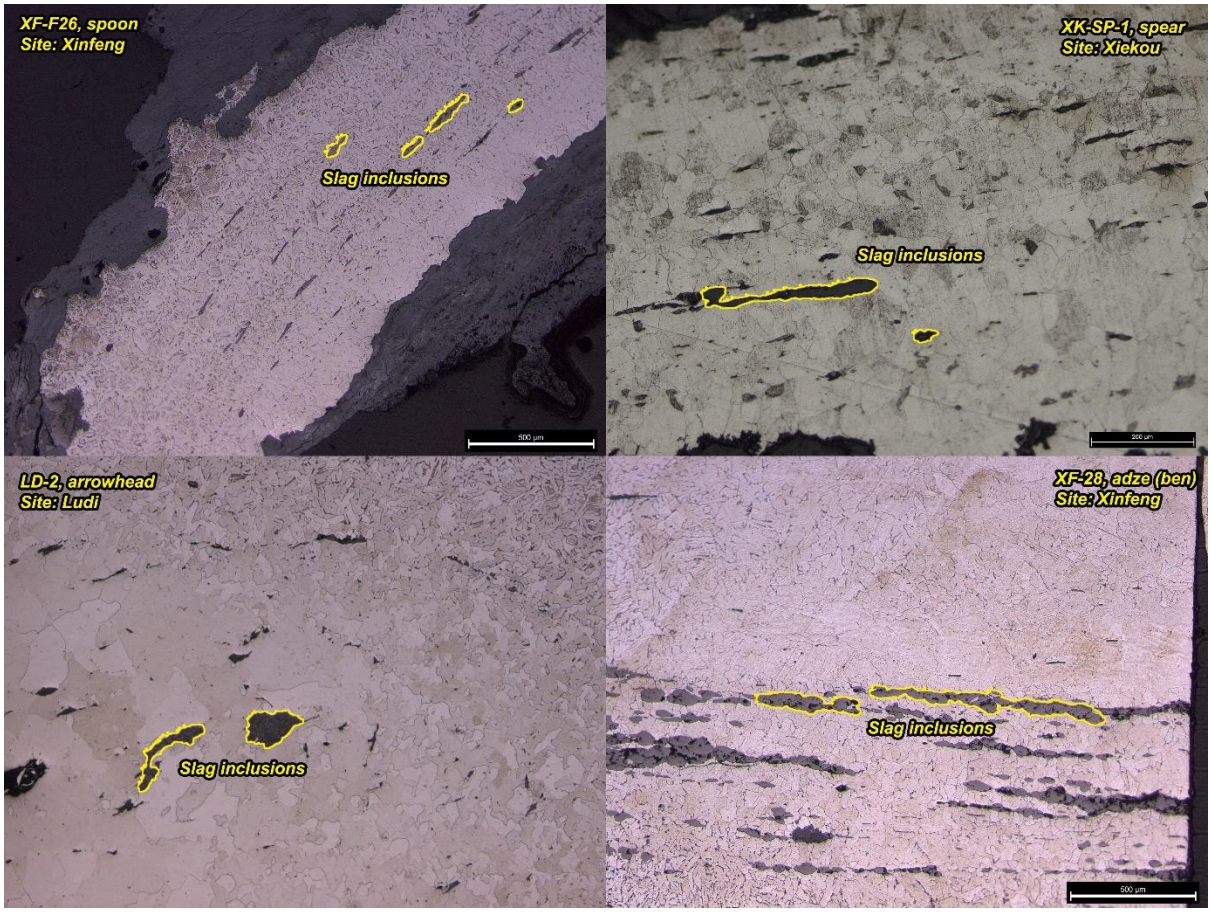

Figure 4.16 Metallography of sample XF-F26, XK-Sp1, LD-2 and XF-28, heterogeneous soft iron/steel microstructure with slag inclusions embedded in the matrix

Table 4.6 List of soft iron/steel samples with slag inclusions embedded in the metal matrix, their microstructure and number of inclusions analysed

Lab No.	Typology	Microstructure	Number of slag inclusions analysed
XF-25	Adze (Ben)	Granular pearlite on ferrite matrix	10
XF-27	Adze (Ben)	Ferrite matrix with increasing amount of pearlite on the surface (Figure 4.23)	47
XF-28	Adze (Ben)	Widmannstätten structure on the tip and ferrite in the middle (Figure 4.27)	35
XF-37	Knife	Large ferrite grains with etching pits of iron phosphide eutectic	17

XF-F17	Awl	Ferritic matrix with martensite structure on one side	61
XF-F19	Chisel	Homogeneous mixture of ferrite and pearlite	65
XF-F26	Spoon	Widmannstätten structure in the centre with ferrite grains on the surface (Figure 4.16)	59
XF-F29	Sword	Widmannstätten structure	49
XK-Sp1	Spear	Ferrite grains (Figure 4.16)	10
XK-Sw14	Sword	Corroded	12
XK-Kn10	Knife	Layered structure of ferrite and pearlite	24
NJG-6	Chisel	Pearlite matrix (Figure 4.63)	26
NJG-7	Chisel	Ferrite matrix in the centre with more pearlite toward the surface (Figure 4.63)	34
NJG-11	Chisel	ferrite grains with small amount pearlite in the grain boundaries (Figure 4.43)	29
NJG-20	Shovel (Chan)	Ferrite grains	28
NJG-34	Fragment	Ferrite grains with pearlite in the grain boundaries, with increasing amount of pearlite toward the surface	14
CXC-1	Sickle	Ferrite grains in the centre, with mixture of ferrite and pearlite on the surface (Figure 4.51)	84
JC-1	Arrowhead	Ferrite grains	18
LD-1	Arrowhead	Mixed microstructure with one side mainly ferrite grains and the other side ferrite and pearlite (Figure 4.55)	66
LD-2	Arrowhead	Ferrite grains in the centre, with increasing amount of pearlite toward the surface (Figure 4.59)	50
NY-2	Shovel (Chan)	Ferrite grains with martensite on one side	11
GX-2	Knife	Ferrite grains with small amount of pearlite in the grain boundaries	19

4.2 Slag inclusion analysis and data treatment

Among the samples analysed, 22 of them contain inclusions embedded in a soft iron or steel microstructure. As demonstrated above, such type of microstructure could either indicate a material derived from the bloomery iron smelting process, where

smelting slag generated from the reduction stage remain entrapped in the metal, or cast iron decarburised through a process where new inclusions were formed or introduced. To further differentiate these two types of material as well as the revealing their manufacturing technique, slag inclusion analysis was carried out and the results are presented below.

To facilitate the presentation of the results as well as the comparison between samples, based on the slag inclusions' morphology, distribution, chemical concentration and their overall homogeneity, these 22 samples are divided into three groups, each group containing similar inclusions that can be analysed using the same methodological approach (Table 4.7). Group 1 includes those samples which do not require additional data treatment on their slag inclusion composition before subjecting to comparison with reference data, either due to their homogeneity within individual samples, and/or too few data collected due to the small sample size and corrosion effect.

Samples categorised in group 2 contain various types of inclusions that fall in different clusters in terms of their morphology and chemical composition, hence it is necessary to understand whether such heterogeneity derives from the use of different material sources in the making of the object, slag inclusions formed at different production stages (smelting, smithing or fining) and/or whether it is the result of inhomogeneous reaction conditions which affected the chemical make-up of the slag inclusions. Dillmann and L'Héritier (2007) proposed a method to eliminate the inclusions affected by the local concentration effect as well as those smithing (forging) slag based on the NRC components, where the ratios of MgO/Al_2O_3, Al_2O_3/SiO_2, K_2O/CaO should remain constant for those inclusions generated from the reduction stage, while the outliers should be removed. Charlton et al. (2012) also proposed a method to identify slag inclusion families based on the NRC component, but focus on the sub-

compositional ratios using multivariate analysis. Following their work, this research adopted a similar approach, yet instead of eliminating those outliers, this research does not seek to remove any data point due to our limited understanding of compositional characteristics of different types of slag inclusions from early China. Additionally, as demonstrated in the following section, most of the compositional difference of the slag inclusions can be considered as continuous variance instead distinct “families”, therefore forcing them into groups may cause misreading the data. In the meantime, when performing multivariate analysis, FeO and P_2O_5 were also included in the variables since we believe they are also important indicators for understanding what is causing the variance. Detailed introduction of the method was introduced in section 4.2.2. Through the data treatment process, subsequent work seeks to identify those inclusions that are diagnostic of the production technology before further comparison with reference data derived from known sources.

Group 3 includes two samples, NJG-6 and NIG-7, both containing inclusions that are different in terms of their morphology and chemical makeup compared with the rest of the samples, hence an independent section is dedicated to this group.

Table 4.7 Groups and corresponding samples

Groups		Samples
Group 1	1a	XF-25, XK-Sw14, XK-Kn10, NJG-34, GX-2, XF-F29
	1b	XF-37, NY-2, XK-Sp1, JC-1
Group 2		XF-F27, XF-28, XF-F17, XF-F19, XF-F26, NJG-11, NJG-20, CXC-1, LD-1, LD-2
Group 3		NJG-6, NJG-7

4.2.1 Group 1

To begin with, samples having glassy silicate slag inclusions with similar chemical composition were classed in Group 1a, including samples XF-25 (adze), XK-Sw14

(sword), XK-Kn10 (knife), NJG-34 (fragment), GX-2 (knife). Inclusions in these samples are predominantly composed of Al_2O_3, SiO_2, CaO and FeO, which together make up over 90 wt.% (Figure 4.17, 4.18).

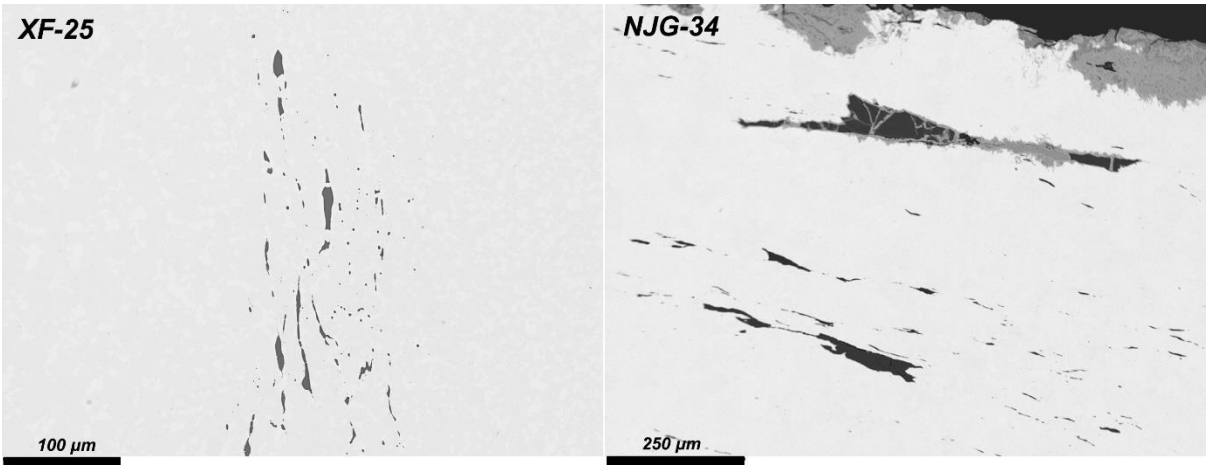

Figure 4.17 Back-scattered electron image of sample XF-25 and NJG-34, with glassy silicate inclusions

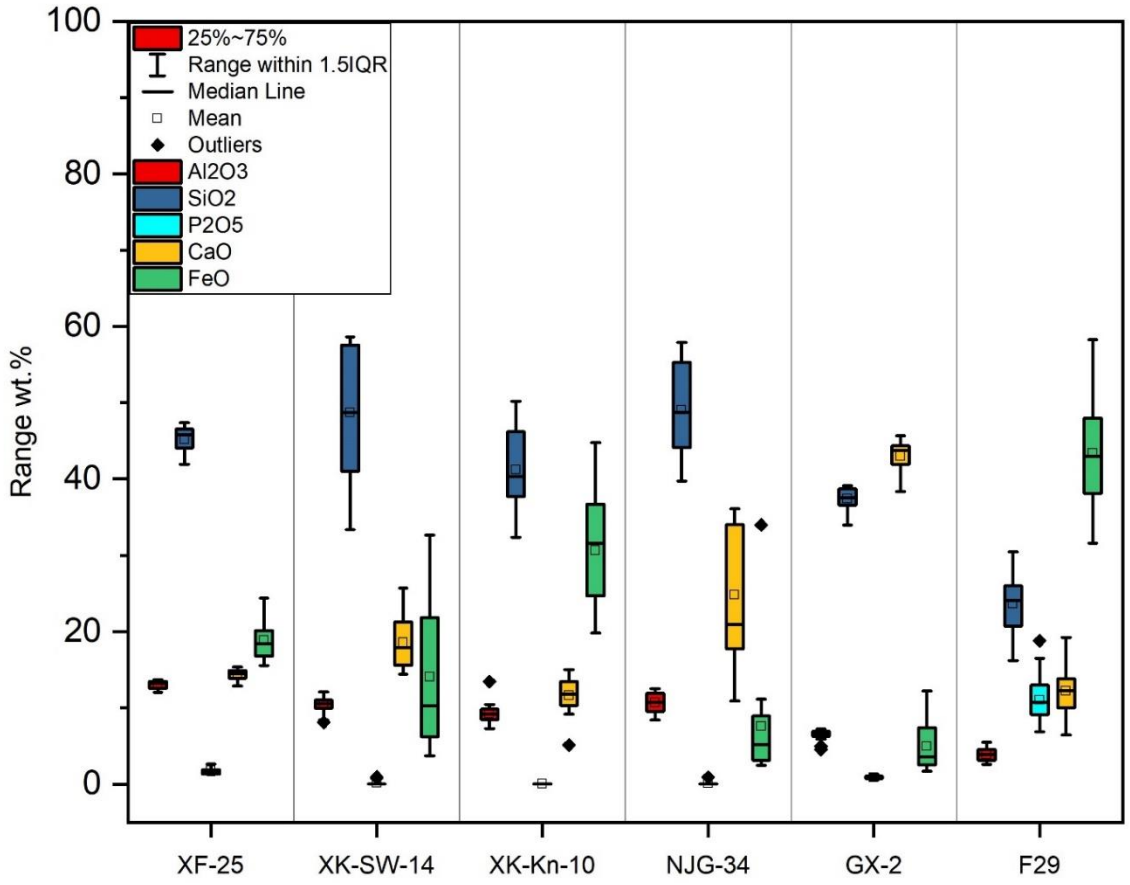

Figure 4.18. Box-whisker plot of Al_2O_3, SiO_2, P_2O_5, CaO and FeO content of slag inclusions in samples XF-25, XK-Sw14, XK-Kn10, NJG-34, GX-2 and XF-F29

Sample XF-F29, a sword sample from the Xinfeng cemetery, also contains glassy silicate inclusions with relatively homogeneous chemical composition (Figure 4.19). Comparing to those five samples mentioned above, slag inclusions in XF-F29 have a much higher P_2O_5 content (mostly around 10 wt.%, Figure 4.18), hence this sample is also categorised in group-1a as these inclusions are most possibly from the same source due to their homogeneity, yet the high P_2O_5 possibly indicates a different technical process compared to the rest of the samples.

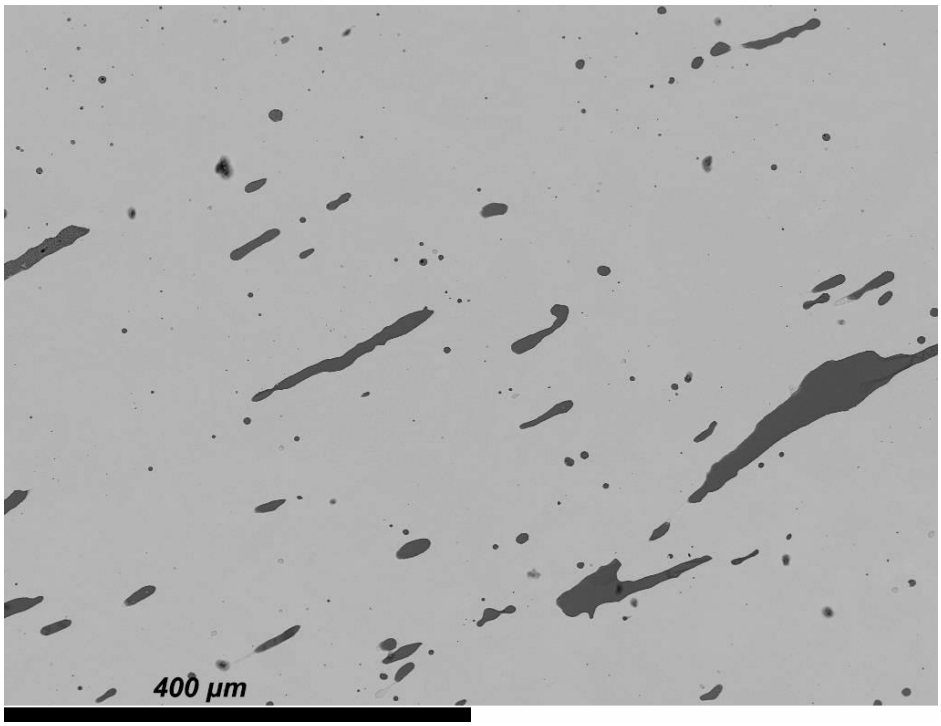

Figure 4.19 Back-scattered electron image of sample XF-F29, glassy silicates elongated toward one direction

In addition, samples without enough slag inclusion data (less than 20) for statistical analysis to differentiate their possible material/technological source are categorised in group 1b, including sample XF-37 (knife, 17 inclusions analysed), NY-2 (shovel, 11 inclusions analysed), XK-Sp1 (spear, 10 inclusions analysed), JC-1 (arrowhead, 18 inclusions analysed). Slag inclusions in these four samples are mostly fayalitic with

wüstite crystals. Metallography and back-scattered electron images are given in Figure 4.20, while box-whisker plots of their main components are given in Figure 4.21.

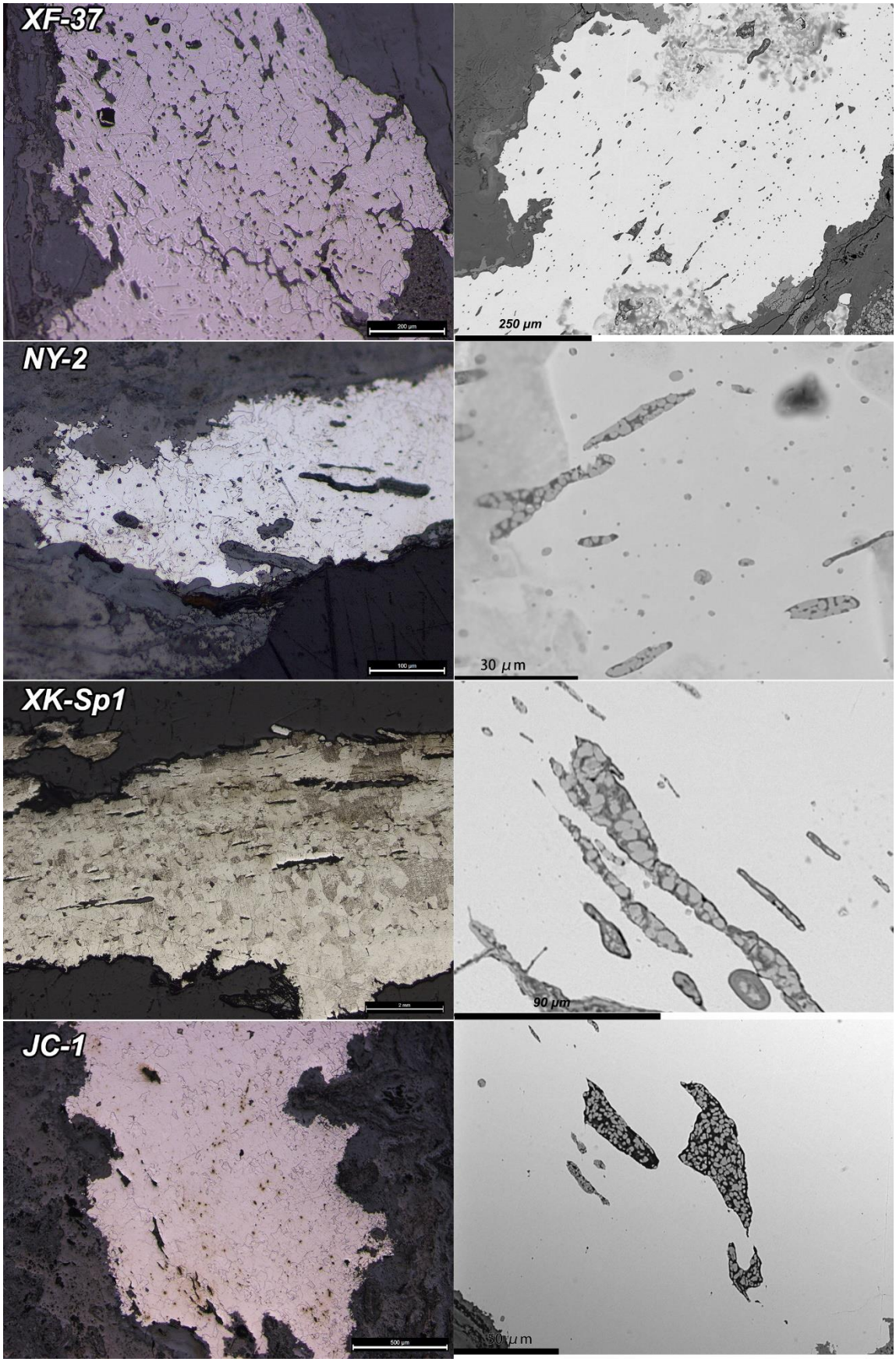

Figure 4.20 Metallography (left) and back-scattered electron image (right) of samples XF-37, NY-2, XK-Sp1 and JC-1

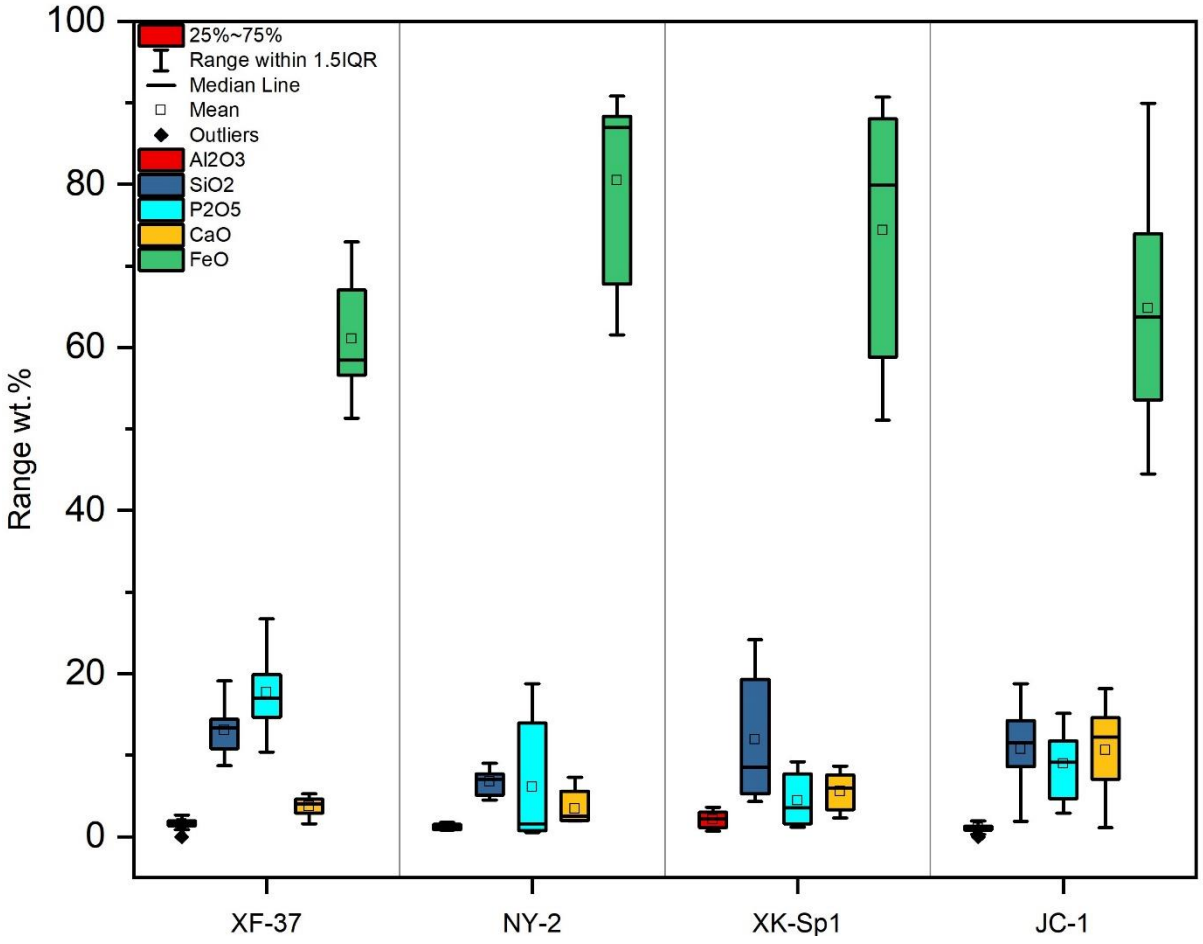

Figure 4.21 Box-whisker plot of Al_2O_3, SiO_2, P_2O_5, CaO and FeO content from sample XF-37, NY-2 and XK-Sp1and JC-1

4.2.2 Group 2

For samples in group 2, a detailed visual examination of the metallographic structure, combined with back-scattered electron images of those inclusions were carried out. This step is aimed at primarily recognising slag inclusion families based on their morphology and distribution pattern. Following this, statistical analysis of their chemical composition is carried out to further examine potential sub-groups.

Two main approaches to the analysis of SI compositional data were employed: an exploration of the non-reduced compounds (NRC), mainly using bivariate scatterplots to investigate correlations among these; and principal component analysis (PCA) of the main oxides. If both analyses showed a consistent group without noticeable

subgroups, i.e., if most of the SI analysed formed a coherent group, it was considered that they had the same material origin, and they could be analysed altogether as indicative of the underlying technical process. Conversely, if clear separation in compositional sub-groups was observed, further data treatment was carried out to assess if such separation was based primarily on NRC differences (hence indicating different material sources) or based on reducible compounds (hence indicative of different redox conditions). Additionally, a data screening process was applied to identify those inclusions that were deemed not to contain significant information regarding the production techniques. These approaches are briefly outlined below.

The method of NRC ratio analysis raised by Philippe Dillmann and Maxime L'Héritier (2007) was first applied. NRC refers to those oxides in the iron smelting system that cannot be reduced under normal conditions or tend to be re-oxidised by the end of the process. Much of the work by these authors is based on the premise that the slag inclusions derived from the same smelting system (including smelting, refining and fining) are based on the same material sources (i.e., gangue, furnace linings, fluxes, fuel ash etc.) and underwent the same set of technical processes. While the absolute concentration of such oxides will fluctuate due to heterogeneous redox conditions, where at certain parts more iron will be reduced or oxidised, causing the change of the concentration of rest oxides in the resulting slag, owing to the similar chemical stability of the NRC under the iron smelting condition, the ratios among these compounds will remain largely constant. If new inclusions are formed or introduced during subsequent technical steps such as smithing/forging, without being homogenised with the original inclusions, such ratios may vary between the original and new inclusions. In addition, during the manufacturing process, if the object was subjected to repeated working,

slag inclusions will be shattered into small particles, in which case, the localised concentration effect may also introduce variations on the NRC ratios.

The compounds used for NRC analysis usually are MgO, Al_2O_3, SiO_2, K_2O and CaO, when present in sufficient amount. To statistically analyse these components and account for their variability, enough representative data needs to be collected. Dillmann and L'Héritier (2007) recommended at least 40 slag inclusions in each area of interest should be analysed, yet in this research, some of the samples analysed do not have enough slag inclusions available for analysis, either due to the limited sample size or the overall scarcity of slag inclusions distributed in the metal matrix, hence the lower limit is set at 20 inclusions. Combinations of MgO vs Al_2O_3, Al_2O_3 vs SiO_2, K_2O vs CaO and SiO_2 vs CaO was used to create bivariate scatterplots when these oxides were mostly presented in sufficient amount.

Principal Component Analysis (PCA) is another statistical method used to explore for structure in a multivariate dataset. It can convert a set of correlated variables into a smaller set of variables which are linearly uncorrelated. The products of this procedure, known as “principal components”, or PC, are a linear combination of the original variables. The number of such components is usually same or less than the original variables. The first principal component accounts for most of the variability, and each of the subsequent components represents less. Under most circumstances, the first two or three can represent at least 70% percent of the variance (Charlton 2007). This is also the case for this research, where the first two PCs usually add up to more than 75% of all variances, hence only the loading plot of PC1 and PC2 will be used in this research to recognise potential subgroups on a multivariate basis. The variables used for PCA analysis includes the NRC (including MgO, Al_2O_3, SiO_2, K_2O and CaO) along with the P_2O_5 and FeO content, which are “reducible” in the iron smelting condition.

The value of 0.1 wt.% was used instead of 0 when the above oxides were below detection limit.

Sample XF-27, adze

Sample XF-27 contains four types of slag inclusions, each of them located in different zones (Figure 4.22). To begin with, glassy silicate inclusions (type-a, 16 analysed) with low FeO content (mostly lower than 10 wt.%) are distributed in Zone 1. Then there are fayalitic inclusions (type-b, 12 analysed) distributed near the welding line which separated the metal matrix into two conjunctive parts (Figure 4.22). These fayalitic inclusions are quite probably derived from sand additives used during welding of these two parts, as their chemical component are predominantly Al_2O_3, SiO_2 and FeO, making up to 95 wt.%. Beyond the welding line, in the small piece of iron attached to the main body (Zone 2), a small number of glassy silicate inclusions with fayalite crystals were also analysed (type-c, 10 analysed). These inclusions have slightly higher FeO content (around 20 wt.%) compared to the glassy silicates in Zone 1. In the centre of the matrix, large iron oxide inclusions were also found. In addition, a small number of an unknown type of inclusions with exceptionally high P_2O_5 and CaO were also analysed (type-d, Zone 3, Figure 4.23).

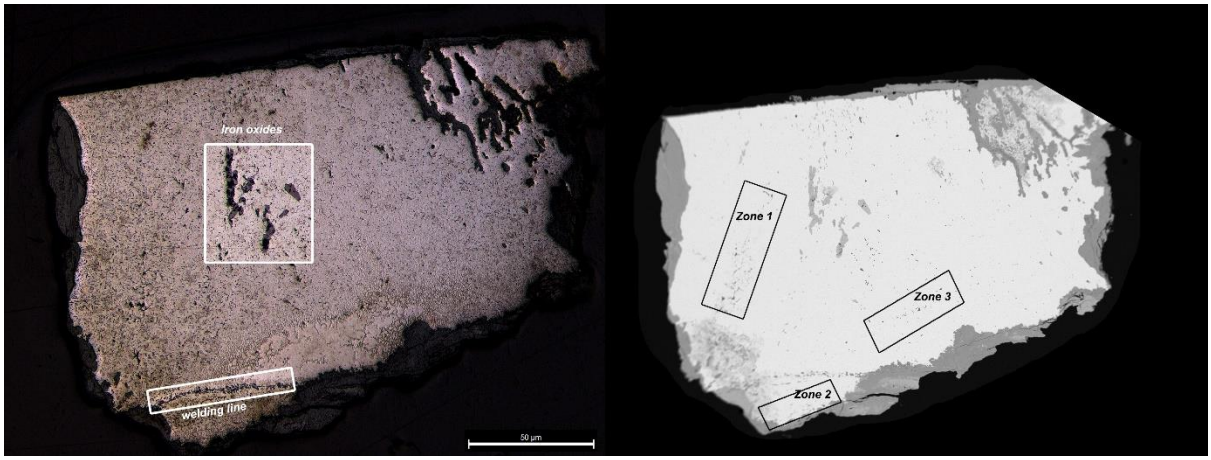

Figure 4.22 Metallograph and back-scattered image of sample XF-27

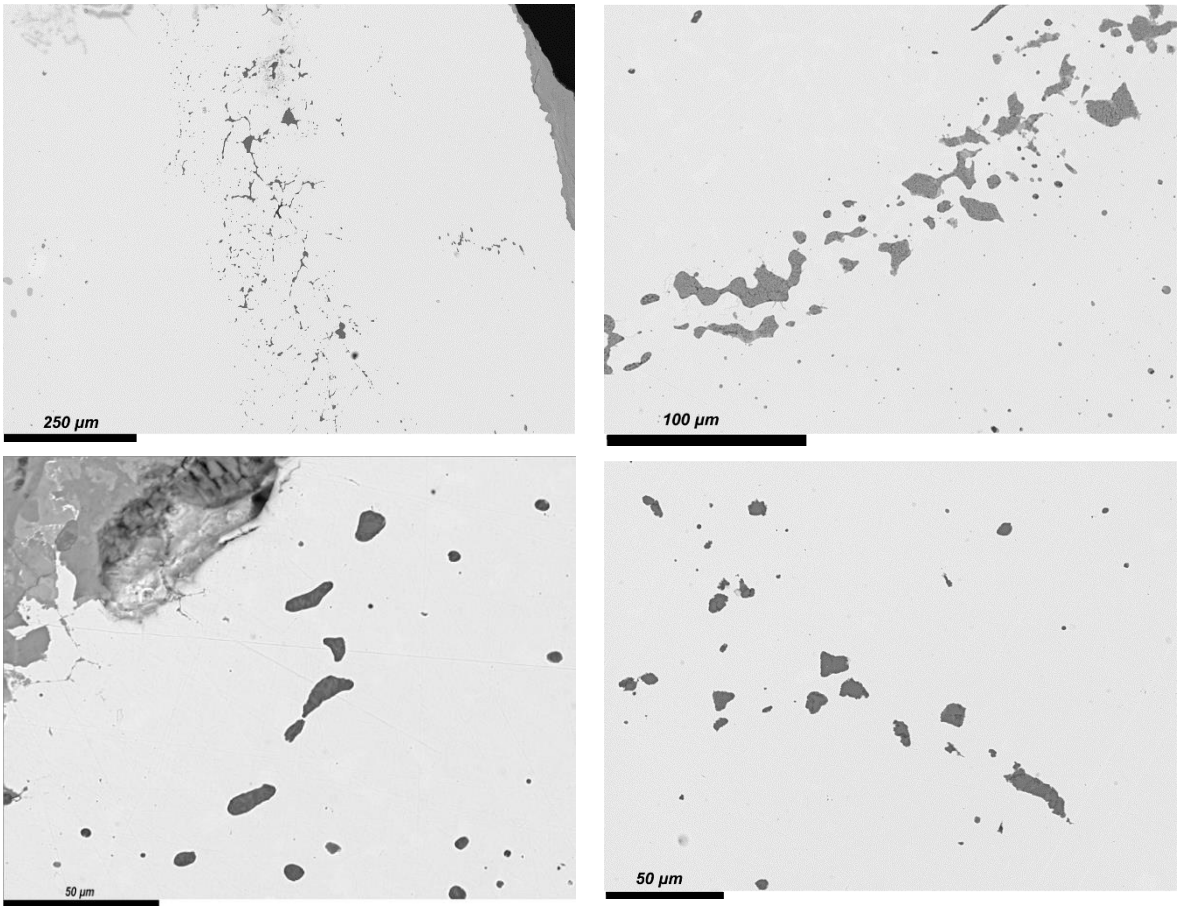

Figure 4.23 Back-scattered image of slag inclusions in sample XF-27. Top left, glassy silicates in Zone 1; Top right, slag inclusions in the welding line, possibly derived from smithing process; Bottom left, glassy silicates in Zone 2; Bottom right, unknow type of inclusions in Zone 3.

Before any further data treatment process, the fayalitic inclusions located near the welding line, and the large iron oxide inclusions in the centre, were excluded from the analysis as it is clear that they do not represent the possible source of the iron or the manufacturing technique. The rest of the inclusions from three different zones were then subjected to more data analysis.

NRC analysis is first carried out using MgO vs Al_2O_3, Al_2O_3 vs SiO_2 , SiO_2 vs CaO and K_2O vs CaO, the results are presented in Figure 4.24.

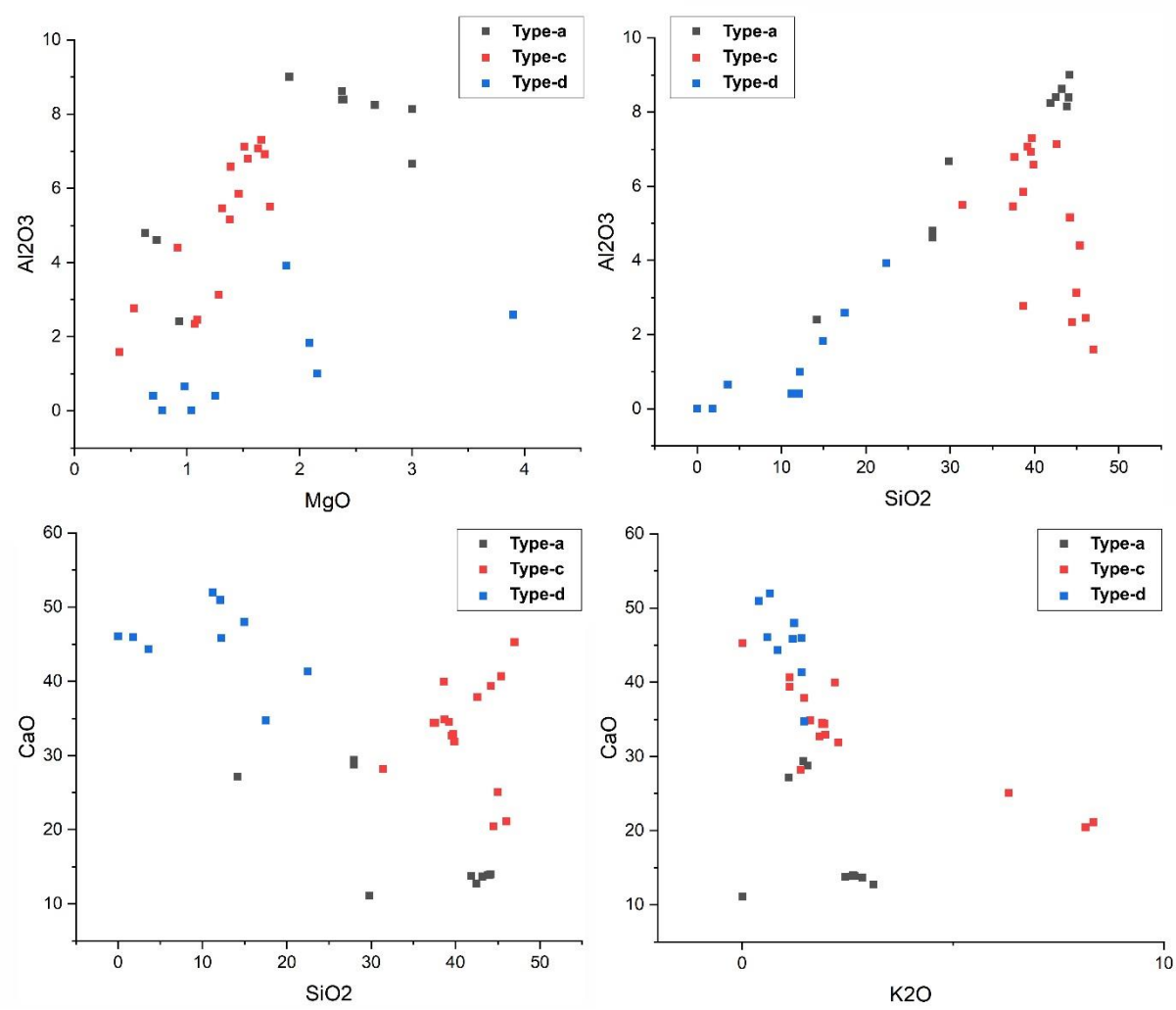

Figure 4.24 Bivariate plots of NRC compounds from sample XF-27 using MgO vs Al_2O_3, Al_2O_3 vs SiO_2, SiO_2 vs CaO and K_2O vs CaO

PCA was then carried out using the concentrations of MgO, Al_2O_3, SiO_2, P_2O_5, K_2O, CaO and FeO as variables. The results again confirmed these three groups of slag inclusions are largely separated. Since no linear correlation is shown in the NRC analysis either, it seems safe to assume these three groups of inclusions could be representing different material sources or technical processes. Based on their chemical composition, it appears slag inclusions in Zone 1 and Zone 2 represents two pieces of iron from different sources. Slag inclusions in Zone 3 are predominantly composed of CaO (34-50 wt.%) and P_2O_5 (18-44 wt.%), which could be the result of a highly localised oxidising condition along with the use flux such as limestone, hence

should not be considered as the slag inclusions representing the source of material or production technique.

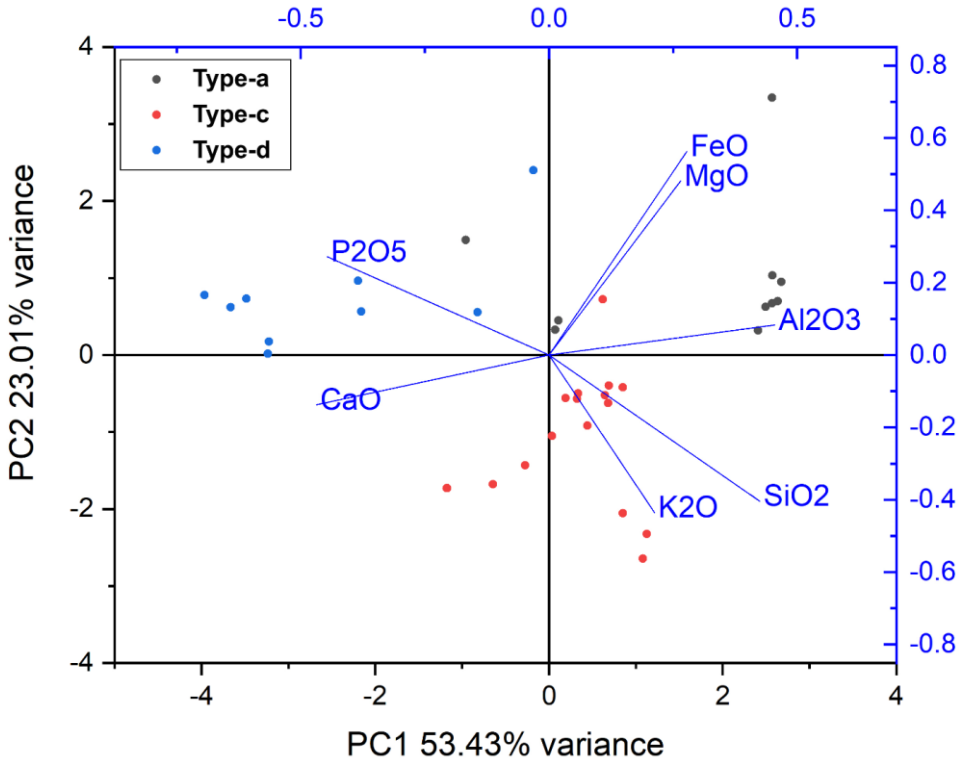

Figure 4.25 PCA plot of SI compositions in sample XF-27

Sample XF-28, adze

Slag inclusions in sample XF-28 are mostly concentrated in two areas, corresponding to the top left and the bottom right part in Figure 4.26, with large iron oxide inclusions in the middle, all linearly distributed towards the edge. In this sample, only the smaller inclusions, mostly glassy silicates and fayalitic inclusions with wüstite crystals, were analysed, whereas the large iron oxide inclusions in the middle were excluded from the analysis since these inclusions do not contain information related to the production techniques.

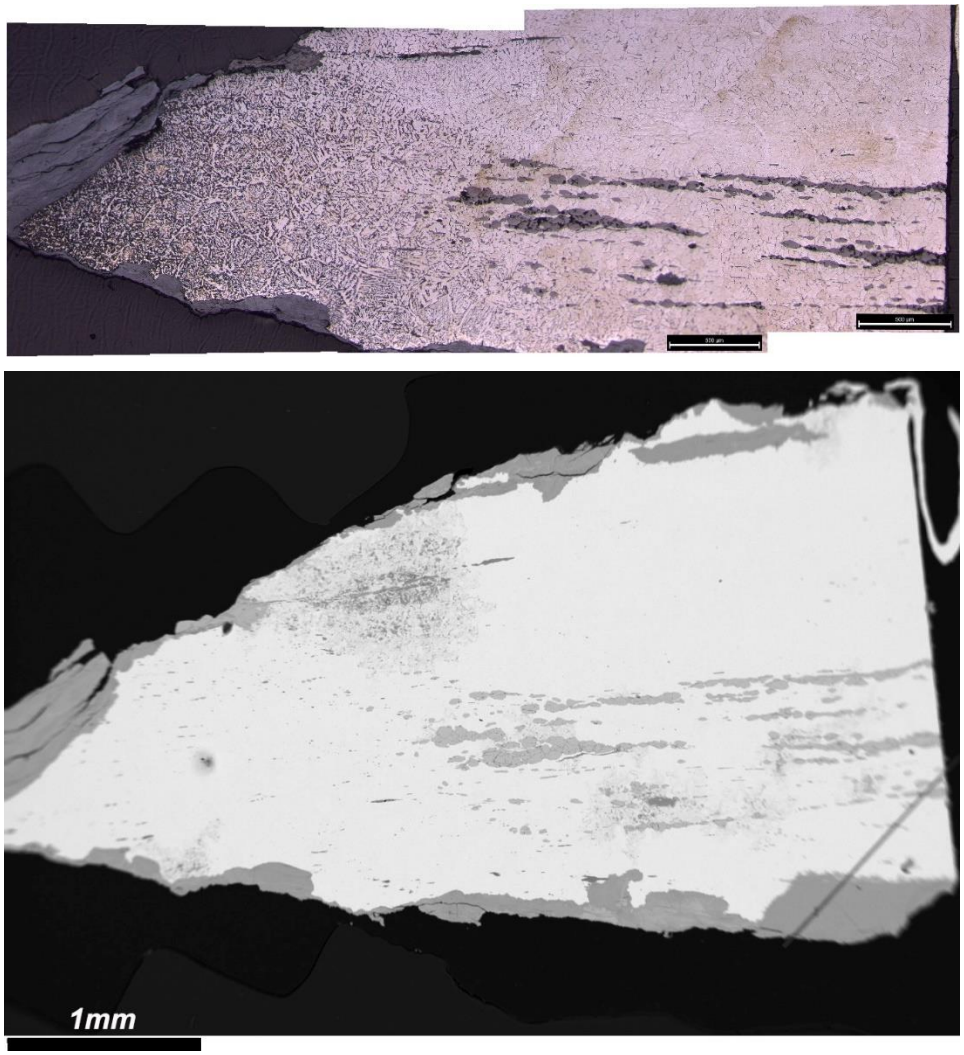

Figure 4.26 Metallography (top) and back-scattered electron image (bottom) of sample XF-28

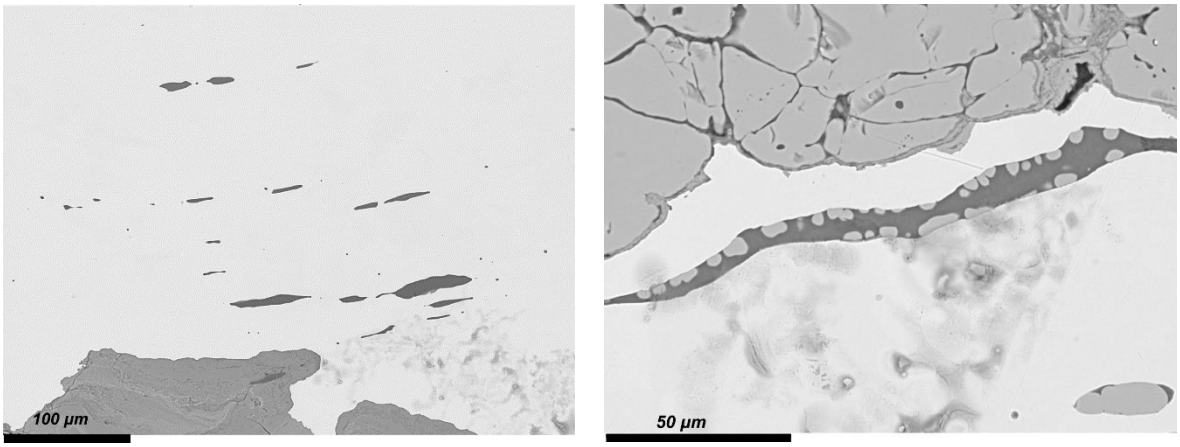

Figure 4.27 Back-scattered electron images of slag inclusions in sample XF-28, glassy silicates (left) and fayalitic with wüstite crystals (right)

Since MgO is not present in sufficient amounts (26 out of 35 inclusions contains detectable amount of MgO), only the combination of Al_2O_3 vs SiO_2, SiO_2 vs CaO and

K_2O vs CaO were used for NRC analysis. The results show these inclusions are generally linearly correlated, with CaO vs SiO_2 showing a more scattered distribution (Figure 4.28).

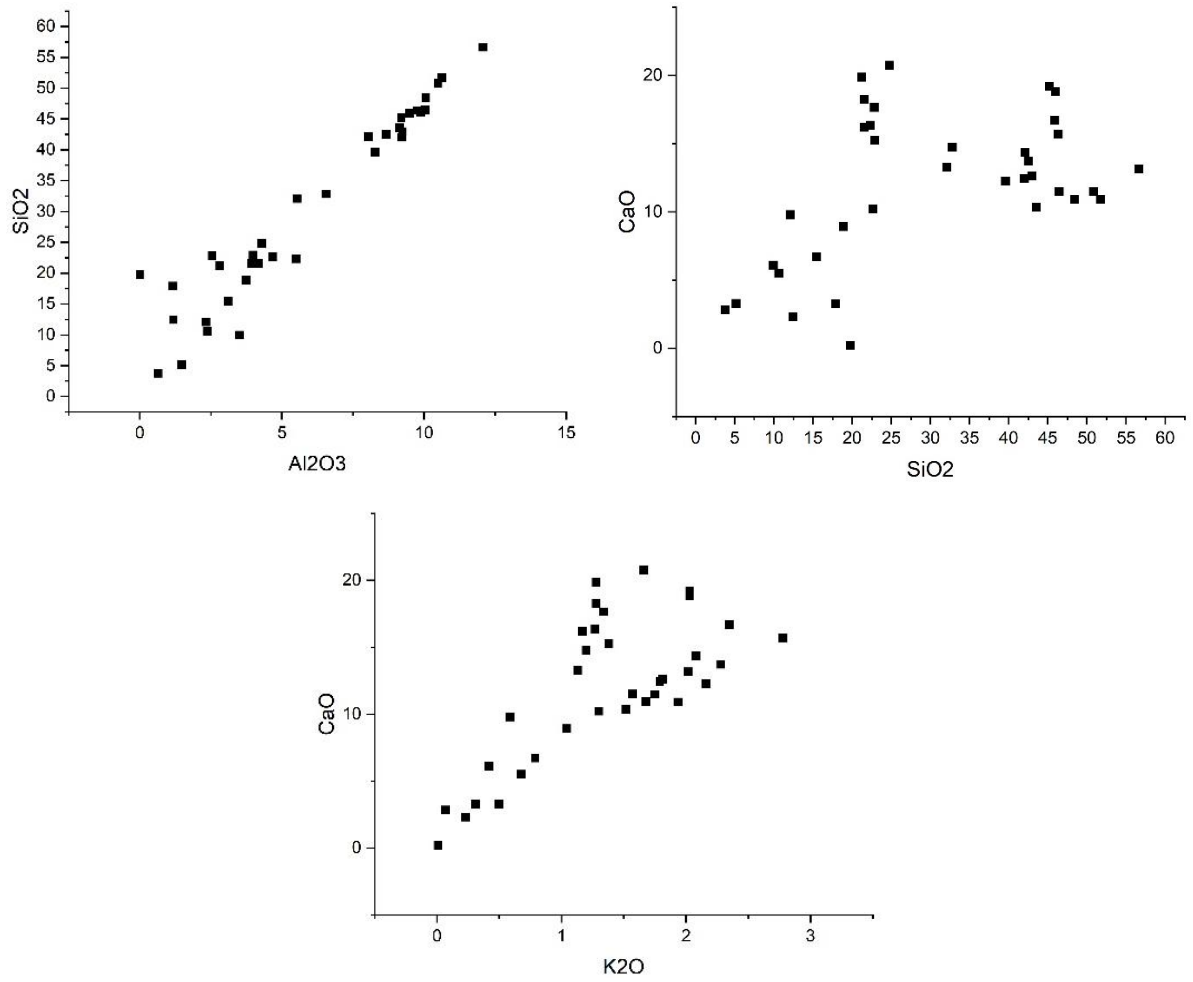

Figure 4.28 Bivariate plots of NRC compounds from sample XF-28 using Al_2O_3 vs SiO_2, SiO_2 vs CaO and K_2O vs CaO

Following NRC analysis, PCA was carried out to examine if sub-groups could be identified (Figure 4.29). Although some outliers may be present, the result show no clear separation among these inclusions, indicating they are mostly derived from the same source.

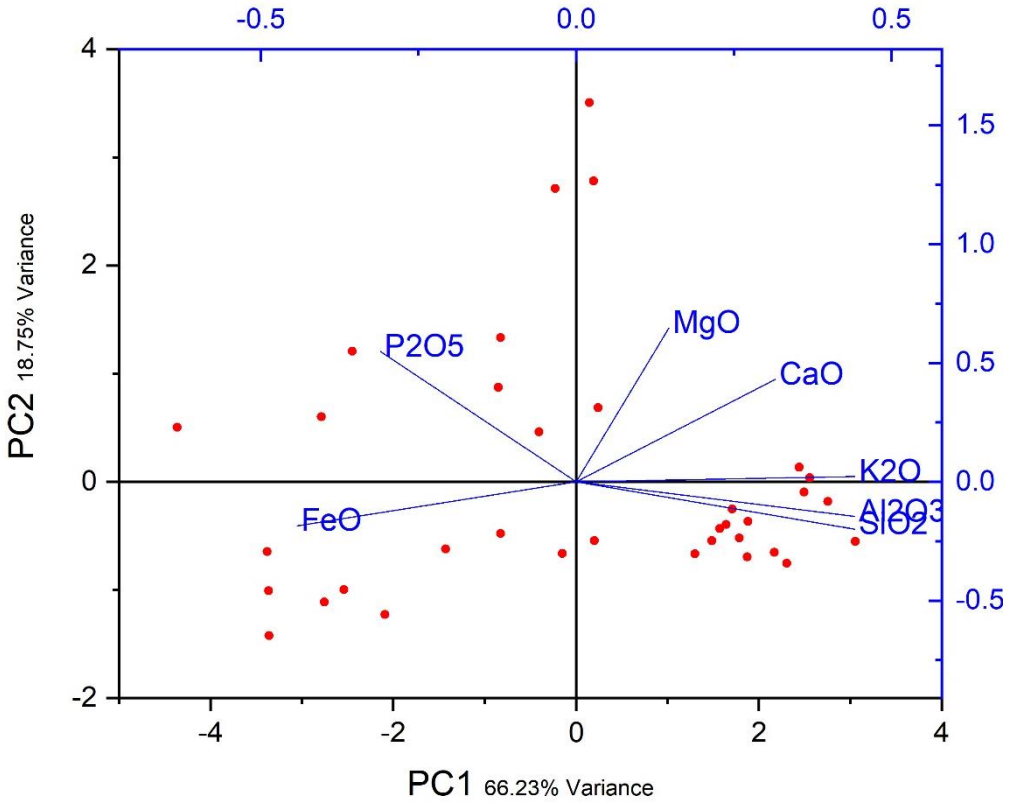

Figure 4.29 PCA plot of SI compositions from sample XF-28

Sample XF-F17, awl

Sample XF-F17 contains slag inclusions randomly distributed in the matrix, mostly glassy silicates and fayalitic inclusions with wüstite crystals (Figure 4.30). NRC analysis (Figure 4.31) shows that most of them are linearly correlated, indicating these inclusions are most likely from the same material source. PCA analysis shows these inclusions are separated into two families, with one family containing higher FeO and P_2O_5 than the other (Figure 4.32). By removing these two variables (FeO and P_2O_5) and re-normalising the NRC components, such separation can no longer be seen (Figure 4.33), confirming that the major difference between these groups of inclusions is the concentration of FeO and P_2O_5, which can be easily affected by the redox condition, hence these inclusions are considered from same material source yet chemically modified by the inhomogeneous reaction condition.

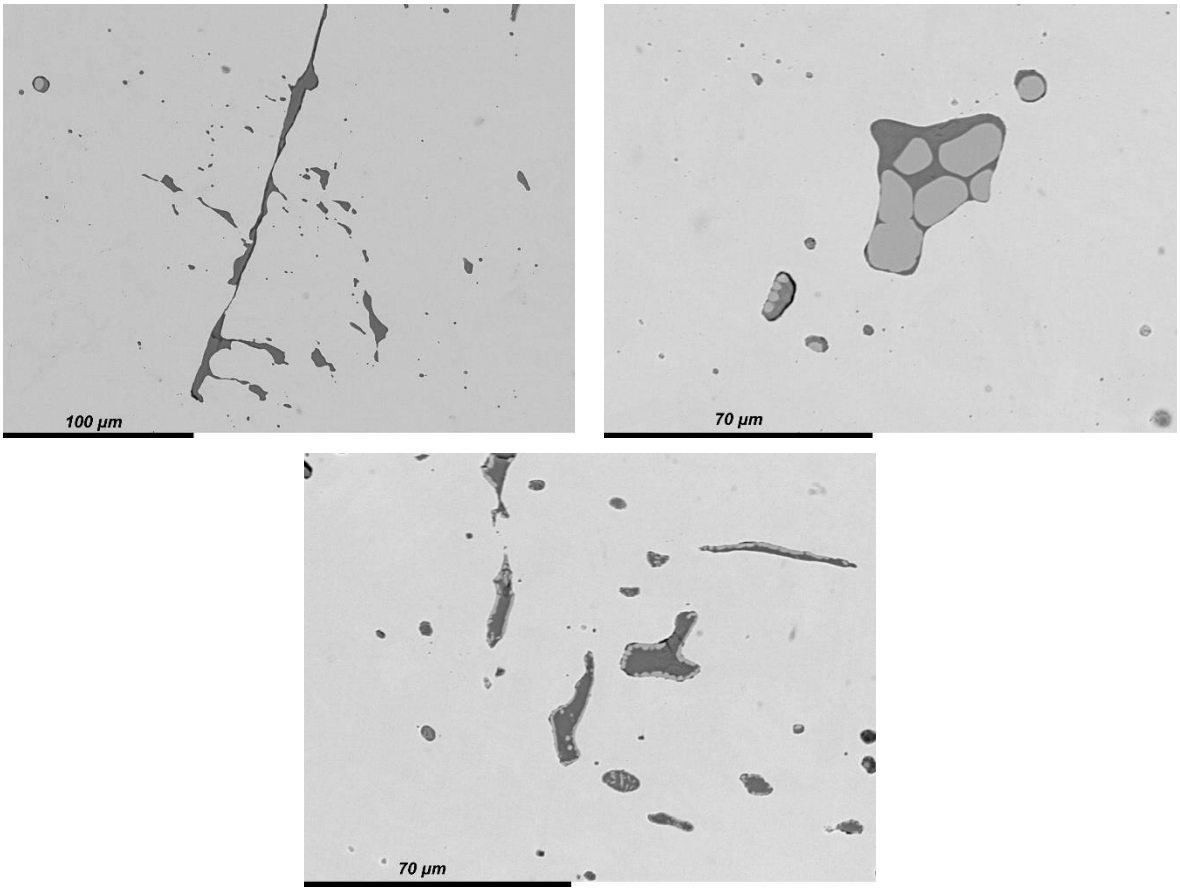

Figure 4.30 Back-scattered electron image of slag inclusions in sample XF-F17, glassy silicates (top left) and fayalitic with wüstite (top right and bottom)

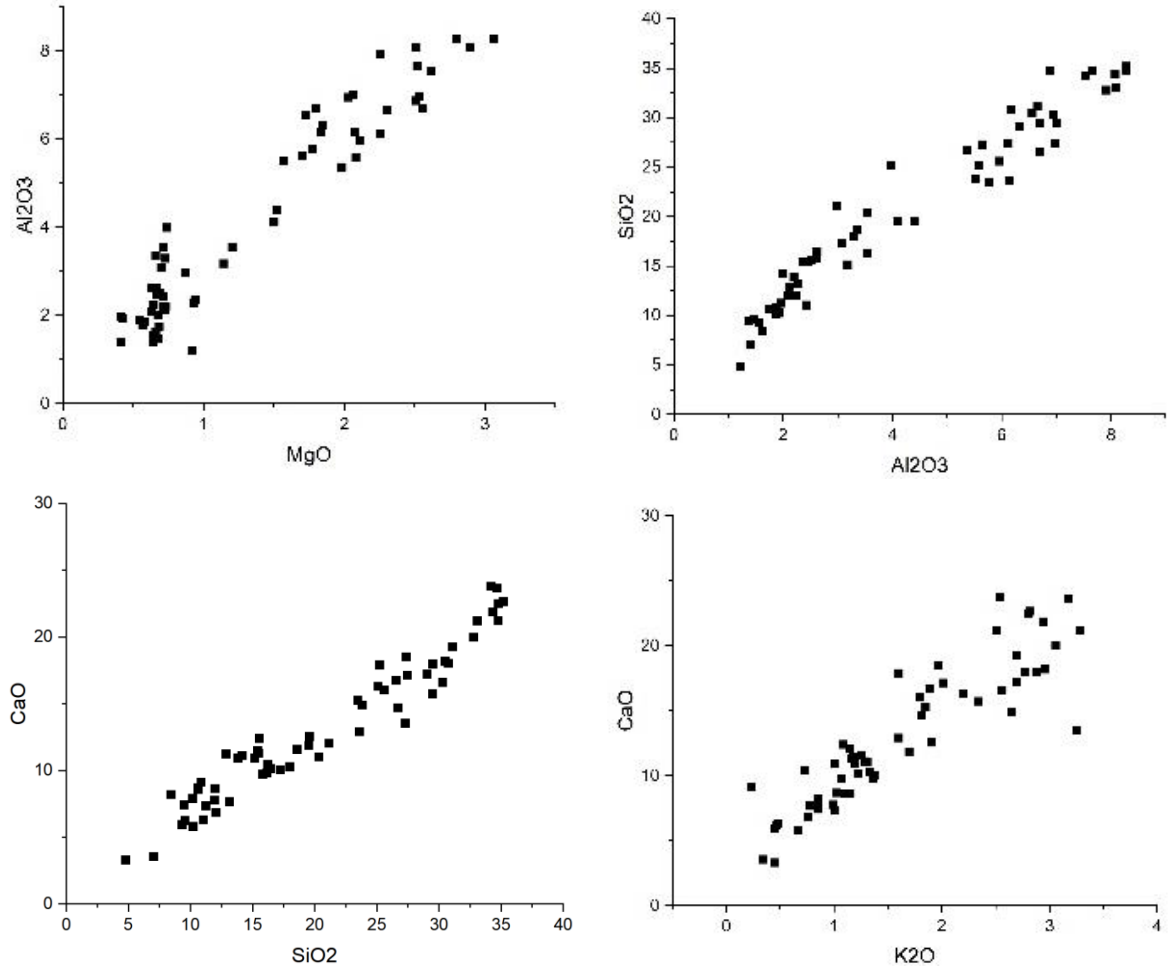

Figure 4.31 Bivariate plots of NRC compounds from sample XF-F17 using MgO vs Al_2O_3, Al_2O_3 vs SiO_2, SiO_2 vs CaO and K_2O vs CaO

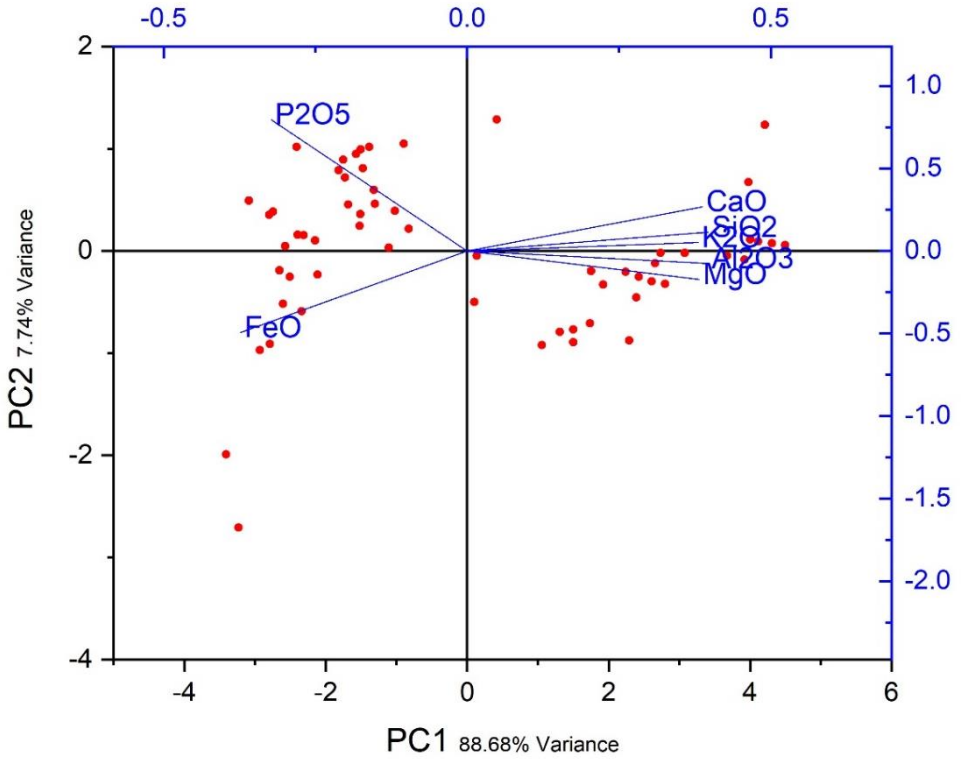

Figure 4.32 PCA plot of SI compositions from sample XF-F17, before re-normalisation

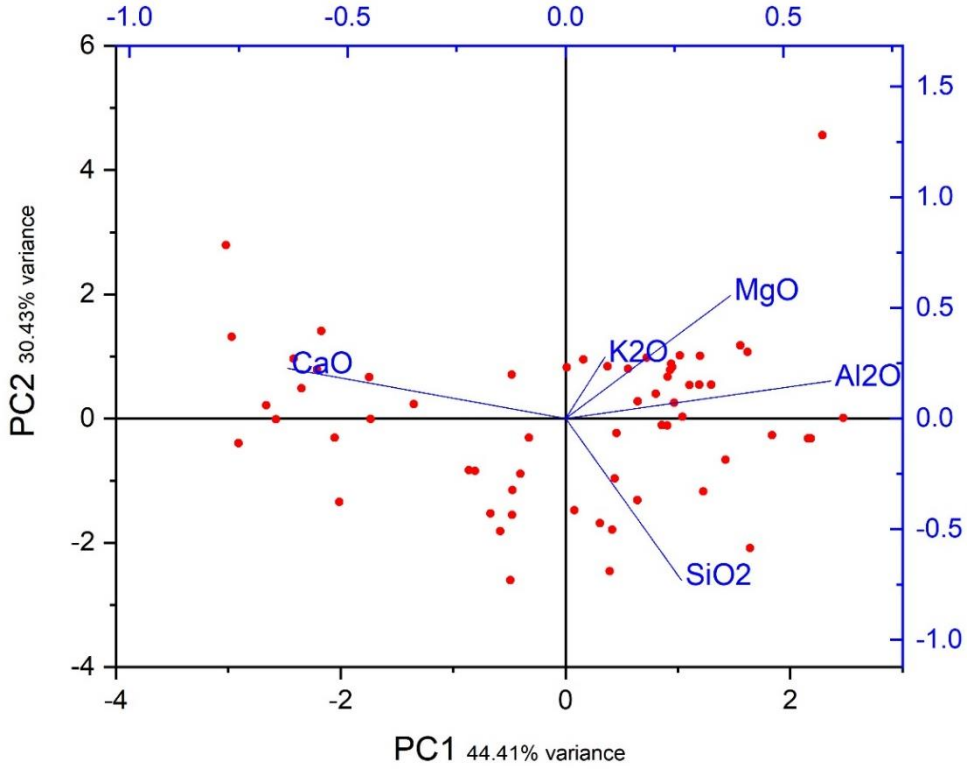

Figure 4.33 PCA plots of SI compositions from sample XF-F17 after re-normalisation

Sample XF-F19, chisel

Slag inclusions in sample XF-F19 are mostly glassy silicates and fayalitic inclusions with wüstite crystals. NRC analysis did not reveal strong linear correlations except for Al_2O_3 vs SiO_2, but in general these oxides are positively correlated. The wides spread could be the result of repeated working, which may have resulted in localised concentration effects (Dillmann and L'Héritier 2007). PCA analysis did not show clear sub-groups either, with the main difference among inclusions simply being the variable concentration of FeO, hence these inclusions will be considered from the same material source.

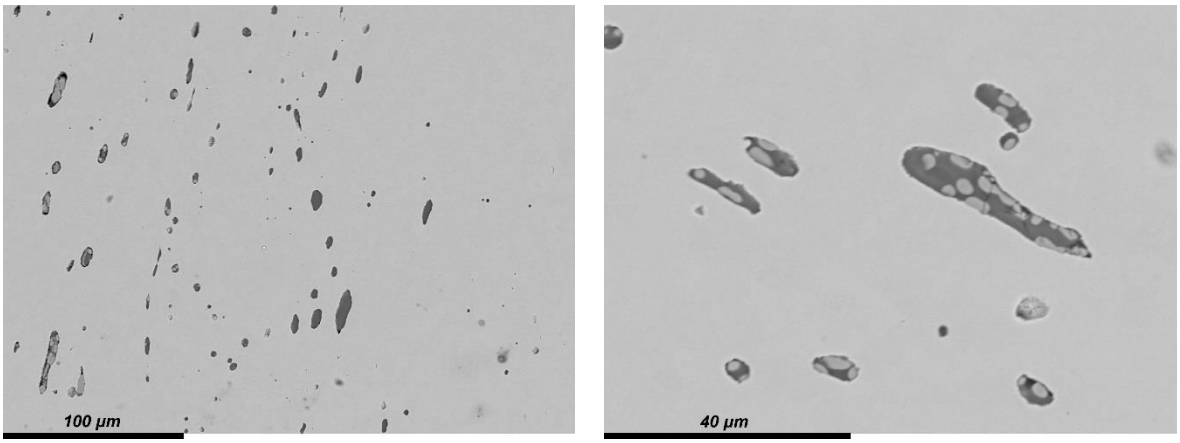

Figure 4.34 Back-scattered electron image of slag inclusions in sample XF-F19

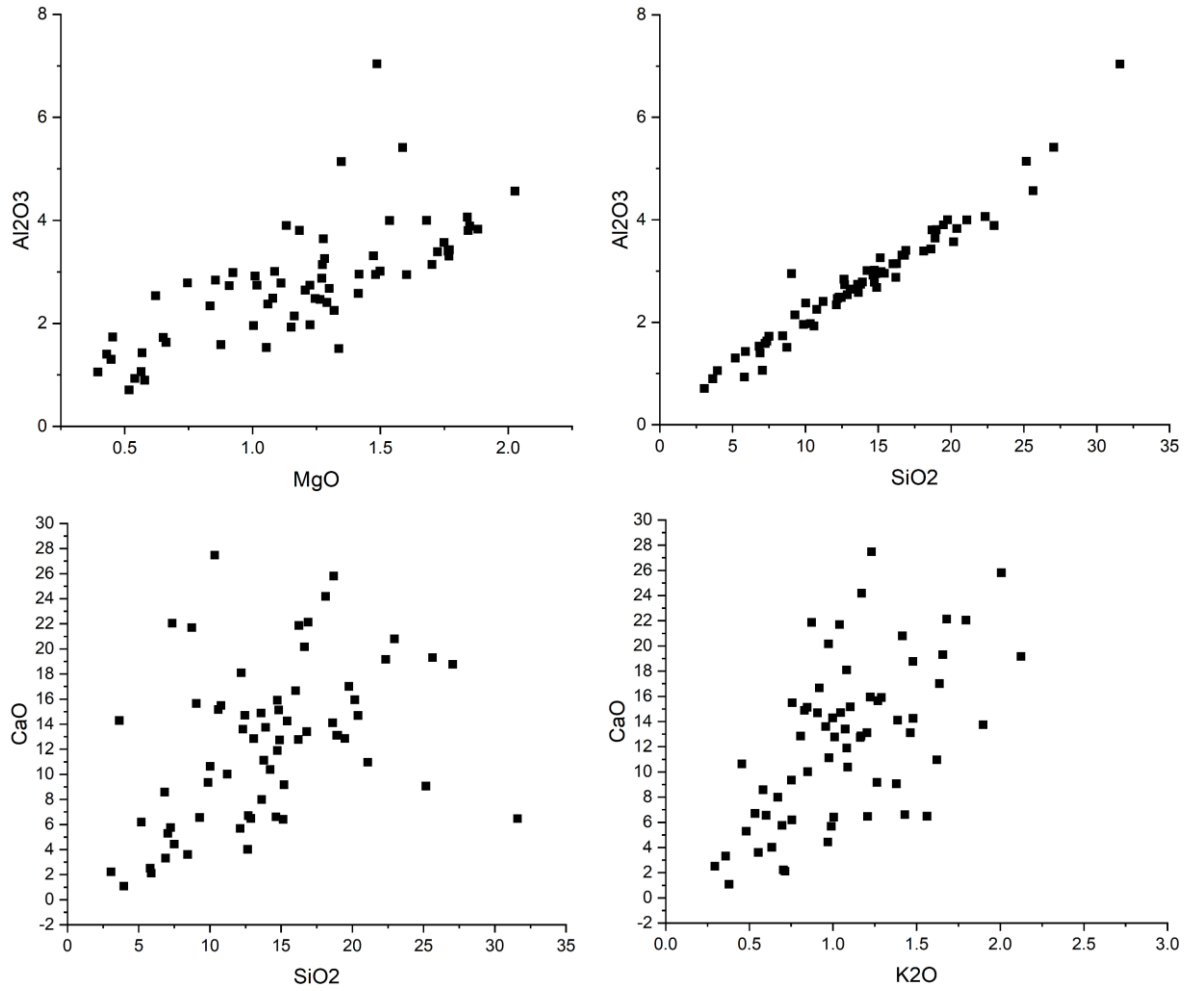

Figure 4.35 Bivariate plots of NRC compounds from sample XF-F19 using MgO vs Al_2O_3, Al_2O_3 vs SiO_2, SiO_2 vs CaO and K_2O vs CaO

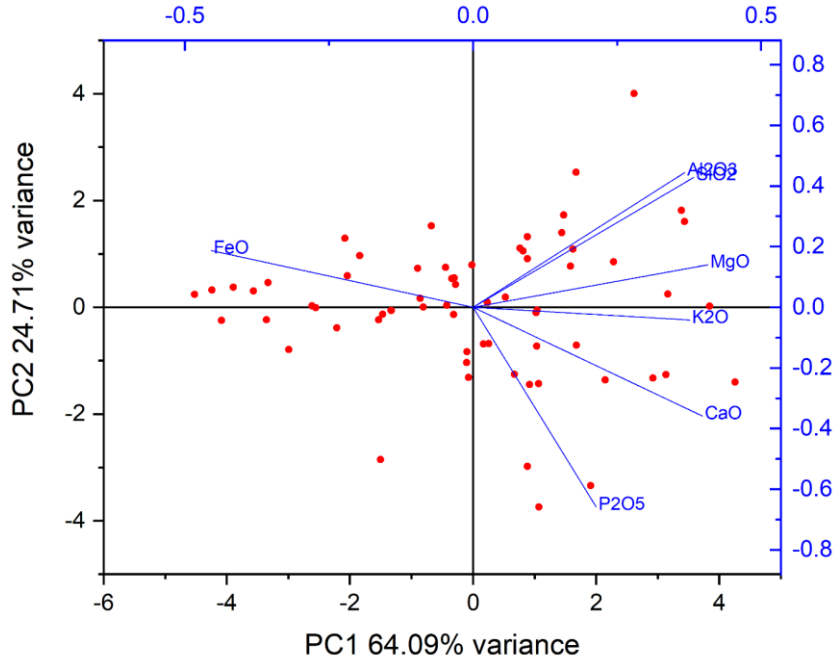

Figure 4.36 PCA plot of SI composition from sample XF-19

Sample XF-F26, spoon

The slag inclusions in sample XF-F26 can be separated into two types based on their morphology and distribution: highly elongated silicates (type-a) and fayalitic inclusions with occasional wüstite (type-b) (Figure 4.37); these two types of inclusions can also be separated based on their chemical compositions, as shown in the NRC analysis (Figure 4.38) and the PCA plot (Figure 4.39).

Since the MgO concentration in fayalitic inclusions is below detection limit, MgO vs Al_2O_3 is excluded from the NRC analysis. The NRC analysis shows the two types of inclusions form two distinct clusters, without evident linear correlation between them. PCA analysis equally indicates these inclusions were divided into two families, with the type-b inclusions containing much higher FeO and P_2O_5 content, and type-a richer in NRC components.

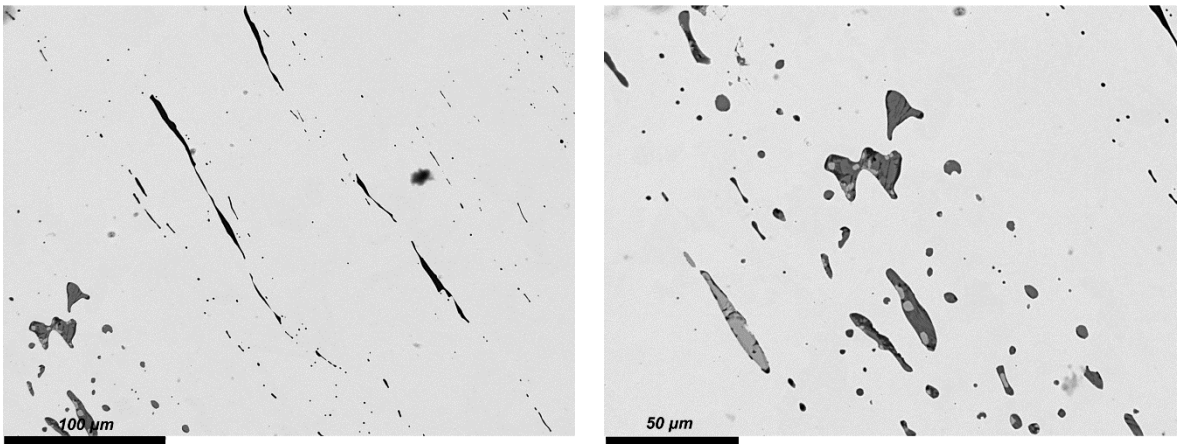

Figure 4.37 Back-scattered electron image of slag inclusions from sample XF-F26, glassy silicates (left) and fayalitic with wüstite crystals (right)

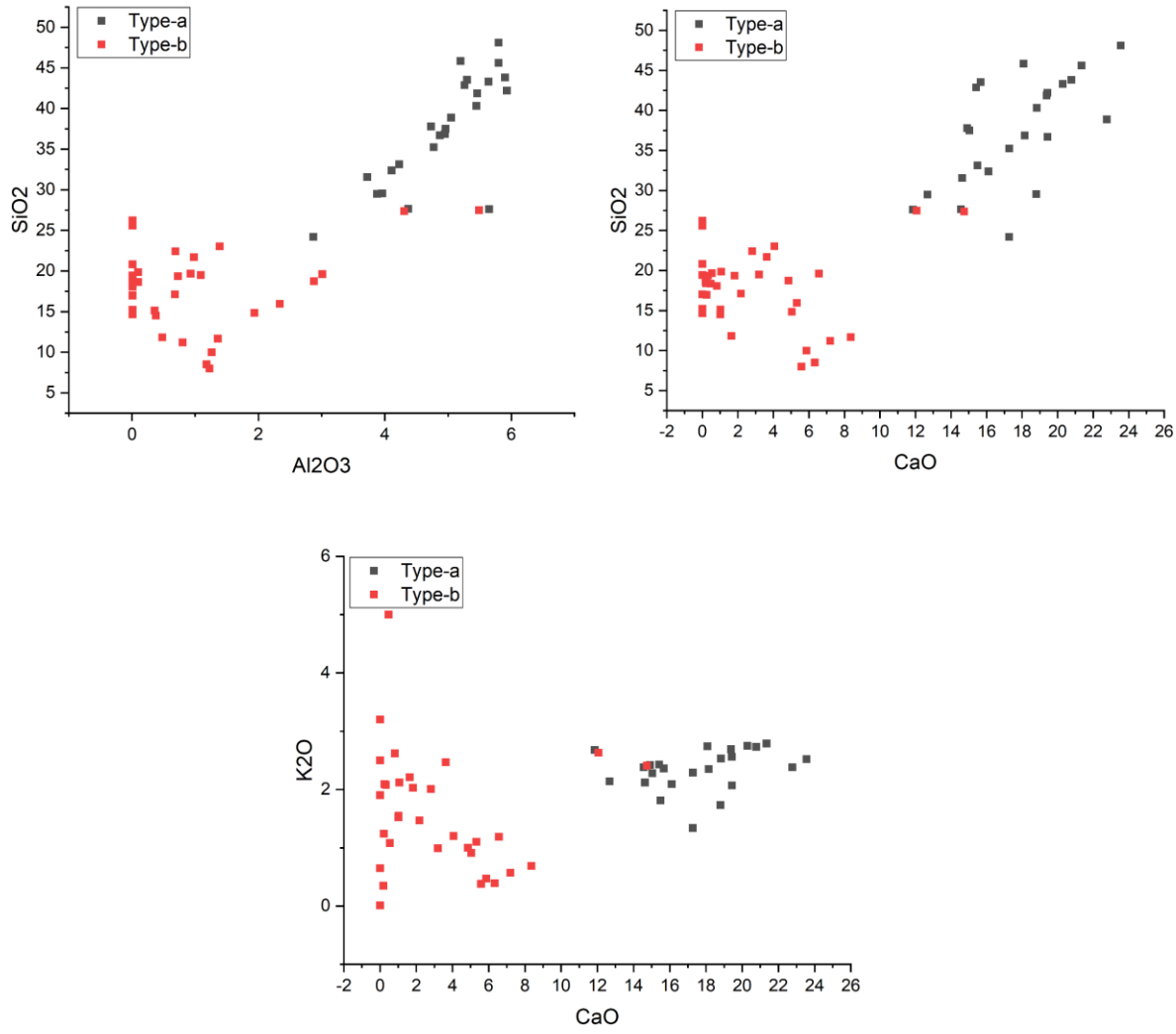

Figure 4.38 Bivariate plots of NRC compounds from sample XF-F26 using Al_2O_3 vs SiO_2, SiO_2 vs CaO and K_2O vs CaO, before re-normalisation

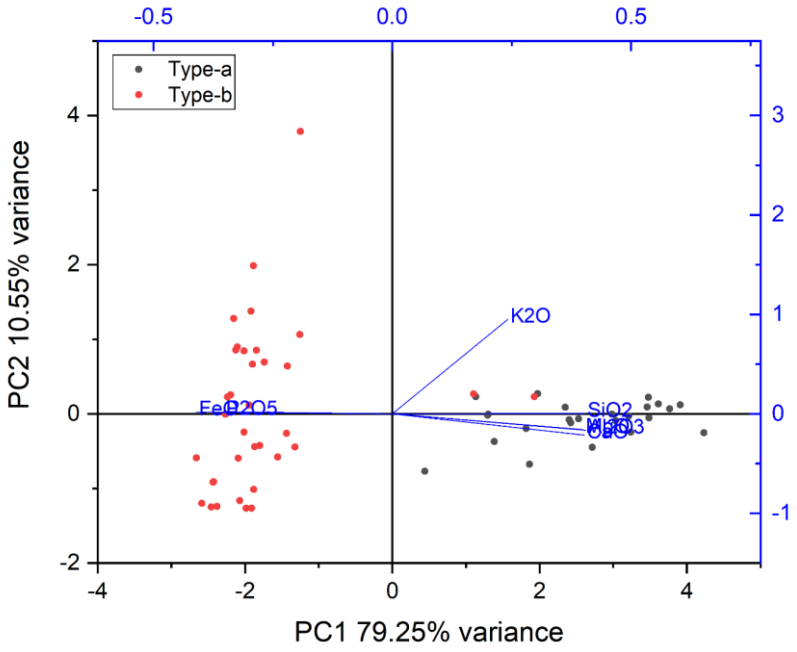

Figure 4.39 PCA plot of SI composition from sample XF-F26, before re-normalisation

In order to neglect the effects of FeO and P_2O_5 fluctuation owing to heterogeneous redox condition, NRC compounds, including MgO, Al_2O_3, SiO_2, K_2O and CaO, were re-normalised and analysed again: the results of NRC and PCA analysis shows that despite some overlap between these two types of inclusions, overall, these inclusions are still distinctively separated, indicating a different material or technological origin for each group (Figure 4.40, 4.41).

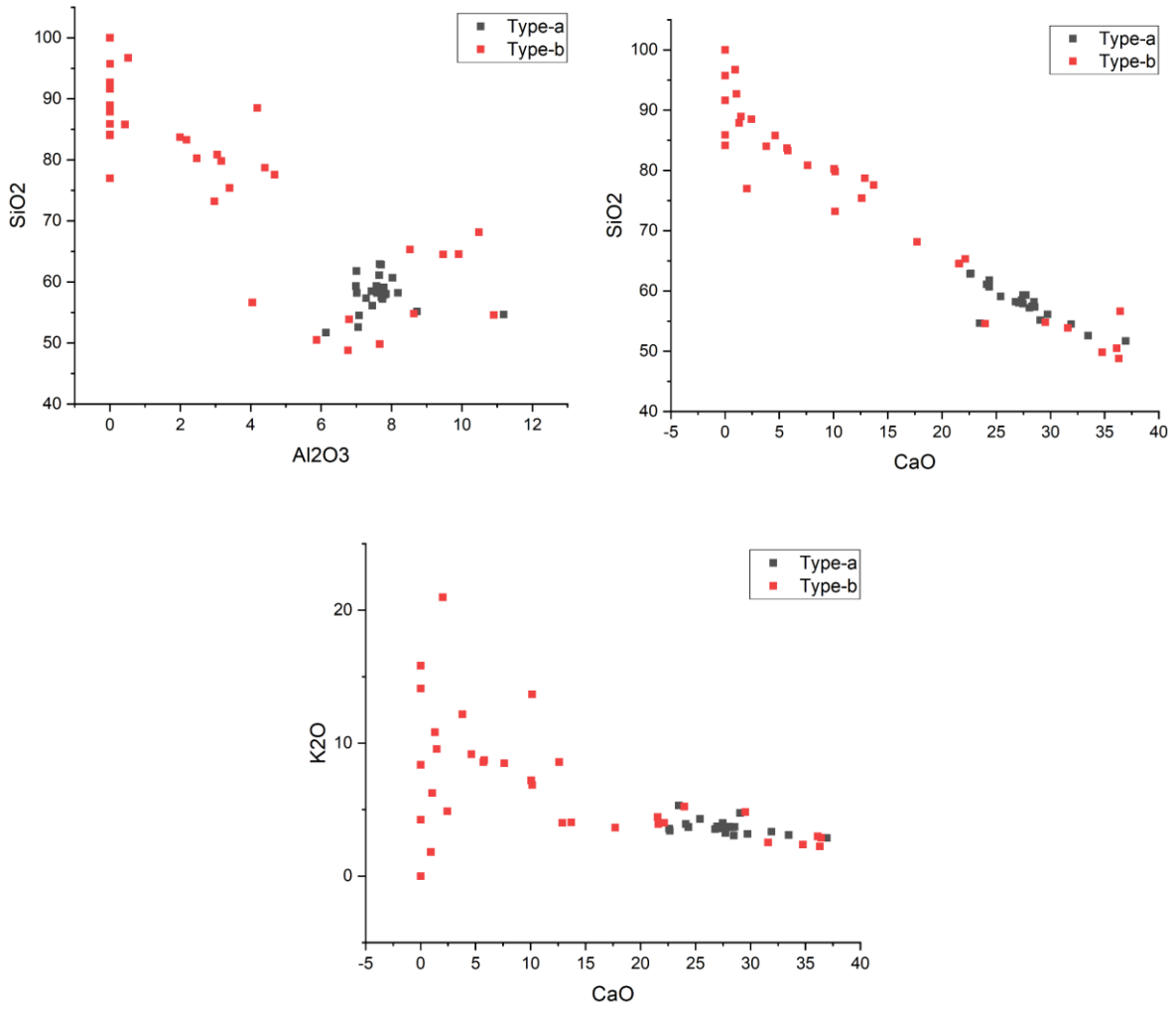

Figure 4.40 Bivariate plots of NRC compounds from sample XF-F26 using Al_2O_3 vs SiO_2, SiO_2 vs CaO and K_2O vs CaO, after re-normalisation

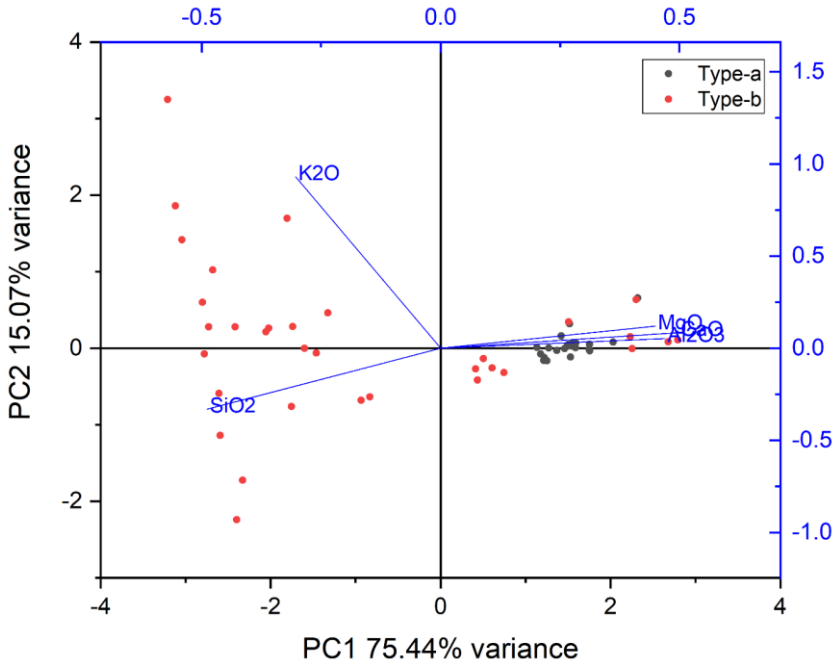

Figure 4.41 PCA plot of SI composition from sample XF-F26, after re-normalisation

Sample NJG-11, chisel

Sample NJG-11 contains a small amount of glassy silicate inclusions and fayalitic inclusions with wüstite crystals (Figure 4.42, 4.43). NRC analysis shows the majority of them are linearly correlated (Figure 4.44). While the PCA plot shows these inclusions can be separated into two groups based on difference of the FeO and P_2O_5 concentration (Figure 4.45). By removing these two variables and re-normalising the NRC components, the separation between them becomes much more blurred (Figure 4.46), hence these inclusions will be considered to derive from the same material source even if subsequently affected by variable redox reactions.

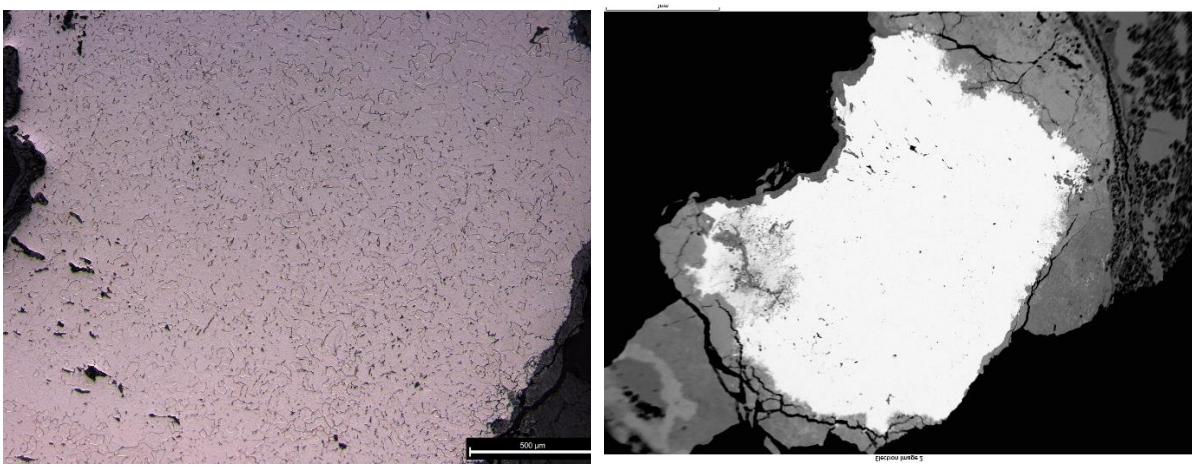

Figure 4.42 Metallography (left) and back-scattered electron image (right) of sample NJG-11

Figure 4.43 Back-scattered electron image of inclusions from sample NJG-11

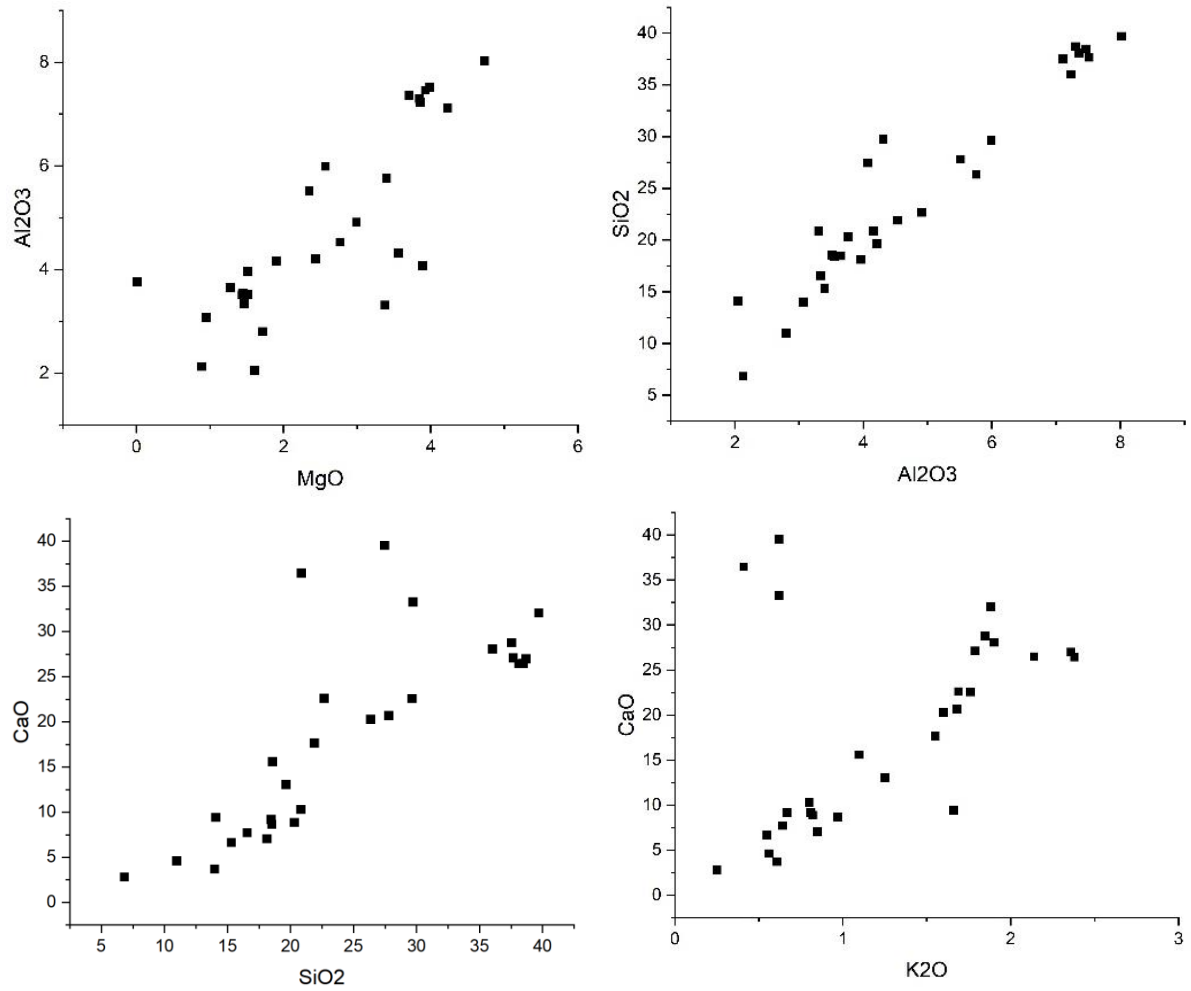

Figure 4.44 Bivariate plots of NRC compounds from sample NJG-11 using MgO vs Al_2O_3, Al_2O_3 vs SiO_2, SiO_2 vs CaO and K_2O vs CaO

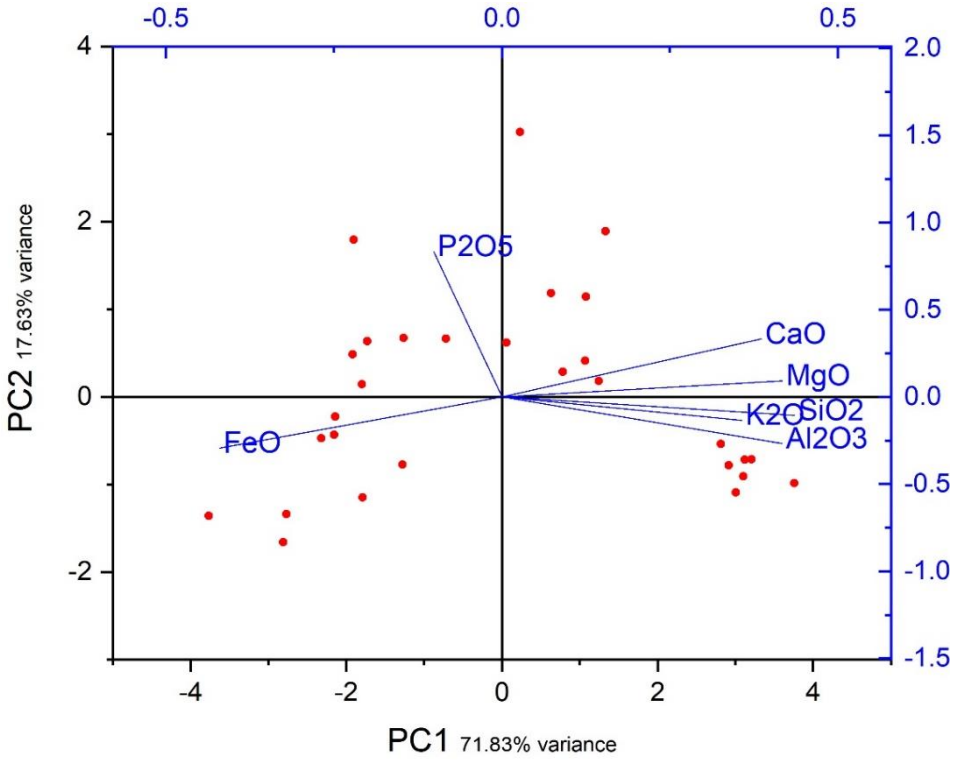

Figure 4.45 PCA plot of SI composition from sample NJG-11, before re-normalisation

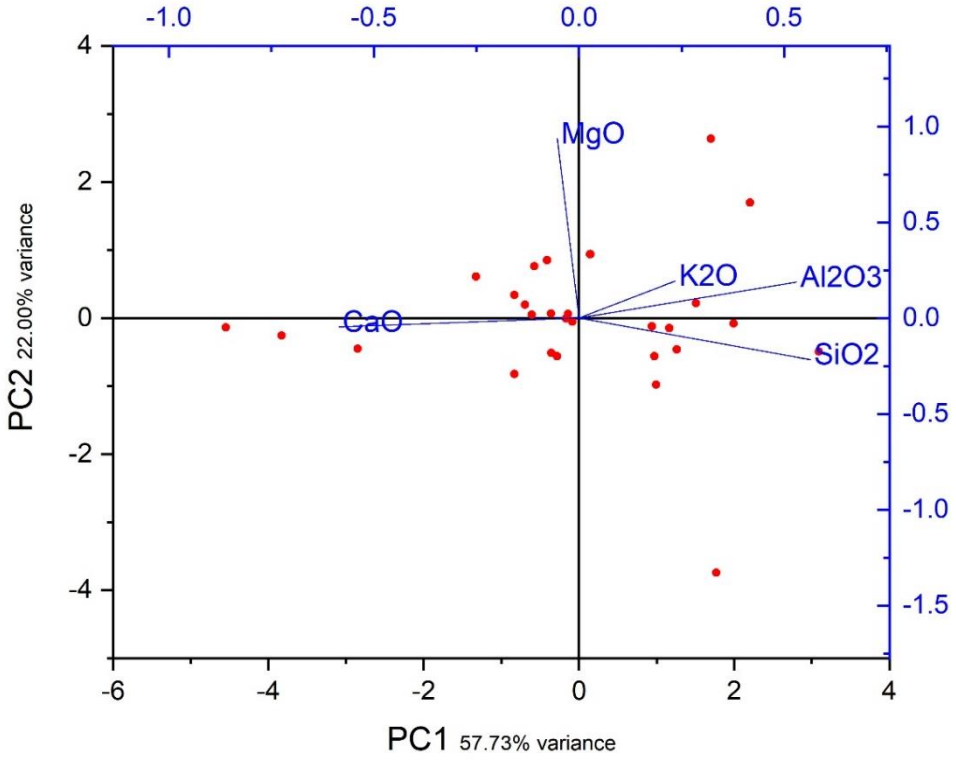

Figure 4.46 PCA plot of SI composition from sample NJG-11, after re-normalisation

Sample NJG-20, shovel

Slag inclusions in sample NJG-20 are mainly glassy silicates and fayalitic inclusions with wüstite crystals (Figure 4.47). Due to the corrosion, only 28 of them in total were analysed. The NRC analysis did not show linear correlation between these inclusions except for Al_2O_3 vs SiO_2 (Figure 4.48). PCA analysis on a multivariate basis did not reveal clear sub-groups either (Figure 4.49). While some outliers can be found in the bottom left corner, this is largely because these four inclusions contain higher than 80 wt.% of FeO, which could have affected the concentration of other oxides. In this case, these inclusions will still be considered as from the same source.

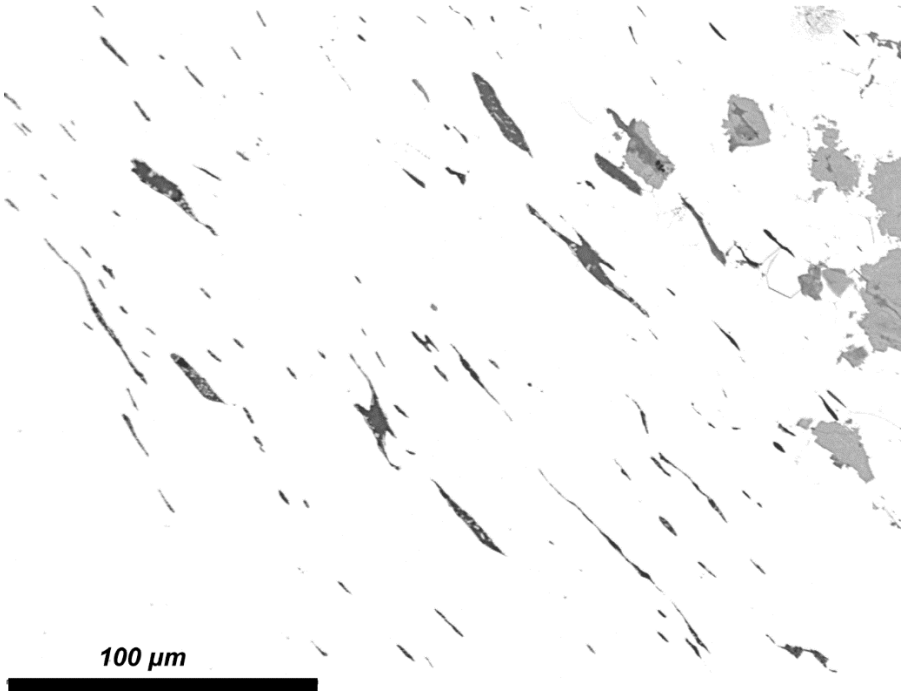

Figure 4.47 Back-scattered electron image of slag inclusions in sample NJG-20

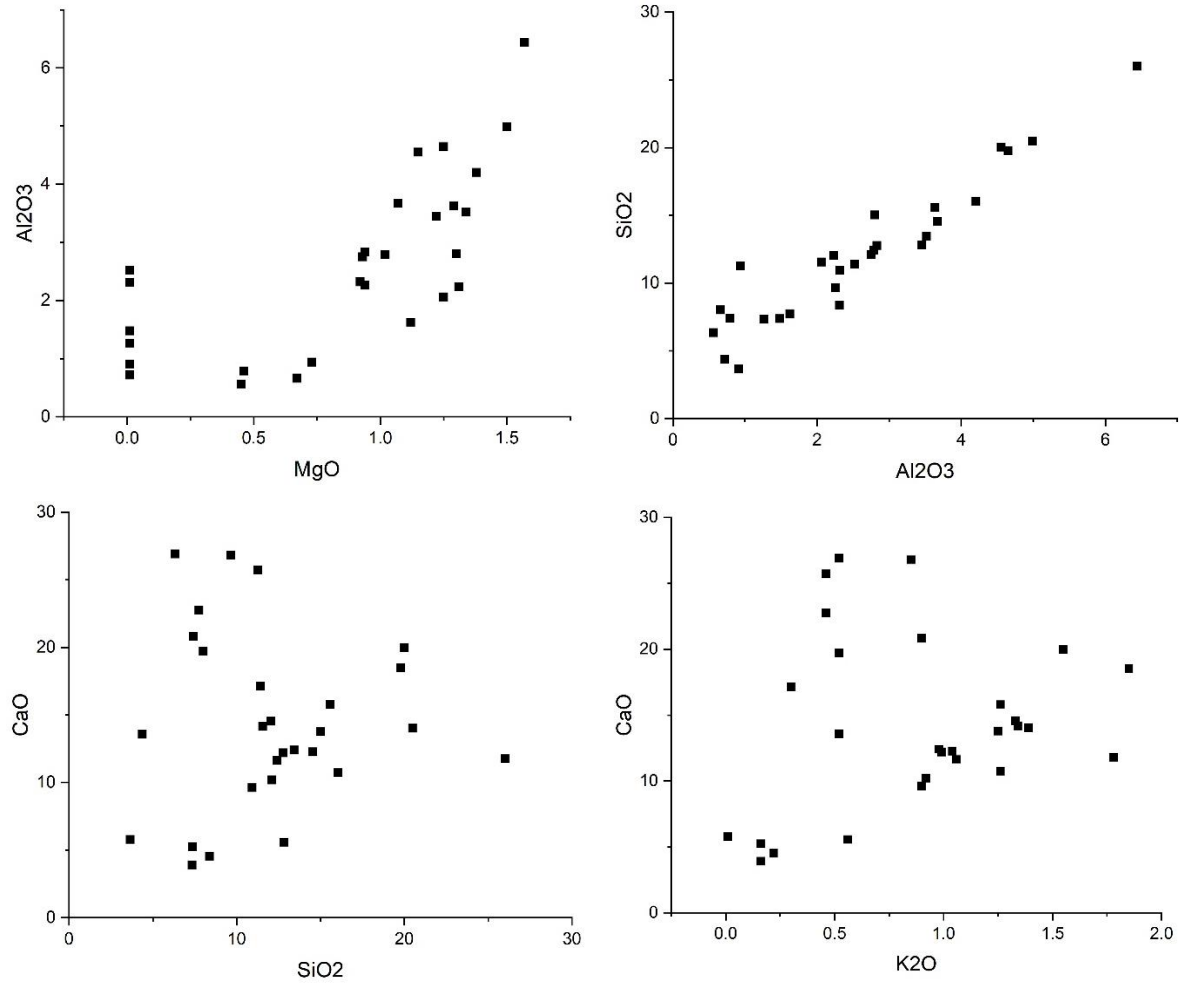

Figure 4.48 FigureBivariate plots of NRC compounds from sample NJG-20 using MgO vs Al_2O_3, Al_2O_3 vs SiO_2, SiO_2 vs CaO and K_2O vs CaO

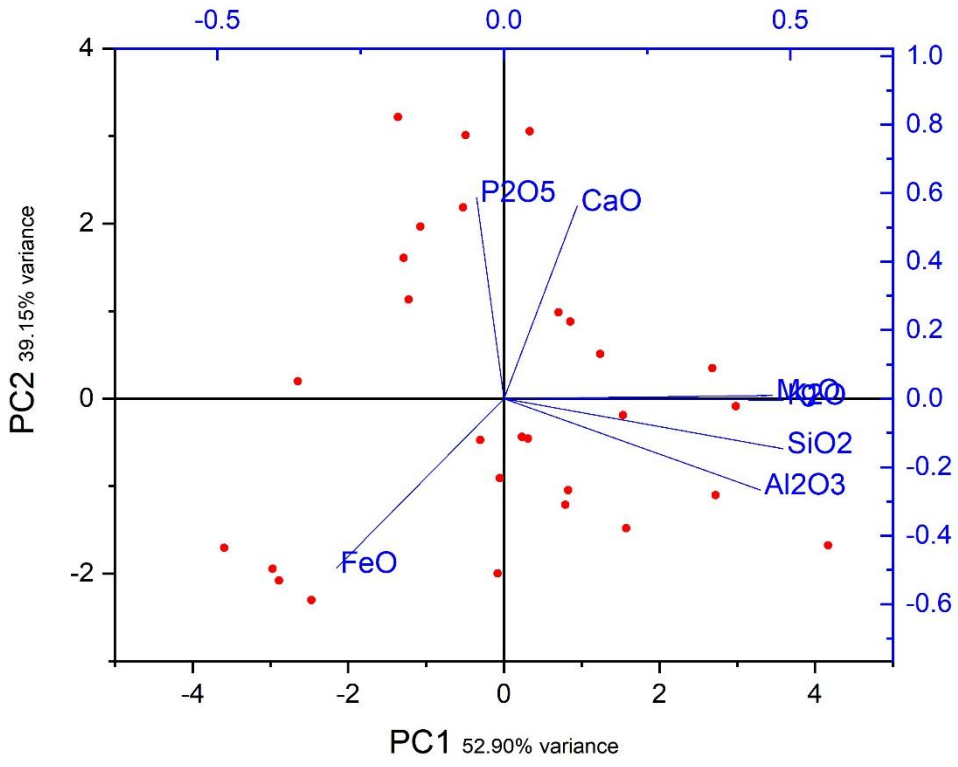

Figure 4.49 PCA plot of SI composition from sample NJG-20

Sample CXC-1, sickle

Sample CXC-1 displayed a microstructure with five layers containing different carbon content (from top to bottom, ferrite, ferrite+pearlite, ferrite, ferrite+pearlite, ferrite, Figure 4.50, left), indicating a carburisation and forging process has been applied during the manufacturing process. The slag inclusions in this sample can be separated into two types, including those larger glassy silicate inclusions (type-a) in the upper part of Figure 4.50 (right), corresponding to the ferrite zone in the middle, and more shattered smaller fayalitic inclusions with wüstite crystals widely distributed in the lower part (type-b). Both types of inclusions were linearly distributed toward one direction. A total number of 84 of them were analysed. Since MgO is below detection limit in type-b inclusions, MgO vs Al_2O_3 is excluded from NRC analysis. Based on the NRC plots, these two types of inclusions were linearly distributed in the NRC analysis, with coefficient of determination (R^2) higher than 0.95 despite the huge variance of

chemical concentration (Figure 4.51). PCA plot shows the majority of the variance is resulted from the FeO and P_2O_5 content, with type-b inclusions containing higher FeO and P_2O_5 content, and type-a inclusions being richer in NRC compounds (Figure 4.52). However, even removing these two components and re-normalising the remaining components (Figure 4.53), the separation is still clear. Thus, these two types of inclusions will be considered to be from different technological or material origins.

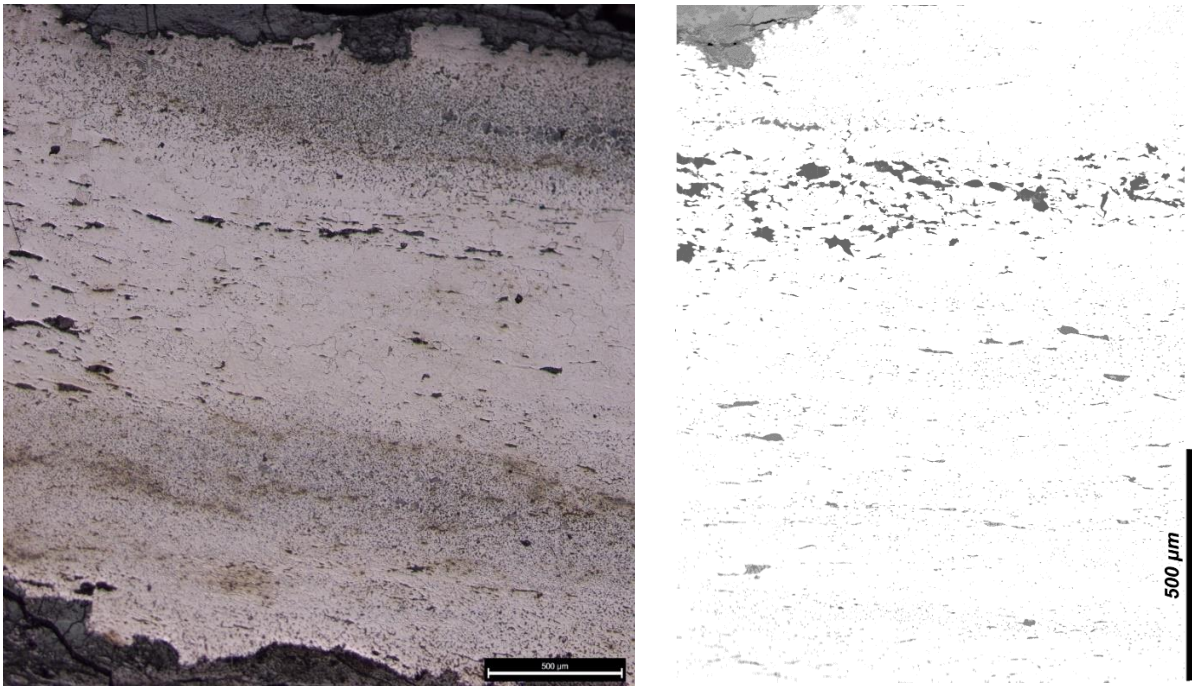

Figure 4.50 Metallography (left) and back-scattered image (right) of sample CXC-1

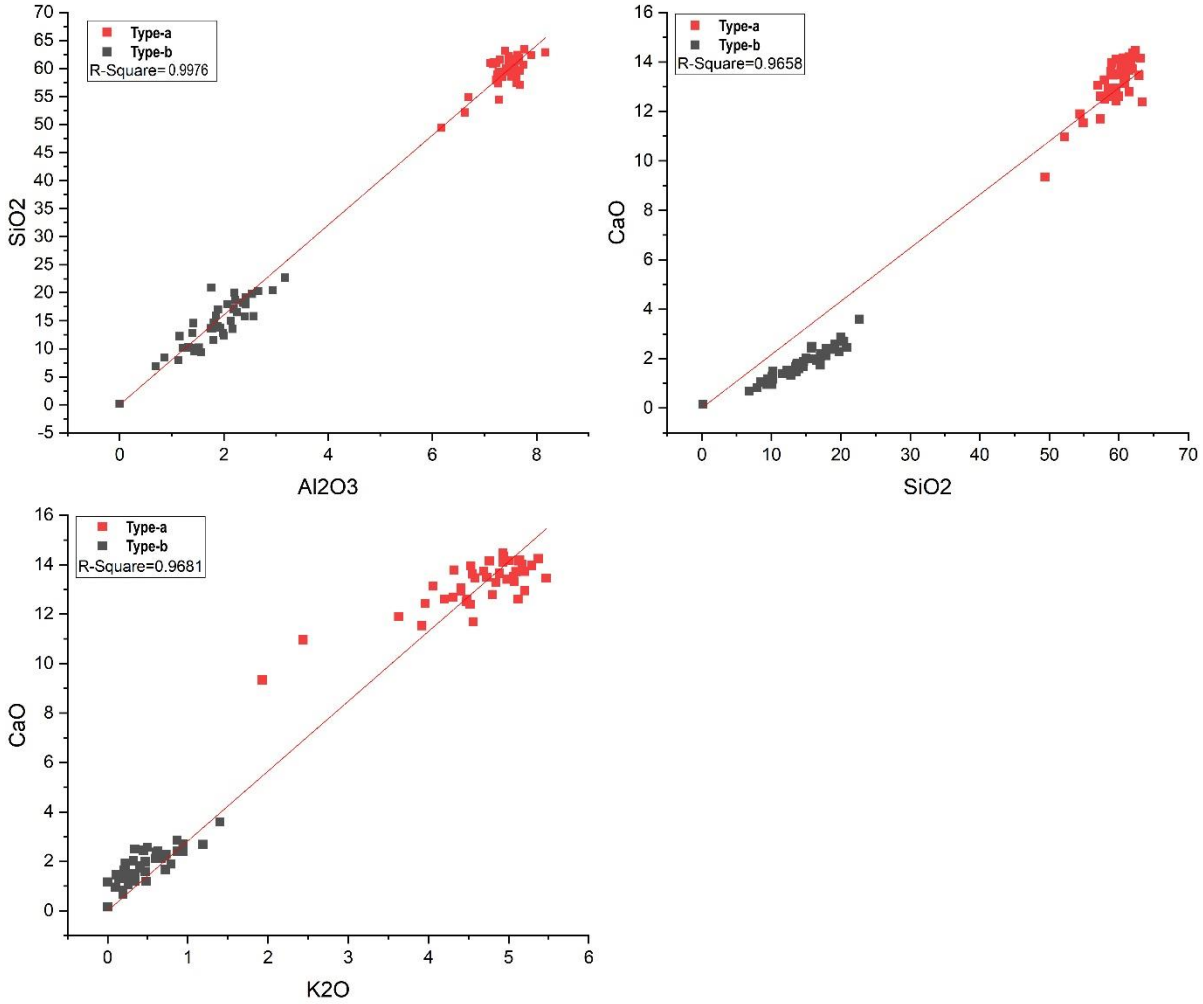

Figure 4.51 FigureBivariate plots of NRC compounds from sample CXC-1 using MgO vs Al_2O_3, Al_2O_3 vs SiO_2, SiO_2 vs CaO and K_2O vs CaO

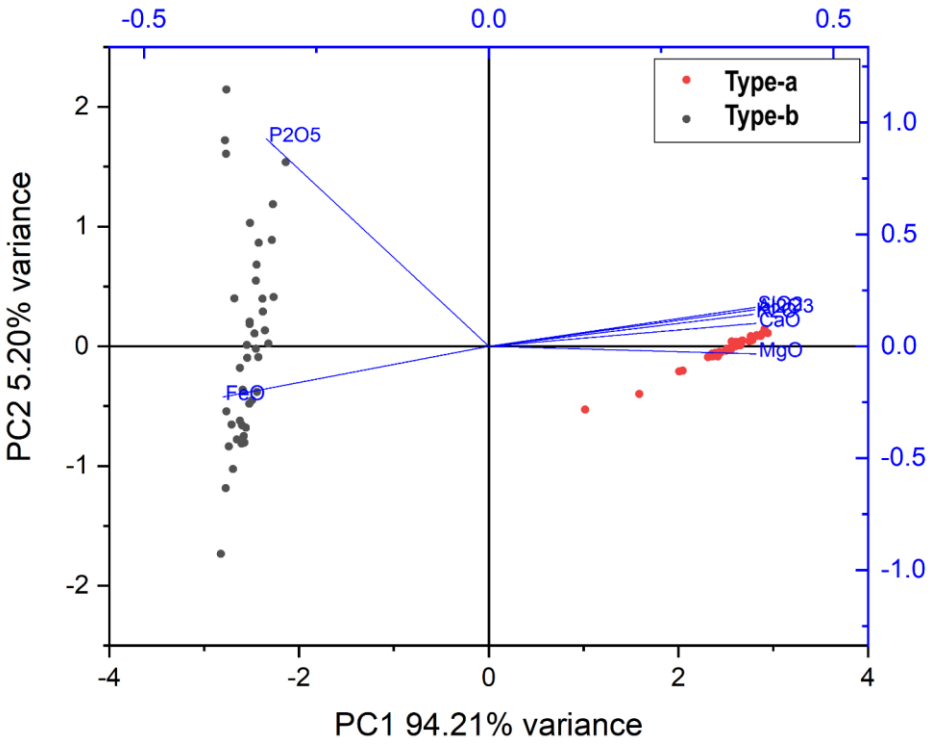

Figure 4.52 PCA plot of SI composition from sample CXC-1, before re-normalisation

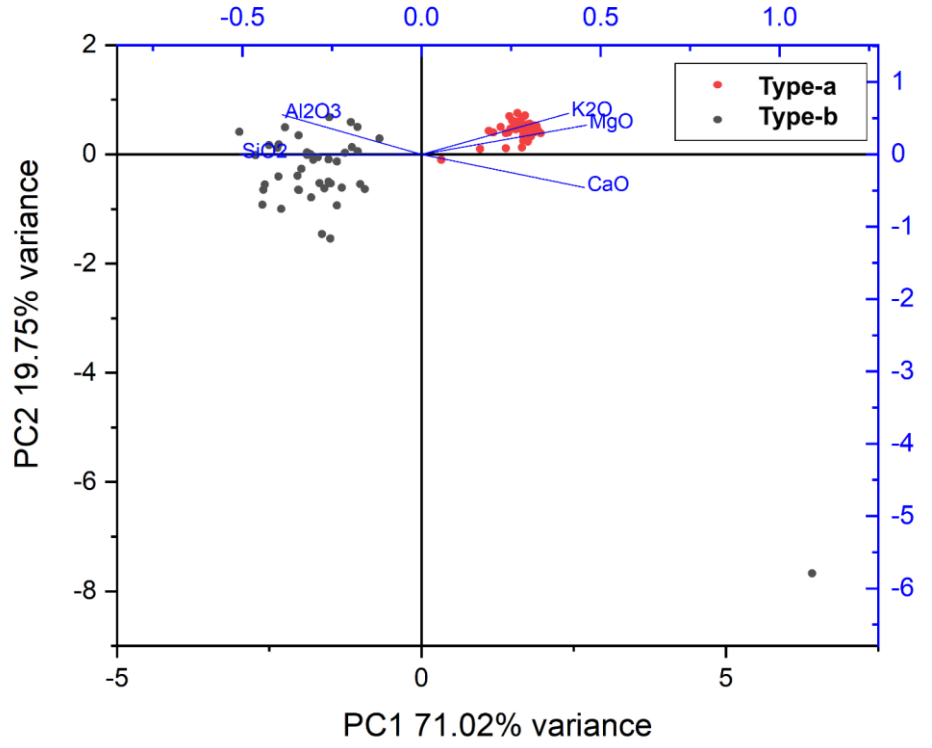

Figure 4.53 PCA plot of SI composition from sample CXC-1, after re-normalisation

Sample LD-1, arrowhead

Based on metallography, sample LD-1 was made of at least two pieces of iron, as clear boundaries can be observed in metallography. On the top part of the sample in Figure 4.54, the metal matrix is ferritic, with very few slag inclusions. On the lower part of the sample, the metal matrix is predominantly composed of pearlite, with many more slag inclusions embedded. Overall, this sample contains three types of inclusions, including two types of glassy silicates (type-a, 19 analysed, and type-b, 23 analysed) and some fayalitic inclusions with wüstite crystals (type-c, 24 analysed). Each type of these inclusions is located separately, with the type-a inclusions mostly found in the upper part of the ferritic iron, and the rest of the inclusions located in the pearlitic iron (Figure 4.55). The fayalitic inclusions are mostly corroded, therefore their chemical composition will be affected, and the data will only be used for indicative purposes. The NRC analysis shows no linear correlation between these three types of inclusions (Figure 4.56), and the PCA plot reveals the same results, with the type-a inclusions dominated by higher CaO and P_2O_5 content, type-b with higher Al_2O_3 and SiO_2, and type-c being richer in FeO (Figure 4.57).

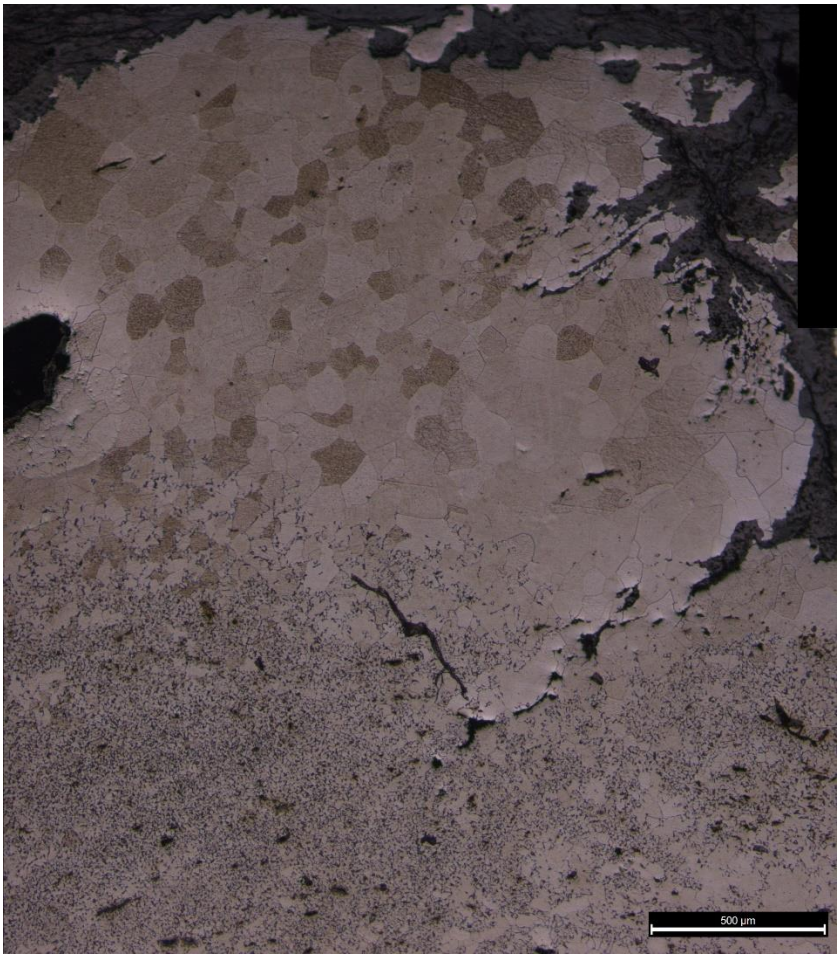

Figure 4.54 Metallograph of sample LD-1, ferrite grains in upper parts with few slag inclusions, lower parts ferrite and cementite with slag inclusions

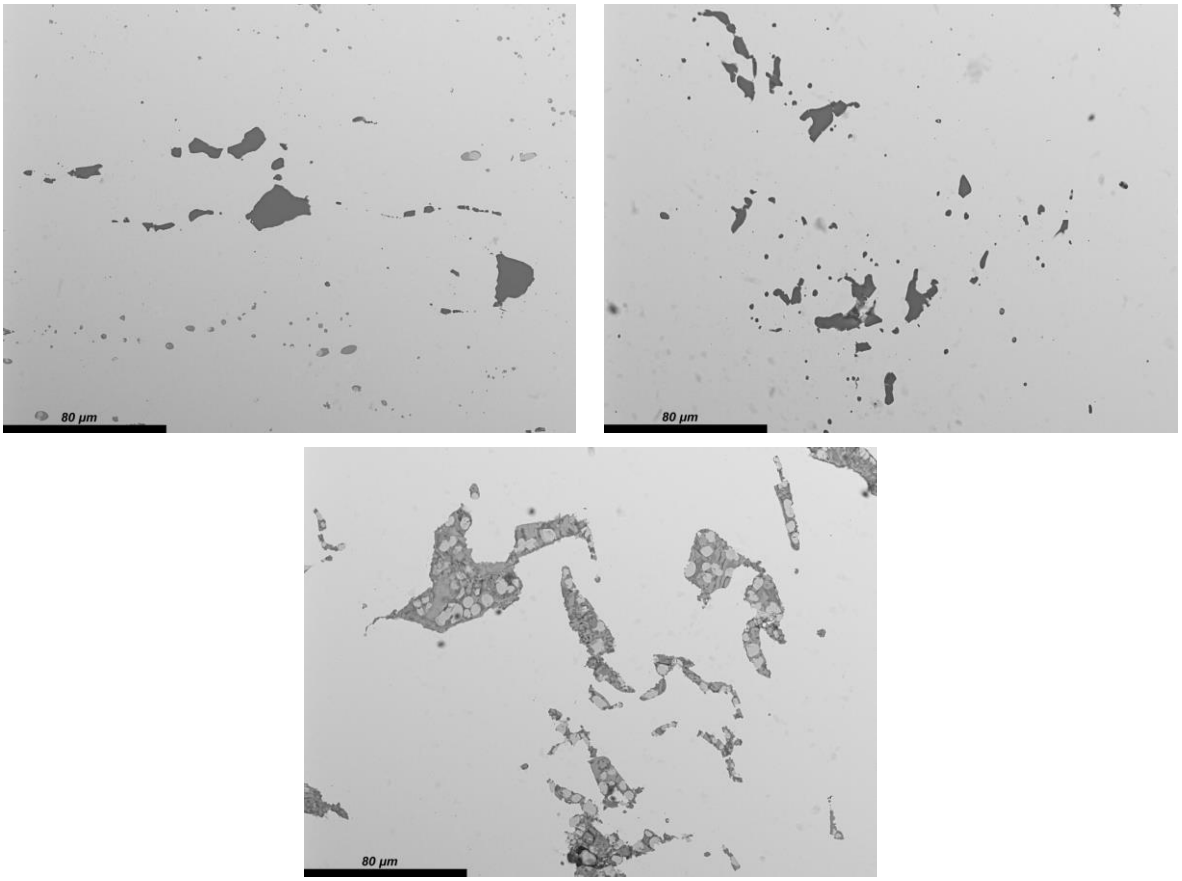

Figure 4.55 Back-scattered electron image of slag inclusions from sample LD-1. Type-a, top left; Type-b, top right; Type-c, bottom

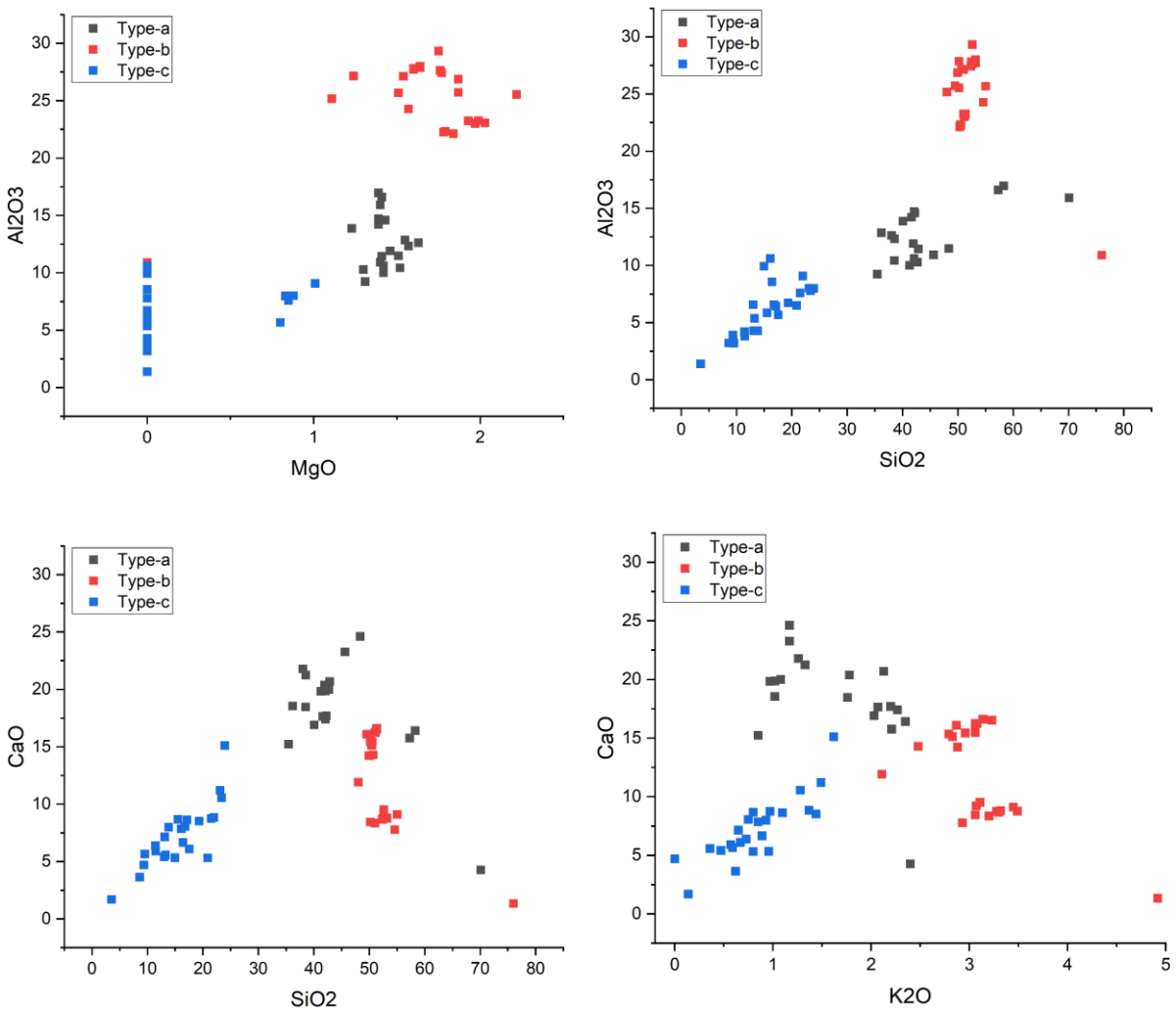

Figure 4.56 Bivariate plots of NRC compounds from sample LD-1 using MgO vs Al_2O_3, Al_2O_3 vs SiO_2, SiO_2 vs CaO and K_2O vs CaO LD-1

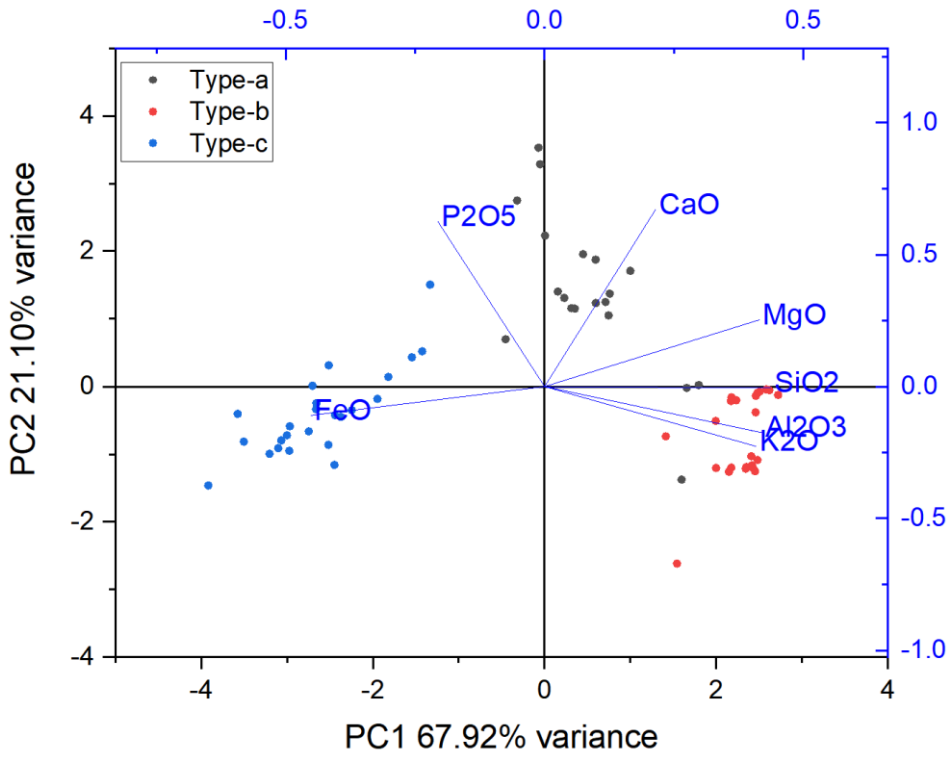

Figure 4.57 PCA plot of SI composition from sample LD-1 showing three types of inclusions separately distributed

Sample LD-2, arrowhead

Slag inclusions in sample LD-2 are mostly glassy silicates and fayalitic inclusions with wüstite crystals. A total number of 50 inclusions were analysed. Metallography study shows the sample has been repeatedly worked, with all inclusions arrange more or less concentrically (Figure 4.58, 4.59). NRC analysis shows a linear correlation between Al_2O_3 vs SiO_2. Between SiO_2 vs CaO, most of the inclusions were linearly distributed, with five outliers containing CaO higher than 25 wt.%. For MgO vs Al_2O_3 and K_2O vs CaO, no clear correlation can be observed (Figure 4.60). As for the PCA analysis, the loading plot shows most of the variance is based on the fluctuation of FeO content, with six outliers (top right in Figure 4.61) containing much higher P_2O_5 content. No clear sub-groups can be seen among the rest of the inclusions (Figure 4.61). In this case, given the good correlation between Al_2O_3 vs SiO_2 and SiO2 vs CaO in the NRC analysis, combining with the PCA analysis showing the major

variance is based on the FeO concentration, this research tends to consider these inclusions to be from the same material source with occasional localised concentration effect resulted from repeated working process.

Figure 4.58 Metallography of sample LD-2, with pearlite structure on the left, ferrite grains in the middle, slag inclusions lined up concentrically

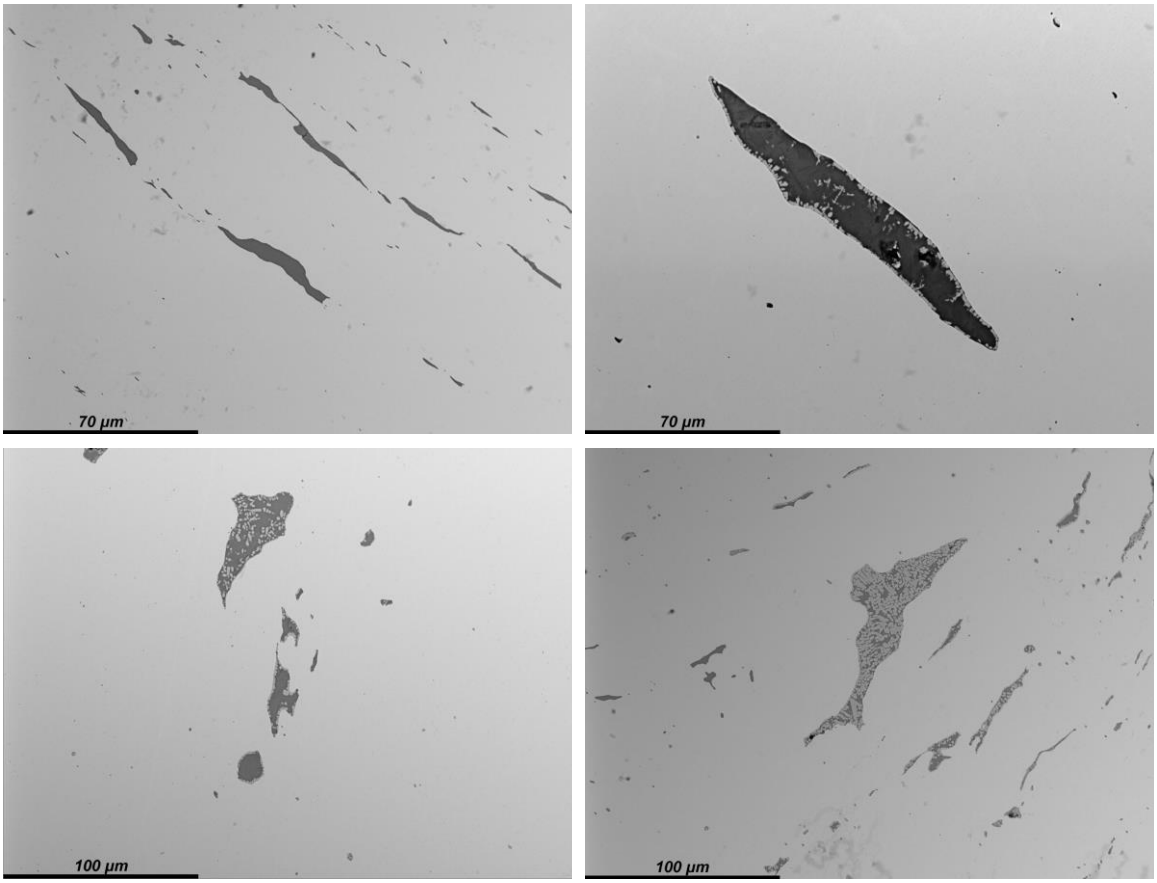

Figure 4.59 Back-scattered electron image of slag inclusions in sample LD-2

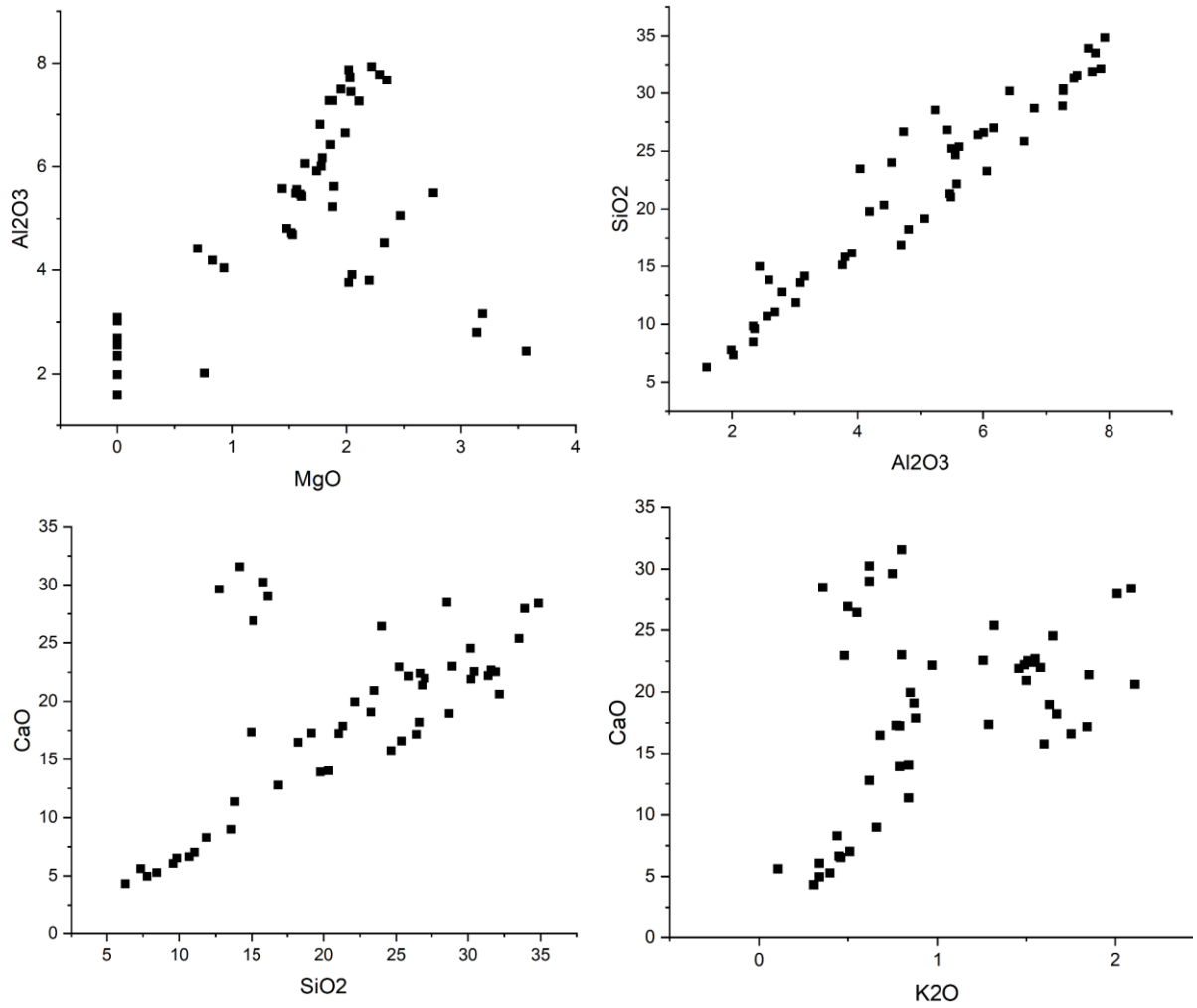

Figure 4.60 Bivariate plots of NRC compounds from sample LD-2 using MgO vs Al_2O_3, Al_2O_3 vs SiO_2, SiO_2 vs CaO and K_2O vs CaO

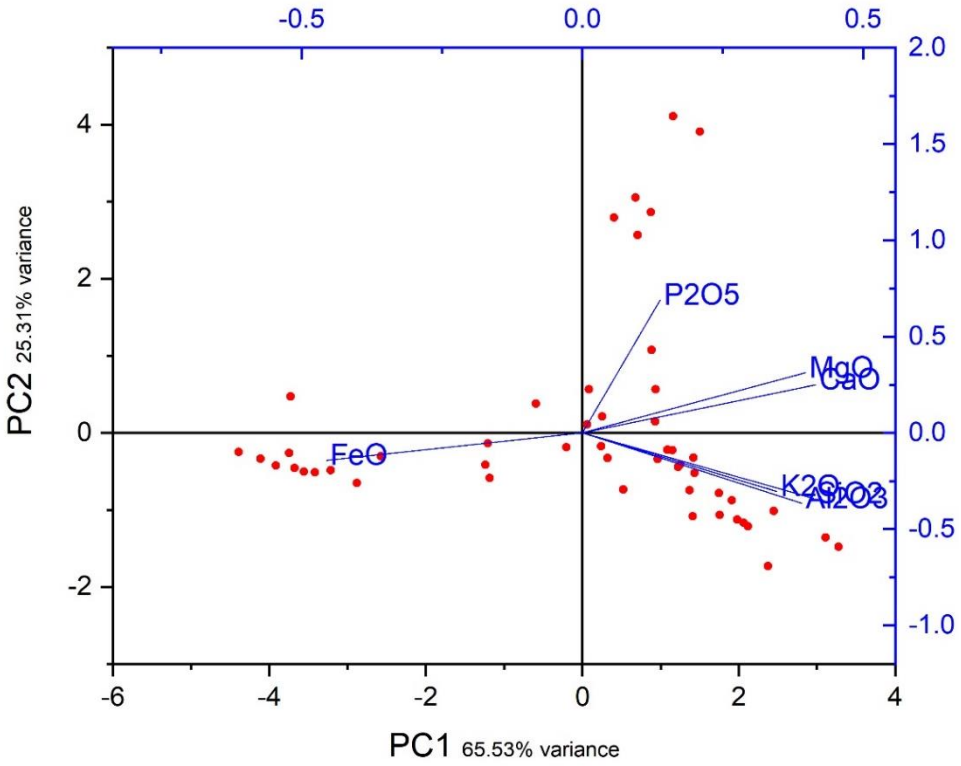

Figure 4.61 PCA plot of SI composition from sample LD-2

4.2.3 Group 3

NJG-6 and NJG-7, both chisels, contain inclusions distinctively different from other samples introduced above. Inclusions in sample NJG-6 are primarily composed of SiO_2, P_2O_5, MnO and FeO, while other elements are mostly below detection limit. These inclusions are highly shattered into small particles, distributed linearly in a homogeneous pearlite matrix (Figure 4.62, top left and top right). As most of the inclusions are too small, only 26 of them were subjected to compositional analysis.

Inclusions in sample NJG-7 are mainly composed of SiO_2, P_2O_5 and FeO, with occasional small amounts of CaO and MnO being detected. Most of the remaining components were below detection limit. These inclusions, mostly small particles, were evenly distributed in the grain boundaries toward the surface of the sample (Figure 4.62, bottom left and bottom right). A total number of 34 representative inclusions were analysed.

The chemical composition of the inclusions in both samples are relatively homogeneous, hence they will be considered to derive from the same material source. Given their unique compositional data, the possibility of them deriving from smelting or smithing slag can be ruled out as none of these inclusions contain detectable/sufficient amounts of MgO or Al_2O_3, which are key components present in most smelting or smithing slag.

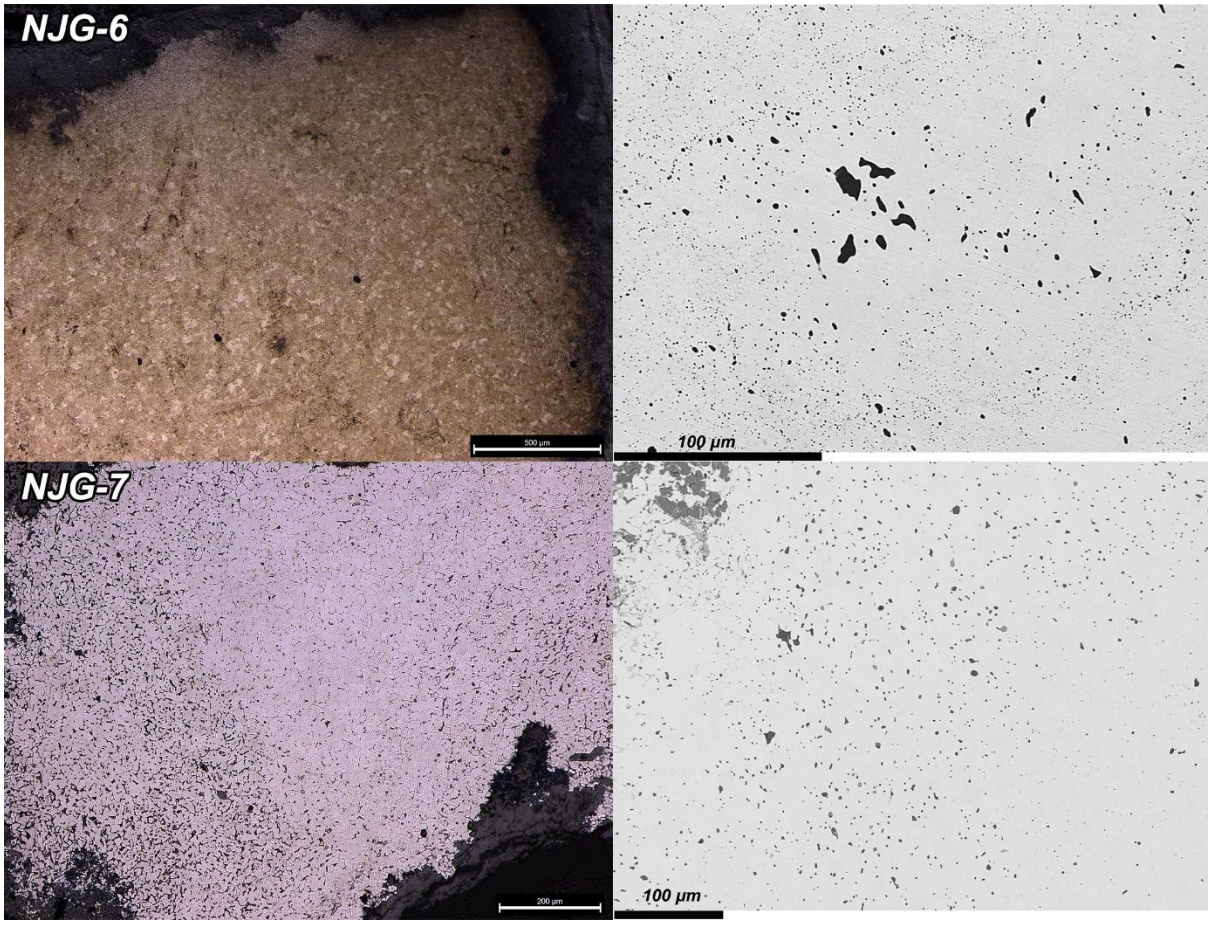

Figure 4.62 Metallography (left) and back-scattered electron image (left) of sample NJG-6 and NJG-7

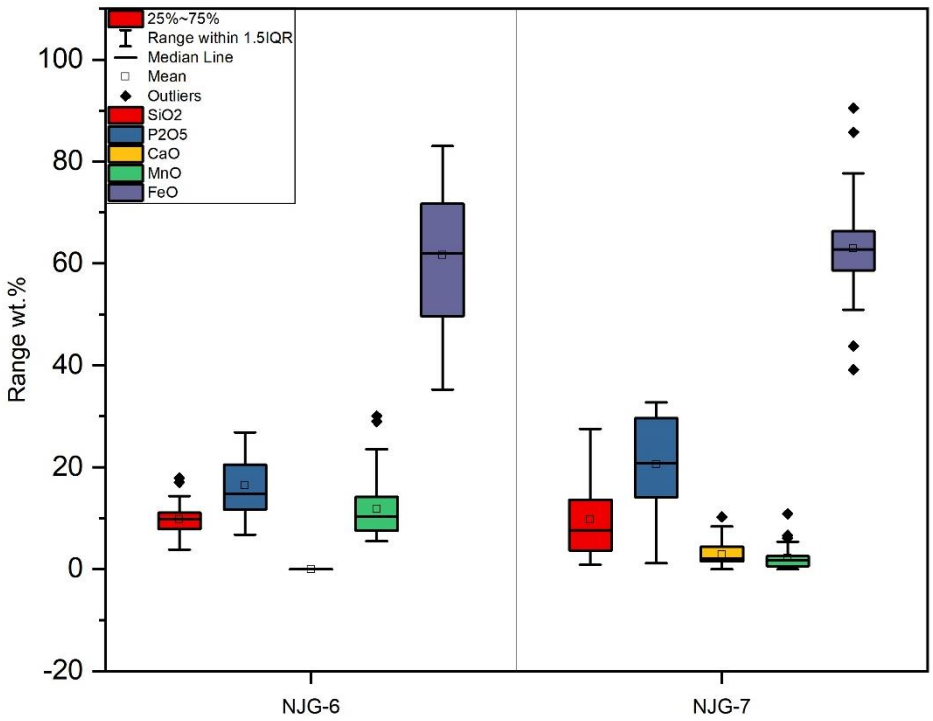

Figure 4.63 Box-Whisker plot of main components of slag inclusions in sample NJG-6 and NJG-7

4.3 Data analysis

Since there are no direct production evidence to inform about the production techniques for the 22 soft iron/steel samples with slag inclusions, therefore it will be necessary to first compare the analytical results with iron products made through known technological sources as an initial step, then further deduce their production techniques.

To begin with, this research adopted the method proposed by Dillmann and L'Héritier (2007), which aimed to differentiate the direct and indirect products by considering several compounds. By plotting the $(MgO+Al_2O_3+K_2O)/FeO$, which largely represents the reduction degree of the smelting system, against the P_2O_5 content, which represents the oxidisation degree, iron products produced from the direct and indirect process can be largely separated with indirect products containing higher amount of P_2O_5 in their slag inclusions, while the direct product contains higher FeO and lower NRC contents (Figure 4.64). By applying the same data treatment process, the slag inclusions data obtained in this research was subsequently plotted into the original plot to make comparisons.

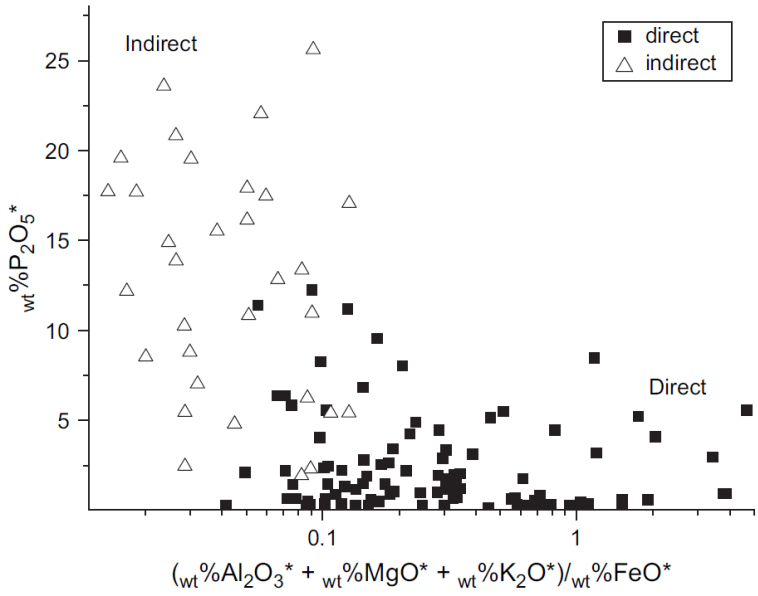

Figure 4.64 Original plot from Dillmann and L'Héritier (2007)

However, as demonstrated in Figure 4.65, this method has been proven to be inconclusive when applied on the iron products from this research. By plotting the slag inclusion data into the original plot, most of the data points would either fall into the intermediate area between direct and indirect products (Figure 4.65, left), or stretching across both the direct and indirect area (Figure 4.65, right).

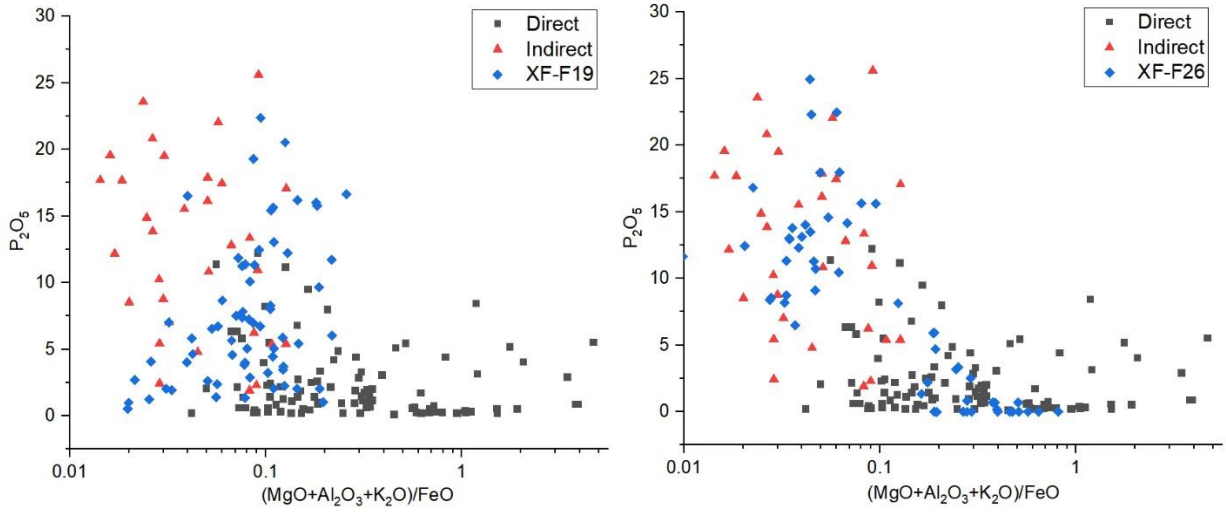

Figure 4.65 Sample XF-F19 and XF-F26 plotted against the original data from Dillmann and L'Héritier (2007)

There are multiple reasons that could be affecting the effectiveness of such a method. To begin with, the original research carried out by Dillmann and L'Héritier includes a data screening process, through which abnormal data has been removed, whereas such a method was not applied in this thesis. In the meantime, the iron objects in the original research were iron reinforcements, which arguably could have been subjected to less working comparing to the craft tools and weapons in this research, therefore could affecting the chemical composition of the resulted slag inclusions. Most importantly, there could be a fundamental difference in the decarburisation techniques adopted in these two regions considering the huge chronological, geological and cultural difference, where the indirect method used in Europe is practiced in a much later time with much more technological developments, while the decarburisation techniques carried out in early China during the 5th to 3rd century BC could be much more primitive. In this sense, it can be problematic to use the differentiation method developed for differentiating direct and indirect products from Europe.

There are alternatives to the approaches conducted here, such as the one proposed by Disser et al. (2014), which utilises discriminant analytical methods on slag inclusions. These approaches have not been applied here based on the aforementioned considerations, although it is clear that additional analytical procedures may resolve the data further in the future work.

As demonstrated in section 4.2, the compositional data of slag inclusion obtained from the 22 samples are highly diversified, therefore using a universal model to discriminate them will be impractical. In this thesis, a different approach has been adopted, which, instead of comparing the samples with indirect products identified in past research and hoping to discern similar patterns, compositional data of bloomery smelting slag, cast iron melting slag, and slag inclusions from bloomery iron products were collected as

reference materials. By comparing the analytical data obtained in this research with these reference data, it was hoped to see general compositional characteristics of the individual samples and make further inferences about their production techniques.

The reference data collected includes bloomery iron smelting slag from three archaeological sites dated to different periods: Clatworthy (**CL**) in the southwest of the UK where smelting spanned the early 1st to late 2nd /early 3rd centuries; Semlach-Eisner (**SE**) in the Carinthia region of Austria where iron was produced during the early 1st to early 4th centuries AD; and the Daye County **(DY)** in Hubei province, China, where bloomery iron smelting was practiced during the 18th century AD. As for cast iron melting slag, I use compositional data from the Taicheng site **(TC)** in Xi'an, Shaanxi province, China dated to Western Han dynasty (around the 2nd -1st c. BC). In addition, slag inclusion data from 31 bloomery iron objects **(NA)** excavated from the North Alpine area, dated between the 6th - 5th century BC was also included. The published compositional data for the latter group was presented in elements but were combined with oxygen by stoichiometry in this thesis to facilitate comparisons. The rest of the compositional data was originally presented in stoichiometry and normalised to 100%. Detailed information regarding the reference data can be found in Table 4.8.

Table 4.8 List of reference data collected in this research

Site	Date	Type of data	Number of data collected	Source
Clatworthy	1st to 3rd c. AD	Bloomery smelting slag	66	Fillery-Travis 2016
Semlach-Eisner	1st to early 4th c. AD	Bloomery smelting slag	70	
Daye county	18th c. AD	Bloomery smelting slag	45	Larreina-Garcia 2017

Taicheng	2nd to 1st c. BC	Cast iron melting slag	95	Lam et al. 2018
North-Alpine area	6th -5th century BC	Bloomery slag inclusions	158	Dillmann et al. 2017

For the comparison, concentrations of MgO, Al_2O_3, SiO_2, P_2O_5, K_2O, CaO and FeO were used as variables for multivariate analysis. Other oxides such as Na_2O, SO_3, MnO, V_2O_5 were mostly below detection limits, hence they were excluded. Components below detection limits are empirically set as 0.1 wt.% to avoid zero values that may affect the results of statistical analysis.

Before running the analysis, centred log ratio transformation was performed on both the raw data from this research and the reference data. The log ratio transformation is often used to deal with compositional data where multivariate analysis was carried out. Since compositions are multivariate in nature, hence even if one part of a composition is reported, it is implicitly related to the other components. By this rationale, an individual variable has no meaning unless it is related to the whole compositional data set. However, the whole data set is rarely (if ever) measured. In other words, the amounts do not add up to a real total. This makes comparisons difficult, as different data sets will have been measured in different ways, often focussing on different parts of the composition. This means that the total amount varies due to missing data, and since the total cannot be determined, the percentage of non-missing variables cannot be calculated. This implies that all compositional data are actually sub-compositional. As long as any analysis conducted on a sub-composition produces the same results regardless of whether only that sub-composition is measured or a larger composition containing other parts, then it should be possible to compare different groups. However, this is not the case, which makes it very difficult to compare results from different studies (Wood and Hsu 2020).

Aitchison (1986) showed that the effects of the constant sum constraint on covariance and correlation matrices disappear if the raw percentage data are expressed as logarithms of ratios, where the denominator is the geometric mean of the percentages in each sample. This works on the principle that transformations are usually used to remove constraints, and the log transformation is used to convert a variable which must be positive into a variable which can take any real (positive or negative) value.

In this research, log ratio transformation is performed following the same procedure. The weight percentage of seven main oxides, MgO, Al_2O_3, SiO_2, P_2O_5, K_2O, CaO and FeO from the reference data and the analytical results was extracted and re-normalised. Centred log ratio transformation was then carried out on the normalised data, and the results were further analysed using principal component analysis (PCA) based on the covariance matrix. The results are presented below.

In the first step, PCA of the reference data was carried out. Based on the loading plots (Figure 4.66), the bloomery smelting slag and slag inclusions can be separated from the cast iron melting slag quite clearly. The loading vector shows the main variance affecting the grouping is the FeO and P_2O_5 content, with the bloomery smelting slag and slag inclusions containing much higher FeO content and cast iron melting slag with much lower FeO and high CaO content. Bloomery iron smelting slag from three different sites are closely clustered despite their differences in geological location and the dating, indicating the slag composition is closely related to the technique itself despite many other variables. The slag inclusions from the iron objects from the North-Alpine area have a wider spread, and can are mostly separated from the bloomery smelting slag by their higher CaO and P_2O_5 content.

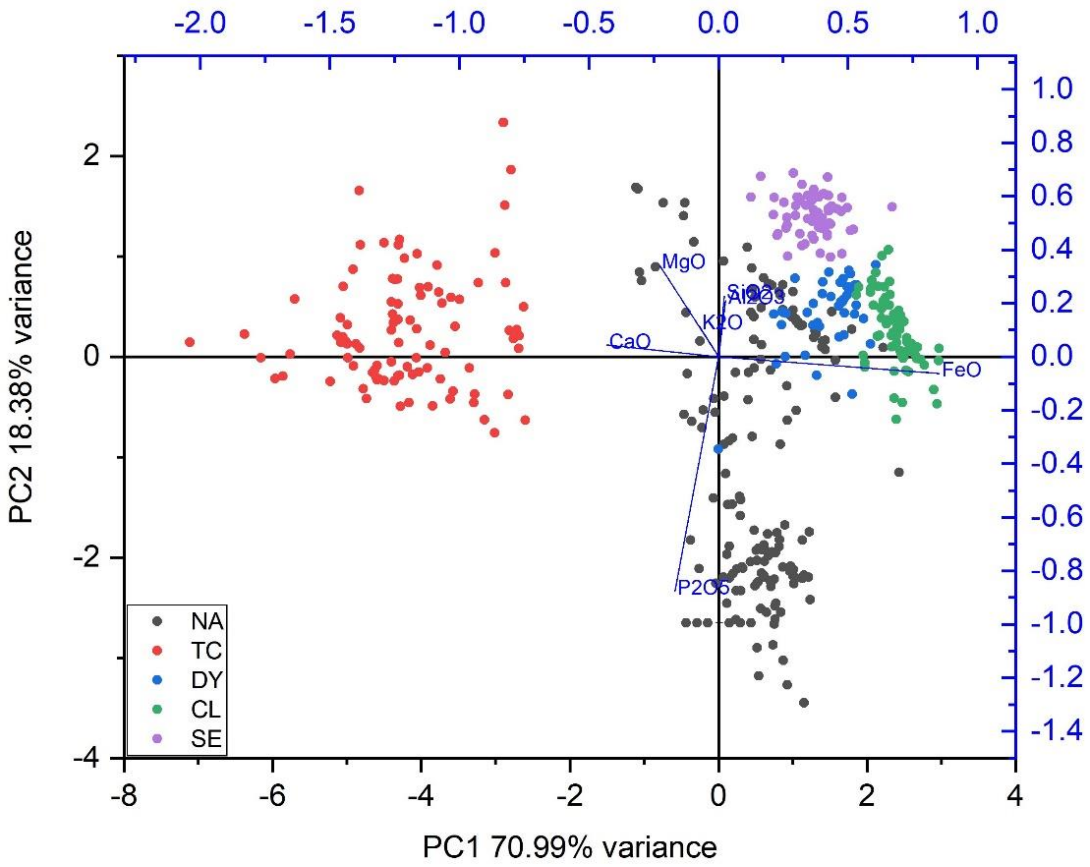

Figure 4.66 PCA plot of the compositions of bloomery smelting slag from Clatworthy (CL), Semlach-Eisner (SE) Daye (DY), cast iron melting slag from Taicheng (TC) and slag inclusions from bloomery iron products from North-Alpine area (NA)

In the next step, the compositional data of slag inclusions obtained in this research was subsequently plotted against the reference data. By plotting the samples from Group 1a with the reference data (Figure 4.67), it can be observed that slag inclusions in sample GX-2 overlapped within the cast iron melting slag. Inclusions in sample XF-25 have a lower amount of CaO, while sample NJG-34, XK-Sw14, XK-Kn10 plot separately from the rest, with lower P_2O_5 content and higher Al_2O_3 SiO_2 and K_2O content. In turn, slag inclusions from sample XF-F29 plot separately too, with a much higher P_2O_5 content than the rest of the samples from group 1a. All samples in group-1a plot away from the bloomery smelting slag and slag inclusions from bloomery iron products.

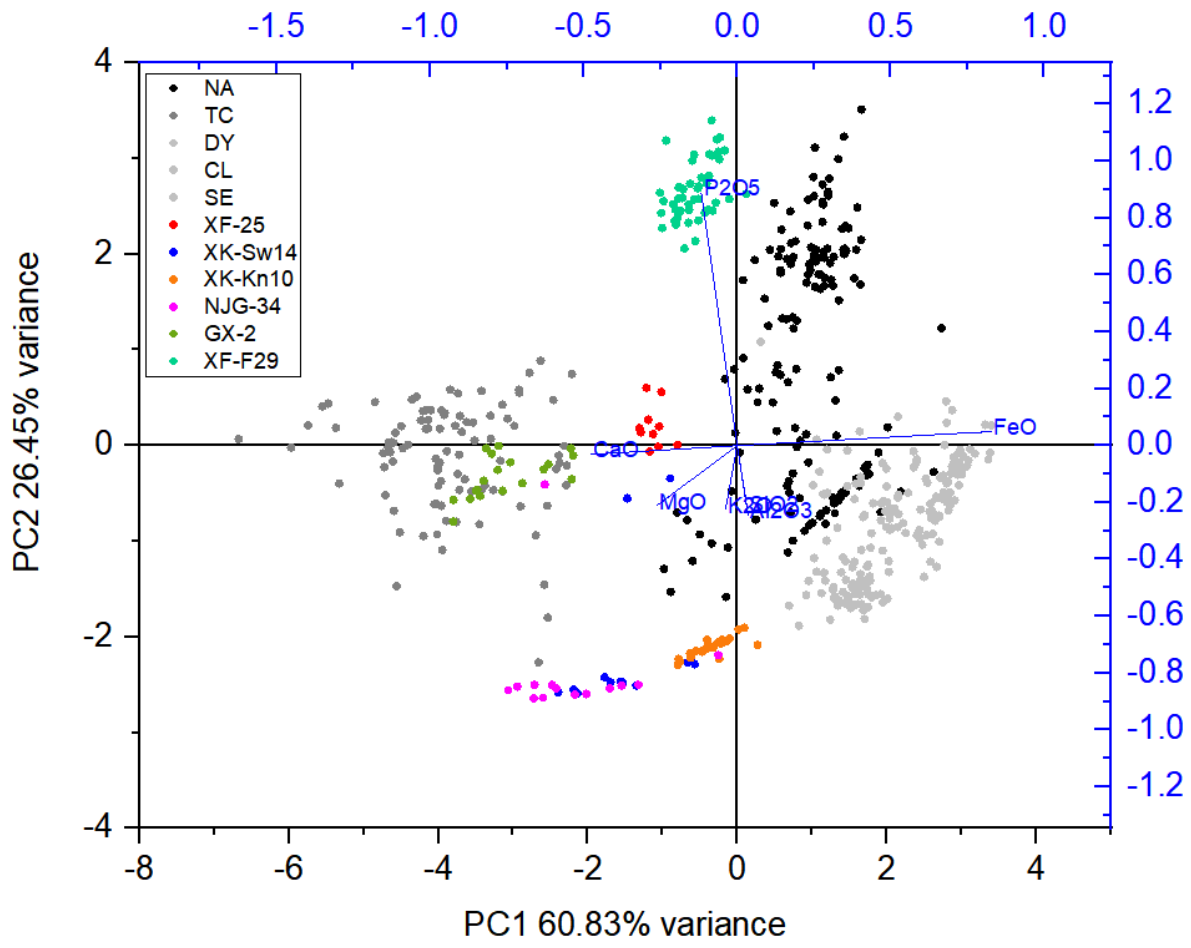

Figure 4.67 PCA plot of samples from Group 1a with the reference data, all bloomery slag data were labelled with light grey points due to their close distribution.

Samples from group-1b show a different distribution pattern compared to group-1a (Figure 4.70). Inclusions from samples JC-1 and XF-37 can be separated from the bloomery iron inclusions from North-Alpine area given their higher P_2O_5 content. The P_2O_5 content in inclusions from samples NY-2 and XK-Sp1 are lower, but still higher than the majority of bloomery slag inclusions.

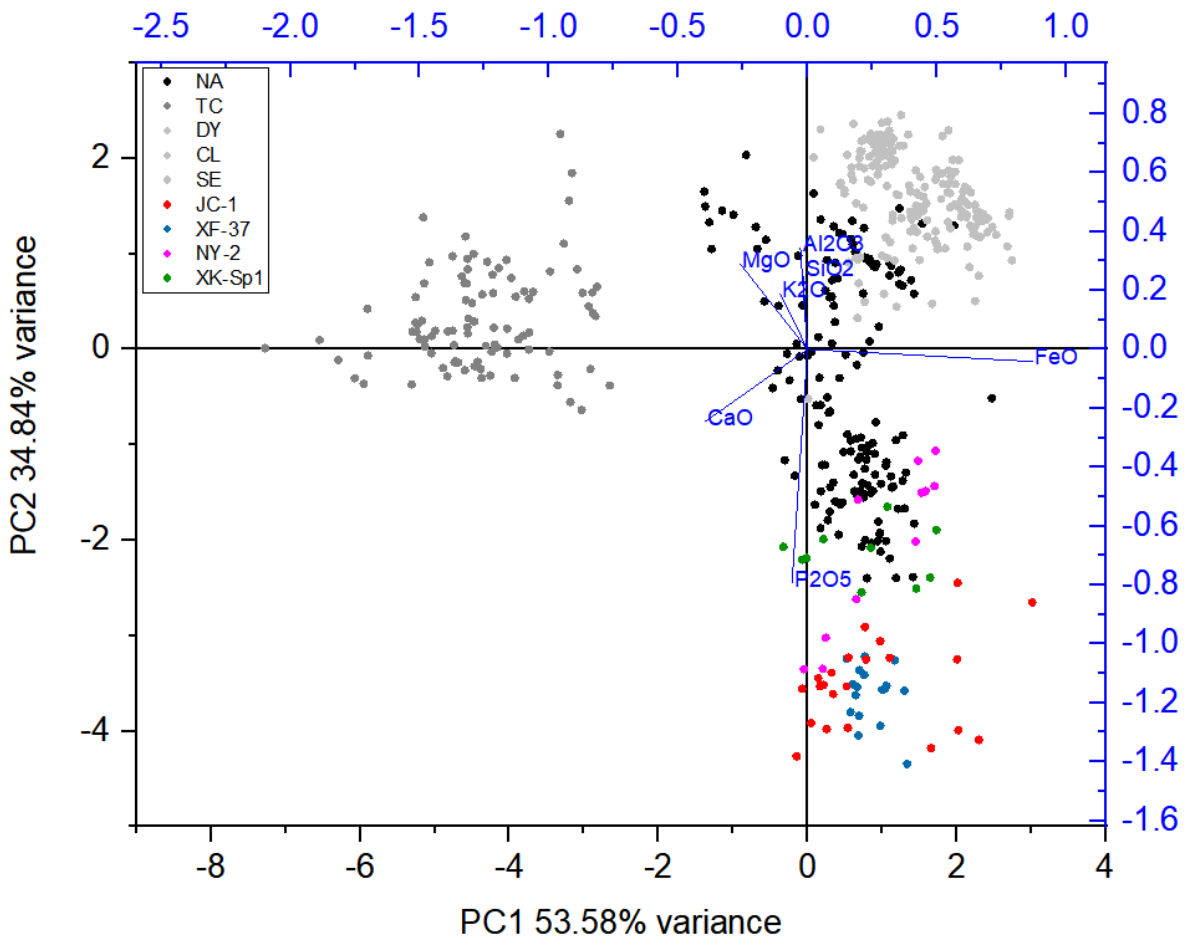

Figure 4.68 PCA plot of samples from group 1b with the reference data.

As for samples from group 2, by plotting them against the reference data, it can be observed that sample XF-27, XF-28, XF-F17, XF-F19, NJG-11, NJG-20 and LD-2 have similar distribution patterns (Figure 4.69). While slag inclusions from these samples have a much wider spread mainly due to the variance of P_2O_5 and FeO content, the majority of them can be separated from the bloomery slag inclusions with higher P_2O_5 and CaO content.

Slag inclusions from sample LD-1 are distributed in three different zones. The type-c inclusions are overlapped with the bloomery slag inclusions from the North-Alpine area; however, as noted above, these inclusions are heavily corroded, therefore their compositional data cannot be validated. Type-a and type-b inclusions are separated

based on the P_2O_5 and NRC content. However, both of them can be separated from bloomery slag inclusions with a higher CaO and lower FeO content.

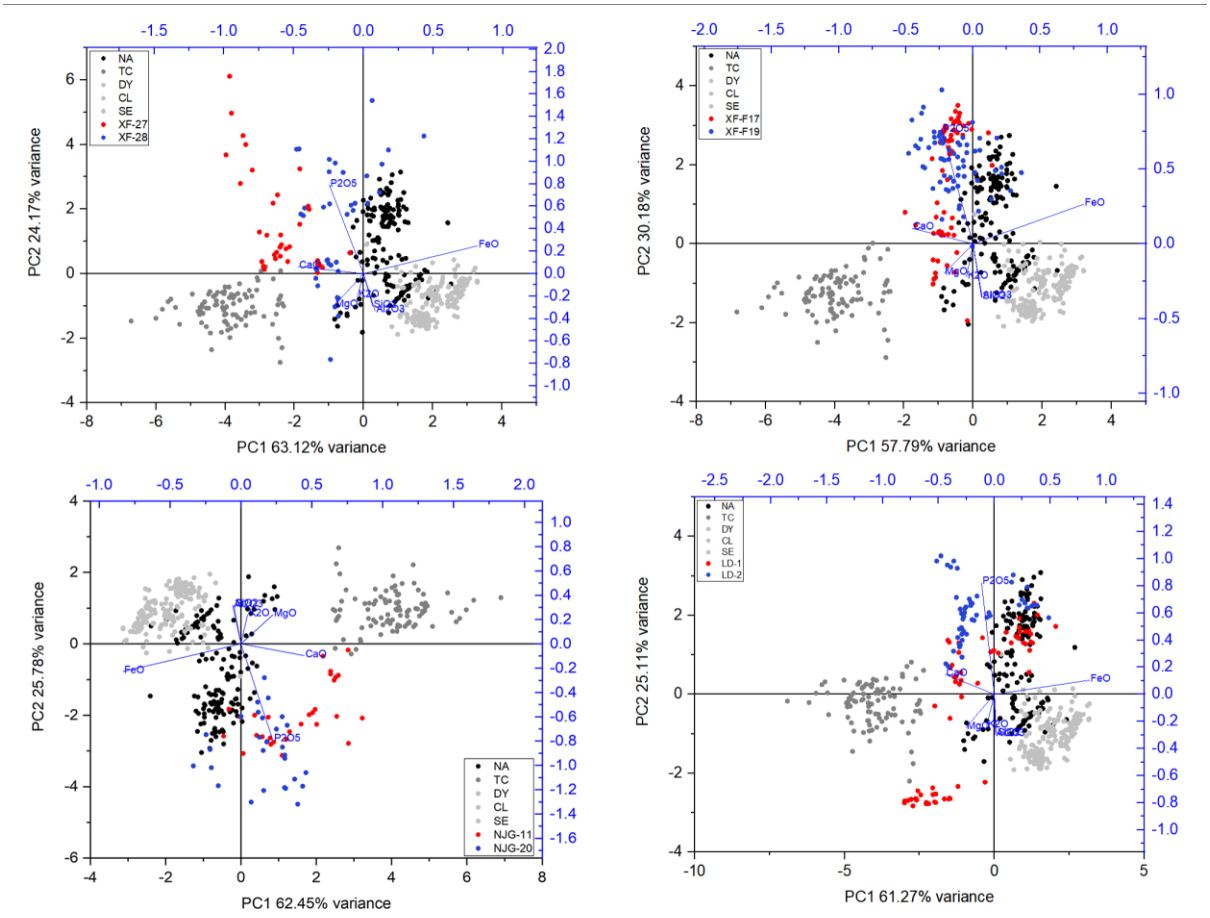

Figure 4.69 PCA plot of samples XF-27, XF-28 (top left), XF-F17, XF-19 (top right), NJG-11, NJG-20 (bottom left), LD-1, LD-2 (bottom right) with reference data

Samples XF-F26 and CXC-1 have similar distribution patterns (Figure 4.72). The type-a, glassy silicate slag inclusions in sample XF-F26 plot separately, with higher NRC components, while the type-b inclusions scatter more broadly. Most of them can be separated from the bloomery slag inclusions through their higher CaO and P_2O_5 content. Slag inclusions in CXC-1 can also be separated from the reference data, with the type-a glassy silicate inclusions containing higher amount of NRC, and the type-b fayalitic inclusions containing higher amounts of P_2O_5.

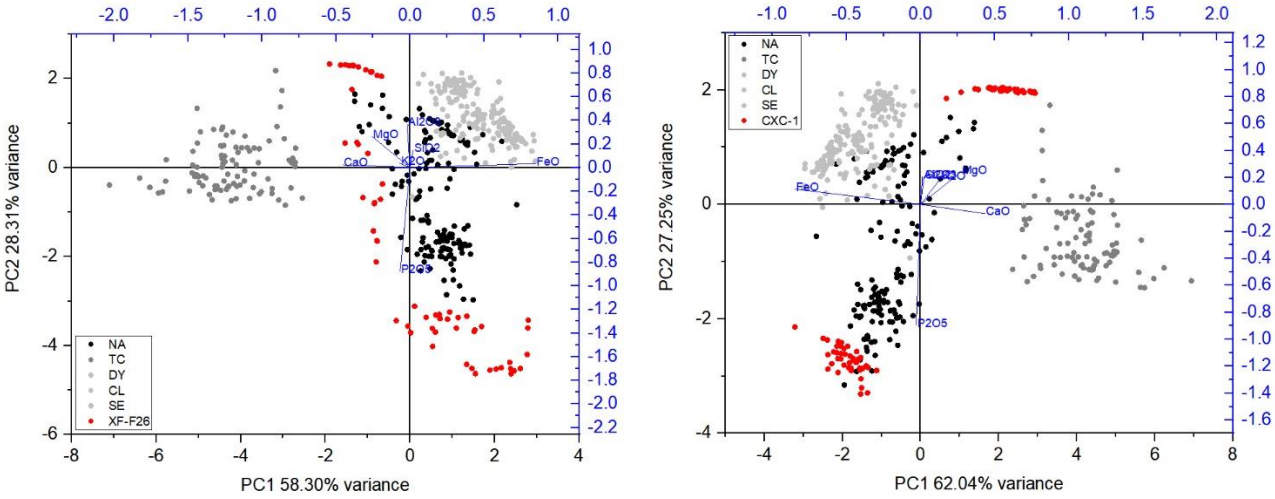

Figure 4.70 PCA plot of sample XF-F26, CXC-1 with reference data

4.4 Summary

In this chapter, based on the metallographic study, the materials and production methods were recognised for the majority of the analysed samples, and the results were presented correspondingly in section 4.1, including white cast iron, grey/mottled cast iron, which were made through mould casting processes, and decarburised cast iron, malleable cast iron, decarburised soft iron/steel, which were made through mould-casting and subsequent annealing process. The rest of the 22 samples are made of soft iron or steel materials with slag inclusions embedded in the metal matrix, and their production method cannot be recognised through metallographic study only, therefore further slag inclusion analysis and associated data process were undertaken. To facilitate the discussion in the following chapter, a brief summary of their slag inclusion type and compositional features is presented in Table 4.9.

Table 4.9 Summary of slag inclusions morphology and compositional features of 22 soft iron/steel samples

Lab No.	Type of slag inclusion	Compositional features

XF-25	Glassy silicate	Predominantly composed of Al_2O_3, SiO_2, CaO and FeO, with FeO mostly below 20 wt.%
XF-27	Glassy silicate + fayalitic + glassy silicate with fayalite crystals	FeO mostly below 30 wt.%, with high CaO content (from 10-40 wt.%)
XF-28	Glassy silicate + Fayalitic with wüstite crystals	From low FeO high NRC to high FeO low NRC, with CaO mostly above 10 wt.%
XF-37	Fayalitic with wüstite crystals	High FeO (50-70 wt.%) and High P_2O_5 (10.4-26.7 wt.%)
XF-F17	Glassy silicate + Fayalitic with wüstite crystals	From low FeO high NRC to high FeO low NRC
XF-F19	Glassy silicate + Fayalitic with wüstite crystals	From low FeO high NRC to high FeO low NRC
XF-F26	Glassy silicate + Fayalitic with wüstite crystals	Low FeO, P_2O_5, high NRC (CaO >15 wt.%) & high FeO, high P_2O_5 (mostly above 10 wt.%) low NRC
XF-F29	Glassy silicate	FeO between 30-60 wt.%, with P2O5 and CaO mostly above 10 wt.%
XK-Sp1	Fayalitic with wüstite crystals	High FeO (50-90 wt.%) and low NRC
XK-Sw14	Glassy silicate	Predominantly composed of Al2O3, SiO2, CaO and FeO, with FeO mostly below 20 wt.%
XK-Kn10	Glassy silicate	Predominantly composed of Al2O3, SiO2, CaO and FeO, with FeO mostly below 20 wt.%
NJG-6	Small shattered single-phase inclusions	primarily composed of SiO2, P2O5, MnO and FeO
NJG-7	Small shattered single-phase inclusions	Mainly SiO2, P2O5 and FeO with small amount of CaO and MnO
NJG-11	Glassy silicate + Fayalitic with wüstite crystals	From low FeO high NRC to high FeO low NRC, with CaO and P2O5 mostly above 10 wt.%

NJG-20	Glassy silicate + Fayalitic with wüstite crystals	From low FeO high NRC to high FeO low NRC, with CaO and P2O5 mostly above 10 wt.%
NJG-34	Glassy silicate	Predominantly composed of Al2O3, SiO2, CaO and FeO, with FeO mostly below 20 wt.%
CXC-1	Glassy silicate + Fayalitic with wüstite crystals	Low FeO, P2O5, high NRC (CaO >10 wt.%) & high FeO, low NRC
JC-1	Fayalitic with wüstite crystals	High FeO (from 44-90 wt.%) low NRC, with CaO and P2O5 mostly above 10 wt.%
LD-1	Glassy silicate + Fayalitic with wüstite crystals	Low FeO (mostly below 20 wt.%), high NRC, CaO mostly between 10-25 wt.% & High FeO low NRC
LD-2	Glassy silicate + Fayalitic with wüstite crystals	From low FeO high NRC to high FeO low NRC, CaO mostly above 15 wt.%
NY-2	Fayalitic with wüstite crystals	High FeO (60-90 wt.%) and low NRC
GX-2	Glassy silicate	Low FeO (mostly below 10 wt.%) high NRC, CaO mostly above 40 wt.%

A data treatment process was then applied on the compositional data of slag inclusions from samples in group 2 to study the underlying cause of their heterogeneity. Through NRC and PCA analysis, it has been determined that samples XF-27, XF-F26, CXC-1 and LD-1 could be made from two or more pieces of iron from different sources, whereas the rest of the samples from group 2 could be considered to be made from one piece of iron, and their slag inclusions were most likely to have been chemically altered during different stages of the manufacturing process.

Additionally, by comparing the transformed compositional data with reference materials, it has been established that these 22 samples can be separated from the direct products mainly with the difference in FeO, CaO and P_2O_5 concentration. The details of their decarburisation method will be discussed and revealed in the following chapter.

5. Technological modelling

In this chapter, based on the analytical results, combining with the understanding of the underlying metallurgical theories, the technologies involved in the production of the analysed iron objects are modelled, while the engineering parameters of the technologies are also evaluated.

5.1 Shaping processes

Since metal, including iron and its alloys, can be both melted and plastically deformed, there are usually two technological pathways available to make an object with a certain shape, namely the mould casting process and the forging process.

The mould casting technique utilises a set of models (the core) and mould with the target shape, and a cavity between them with the desired thickness. During casting, melted metal will be poured into the mould to fill the cavity, then allowed to solidify. Building on this method, craftspeople in Bronze Age China developed a set of sophisticated piece-mould casting technique to produce bronze vessels as well as other artefacts with complicated shapes and decorations (Figure 5.1), which was later inherited by the craftspeople in the Iron Age.

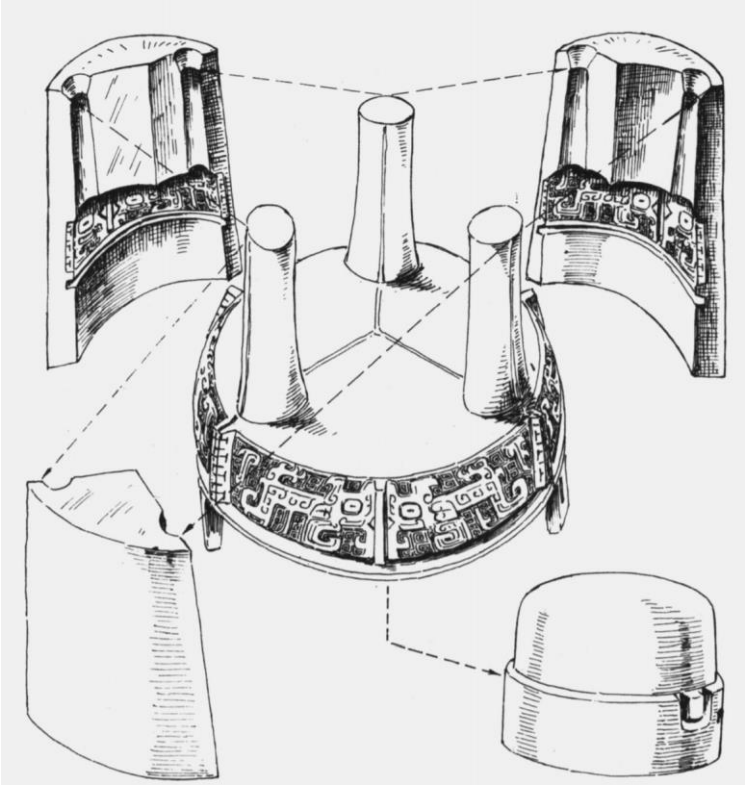

Figure 5.1 Diagram of the mould casting process for making a bronze caldron, from (Wan 1976)

The forging process, on the other hand, involves plastically deforming the metal into the desired shape through the application of physical pressure such as hammering, while the metal itself remains in solid state. Through the forging process, the grains of the metal can be significantly deformed and reduced while the metal itself also becomes consolidated.

While both the casting and forging process are potential pathways to manufacture iron products, normally these techniques require different types of iron as raw material. Iron used for casting needs to have a relatively low melting point which can be reached by early smelting/melting furnaces, hence a higher carbon content (usually between 3-5 wt.%), namely cast iron, is needed for the mould casting production. Whereas for the forging process, to allow the plastic deformation of the metal to happen, soft iron or steel with lower hardness compared to cast iron will be needed. While it has been pointed out that cast iron with a carbon content up to 3 wt.% can also be hot forged

(Wadsworth & Sherby 1980 in Redher 2000, 141), this clearly is not the common case for early iron production.

Through metallographic study, samples made through casting or forging process can be recognised. A reconstruction of the technique as well as certain engineering parameters is presented below.

5.1.1 The mould casting technique

Based on the analytical results, large quantities of mottled and grey cast iron samples along with white cast iron were observed among the samples, suggesting that different types of the mould casting techniques were applied for iron production in the Qin state.

As demonstrated in section 2.1.2, the main factor affecting the resulting microstructure of cast iron is the cooling rate. The chemical composition (alloying elements) of the cast iron, on the other hand, is also a key factor that affects the final microstructure of the mould casting product. In theory, certain elements in cast iron will favour the formation of graphite, including carbon, silicon, aluminium, phosphorus, while others prevent its formation, such as sulphur, magnesium and vanadium (Cui and Tan 2000: 366, Craddock et al. 2003, Wagner 1989). The most important elements here are carbon and silicon. As shown in the phase diagram (Figure 2.5), when the carbon content rises beyond the eutectic point (4.3 wt.%), the crystallisation temperature of iron-graphite increases drastically, while that of iron-cementite increases much more slowly, hence creating a larger temperature interval which allows a longer time window for graphite to crystallise. The presence of Si will also promote this process by decreasing the crystallisation temperature of the iron-cementite system. An amount of 0.5 wt.% of Si will expand this interval by 10 ˚C while 2 wt.% of silicon will increase it by 30 ˚C (Figure 5.2) (Li 2004, 2005). The effect of carbon and silicon contents on the

crystallization of cast iron can be simplified as carbon equivalent, which is expressed as $C_{eq}= \omega_C+1/3\omega_{Si}$. A higher carbon equivalent favours the formation of flake graphite. However, published analyses have shown that most of the cast iron from early China contain very low silicon content, which means that the main element affecting the microstructure of these artefacts is carbon (Beijing University of Iron and Steel Technology 1976, Hua et al. 1960, Ko et al. 1993, Li 1982, Rong et al. 2013, Yang 1960, Zhao et al. 1985). In this research, EDS analysis was also performed on the metal matrix of uncorroded cast iron samples to qualitatively evaluate the silicon content. Most of the samples yielded values for silicon at or below the detection limits, which were empirically established to be around 0.5 wt.%. While the specific values are unreliable as they are too close to the detection limits, the low contents of Si are in line with previous analyses of cast iron in early China.

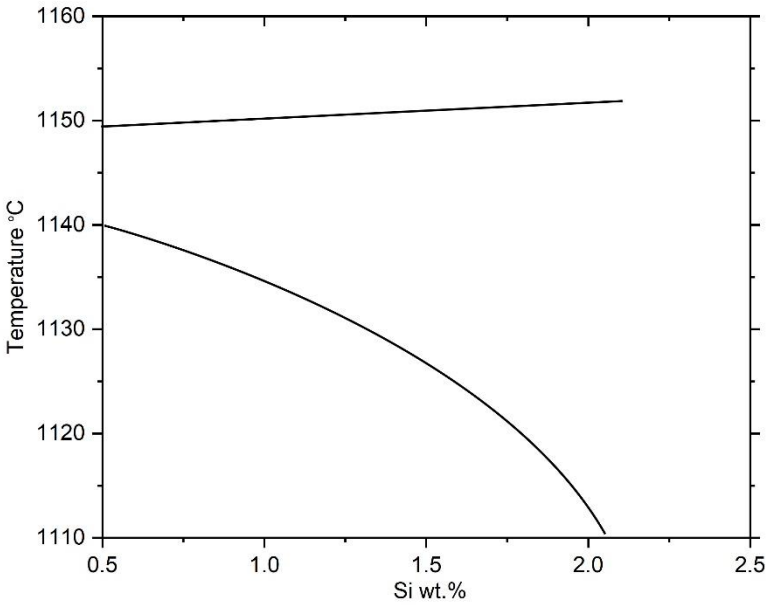

Figure 5.2. Effects of silicon on equilibrium temperature of iron-carbon alloy (Li 2004, Li 2005a)

Among the samples analysed in this research, two distribution patterns of the graphite flakes have been identified. The type-C´ graphite, also known as primary graphite, which is found in most of the samples, is the result of the slow solidification of

hypereutectic cast iron. In this case, the presence of such graphite flakes indicates that the iron used for casting has a carbon content greater than 4.3 wt.%. The type-A graphite found in sample XF-1, on the other hand, is formed when hypoeutectic cast iron (carbon content between 2.1 - 4.3 wt.%) is solidified with a low to intermediate degree of undercooling (International Standard Organisation 2008). Despite such differences, both types of graphite are distributed on a pearlite matrix, which means the liquid cast iron was solidified at a relatively slow rate before reaching the eutectoid point (738 ˚C), then quickly cooled down afterwards. Current research suggests that this could be achieved either by using a thicker mould to contain the heat, or by preheating the mould before casting (Ko et al., 1993, Craddock et al. 2003, Wagner 2008:162). Since the cooling rate needs to be increased again after reaching the eutectoid point, a more reasonable technological choice will be preheating the casting mould, since using a thicker mould will result in a slow cooling rate throughout the whole cooling process, which will lead to a ferritic matrix instead of pearlite. Such a method is also reported to have been used in Europe during the 17th to 18th centuries: here, cast iron produced from charcoal-fuelled furnaces could not solidify into grey cast iron in a cold thin-wall cooking pot casting mould, therefore the craftsman had to heat up the moulds before casting to slow down the cooling rate. It is only after the application of coke fired blast furnace, when smelted cast iron contains sufficient amount of silicon, that cold moulds can be used to produce grey cast iron (William 2013).

It is unclear the extent to which the carbon content was also controlled intentionally. Based on estimates from the metallographic examination, the carbon content of the white cast iron samples analysed in this thesis ranges significantly, from around 2.2 to 4.5 wt.%. Theoretically, a lower carbon content is favourable for a solidification into

white cast iron, whereas a higher carbon content facilitates the formation of grey/mottled cast iron, hence it would be reasonable to expect the craftspeople to control the carbon content depending on the intended product; more research data will be needed to further verify this observation.

Due to the relatively limited archaeological findings and different research focus, previous studies have not considered the production of grey/mottled cast iron as an independent technological choice as in essence it follows the same technological routine with the mould casting of white cast iron. However, based on the systematic study of the mould casting products in this research, it appears that the mould casting process for producing white cast iron and grey/mottled cast iron in this area are essentially two independent technological pathways.

Among the mould casting products which did not undergo further annealing processes, around 70% of them were made of mottled or grey cast iron (Table 5.1), which shows a clear preference for such materials. In addition, the material type seems to be related to product typology as well. Among the 15 cooking pots analysed, only two of them are made of white cast iron. For the seven lamps analysed, all of them were made of grey or mottled cast iron. In comparison, seven out of ten belt-hooks analysed were made of white cast iron. Considering those belt-hooks that underwent an annealing process were originally white cast iron, the proportion of white cast iron belt-hooks raises up to 12/15 (Figure 5.3). In this sense, a strong connection between materials and the typology can be observed, which suggests the production technique has been intentionally selected for different product categories.

It can be argued that the difference in cast iron material types could be the result of variations on how the mould casting process were performed by different craftsmen

with different knowledge backgrounds. However, it has to be pointed out that grey or mottled cast iron cannot be decarburised or malleablised through annealing, as the decomposed carbon atoms will preferentially grow on the existing flake graphite instead of being oxidised or form into tempered carbon (Hua 1982). In this sense, the production of white cast iron is a non-optional choice if the product needs to be further annealed. Since all the decarburised cast iron and malleable cast iron analysed in this research showed no signs of flake graphite, it is safe to assume that the craftsmen in this area clearly knew how to produce white cast iron, yet for certain types of artefacts, they chose to control the cooling rate to produce a different type of cast iron. The reasons behind such a technological choice will be discussed in the following chapter.

Table 5.1 List of cast iron products analysed in this research

Site	Typology	WCI	MCI&GCI
Xinfeng	Tripod	2	2
Xinfeng	Pot	1	10
Xinfeng	Mou		1
Xinfeng	Belt-hook	1	
Xinfeng	Lamp		2
Xiekou	Pot	1	2
Xiekou	Lamp		5
Niejiagou	Shovel(Chan)	1	
Yancun	Belt-hook	1	1
Hejia	Belt-hook	5	2
Airport	Vessel		1
Ningyuan	Pot		1
Total		12	27

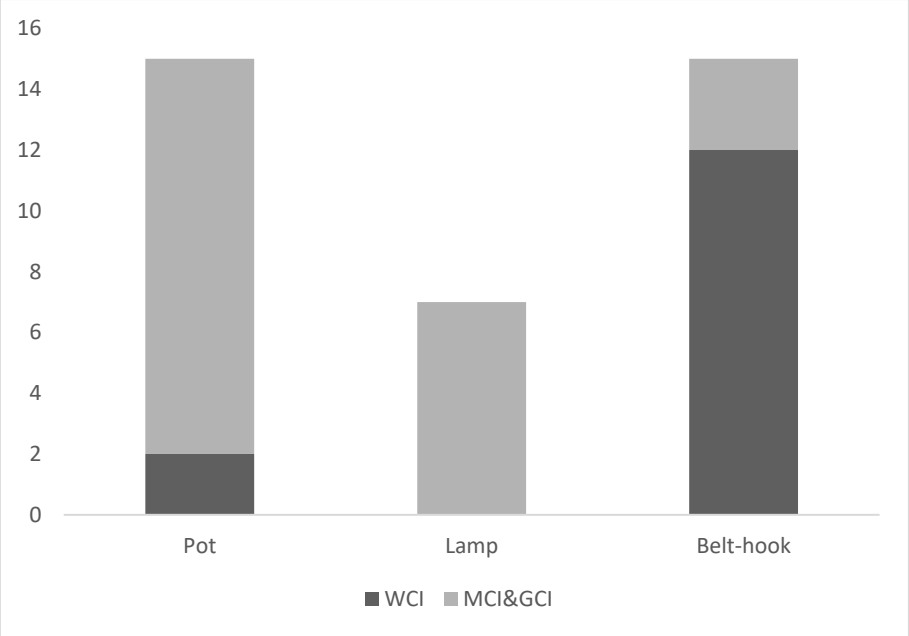

Figure 5.3 Number of white and grey/mottled cast iron among three types of objects

In sum, the mould casting technique used to produce the iron products analysed in this research can be divided into two technical branches based on their engineering parameters. The white cast iron and decarburised/malleablised cast iron products were possibly produced using a thin clay mould or an iron mould with low heat capacity, therefore favouring a faster cooling rate during solidification and facilitating the crystallisation into white cast iron. Grey or mottled cast iron products, on the other hand, were more likely produced through a controlled mould casting process, where the moulds were pre-heated before casting, hence the solidification rate was slowed down to facilitate the formation of graphite flakes to produce grey or mottled cast iron.

5.1.2 The forging technique and heat-treatment processes

While the analytical results have shown that the mould casting process was the dominant technique for iron production in the Qin state, with the annealing process applied to reduce the hardness for those farming implements, however, for certain types of iron products, such as knives, swords, a forging process is still necessary to

consolidate the iron as well as reducing the grain size to increase overall toughness and strength.

Samples made through the forging process have specific microstructural features that can be recognised under the optical microscope. To begin with, since deformation has been applied to the iron, the internal grains as well as slag inclusions will also be deformed. In some cases, the grain deformation can be removed through an annealing process where the grains could re-grow in the solid state, however, non-metallic slag inclusions can hardly change its shape through recrystallisation, hence the initial deformation will be retained. In the meantime, the forging process can also reduce the grain size by breaking up larger grains; therefore, the deformed grains, elongated slag inclusions and the evidently reduced grain size will serve as evidence of the forging process (Figure 5.4). Additionally, when repeated forging and folding have been applied, layered microstructures can also be observed with the separation between different zones (Figure 5.5).

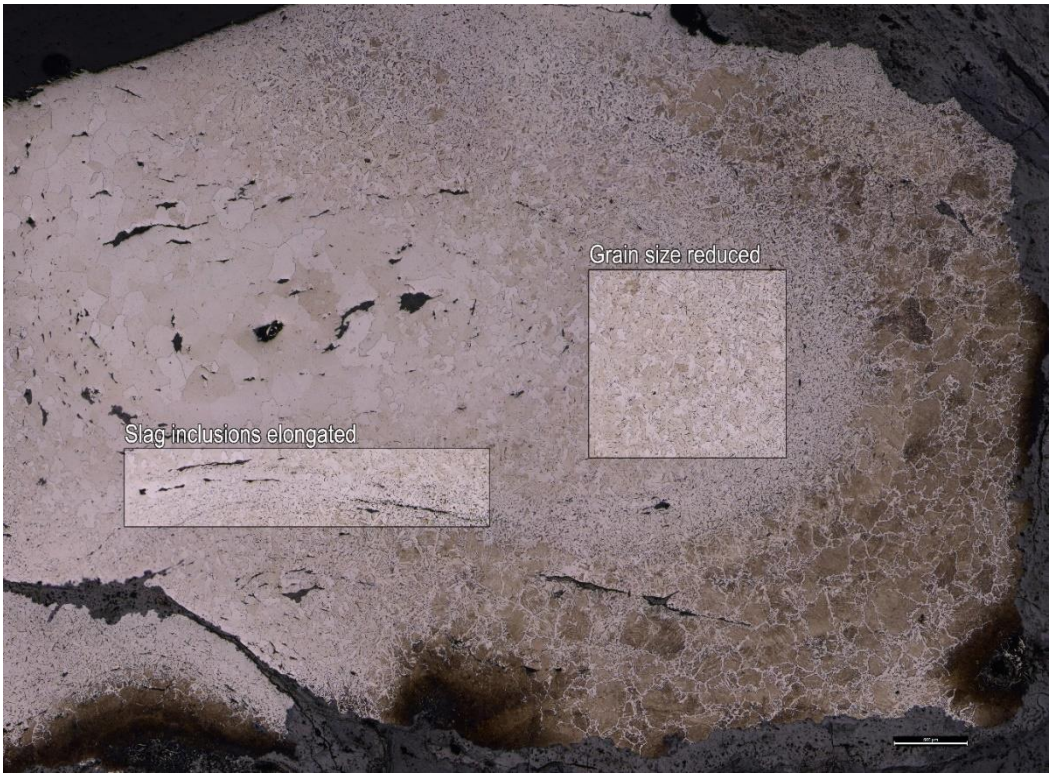

Figure 5.4 Metallography of sample LD-2, with elongated slag inclusions in the metal matrix and grain size reduced

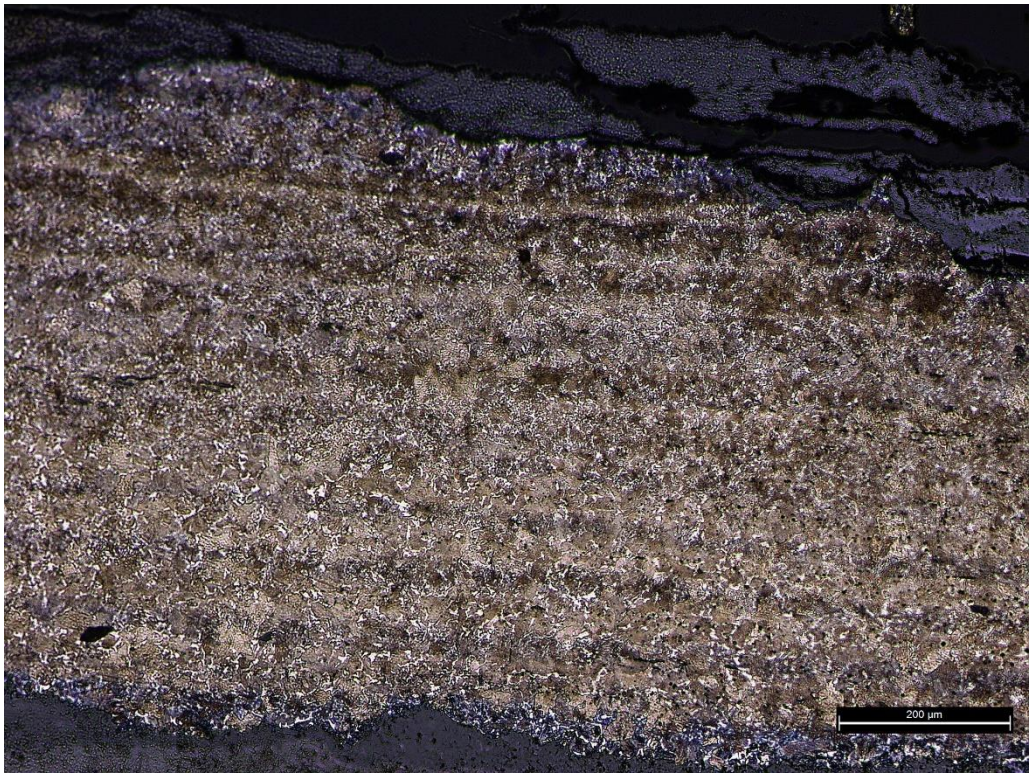

Figure 5.5 Metallography of sample XK-Kn10, layered microstructure with different carbon contents, along with bands of slag inclusions

To begin with, all 22 soft iron/steel samples made from the *chaogang*/fining process (see section 5.2.2) can be assumed to have been shaped by forging, since their raw material has a low carbon content, which cannot be melted and cast. In the meantime, samples thoroughly decarburised through the annealing process can also be further forged after casting, yet the absence of slag inclusions made it difficult for recognising them. Based on the metallographic study, only sample XK-Saw1 and XK-Kn11 can be confirmed to be manufactured through forging process given their various grain size, while the rest decarburised soft iron/steel samples do not have clear evidence suggesting forging has been applied.

In addition, during the metallographic study, certain characteristic microstructures such as martensite structure, Widmannstätten structure, granular pearlite were observed, indicating different types of heat-treatment had been applied during the manufacturing of the iron product.

The most common heat treatment processes for iron/steel include quenching, annealing, tempering and normalising. Such processes are aimed to change the internal structure to improve the mechanical properties of the metal in different ways (Cui and Tan 2000: 290 - 306). Each of such treatments applied on iron will create a distinctive microstructure that can be recognised under optical microscope. For instance, martensite (Figure 5.6) is a needle-shaped structure which is formed in carbon steels by rapid cooling (quenching) from above 912˚C. Widmannstätten structure (Figure 5.7) is another type of microstructure where needle-shaped ferrite or cementite formed on the pearlite matrix along the direction of the grain. Both martensite and Widmannstätten structures are the products of a rapid cooling process, namely quenching, with minor differences in the original temperature and cooling rate.

In the meantime, granular pearlite (Figure 5.8) or similar structures were also observed among the analysed samples. Granular pearlite is a type of pearlite in which the cementite is presented in the shape of globules distributed on the ferrite matrix. Such a structure can be formed through several technical processes, including directly spheroidising annealing or excessive tempering after quench hardening. Both processes can create a similar structure, yet the former are less likely to be intentionally employed since such a method require precise control of operation which can hardly be practiced in early China. Another more plausible explanation is that the artefact was forged at inappropriately low temperatures (around 700-900 ˚C) (Wagner 1993: 281-282), which was used to explain the similar structure found in several African artefacts (Gordon and Van Der Merwe 1984).

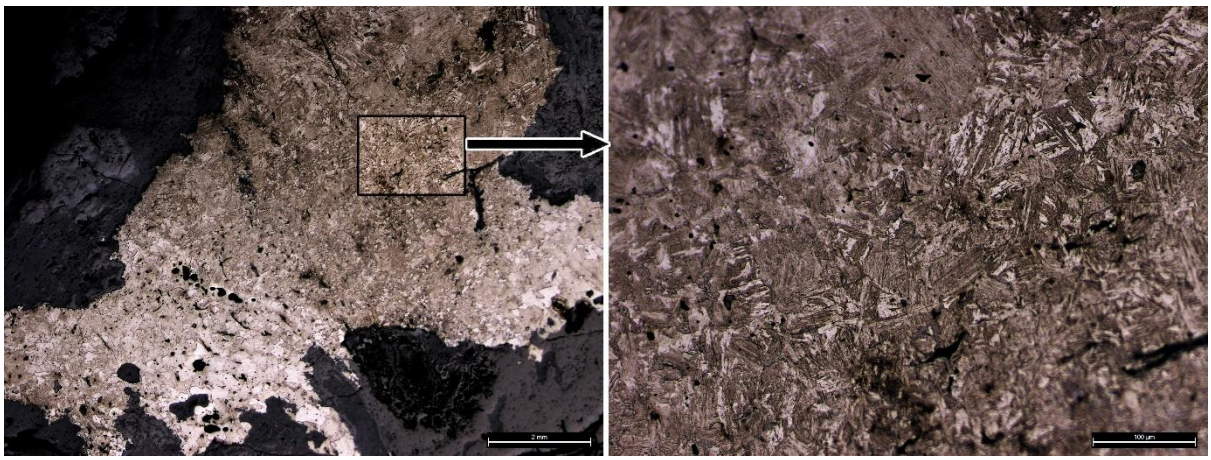

Figure 5.6 Metallography of sample XF-F17, martensite structure can be observed on the upper part. The lower part is mainly composed of ferrite grains with small amount of pearlite.

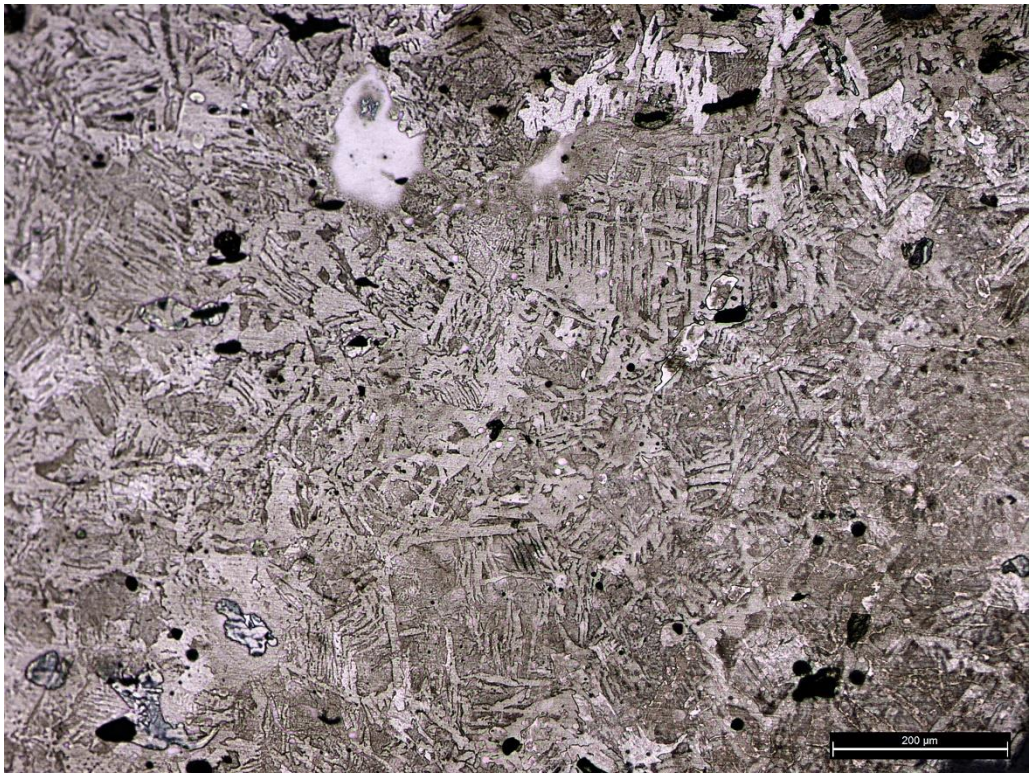

Figure 5.7 Metallography of sample XF-F29, Widmannstätten structure.

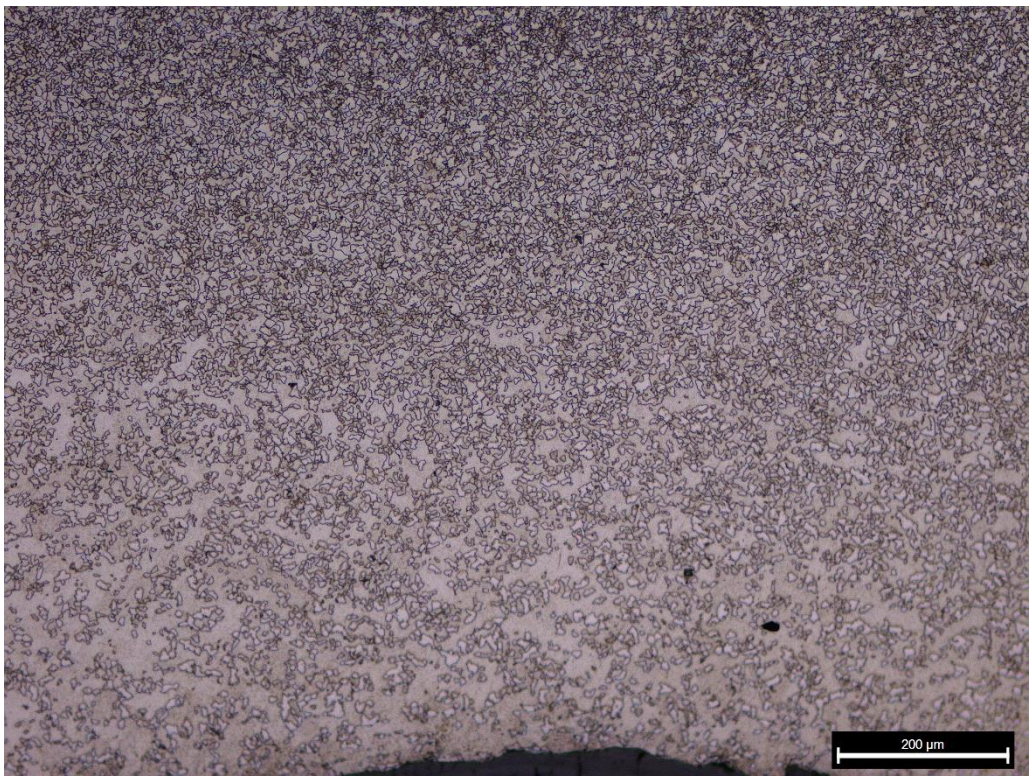

Figure 5.8 Metallography of sample XF-25, granular pearlite

Among the samples analysed, martensite structure was observed in sample XF-F17, a chisel. Along with the martensite structure, ferrite grains were also observed on the other side of this sample. This suggests the chisel itself was made using soft iron with low carbon content, then further carburised and quenched to increase the hardness. In sample XF-27 (adze), XF-28 (adze), XF-F26 (spoon), XF-F29 (sword), NJG-4 (Chisel), NJG-7(chisel), NJG-34 (fragment), Widmannstätten structures of various sizes were observed. The presence of such a structure indicates the sample also went through a rapid cooling process. Altogether, the evidence suggests that the quenching process was widely used for iron production in the Qin state to increase the hardness of iron products. Granular pearlite was observed in sample XF-25 (adze), indicating the object were possibly subjected to an forging process at low temperature or excessively tempered after forging.

Additionally, the majority of the iron tools and farming implements excavated from the bone workshop in Niejiagou (including samples NJG-1, 2, 3, 4, 5, 6, 8, 9, 12, 13, 16, 17, 18, 19, 21, 23, 31 and 32) and few samples from other sites (including XF-F19, XK-Saw1, XK-Kn11, XK-36) have an extremely fine pearlite matrix or a mixture of pearlite and ferrite (Figure 5.10). Such a microstructure should theoretically be the result of a normalising operation, which involves heating the iron to 30-50 ˚C above the 912 ˚C, maintaining it for a period of time, then quickly cooling it down through air cooling (Cui and Tan 2000: 290 - 306). The prevalence of such microstructure in the Niejiagou site indicates the production method was a common technological choice in this area. In comparison, only few samples with such microstructure were found in other burial sites. However, since all the samples from the Niejiagou site along with sample XK-Saw1, XK-Kn11, XF-36 were made by decarburising cast iron in solid state, whether such microstructure was the result of an intentional normalising operation

cannot be confirmed, as in essence the normalising process can be considered as part of the annealing for decarburisation operation. In this sense, only sample XF-F19 can serve as the evidence of an intentional normalising operation since it was made through the fining process.

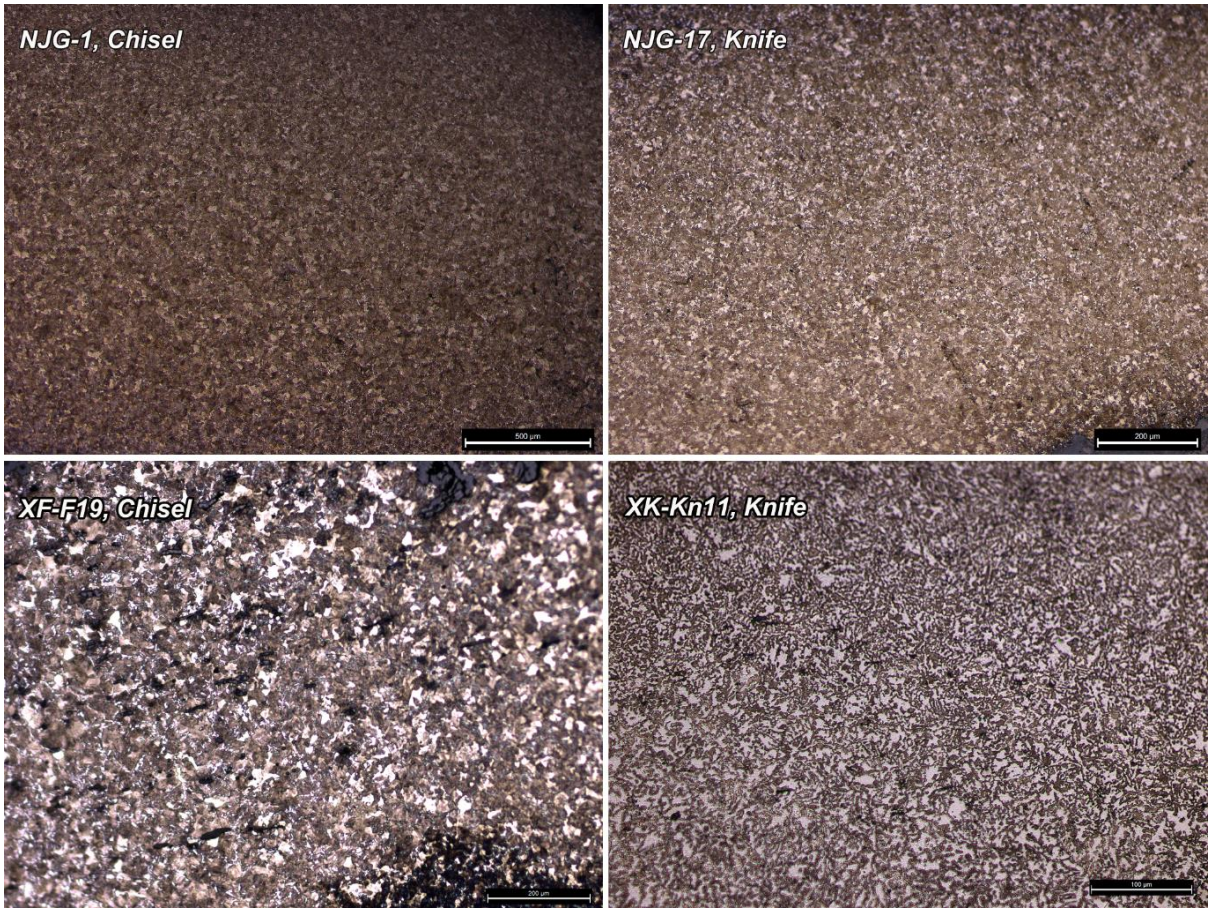

Figure 5.9 Metallograph of sample NJG-1(chisel) and NJG-17 (knife), XF-F19 (chisel) and XK-Kn11(knife). Sample NJG-1 were constituted of fine pearlite. Sample NJG-17, XF-F19 and XK-Kn11 were constituted of pearlite and ferrite.

5.2 Decarburisation/malleablisation techniques

5.2.1 Solid state decarburisation/malleablisation

The solid-state decarburisation/malleablisation technique, namely the annealing technique, applied on white cast iron in early China has been studied comprehensively both by metallurgists and non-metallurgists (Yang and Wu 1985, Wagner 1989, Beijing University of Iron and Steel Technology 1976, Li et al. 1983, Kunming Institute of

Technology 1988, Li 1976b). However, due to the limited understanding of the underlying mechanism and numerous variables involved in this practice, there is by far no conclusive method for precise evaluation of the engineering parameters based on the sample analysis. For a given sample, the chemical composition, annealing time, annealing temperature as well as the atmosphere control will all affect the resulting microstructure, and reverse engineering is especially hard in early iron making practices, where such parameters might not always have been maintained constant in time, or regular throughout the metal objects.

Experimental work and modern metallurgical practices have provided a source of information, which, while not always perfectly matching early metallurgical practices, can be used to qualitatively assess the parameters by comparing the analytical data with other considerations. In this chapter, building on the theoretical basis of the annealing technique and modern metallurgical practices demonstrated in section 2.1.2, attempts will be made to evaluate the general range of the annealing parameters for the production of the artefacts analysed in this research.

To begin with, the annealing atmosphere can be directly recognised through metallographic study, where those decarburised cast iron, decarburised soft iron/steel were annealed under an oxidising atmosphere, and malleable cast iron samples annealed in a neutral or reducing condition. Based on the study of the annealing furnace excavated in Tieshenggou site, Henan province (Figure 2.18), the main oxidising agent used in early China for decarburisation appears to have been in the gaseous state, namely the carbon dioxide from the fume generated through the combustion of charcoal in the fire pit (Zhao et al. 1985). In addition, excessive oxygen pumped into the chamber will also react with the casting to oxidise the carbon as well as the iron itself, however it is impossible to evaluate this factor due to our limited

understanding of early annealing practices. In terms of the malleablisation process, the annealing atmosphere should have been maintained neutral or reducing, this can be achieved by reducing the air supply so the combustion of charcoal will be incomplete, hence creating a reducing condition in the annealing chamber. In the meantime, sealing the castings using clay can also isolate the cast iron from gaseous oxidants to avoid decarburisation. The actual method employed remains unknown until further archaeological evidence may be found.

The annealing temperature and duration are much more complicated to be evaluated. Wagner (1989) proposed a method based on a series of theoretical calculations, however, such a method was later pointed out to be impractical since it is based on too many premises such as quickly raising to the desired annealing temperature, maintaining the exact temperature for days as well as quick cooling, which are either possible or desirable in premodern practices. In this sense, the calculation of annealing time and temperature for decarburisation process will be impractical, especially for those decarburised cast iron samples, whose surface has been lost to corrosion, making it even more complicated to evaluate the annealing parameters. However, the general range of annealing temperatures for those samples with a pearlitic matrix or a mixture of pearlite and ferrite can be deduced according to results from Wagner (1989), with reference to with the annealing practices demonstrated in section 2.1.2, and the results are presented in Table 5.2

Table 5.2 Estimated annealing temperature.

Sample	Matrix	Estimated annealing temperature (˚C)
XF-36	Ferrite with pearlite	727-912
XK-Saw1	Ferrite with pearlite	727-912
XK-Kn11	Ferrite with pearlite	727-912
NJG-1	Pearlite	>912

NJG-2	Ferrite and pearlite	727-912
NJG-3	Pearlite	>912
NJG-4	Ferrite and pearlite	727-912
NJG-5	Pearlite	>912
NJG-8	Ferrite and pearlite	727-912
NJG-9	Ferrite and pearlite	727-912
NJG-12	Ferrite and pearlite	727-912
NJG-14	Ferrite and pearlite	727-912
NJG-16	Ferrite and pearlite	727-912
NJG-17	Ferrite and pearlite	727-912
NJG-18	Ferrite and pearlite	727-912
NJG-19	Ferrite and pearlite	727-912
NJG-21	Ferrite and pearlite	727-912
NJG-23	Perlite	>912
NJG-31	Ferrite and pearlite	727-912
NJG-32	Ferrite and pearlite	727-912

As for those malleable cast iron samples, retrieving the engineering parameters based on the analysis is more complicated. Published research has not suggested any method to theoretically calculate the annealing parameters, hence this research has related the samples to the annealing practices introduced in section 2.1.2 for reference purpose (Table 5.3). Additionally, for the two samples with spheroidal graphite (NJG-35 and HJ-11), the raw cast iron should have a Mn/S ratio around 1 based on the experimental work carried out by Li and Li (1983).

Table 5.3 Estimated annealing temperature of the malleable cast iron samples.

Sample	Graphite morphology	Matrix	Possible annealing settings
XF-20	Flocculant	Pearlite and ferrite	Figure 2.11
XF-21	Flocculant	Corroded	
XF-34	Flocculant	Pearlite and ferrite	Figure 2.11
XK-Pl1	Vermicular	Pearlite, with cementite remains	Annealing imcomplete
NJG-24	Flocculant	Pearlite and ferrite	Figure 2.11
NJG-35	Spheroidal	Ferrite	Figure 2.10

YC-1	Flocculant	Ferrite	Figure 2.10
LD-3	Spheroidal	Pearlite	Figure 2.9
NY-1	Flocculant	Pearlite and ferrite	Figure 2.11
NY-3	Flocculant	Pearlite	Figure 2.9
NY-4	Flocculant (close to flake)	Pearlite and ferrite	Figure 2.11
NY-6	Flocculant (large size)	Pearlite	Figure 2.9
HJ-7	Flocculant	Pearlite	Figure 2.9
HJ-8	Flocculant	Pearlite and ferrite	Figure 2.11
HJ-11	Spheroidal	Pearlite and ferrite	Figure 2.11

5.2.2 Liquid state decarburisation

In addition to the annealing products, this research has also identified soft iron or steel materials with slag inclusions embedded in the metal matrix. Since there is no direct archaeological evidence providing the information regarding the production technique for such materials, this thesis took the approach of exploring all the possible technical pathways available in premodern times (Figure 5.10), before then using the analytical results and our understanding of these techniques, to make reasonable inferences while acknowledging other possibilities.

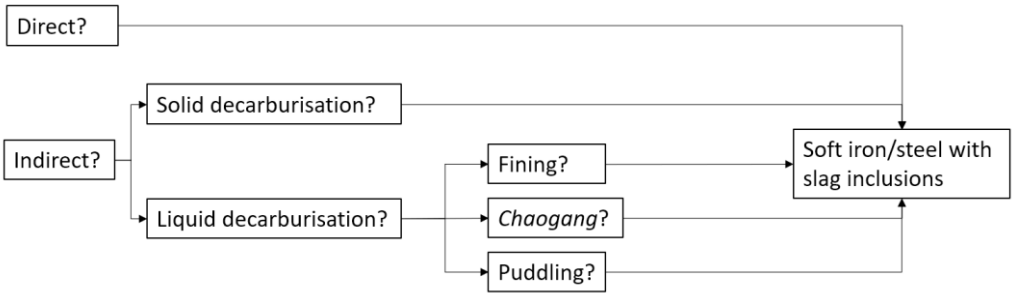

Figure 5.10 Flow chart of the possible technological pathways to obtain soft iron or steel in early China

In early metallurgical practices, soft iron or steel with slag inclusions embedded can be the result of either the direct process, namely bloomery smelting, or the indirect process, which converts cast iron into soft iron or steel through a decarburisation

process. Depending on the decarburisation temperature and the state of the cast iron, the indirect process can be further divided into solid-state decarburisation, namely the annealing process, and the liquid decarburisation process. In the case of liquid decarburisation, past research has invariably categorised artefacts in this category as resulting from the *chaogang*/fining technique, despite the possible differences in operating parameters, which often correspond to a different technology. For instance, both the fining and puddling process can be considered as liquid state decarburisation; the main difference between them normally lies in whether the fuel is mixed with the cast iron. In the fining process, the charcoal is directly mixed with the cast iron during the operation, while the puddling furnace uses a reverberatory system where the heat generated through the combustion of charcoal is directed into an independent chamber in which cast iron is melted and decarburised (Figure 5.18) (Yang 2014: 235-242). As for the fining process, there are also several technological choices regarding how such a process will be carried out. To begin with, according to the description from the *Tiangong Kaiwu* encyclopaedia, the traditional *chaogang* process is carried out in a manner where cast iron was first smelted/melted in a cupola furnace, then directly induced into a pond (fining hearth) and stirred for decarburisation (Figure 2.19), whereas according to the description of the modern fining process, cast iron will be re-melted in the fining hearth instead of using liquid cast iron directly (Han and Ko 2007: 612). In this sense, the *chaogang* process and the fining process, while both referring to the liquid state decarburisation technique, are different in many ways. First, directly using liquid cast iron for decarburisation will not involve the heating up process, where fuel was charged into the fining hearth in mixture with the cast iron to re-melt it. Second, according to the modern description of the fining process, the decarburisation was carried out where cast iron was in a semi-molten state instead of being fully liquified.

Such differences will therefore involve different operating procedures and materials, while the final product will also retain some distinct features. Overlooking such differences can lead to an underestimation of the diversity of early decarburisation techniques as well as causing confusions, since these techniques always result in materials with different technical features. In this sense, this thesis will consider the *chaogang* process as a different form of liquid decarburisation technique comparing to the fining process.

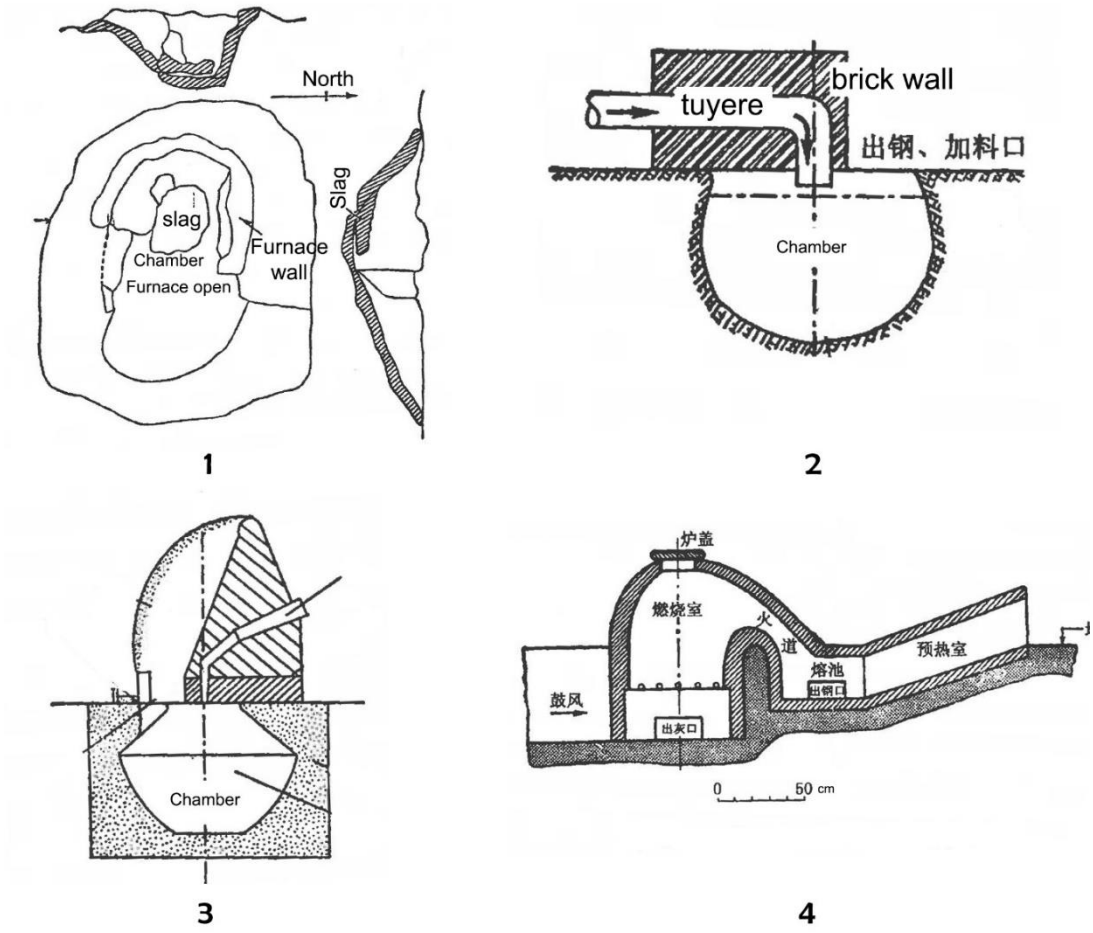

Figure 5.11 diagram of early fining and puddling furnaces. 1, possible fining hearth found in Wafangzhuang, Nanyang, Henan province; 2&3: traditional fining hearth designs in Henan during the 1950s. 4, reverberatory furnace for the puddling process (Yang 2014: 235-242)

To differentiate these technical pathways and find out the corresponding techniques for the analysed samples, the key lies in the chemical composition of slag inclusions. To begin with, the smelting slag from the direct and indirect processes has some

fundamental differences, which should be reflected in their slag inclusions. As introduced in section 2.1.1, the bloomery smelting process strives to obtain a fayalitic slag (Fe_2SiO_4), which is an ideal technological choice as it has both the desirable low melting temperature and a relatively low iron content (Charlton et al. 2010). In this sense, most of bloomery smelting slag or slag inclusions should be fayalite based, with a small amount of hercynite, glass and/or wüstite depending on the actual smelting conditions and charge composition. On the other hand, during the cast iron smelting process, which is carried out in more reducing conditions, most of the iron will be reduced into the metal; consequently, the smelting slag will have a much lower iron content, especially when a calcium-rich flux such as limestone was used (Chen and Zhang 2016; Lam et al. 2018). Meanwhile, the use of such flux will also create a distinctive high calcium concentration, which is rarely seen in the slag produced from the direct process.

On the other hand, the P_2O_5 concentration in slag inclusions is also an indicator for different technical processes. Both the ore and the charcoal may contain certain amount of phosphorus oxide. In cast iron smelting, most P_2O_5 is reduced into the metal due to the high reducing condition. The reduced phosphorous will form Fe-P eutectic (Fe_3P) in the metal, with little to no phosphorus left in the slag. In contrast, in the bloomery process, phosphorus oxide is only partially reduced due to the relatively weak reducing condition, and the reduced phosphorus can hardly be absorbed by the iron bloom which is in solid state; therefore, the P_2O_5 content in bloomery slag is generally higher than in blast furnace slag (Dillmann and L'Héritier 2007).

When cast iron is subjected to a decarburisation process, the phosphorus levels may also change accordingly. If the decarburisation was carried out in a liquid state, the phosphorus in the metal will be re-oxidised and, theoretically, form a stable compound

such as $Ca_3(PO_4)_2$ with the calcium oxides in the system (Dillmann and L'Héritier 2007; Chen and Zhang 2016; Lam et al. 2018). This process will lead to a decrease in the P concentration in the metal and significant high P_2O_5 levels in the resulting slag and slag inclusions, higher than those normally expected from the direct process. Alternatively, if the decarburisation was carried out in solid state, namely the annealing process, phosphorus will not be removed from the metal as the diffusion rate of phosphorous in solid iron is too low under the annealing conditions and impossible to be removed as P_2O_5 gas. Thus, the different behaviour of phosphorous in solid and liquid decarburisation processes can give us a chance to discriminate their products based on the P_2O_5 content in slag inclusions. Based on the above parameters, it may be proposed that the FeO, CaO and P_2O_5 concentration in the slag inclusions can be used together with metallographic information as the main markers to differentiate iron objects made from direct and indirect processes, but also the specific decarburisation technique used to convert cast iron into soft iron or steel.

It is worth noting that there are certain limitations for these criteria to be applied on different sample sets. On the one hand, in some cases, if the iron ore used for smelting contains lime-rich gangue, and/or other raw materials such as technical ceramics or charcoal can lead bloomery smelting systems to produce slag with high CaO concentration (Iles and Martinón-Torres 2009, Veldhuijzen and Rehren 2007). However, these are very rare cases as most of the early bloomery smelting slag analysed does not contain such high amounts of CaO which cannot be distinguished from cast iron smelting slag. On the other hand, if neither the iron ore nor the fuel used for smelting contains phosphorus, or cast iron used was recycled, which means it has been subjected to a refining process, the phosphorous will not be present in the metal or the slag inclusions, which will render the P_2O_5 content less effective as an indicator

for the production techniques. However, analyses of early cast iron from China show most of them have phosphorus levels between 0.1 and 0.6 wt.% (Hua 1982; Li 1982; Zhao et al. 1985; Miao et al. 1993), and thus, the aforementioned criteria are arguably appropriate for this research.

For the 22 soft iron/steel samples with slag inclusions in this thesis, through the compositional analysis and comparison with reference data in chapter 4, it is clear that the majority of their slag inclusions can be distinctively separated from the bloomery smelting slag or slag inclusions. While some inclusions from samples in group 1b and group 2 overlap with the bloomery slag inclusions (Figure 4.66, 4.67), overall, the slag inclusions analysed in this research can be separated from the reference data by their relatively higher P_2O_5 and CaO content, hence these 22 samples should most likely have been made through the indirect process.

As noted above, the indirect process includes both solid and liquid decarburisation processes. The solid decarburisation, namely the annealing process, is carried out in the solid state, hence no slag inclusions will be formed or introduced during decarburisation as such. However, it is possible that new smithing slag can be introduced when the fully decarburised cast iron was subjected to a forging process during the manufacturing of the final object. Smithing slag is mostly formed during the secondary smithing process, such as forging, welding or repairing. In such processes, sand fluxes or clay were often used on the surface of the metal to prevent oxidisation by forming a layer of fayalite through the reaction between silica and the oxidised iron (Figure 5.12). Other sources such as the hearth lining or fuel ash will also contribute a small number of minor elements (Serneels and Perret 2003). After smithing slag was formed on the surface, through repeated folding and hammering, such slag can be incorporated into the metal matrix and become slag inclusions. In terms of chemical

composition, smithing slag should be predominantly composed of SiO_2 and FeO, with lower concentrations of other components (such as CaO) compared to smelting slag, hence compositional analysis should be able to tell them apart. Slag inclusions found near the welding line in sample XF-27 can serve as an example of the smithing slag inclusions (see section 4.2.2). In addition, the metallographic study has shown that while some of the decarburised soft iron or steel samples (XK-Saw1, XK-Kn11) showing deformed grain or layered microstructure has been repeatedly hammered, their metal matrix remained clean without inclusions being spotted (Figure 5.5, 5.13), indicating the forging process does not necessarily introduce new inclusions. In this sense, the bulk of the slag inclusions analysed among these 22 samples are unlikely to derive primarily from smithing slag, hence the possibility that such samples were produced through the annealing process can be ruled out.

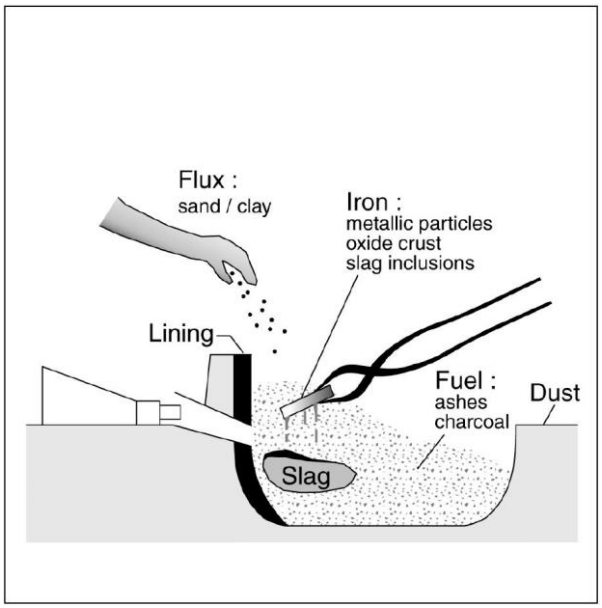

Figure 5.12 Diagram of the smithing process (Serneels and Perret 2003)

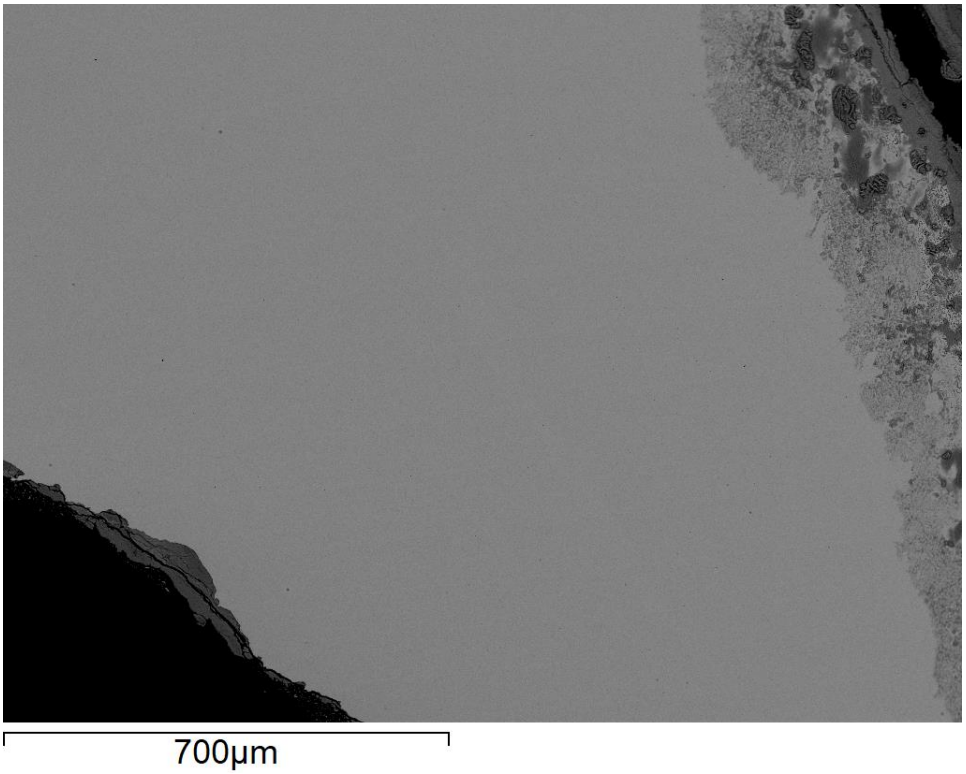

Figure 5.13 Back-scattered electron image of sample XK-Kn11, clean metal matrix

By excluding the possibility of both the bloomery smelting and annealing, we arrive at the conclusion that these 22 samples should have been made from an indirect process where liquid state decarburisation was applied. As noted above, the liquid state decarburisation includes several possible pathways, which will theoretically generate various types of inclusions, hence a significant research focus of this thesis is to recognise such differences, then further reveal the technological details.

To begin with, slag inclusions in samples from group 1a are invariably glassy silicate, and their chemical compositions within individual samples are homogeneous, indicating the reaction during which the inclusions were generated was in liquid state. Sample XF-F29 contains inclusions both high in P_2O_5 and CaO, indicating the reaction was strongly oxidising and a calcium-rich flux was used. Based on this evidence, this sample was probably produced through a process where the cast iron was fully liquified, which fits the description of the *chaogang* process from *Tiangong Kaiwu*.

The rest of the samples from group 1a contain little to no P_2O_5, with lower FeO compared to sample XF-F29. Such inclusions resemble cast iron melting slag in terms of chemical composition (see section 4.3). A possible explanation is that such inclusions were generated during a *chaogang* process, as with sample XF-29, but under weaker oxidising conditions, hence less iron was oxidised into the slag. While the low P_2O_5 content might seem to contradict the assumption that liquid decarburisation always removes phosphorous from the cast iron and enriches in slag inclusions, EDS analysis carried out on the metal matrix has shown no detectable amount of phosphorous either, indicating the raw cast iron used for decarburisation contained little to no phosphorous. Such cast iron could either be recycled cast iron, which would have been dephosphorised before, or smelted with phosphorous-poor iron ores. There is another possible, yet less likely, alternative scenario, which is that these samples were made through the bloomery smelting process, where the gangue of the ore contained sufficient amount of calcium, or fluxes were used during smelting, creating a homogeneous slag with high CaO content.

Slag inclusions in samples from group 1b and group 2 are more heterogeneous in terms of their chemical content. While samples XF-F26, CXC-1 and LD-1 displayed distinctive subgroups (Figure 4.69, 4.70), the rest of the samples showed continuous variance of the chemical concentration among the slag inclusions. The relatively high and variable P_2O_5 in the inclusions suggests the decarburisation temperature was above the melting temperature, yet the cast iron may not have been fully liquified, resulting heterogeneous redox conditions reflected in the variable chemical concentration of certain elements. Such a process fits the description of the fining process where the cast iron was decarburised in a semi-molten state, causing heterogeneous reaction conditions inside the fining hearth: at certain parts, the

condition was more oxidising, hence more iron and phosphorous were oxidised into inclusions, diluting the concentration of other oxides; conversely, at the less oxidising parts, the inclusions will contain less P_2O_5 and FeO.

Furthermore, the morphology of the slag inclusions also offered information regarding the production process. In samples XF-F17, XF-28, NJG-11 and LD-2, a specific type of slag inclusion was observed, in which wüstite crystals were formed on the inner edge of the inclusions, while fayalite crystals can also be observed in the glass matrix, along with glassy silicate inclusions. This type of inclusion represents a reaction phase where the oxidisation of iron was still going on after the formation of the inclusions, hence more iron was oxidised into the glassy silicate, forming fayalite and wüstite crystals on the interface. This, in turn, indicates the production process of such samples was heterogeneously oxidising, which also supports the above conclusion of the fining process.

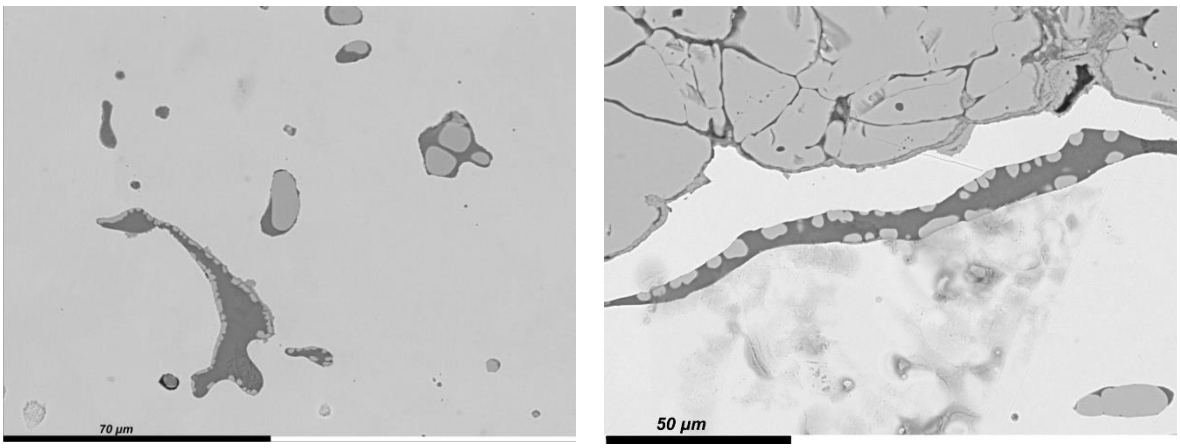

Figure 5.14 Back-scattered electron image of slag inclusions in samples XF-F17 and XF-28, with wüstite crystals formed at the interface.

In samples XF-F26 and CXC-1, slag inclusions show a similar pattern, with glassy silicate inclusions having lower FeO and higher MgO, Al_2O_3, SiO_2, K_2O and CaO, and fayalitic inclusions showing higher FeO and P_2O_5 (see section 4.2.2). Since the NRC and PCA analysis is not clear enough to suggest these two types of inclusions came

from the same source, it remains possible that their manufacture involved the welding of iron from different sources. However, the fayalitic inclusions with high FeO and P_2O_5 content in both samples still suggest this part of iron came from an indirect process where cast iron was decarburised in liquid state, yet the limited evidence is not enough to suggest whether the specific technique was *chaogang* or fining. In the case of sample LD-1, combining the metallography with the slag inclusion study, it should be safe to assume that the object was made of more than two pieces of iron from multiple sources. The type-a and type-b silicate inclusions are most possibly generated in the *chaogang* process given their high CaO concentration and overall homogeneity (Figure 4.56, 4.57, 4.69). In the meantime, we should again acknowledge the possibility that these two parts of iron were made through the bloomery smelting process with a calcium-rich ore and/or flux.

Slag inclusions in samples from group 3 are predominantly composed of oxides that are sensitive to redox conditions. These oxides, including P_2O_5, SiO_2 and MnO, can be partly or fully reduced during cast iron smelting, and tend be re-oxidised in the following decarburisation process, hence they will be enriched in slag inclusions. The presence of such inclusions indicates the iron was produced through the indirect process. Based on the compositional analysis, slag inclusions in NJG-6 and NJG-7 showed no significant amount of other oxides such as Al_2O_3, K_2O, indicating the furnace linings or fuel ash did not contribute to the formation of such inclusions, which excludes the possibility of the *chaogang* or fining process. In addition, the size and morphology of such inclusions also differs from the inclusions seen from the *chaogang* or fining products mentioned above (Figure 4.62), indicating a totally different decarburisation technique was applied for the production of these two samples.

However, current research has not found a corresponding technique in early China that could yield such a material.

In conclusion, among the 22 soft iron/steel samples with slag inclusions, samples from group 1a (XF-25, XK-Sw14, XK-Kn10, NJG-34, GX-2 and XF-F29) were most possibly produced through the *chaogang* process as described in the *Tiangong Kaiwu*, where liquid cast iron was directly stirred and decarburised in the furnace. Samples from group 1b and group 2 (excluding CXC-1, XF-F26 and LD-1) were possibly produced through the fining process, where cast iron was re-melted in the fining hearth, then further stirred and decarburised. Samples CXC-1 and XF-F26 were possible manufactured using two pieces of iron made from indirect process, and the exact decarburisation technology cannot be recognised due to the inconclusive evidence. Sample LD-1 was made using no less than two pieces of iron pieced together, and the glassy inclusions indicate these two pieces of iron were possibly made from the *chaogang* process. Samples NJG-6 and NJG-7 have unique slag inclusions, which were most possibly formed through a decarburisation process without melting the iron, yet the specific detail of the technique remains unknown until further evidence. A summary of the production techniques of these 22 samples is provided in Table 5.4.

Table 5.4 Production method of 22 soft iron/steel samples

Lab No.	Typology	Production method	Remark
XF-25	Adze (Ben)	*Chaogang*	
XF-27	Adze (Ben)	Fining	
XF-28	Adze (Ben)	Fining	
XF-37	Knife	Fining	
XF-F17	Awl	Fining	
XF-F19	Chisel	Fining	
XF-F26	Spoon	Unknown	Two pieces of iron combined
XF-F29	Sword	*Chaogang*	
XK-Sp1	Spear	Fining	

XK-Sw14	Sword	*Chaogang*	
XK-Kn10	Knife	*Chaogang*	
NJG-6	Chisel	Unknown	
NJG-7	Chisel	Unknown	
NJG-11	Chisel	Fining	
NJG-20	Shovel (Chan)	Fining	
NJG-34	Fragment	*Chaogang*	
CXC-1	Sickle	Unknown	Two pieces of iron combined
JC-1	Arrowhead	Fining	
LD-1	Arrowhead	Fining	More than two pieces of iron combined
LD-2	Arrowhead	Fining	
NY-2	Shovel (Chan)	Fining	
GX-2	Knife	*Chaogang*	

6. Technological system and technological choices

In this chapter, based on the relationships between sample typology, function and their predominant production techniques, the general technological system employed in this area for iron production is modelled. The possible reasons behind technological choices are further discussed based on the consideration of broader technological and social factors.

6.1 Technological system

After revealing specific aspects of the production techniques for each of the analysed samples, and initiated a comparison, we can begin to develop broader inferences about the general technological system by linking the typology and function of the iron products with the observed production techniques.

To begin with, since no concrete evidence of bloomery iron products has been found among the analysed samples, it appears that the cast iron smelting technique was the primary technological choice to extract iron in the Qin state.

For the artefacts designed for daily use, including all types of vessels, belt-hooks, lamps etc., the materials used are mainly various types of cast iron produced through the mould casting technique. For specific types of objects including cooking pots and lamps, a slower cooling was applied to obtain mottled or grey cast iron. In addition, five belt-hooks from different sites were annealed under reducing or neutral conditions, which converted white cast iron into malleable cast iron to reduce the hardness.

Table 6.1 Material types of artefacts for daily use

Site	Typology	WCI	MCI&GCI	Malleable cast iron	Sample code
Xinfeng	Tripod	2			XF-2, XF-4
Xinfeng	Pot	1			XF-17
Xinfeng	Belt-hook	1			XF-22
Xiekou	Pot	1			XK-Pot8
Yancun	Belt-hook	1			YC-4
Hejia	Belt-hook	5			HK-1, 5, 6, 9, 10
Xinfeng	Tripod		2		XF-1, XF-3
Xinfeng	Mou		1		XF-5
Xinfeng	Pot		10		XF-7, 8, 9, 10, 11, 12, 14, 15, 16, 18
Xinfeng	Lamp		2		XF-24, XF-F27
Xiekou	Pot		2		XK-Pot7, XK-Pot9
Xiekou	Lamp		5		XK-La13, 14, 15, 16, 17
Yancun	Belt-hook		1		YC-5
Airport	Vessel fragment		1		JC-5
Ningyuan	Pot		1		NY-9
Hejia	Belt-hook		2		HJ-2, HJ-4
Xinfeng	Belt-hook			2	XF-20, XF-21
Ningyuan	Belt-hook			1	NY-4
Hejia	Belt-hook			2	HJ-7, HJ-8
Total		11	27	5	43

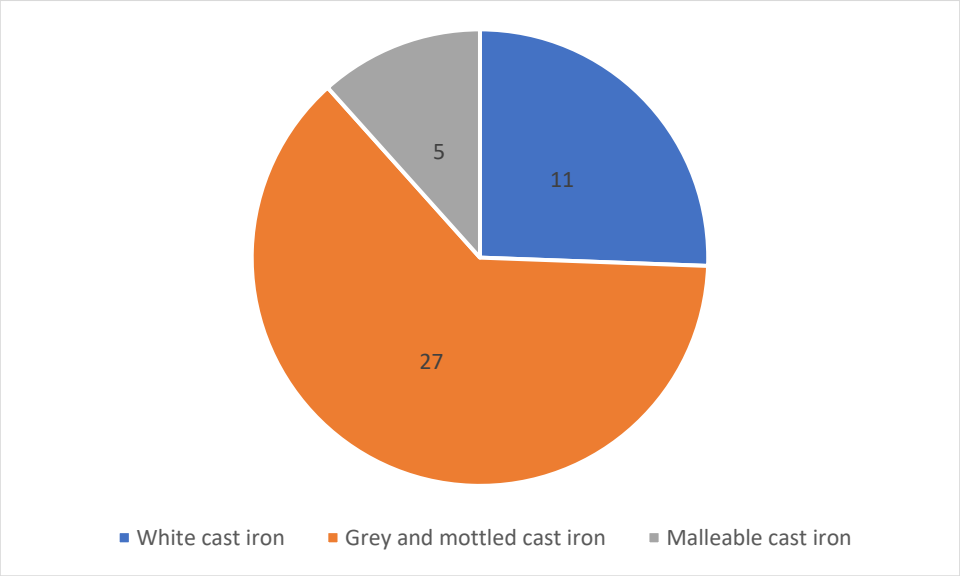

Figure 6.1 Pie chart of material types for daily use artefacts

For the farming implements designed to work on soils, the analytical results have shown the main production technique was to first cast the metal as white cast iron, then apply an annealing process to decarburise or malleablise it to improve its mechanical strength. Additionally, these products were also produced using a range of alternative techniques. Among the samples analysed, a shovel from the Niejiagou site was made of white cast iron without evidence of further annealing treatment. Three adzes from the Xinfeng cemetery, one shovel from Niejiagou site and one shovel from Ningyuan site were made of soft iron derived from cast iron decarburised through liquid decarburisation process.

Table 6.2 Material types of analysed farming implements

Site	Typology	WCI	Decarburised cast iron	Malleable cast iron	Decarburised soft iron/steel	Soft iron/steel	Sample code
Niejiagou	Shovel (Chan)	1					NJG-22
Xinfeng	Shovel (Chan)		2				XF-30, XF-31
Xinfeng	Spade (Cha)		2				XF-33, XF-35
Yancun	Spade (Cha)		2				YC-2, YC-3
Gaoxin	Spade (Cha)		1				GX-3
Xinfeng	Spade (Cha)			1			XF-34
Xiekou	Ploughshare			1			XK-Pl1
Yancun	Spade (Cha)			1			YC-1
Lüdi	Spade (Cha)			1			LD-3
Ningyuan	Spade (Cha)			1			NY-1
Ningyuan	Adze (Ben)			1			NY-3
Xinfeng	Adze (Ben)				1		XF-29
Niejiagou	Shovel (Chan)				1		NJG-21
Niejiagou	Adze (Ben)				1		NJJG-23

Lüdi	Shovel (Chan)				1		LD-4
Xinfeng	Adze (Ben)					3	XF-25, XF-27, XF-28
Niejiagou	Shovel (Chan)					1	NJG-20
Ningyuan	Shovel (Chan)					1	NY-2
Total		1	7	6	4	5	23

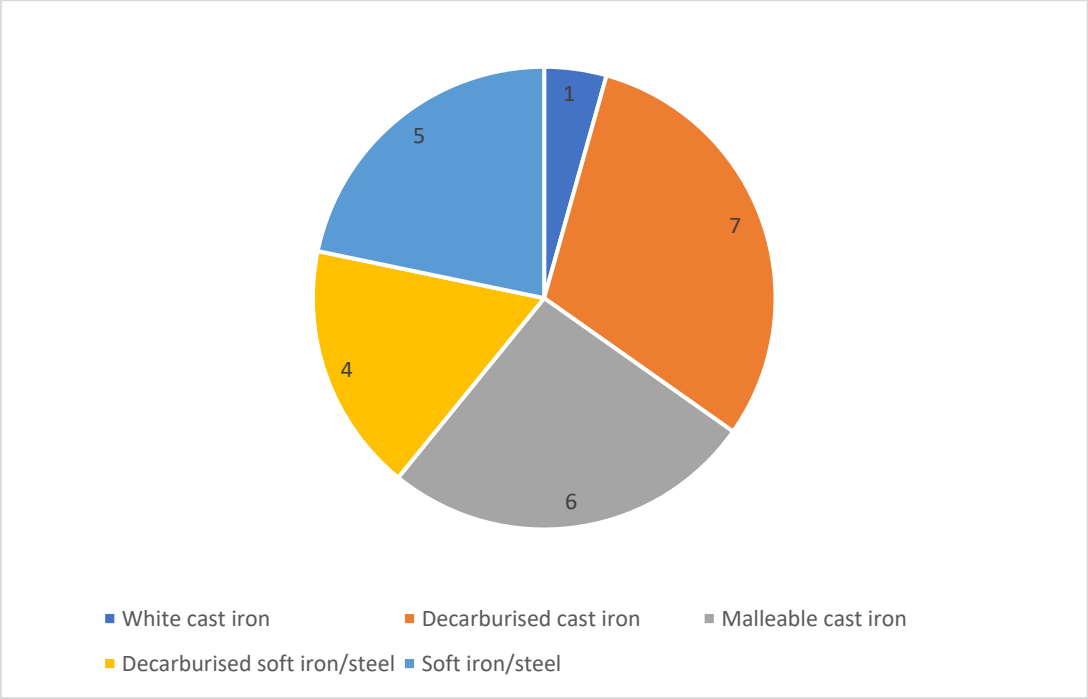

Figure 6.2 Pie chart of material types for farming implements

For craft tools that were designed to work on harder surfaces, including knives, chisels and awls, the material types are predominantly soft iron or steel. A sickle sample (CXC-1) from Changxingcun site is also classified in this category since it is designed for harvesting crops instead working against soil. The production techniques involved in making such products includes converting cast iron into soft iron or steel, prior to being further forged into shape. The decarburisation of cast iron included the solid-state decarburisation via the annealing process, and liquid state decarburisation,

namely the *chaogang* and fining process. Additionally, one knife from the Ningyuan site, sample NY-6, was made of malleable cast iron.

Table 6.3 Material types of analysed craft tools

Site	Typology	Malleable cast iron	Decarburised soft iron/steel	Soft iron/steel	Sample code
Ningyuan	Knife	1			NY-6
Xinfeng	Knife		1		XF-36
Xiekou	Saw		1		XK-Saw1
Xiekou	Knife		1		XK-Kn11
Niejiagou	Chisel		8		NJG-1, 2, 3, 4, 5, 8, 9, 12
Niejiagou	Knife		5		NJG-14, 16, 17, 18, 19
Xinfeng	Knife			1	XF-37
Xinfeng	Awl			1	XF-F17
Xinfeng	Chisel			1	XF-F19
Xiekou	Knife			1	XK-Kn10
Niejiagou	Chisel			3	NJG-6, 7, 11
Changxingcun	Sickle			1	CXC-1
Gaoxin	Knife			1	GX-2
Total		1	16	9	26

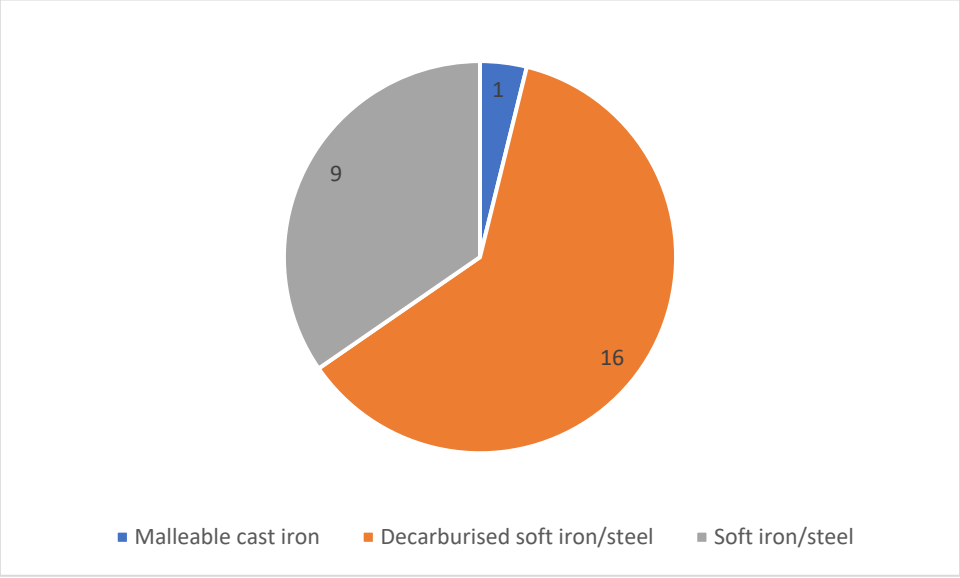

Figure 6.3 Pie chart of material types for craft tools

As for the weapons, only a few types of them were excavated and available for analysis. In this research, two swords, one spear and six arrowheads were analysed.

The results showed the swords and the spear were made by decarburising cast iron in liquid state, then forging into shape. For the production of arrowheads, multiple methods were used, including mould casting with further annealing for partial decarburisation, fully decarburising cast iron through annealing, and decarburisation through the *chaogang* and fining process.

Table 6.4 Material types of analysed weapons samples

Site	Typology	Decarburised cast iron	Decarburised soft iron/steel	Soft iron/steel	Sample code
Airport	Arrowhead	2			JC-2, JC-4
Airport	Arrowhead		1		JC-3
Xinfeng	Sword			1	XF-F29
Xiekou	Spear			1	XK-Sp1
Xiekou	Sword			1	SW-14
Airport	Arrowhead			1	JC-1
Lüdi	Arrowhead			2	LD-1, LD-2
Total		2	1	6	9

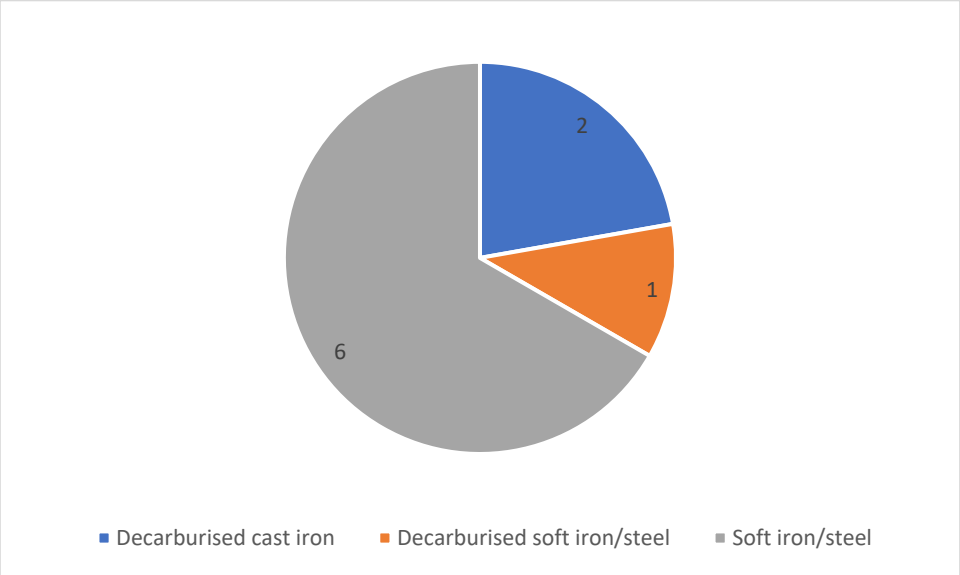

Figure 6.4 Pie chart of material types for weapons

A flow chart of the technological system based on the analytical results is given in Figure 6.5.

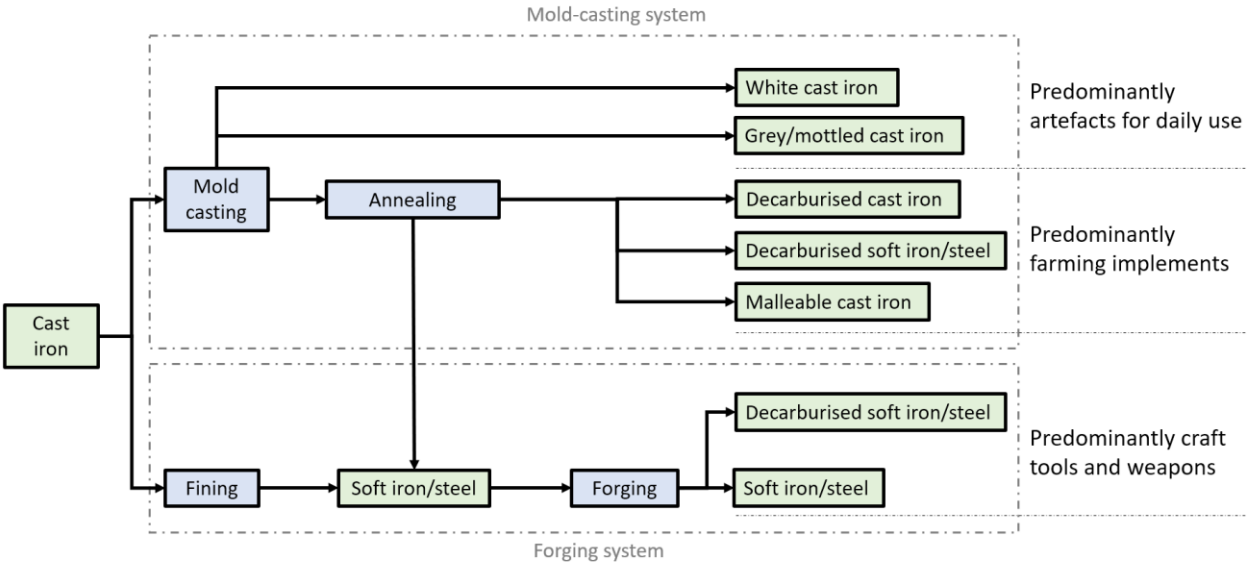

Figure 6.5 Summary of the technological system for iron production in the Qin state recording the main technological choices/pathways as derived from research in this thesis.

In sum, the results suggest that from the later stages of the middle Warring States period, iron production in the Qin state was based on cast iron smelting to extract metallic iron from the ore. Building on this method, a complicated and well-developed technological system was established to make an array of iron products for different functions and activities. Depending on how the final product was shaped, the overall system can be divided into the mould casting and forging branches. The mould casting system was mainly designed for iron products that did not require excellent mechanical strength, such as daily use vessels, ornaments and farming implements. For daily use artefacts such as tripods, cooking pots, or lamps, a direct casting process with different extents of cooling control was applied. For most of the farming implements, an annealing process was adopted after casting to decarburise or malleablise the cast iron to reduce the hardness and brittleness while also improving its toughness. The forging system was mainly designed for making craft tools and weapons, which generally required higher toughness. The raw material used for the forging process were cast iron converted through a decarburisation process, including solid-state

decarburisation, namely the annealing process, and liquid state decarburisation, including the *chaogang* and fining process. Occasionally, farming implements were also produced through the forging process using soft iron/steel made through liquid decarburisation processes, while some arrowheads, which can be considered as consumables, were made by mould casting followed by a decarburisation process.

In this thesis, no clear technological difference has been observed between the sites distributed near Xi'an and the Xianyang city and dated to various periods. Due to the limited number of samples from the Baoji city, it is hard to evaluate the overall technological system there. However, based on the study of the spade and knife sample from the Gaoxin site, it appears that cast iron smelting, casting, annealing for decarburisation and *chaogang* technique had all been adopted for iron production in this area. From a chronological perspective, the production technologies remain the same from the later stage of the middle Warring States period to the Qin dynasty. However, the quality of the iron between the burial goods and the iron products unearthed from the bone workshop in Niejiagou was different. As noted above, the majority of iron tools and implements from the Niejiagou site have an extremely fine grained pearlitic matrix or mixture of pearlite and ferrite, which confers good hardness as well as toughness. While the production technique is also available in other sites, such microstructure was rarely seen elsewhere, indicating the craftsmen making iron products for the Niejiagou workshop had a better control of the annealing and associated production processes.

6.2 Technological choices

6.2.1 Iron smelting: Direct vs indirect

Based on the analytical results, it appears that by the late Warring States period, cast iron smelting had become the dominant method to smelt iron in the Qin state. Given the fact that bloomery iron products have also been found in Qin burials dating back to the 5th century BC, it is safe to assume that the iron production industry in State of Qin had gone through a transition period where bloomery iron smelting was replaced by cast iron smelting. Such a phenomenon will be discussed in this chapter, with consideration of both the technological and social factors that may affect the decision-making process.

Due to the cultural continuities between the state of Qin and other vassal states of the Zhou royalty, the discussion of the technological choice between direct and indirect smelting in the Qin state, inevitably engages broader consideration of the adoption of cast iron smelting in the general central China area. As introduced in section 2.1, both the bloomery iron smelting and cast iron smelting systems have their own technological features, which are generally associated to different models of production that fit different social and technological contexts. For bloomery iron smelting, the initial investment is relatively small, the final product is directly workable, and it does not require a complicated technical system for manufacture, but the yield per smelting is relatively low and the production is discontinuous. In this sense, iron production based on bloomery iron smelting is inherently a small-scale enterprise. In comparison, cast iron smelting requires a much larger initial investment, specialised labour force as well as the necessary skills of planning and organising the production (Wagner 2008: 147; Franklin 1983). It also needs a complicated technological system

to utilise the cast iron. As such, cast iron smelting is only cost-effective when the production is carried out continuously and on a large scale, along with a stable market and efficient distribution system to consume the products.

However, when such conditions are met, cast iron smelting has some advantages over bloomery iron. To begin with, in cast iron smelting, the iron ore utilisation rate is much higher. With the use of flux, cast iron smelting can use iron ores with much lower iron content compared to the bloomery smelting process. This will allow the exploitation of low-grade iron ores and will remove considerable limitations in terms of the location of smelting sites. Second, the final product of the smelting process, cast iron, has a much lower melting temperature, and can be melted in the furnace, which makes the mould-casting of iron possible. Mould casting is suitable for making products with complex shapes; it is also apt for mass production and capable to produce objects with a high degree of standardisation. More importantly, cast iron smelting can be conducted continuously, hence large quantities of iron can be produced easily at a lower cost compared to the bloomery iron smelting system.

Such features of cast iron smelting, while not always necessarily beneficial in all social backgrounds, were a perfect fit for the context of the central China as well as the Qin state in the early Iron Age. To begin with, the technological tradition of mould casting for metal production laid the technological foundation for cast iron smelting to be adopted in early China. Prior to the Iron Age, bronze production in central China had followed a unique trajectory compared to those in the Eurasian Steppe and beyond and entered a “Heavy Casting Era” (重器时代) shortly after the adoption of copper/bronze smelting technique (Hwang 2014). Featuring a highly complicated piece-mould casting process, bronze was mostly used to cast large ceremonial

vessels as well as weaponry, both of which were primarily used to reinforce the political control of the royalty (Figure 6.6). Such a tradition laid down the technological trajectory for future metal production within central China, where liquid metal will always be desired, and the mould casting process was deeply rooted in the craftspeople's knowledge system, hence typically serving as the primary technological choice.

Figure 6.6 Shang Bronze from Metropolitan Museum, dated to 11th c. BC, overall (table): Height, 18.1 cm; Width, 46.4 cm; Depth: 89.9 cm. Source: https://www.metmuseum.org/toah/works-of-art/24.72.1-14/

With no signs of bloomery smelting sites and very limited findings of bloomery iron products dated before the 5th century BC, it is still largely under debate whether bloomery iron smelting was widely practiced in central China during early Iron Age (see section 2.2.2). However, it is reasonable to believe that through the handling of early meteoritic iron and bloomery iron products, iron as a useful and precious material, arguably with better material properties than copper and its alloys, was recognised by

the craftspeople as well as the general society, which could have created a demand for the invention or adoption of a smelting technique. Early iron smelting practices in this area would have followed the bloomery smelting recipe with the same ingredients, yet the established mould-casting technological tradition would have provided a fertile ground so that occasional or accidental production of liquid cast iron would be immediately recognised as a much more preferred material compared to a hot spongy bloom; thus, it is easy to imagine that such a practice would be repeated by the craftspeople again and again to in order get the same materials, leading to the establishment of the cast iron smelting technique.

In the meantime, the access to bronze was largely restricted during the Bronze Age, hence iron would become a suitable alternative material in different aspects of social activities, which created a market for the cast iron production. During the Bronze Age, pottery vessels strictly imitating their bronze counterparts (Figure 6.7) were used across central China, dating to different periods including Shang and Zhou dynasty as well as the Qin burials during Warring States period (Kang 2013; Tian 2014; Zhang 2015; Zhang 2017). The use of such pottery vessels indicates that during the Bronze Age, owing to the limited availability of bronze, certain people had to use pottery as a compromise to produce ritual vessels for burial in order to be in conformity with the funerary tradition. In the meantime, it is also unlikely that bronze was available for making daily use artefacts for the common people. In this sense, the presence of cast iron, even without the aesthetic appearance as bronze, was likely still good enough to enter the market competing against bronze with a lower price, and against pottery as a metallic material that could be mould cast and have better qualities in terms of their overall strength.

Figure 6.7 Pottery vessels imitating bronze vessels dated to Western Zhou period (Zhang 2017)

Furthermore, central China provided vast land with a suitable environment for the development of agricultural economies. However, as demonstrated in the introduction part, agricultural production in early Bronze Age China rarely benefited from the adoption and development of the bronze industry (Yu 1957; Bai 1985; Bai 1989; Han and Chen 2013). Among the few bronze farming implements excavated during the Shang and western Zhou dynasty, the majority of them were found in burials along with large quantities of ritual vessels, symbolising the high social status of the owner, whom were arguably not participants of the actual farming activity; It has also been argued that such farming implements may not have been designed for agricultural production, instead, they were more likely to be used for construction purposes. At the same time, the majority of craft tools and farming implements excavated dating to this period were made of stone, wood and bone in various composite designs, indicating the main materials for agricultural production remained unchanged (Yu 1957, Bai 1985,

Bai 1989, Chen 2013, Rostoker et al. 1983). A dialogue between the philosopher Guan Zhong and the Duke *Huan* of Qin took place in the 7th century BC, as recoded in *Guo Yu*, states that “lovely metals shall be used for casting weaponries, and tried on dogs and horses; ugly metal shall be used for casting tools or implements, and tried on the soil” (Dong 1993). Despite the plausible argument on whether the “ugly metal” refers to low quality bronze or cast iron, this statement in any case indicates that the agricultural economy was eagerly ready for a cheap metal to produce farming implements (Bai 2004). With the development of cast iron smelting, iron as a potentially less aesthetically pleasing but sufficient material, began to be widely adopted to make farming implements for agricultural production. Cast iron is relatively cheap when produced on a large scale, and it can be easily cast into shape; above all, the solidified cast iron has high hardness and abrasive resistance, rendering it suitable to work against soil, hence it could be directly used for the production of farming implements. In the meantime, the agricultural economy guaranteed the food surplus for the labour supply, the planning and organisation skills is also no stranger to the Chinese craftspeople from the experiences of bronze casting industry (Lam 2014).

With cast iron smelting technique widely adopted for iron production, the development of the annealing technique for iron decarburisation and malleablisation in the 6th to 5th century BC, the development of the *chaogang* and fining technique around the 3rd century BC further consolidated the dominance of cast iron smelting in the iron production industry. Since the majority of the iron products, such as artefacts for daily use and farming implements, could be directly cast and did not need the utmost mechanical strength, cast iron still constituted a better choice for these products than bloomery iron, with a lower cost and simpler manufacturing method. While the production of bladed tools and weapons still required the forging of soft iron or steel,

the availability of various decarburisation methods meant that cast iron could also be used as the raw material for their production. In this sense, the necessity of bloomery iron smelting no longer existed in central China. While bloomery iron products are still found in several sites (see section 2.3.2), overall, the limited findings suggest the scale of production is largely restricted.

Table 6.5 A performance matrix for the iron smelting system

	Bloomery iron smelting	Cast iron smelting
Small initial investment	+	-
Able to produce directly workable iron	+	-
Does not require complex knowledge and expertise	+	-
Able to carry out continuous production	-	+
High utilisation rate of iron ore	-	+
Able to produce liquid iron/able to separate slag/metal in liquid state	-	+
Apt for mass production	-	+
Fits the established technological tradition	-	+
Able to meet the social demand	-	+

The state of Qin, which officially become a vassal state of the Zhou royalty in 770 BC, was both culturally and economically similar to its counterparts in the eastern part of the Central Plains. In 770 BC, the capital city of Zhou was moved from Xi'an in Shaanxi province to Luoyang in Henan Province. Gradually expanding eastwards, the Qin state took over the vast land in the Guanzhong plain and adopted a similar cultural, economic and technological system to that of the Zhou royalty in the following centuries. While cast iron smelting started much earlier in the eastern part of central China, with the social turmoil and constant warfare during the Warring States period, exchange of personnel between the vassal states will be frequent through migration and military conquer, which would make technological transmission anticipated. The conditions for adopting an industrial iron production based on cast iron smelting in the

Qin state were also facilitated by the similar social background the Qin state shared with its eastern counterparts. As such, the technological transformation would be inevitable in the Qin state.

After the Shang Yang reform in the middle stage of the Warring States period, the Qin state further consolidated the agricultural production as its economic foundation. To facilitate the agricultural production, large quantities of iron farming implements were required, which created a stable domestic market for the iron industry. In the meantime, the Qin state has also started regulating iron production, setting up iron officials to manage mining and smelting during the late Warring States period (Dai 2012; Chen 2017; Liu 2019). The social demand and a series of state endeavours greatly promoted the adoption and development of the iron production industry based on cast iron smelting.

In conclusion, the technological tradition of mould casting process for metal production in the Central Plains area is the most important factor allowing for the innovation and adoption of the cast iron smelting technique. The demand of farming implements for agricultural production, the cultural tradition for using mould casting products in daily life in the Qin state as well as other vassal states created a large, stable and profitable market, which is also the essential element for the adoption and development of the iron production industry based on cast iron smelting technique. The development of decarburisation techniques made it possible to produce soft iron and steel from cast iron, which further consolidated the dominant position of cast iron smelting technique in iron production, while rendering bloomery iron smelting technique largely obsolete at the same time.

6.2.2 Mould casting: white vs grey/mottled cast iron

Based on the analytical results, the mould casting technique appears to be the primary production technique for most of the analysed iron artefacts, especially for those employed as daily use and farming activities. However, among those iron products made through the mould casting process, grey and mottled cast iron appear to be more preferred than white cast iron. For iron products directly cast without further post-casting treatments, grey/mottled cast iron makes up to 2/3 of all samples (Table 6.6), suggesting the latter appears to be a more preferred technological choice in the Qin state.

Table 6.6 List of cast iron produced through mould casting process.

Site	Typology	White cast iron	Grey/mottled cast iron
Xinfeng	Tripod	2	2
Xinfeng	Pot	1	10
Xinfeng	Belt-hook	1	
Xinfeng	Mou		1
Xinfeng	Lamp		2
Xiekou	Pot	1	2
Xiekou	Lamp		5
Niejiagou	Shovel (Chan)	1	
Yancun	Belt-hook	1	1
Hejia	Belt-hook	5	2
Airport	Vessel fragment		1
Ningyuan	Pot		1
Total		12	27

Grey or mottled cast iron objects have previously been found in different sites across the central China (Table 2.4). However, despite the quantity of these findings, the evidence was still not sufficiently strong to verify that the production of grey or mottled cast iron in these sites was based on intentional technological choices. To begin with, there was no clear correlation between the materials and typology/function among the earlier findings, with grey/mottled cast iron identified in craft tools, farming implements

as well as daily use vessels and casting moulds in small numbers. Secondly, it may be argued that grey or mottled cast iron is not the ideal choice for all types of products, especially for craft tools or farming implements; in these cases, white cast iron may be argued to constitute a better choice due to its abrasion resistance and high compression strength, while the graphite flakes in grey cast iron will reduce such properties as they are soft and act as internal gaps (Wagner 2008: 163). This raises the question as whether the craftspeople produced such products understood the materials and technologies, and made intentional choices based on them. However, as demonstrated in section 5.1.1, the production of grey/mottled cast iron appears to be an intentional technological choice in the Qin state.

Grey cast iron is an important engineering material in modern industry due to its relatively low cost and good machinability, which results from the graphite lubricating the cut and breaking up the chips. Furthermore, the material has good vibration dampening properties (Collini et al. 2008; Wagner 1989). In grey cast iron with 4 wt.% carbon, this element makes around 13% by volume. Since graphite is soft, the presence of such a material can absorb most of the shockwave. In addition, it has also been pointed out that grey cast iron has greater tensile strength than white cast iron and can even exceed that of wrought iron, or low carbon steel (Wagner 1989). While some of these properties may have been unknown to early Iron Age craftspeople, through empirical experience, they would certainly be able to determine whether the objects they made had an acceptable quality and service life, and they could have gained some understanding of how to selectively make and use these materials.

For example, in the technological treatise *Tiangong Kaiwu*, a method to examine the quality of a cast pot is described; the text notes that “by knocking on the pot, a sound like knocking on the wood indicates the pot is in good quality, otherwise it will be easy

to be broken in the future" (Song 1997:110). This is in fact one of the properties of grey/mottled cast iron, as the graphite flakes will dampen the transmission of the sound. Although this treatise was written in a much later period, it is still informative evidence suggesting that craftsmen in preindustrial China were able to tell the difference between these two types of cast iron without modern analytical methods, and further realised that the nature of grey/mottled cast iron was such that the products had a longer service life than white cast iron.

While grey cast iron does not possess a high toughness compared to wrought iron or steel, it does have lower hardness than white cast iron. Grey cast iron with a fine pearlite matrix has the Brinell Hardness between 200 - 270, while white cast iron has hardness values between 400 - 500 (Atlas Foundry Company 2001). Mottled cast iron will have a hardness between these two materials. As explained, lower hardness corresponds to higher toughness and lower brittleness, along with the vibration dampening properties due to the presence of flake graphite, which makes the iron products made of grey/mottled cast iron considerably more durable than those made of white cast iron.

Furthermore, the production process of grey/mottled cast iron, which only includes a mould casting process, is theoretically more cost-effective in terms of labour use and fuel consumption compared to the other technical solutions aiming to reduce the hardness of white cast iron. In early Iron Age China, this could be achieved through the annealing process, which decarburise or malleablise white cast iron under high temperature. While annealing arguably produced metal with better material quality, this process usually takes from hours to days depending on the actual parameter settings, hence more fuel and labour will be needed. Decarburised iron was therefore arguably less cost-effective compared to grey/mottled cast iron production.

In conclusion, both white cast iron and grey/mottled cast iron were used for casting daily use artefacts in the Qin state. However, for certain types of artefacts such as vessels and lamps, grey or mottled cast iron appears to be preferred. Such a technological choice is possibly based on a consideration of cost efficiency, as grey/mottled cast iron offers better material properties overall which leads to a longer service life, yet cost significantly less comparing to other alternative techniques aiming to reduce hardness and brittleness, such as the annealing process.

6.3.3 Decarburisation: annealing vs *chaogang* and fining

For the production of soft iron or steel for further processing via forging, both the solid and liquid state decarburisation technique were adopted. These two types of techniques are fundamentally different in theory and practice, as a result, their products as well as the cost/benefit are also different.

To begin with, the annealing process decarburises cast iron in solid state. Since the main reaction for decarburisation ($C+CO_2=2CO$) is endothermic, and the migration of carbon atoms in cast iron needs continuous supply of energy, hence the annealing process requires continuous heating until the decarburisation is complete. As for the *chaogang*/fining process, since the reaction took place in liquid state, and the main reaction ($C+O_2=CO_2$) is exothermic, hence this process only requires an initial heating up process to melt the cast iron, and the following decarburisation process can be kept going from the heat released from the oxidisation of carbon.

The fuel consumption of the annealing process cannot be accurately measured with too many key parameters missing. For the fining process, on the other hand, it can be evaluated based on the investigation into the traditional fining process in early China. In most of the fining practices in Henan province, China during the 1950s, the typical

charge of the fining operation is reported in a weight ratio between wood, charcoal and cast iron at around 1:1:10 (Wagner 1985: 25). For instance, based on the recoding of one fining practice, 7 kilograms of wood and 7 kilograms of charcoal were used to decarburise 70 kg of cast iron. As a comparison, to maintain an annealing kiln at a temperature above 700 ˚C for days will undoubtedly consume much more fuel. In this sense, the *chaogang* and fining process will be much more cost-effective than the annealing process.

As aforementioned in section 5.2.1, the annealing process usually takes many hours to days to complete. The actual time varies depending on the annealing temperature, the initial carbon content and the amount of cast iron to be decarburised, and it is impossible to be accurately evaluated. According to the annealing practices in the early 20th century, to fully decarburise white cast iron into soft iron or steel, the annealing duration was around 144-240 hours (6-10 days) (Hua 1982). In comparison, the *chaogang* and fining process takes much less time since the reaction is much more intense with the stirring being applied on melted cast iron. According to the traditional fining practices, a typical fining operation takes around one hour to complete, including 20 minutes of heating up, 20 minutes of stirring (puddling) and another 20 minutes to remove the charge and hammering (Wagner 1985: 25).

As for the c*haogang* practice, that is when fully liquified cast iron instead of solid cast iron lumps were used for decarburisation, lesser fuel and time will be needed for the whole process (Wagner 1985: 65). However, melting the cast iron in the cupola furnace will also take time and consume certain amount of charcoal. But in general, it should be more economic compared to the annealing process.

While it appears that the annealing process is more costly in terms of time and fuel consumption compared to the *chaogang*/fining process, it does have some advantages. To begin with, since the annealing process decarburises cast iron in solid state, no slag inclusions will be introduced during this process, and the final product will keep the clean matrix from cast iron. Conversely, the fining process will generate large amounts of slag inclusions in the final product. Slag inclusions in the metal matrix are defects that will affect the overall strength of the metal, as they constitute point of stress concentration that will cause fatigue fracture, reducing the ductility while also promoting corrosions to develop (Bowman et al. 1984). In this sense, the annealing products will have a better overall mechanical strength comparing to the *chaogang*/fining products.

At the same time, the annealing process made it possible to decarburise iron products with a complicated shape, whereas the *chaogang* and fining products are largely limited due to the fact that the final artefact shape had to be obtained through the forging process. In addition, the annealing process can decarburise iron products in batches with a higher degree of standardisation in terms of their shape and size, which is also impractical for the *chaogang*/fining process to deliver. In this sense, the annealing process produces soft iron/steel with a better quality.

Table 6.7 A performance matrix for the decarburisation techniques

	Annealing	*Chaogang*/fining
Fuel efficient	-	+
Short operation time	-	+
Low production cost	-	+
Able to produce high quality soft iron/steel	+	-
Able to produce soft iron/steel products with complex shape	+	-
Able to produce soft iron/steel products in batches	+	-

To sum up, both the annealing technique and the *chaogang*/fining technique have their own advantages in different aspects. The annealing technique is more costly in terms of time and fuel consumption, yet the products generally have better mechanical properties. The *chaogang*/fining technique is more cost-effective compared with the annealing technique, yet its products tend to have a lower quality due to the nature of such techniques. The choice between these two types of techniques should mainly rest on the consideration between the performance and the cost. In this thesis, it has been demonstrated that most of the iron tools unearthed from the Niejiagou site, which is a bone workshop attached to the Qin royalty, adopted the annealing technique for decarburisation. Most of these objects have a clean metal matrix with uniform microstructure and fine grains, indicating a high mechanical strength. In comparison, iron tools unearthed from the civilian cemeteries were mostly produced though the *chaogang*/fining process, which appears to be a compromise considering both the quality and the production cost (Table 6.8).

Table 6.8 List of soft iron/steel tools analysed in this thesis.

Site	Typology	Decarburised soft iron/steel	Finned iron
Xinfeng	Knife	1	
Xiekou	Knife	1	
Niejiagou	Chisel	8	
Niejiagou	Knife	5	
Xinfeng	Knife		1
Xinfeng	Awl		1
Xinfeng	Chisel		1
Xinfeng	Spoon		1
Xiekou	Knife		1
Niejiagou	Chisel		3
Gaoxin	Knife		1

7. Technology within society

In this chapter, I synthesise existing archaeological and historic evidence with my own scientific results and propose a framework for developmental trajectory of iron production in the Qin state. This will be followed by a discussion on the impact of iron production on agricultural development and weapon production in the Qin state.

7.1 Development of iron production in the Qin state

According to current archaeological findings, iron was used in the Qin state since the beginning of the Spring and Autumn period (around the 8th century BC). In addition to the 20 iron swords and knives found in the Tomb No.2 in Yimencun, Baoji, Shaanxi province (Zhao 1997), other findings of iron objects have also been reported in Qin burials dated to the Spring and Autumn period (770 - 476 BC) (Table 7.1). These include an iron sword with bronze handle, reported to be found in a Qin burial in Long county, Shaanxi province, and dated to the early Spring and Autumn period (Zhang 1993); and an iron dagger, unearthed in *Changwu* county, Shaanxi province, dated to early Spring and Autumn period (Yuan 1990). Neither of these two findings has solid archaeological context, and no analytical work has been carried out on them. In 1986, a few iron objects, including several shovels, adzes and knives were found during the excavation of the tomb of the Duke *Jing* of the Qin state in Fengxiang county, Baoji city, Shaanxi province (Han and Jiao 1988). The tomb was dated to late Spring and Autumn period. Metallographic study carried on the shovels has shown they were made of cast iron. However, these iron objects were allegedly collected from the excavated backfill deposits from the tomb without precise contextual information, hence their actual dating is questionable and cannot be used as valid archaeological evidence. During the excavation of a sacrificial pit in *Fengxiang* county during 1981-

1984, an iron adze was also found in the backfill, which could be dated to late Spring and Autumn period (Han et al. 1985). Instead of being collected, this adze was excavated, which indicates such an adze was possibly discarded during the construction of the sacrificial pit.

Further to the western region, some of early Qin burials in the Gansu province also yielded small numbers of iron objects. From the Tomb no.1 at *Jingjiazhuang*, Gansu province, which was dated to early Spring and Autumn period, an iron sword with bronze handle (M1:14) was unearthed (Liu and Zhu 1981). In the horse and chariots pit No.1 in Li county, Gansu province, “heavily corroded iron objects” were mentioned in the excavation report, which could be dated to the beginning of the Spring and Autumn period (Dai 2000). In 1998, an iron sword with a bronze handle was excavated from an elite burial in Li county in Gansu, which could be dated to the early Spring and Autumn period (Dai 2000).

Table 7.1 List of findings of early iron in Qin burials dated before the Warring States period

Site	Dating	Typology
Horse and chariots pits no.1 in Li county, Gansu	Beginning of the S&A* period, 8th c. BC	Unknown corroded iron objects
Tomb no.1 in Jingjiazhuang, Gansu	Early S&A period, 8th c. BC	Iron sword with bronze handle
Elite burial in Li county, Gansu	Early S&A period, 8th c. BC	Iron sword with bronze handle
Unknown Qin burial in Long county, Shaanxi	Early S&A period, 8th c. BC	Iron sword with bronze handle
Unknown Qin burial in Changwu county, Shaanxi	Early S&A period, 8th c. BC	Iron dagger
Tomb of Duke Jing in Fengxiang, Shaanxi	Late S&A period, 6th c. BC	Shovels, Adzes and Knives
Sacrificial pit in Majiazhuang, Fengxiang, Shaanxi	Late S&A period, 6-5th c. BC	Adze
Tomb no.2 in Yimen, Baoji, Shaanxi	Late S&A period, 6-5th c. BC	20 iron swords and knives

*:Spring and Autumn period

Overall, the majority of such findings are iron weapons with bronze or gold accessories and decorative parts. The burials that yielded such findings were mostly associated with tomb occupants of high social status. Due to the absence of production sites, whether these iron products were locally produced or imported from outside remains unclear. Nevertheless, such phenomenon still indicates that during the Spring and Autumn period, iron was a rare and valuable material in the Qin state and only available to a small group of social elites. It is surmised that even if iron smelting was practiced locally, the scale of production would have been limited.

While these early iron findings in Qin burials serve as evidence for iron usage in the Qin state, most of them have not been subjected to scientific study, therefore their smelting and manufacturing techniques remain unknown. The only scientific study, carried out on the iron sword from tomb No.2 in Yimencun, showed it was made of bloomery iron, which suggests that during the late Spring and Autumn period, bloomery iron was still being produced or imported in the Qin state. Based on the typology of these early scattered findings of iron objects in the Qin state, I suggest that these iron objects were most possibly produced through bloomery smelting process, since cast iron smelting is inherently large-scale production, which contradicts the high social value of iron in this findings.

During the early to middle stage of the Warring States period, iron was rarely, if ever, found in all sorts of Qin burials. This is an intriguing archaeological phenomenon compared to the other vassal states in the east, where large quantities of iron dating to this period have been recovered. The absence of iron in the Qin burials during this period may be affected by multiple factors such as limited archaeological excavations and the transformation of mortuary traditions in the Qin state. The most plausible

explanation is, however, the decline of iron production due to a deteriorating political situation in the Qin state during the time, as also documented in historical records, which could have led to a tighter control over the production and distribution of iron by the state. According to related historical records, from the beginning of the Warring States period to 384 BC, the Qin state suffered from a series of internal unrest and external military failures. It is not until Duke Xian came in position in 384 BC, who led a series of reforms including abolishing the human sacrifice tradition, moving the capital to Yueyang city as well as encouraging trade and implementing a new administration system that the situation eventually stabilised (Pines 2013: 2-4).

From the middle Warring States period onward, iron products started to appear and become increasingly common in Qin civilian burials. To demonstrate this profound change, this research has examined two Qin cemeteries, which includes burials dated from the Spring and Autumn period to the Qin dynasty, and shown the rising number of iron products in Qin burials.

To begin with, in the Qin cemetery at *Gaozhuang*, Fengxiang county, Shaanxi province, 46 tombs dated between late Spring and Autumn period to the Qin dynasty were excavated. Among these 46 tombs, two of them were dated to the late Spring and Autumn period, with no iron being unearthed. 16 tombs were dated to early Warring States period, with only one iron belt hook unearthed from tomb no.26. Among the 15 tombs dated to the middle Warring States period, five belt hooks and two rings were unearthed from three tombs. As for the three tombs dated to the late Warring States period, all of them contains iron products, including two belt hooks, one knife and one tweezer. For the ten tombs dated to the Qin dynasty, nine of them have iron products being unearthed, including chisel, awl, adze, knife, sword, cooking pot and belt hook etc. (Figure 7.1) (Wu and Shang 1981).

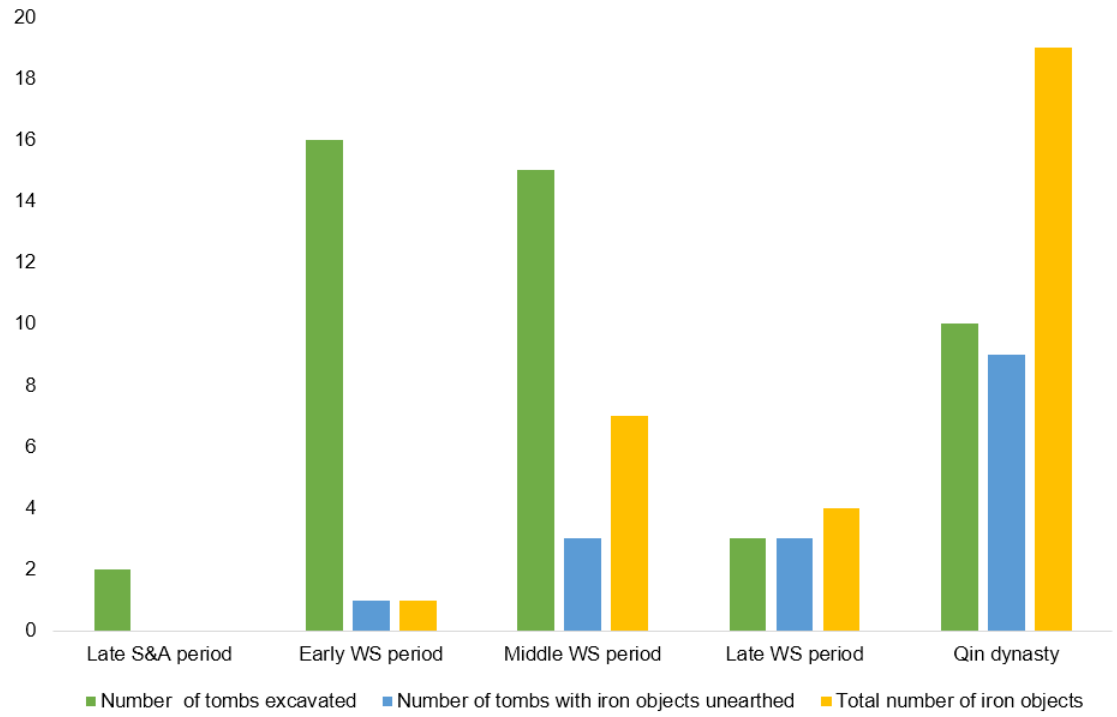

Figure 7.1 Comparisons of tomb excavated/number of tombs with iron findings/total number of iron objects between different period in the Gaozhuang Qin cemetery

Another representative Qin cemetery is the *Dianzi* cemetery at Long county, Shaanxi province. In this cemetery, 224 tombs dated between middle stage of the Spring and Autumn period to the Qin dynasty were excavated. Among these tombs, iron products only begin to occur in the tombs dated to the late Warring States period. Among the 40 tombs dated to this period, two of them yielded two iron objects, including an iron spindle whorl and an unrecognisable fragment. As for the 54 tombs dated to the Qin dynasty, nine of them yielded 15 iron objects, including four cooking pots, one jug, seven farming implements, two knives and an unrecognisable fragment (Shanxi Privincial Institute of Archaeology 1998).

While the burial findings do not necessarily reflect the use of iron in actual life, the presence of them in civilian burials does suggests the scale iron of production has increased, and iron has become an affordable material for the common people. Along with the increase in the absolute quantities, the category of iron products is also

becoming more diversified in the following late Warring States period. In the middle Warring States period, iron found in Qin burials was mostly in the form of small ornaments, such as belt hooks and rings, which use very small amount of iron and are easy to manufacture. During late Warring States period, iron products unearthed from Qin burials covered basically every aspect of daily life, including large cooking vessels, ornaments, craft tools, farming implements as well as weapons (Di 2012), which shows the increase in both the scale of iron production as well as the complexity of production techniques. Along with the growing ubiquity of iron in Qin burials, the analytical results obtained in this research also shown the production techniques have changed, from the possible bloomery iron smelting during the Spring and Autumn period, to a fully developed cast iron smelting-based technological system during the late Warring States period and Qin dynasty.

The study of organisation of the iron production in the Qin state has been severely fraught with the lack of archaeological findings of actual production sites for iron smelting and manufacturing. Current archaeological research has located three possible iron manufacturing workshops dated to Warring States period, located in the Yong city, Yueyang city and Xianyang city respectively, all of which were Qin capital cities (Liu and Li 1985; Tian 2013; Shaanxi Provincial Institute of Archaeology 2018), yet no systematic excavation has been carried out so far. It is likely that such sites were mainly designed for manufacturing iron products rather than smelting since the smelting site should ideally be located closer to the fuel source and ore deposit to reduce the cost of transportation.

In addition to the archaeological evidence, there is plenty of historical literature as well as palaeographic materials that carries valuable information about the society during the Warring States period, such as the Qin bamboo texts unearthed from different

locations. This line of evidence also provides detailed description about the administrative details of the government as well as the daily life of the Qin people (Chen 2012; Peng 2002). Based on these evidence, a high level of state involvement in iron production has been established during the late Warring States period. According to the bamboo texts excavated from *Liye* in Hunan province, and *Shuihudi* in Hubei province, the Qin government has developed a complicated administrative system to regulate the iron production during the unification war period. Officials including "*Cai tie (采铁)*", "*Ye tie (冶铁)*" and "*Tie guan (铁官)*" were set up both in the central and local government to manage mining, smelting, manufacturing and trade (Dai 2012; Tang 2019). In this system, the private and state-owned iron foundries co-existed in the iron production industry. The private iron production was run under the supervision of the state iron office, who was also responsible for collecting a fixed rate of tax from both smelting and manufacturing workshops. The iron products produced from these foundries would be further sold on the market, which is believed to have been highly profitable. The *Shiji* recorded three iron smelting families, *Zhuo*, *Chengzheng* and *Kong*, which were deported/relocated by the Qin state after military conquer of their original state, quickly got enriched to own thousands of servants and become social elites (Sima 2010: 7615-7616). The state-run iron foundries belong to dedicated departments in the central government, including the *shaofu* (少府) and *neishi* (内史). The *shaofu* department was tasked with making weapons for the military and all types of craft tools for construction workers. The *neishi* department was mainly in charge of regulating the production of craft tools and farming implements for civilian use (Tang 2019). The majority of iron products produced from the state-owned iron foundries were distributed through local governments, where they were let to craftsmen and peasants but should be returned after usage. In addition, the state also

set iron officials managing the trade, where certain amount of iron products made in the state-owned workshops were sold on the market to make a profit. The main source of labour for the state-owned mining and smelting workshops were convicts and captives, who were centrally regulated by the local government. As for the private ones, the main source of labour should be hired civilian workers.

The Qin involvement in iron production is not unprecedent. During the Warring States period, both the Qi state and Yan state also set up state-owned iron workshops. It has been argued that such a tradition can be traced back to middle Spring and Autumn period (Dai 2012). However, it can be argued that the Qin state management of iron production was most comprehensive and should be the seen as the root of the Han iron monopoly. It is as yet unclear when the state involvement of iron production started in the Qin state. Most of the evidence is based on palaeographic materials excavated in the later conquered areas and dated to the unification war period (236-221 BC) and the following Qin dynasty. The *Liye* bamboo text is dated to around 222 BC, the *Shuihudi* bamboo text can be dated to 217 BC. The relocation of the iron smelting families also took place during the unification war. In this sense, the effect of state control on the development of iron production during the Warring States period cannot be precisely evaluated.

To sum up, the archaeological and historical evidence has provided a general picture of the development of iron production in the Qin state. During the Spring and Autumn period, limited amount of bloomery iron, whether locally produced or imported, was used to make weapons for ritual purpose. From the early to middle stage of the Warring States period, there is a sharp decline of iron in archaeological findings, which could be indicative of a decline of iron production in the Qin state. From the middle stage of the Warring States period onward, after the Shangyang reform, the iron

production industry seems to have enjoyed a great time for development, where large market demand for iron was created by the developing agricultural production, along with population growth as well as migration, which could have provided specialised labour force as well as introducing new techniques. I would argue that during this period, iron production based on cast iron smelting was greatly developed, along with technological innovations taken place. From the later stage of the middle Warring States period, a well-developed iron production industry based on cast iron smelting and associated production techniques were established across the Guanzhong Plain. By the end of the Warring States period, a high level of state involvement in the iron production industry was implemented, which further laid the technological and economic foundation for the following unification war and the establishment of the Qin empire.

6.2 The social and economic impact of the iron production industry

With iron becoming an inherent part of social life in the Qin state during the late Warring States period, there would undoubtedly be a great social impact on the development of the Qin state. In 362 BC, the Duke Xiao of Qin came into power. Under his governance, Shang Yang (or Gongsun Yang), who was one of the earliest legalists in China, was appointed as the chief adviser and led a series of reforms which significantly transformed the Qin state in many aspects. Lord Shang himself personally holds the ideology of “Agricultural-Military principle (耕战)”, which states that the key to run a state successfully lies in the development of agricultural production, which can further provide food for a larger population as well as allowing a bigger military (Liu 1983).

Following this principle, the Shangyang reform was carried out in 356 BC and 350 BC. The reform includes a series of state policies which fundamentally aimed to increase the agricultural production as well as the military power, and successfully enabled the Qin state to unify the seven states and establish the first empire in Chinese history. In this sense, this section will look into the use of iron farming implements and weapons in the Qin state, and explore its relationship with the agricultural development as well as the military success, hence developing discussion on the social impact of the iron production industry in the Qin state during the late Warring States period.

7.2.1 Agricultural development

As the economic foundation, agricultural production in early China largely depended on certain factors including the amount of arable land, weather, water supply and the use of farming tools (Rostoker et al. 1983). In other words, to increase food production, the common method was to exploit more land for farming and/or to increase the yield per unit area through regulating water supply and implementing better soil management. In order to do so, the use of high-quality iron tools would be essential as it could be both used for land cultivation, soil management as well as building hydraulic systems for irrigation, therefore increasing the output per person-hour/unit area and releasing a larger part of the population for non-agricultural activities (Boserup 1965: 17-19). This argument is also in line with past research, where the impact of iron farming implements on the development of agricultural production in early China has been studied in detail (Yang 1980; Lei 1980; Lei 1986; Wang 2004; Li 2005b).

In terms of the Qin state, based on current archaeological findings, several types of farming implements have been found in Qin burials during the late Warring States

period, including shovels (*chan*), adzes (*ben*), spades (*cha*), sickles and ploughshares, which would have been used in a wide range of farming activities from reclaiming land to harvesting crops. These farming implements have shown a high level of consistency in terms of their size and shape, indicating they were most likely mass produced (Chen 2017; Liu 2019). The analytical results presented in this research have also shown the production technique is highly developed and possibly centrally regulated. In this sense, I argue that the availability of a well-developed iron production industry supplying large quantities of affordable farming implements enabled the Qin state to further make progresses on agricultural development as well as initiating a series of reforms to accommodate the increasing productivity, which laid the economic foundation for the unification war and the establishment of the Qin empire.

As aforementioned, one of the most important policies of the Shangyang reform was the abolishment of the allegedly “nine squares system” (井田制) of land ownership, under which the land was owned by the local ruling class, while peasants working there only got to keep a small part of the output. In the new system, land was privatised to each peasant and a fixed amount of taxes would be collected (Ye 1999). This is a critical step in the change of social structure and greatly motivated the initiative of the peasants. Meanwhile, aiming to increase the total acreage of arable land, the reform also broke up large families into small ones and assigned each new family large number of lands for them to cultivate. Land was also used as rewards, given to people who have made contributions in the military (Zhang 2017).

In the meantime, according to the *Shuihudi* bamboo text, the Qin government also promoted the usage of iron implements and the cattle for farming during the late Warring States period and Qin dynasty, deploying iron officials to let implements to

those who could not afford to purchase them, which would undoubtedly increase the overall productivity of the peasants as well as the yield per unit area.

Additionally, to further facilitate agricultural production, the Qin government also invested in irrigation systems for farming. During the late Warring States period, two large hydraulic systems were built, aiming to provide irrigation as well as harnessing the flood, including the Dujiangyan irrigation system and the Zhengguo canal. The Dujiangyan irrigation system was located in the modern-day Sichuan province. During 256 BC-251 BC, the governor, Li Bing, managed to construct the Dujiangyan irrigation system, which harnessed the Min river using a new method of channelling and dividing the water rather than simply damming it. This system, which is still in use today, successfully solved the flood problem and made the Sichuan Basin one of the most productive agricultural regions in early China (Li and Xu 2006).

The Zhengguo canal, which is another hydraulic system named after its designer, is located in the Guanzhong Plain. This work started in 246 BC and was finished roughly ten years later. The canal stretches around 300 kilometres and connects the Jing River with the Luo River (Figure 7.2), irrigating the vast land along it, allegedly around 733 square kilometres, making the Guanzhong Plain “a fertile land without famine year” (Sima 2010: 2317). The Zhengguo Canal is especially important since it is located in the heartland of the Qin state and runs through several Qin capitals and surrounding lands, hence it would have played a vital role in promoting agricultural production in a sense that it can secure reliable agricultural yields. It has also been argued that such irrigation systems fundamentally changed water management and farming patterns, therefore significantly increased productivity by converting previously unoccupied land into fertile ground and pushed population threshold to a new level (Zhuang 2017). The construction and maintenance of these two hydraulic/irrigation systems, which

involved massive work of excavation on different types of geological conditions, undoubtedly required large amounts of reliable iron tools and implements, which could only be supplied through an efficient and well-developed iron production system based on cast iron smelting.

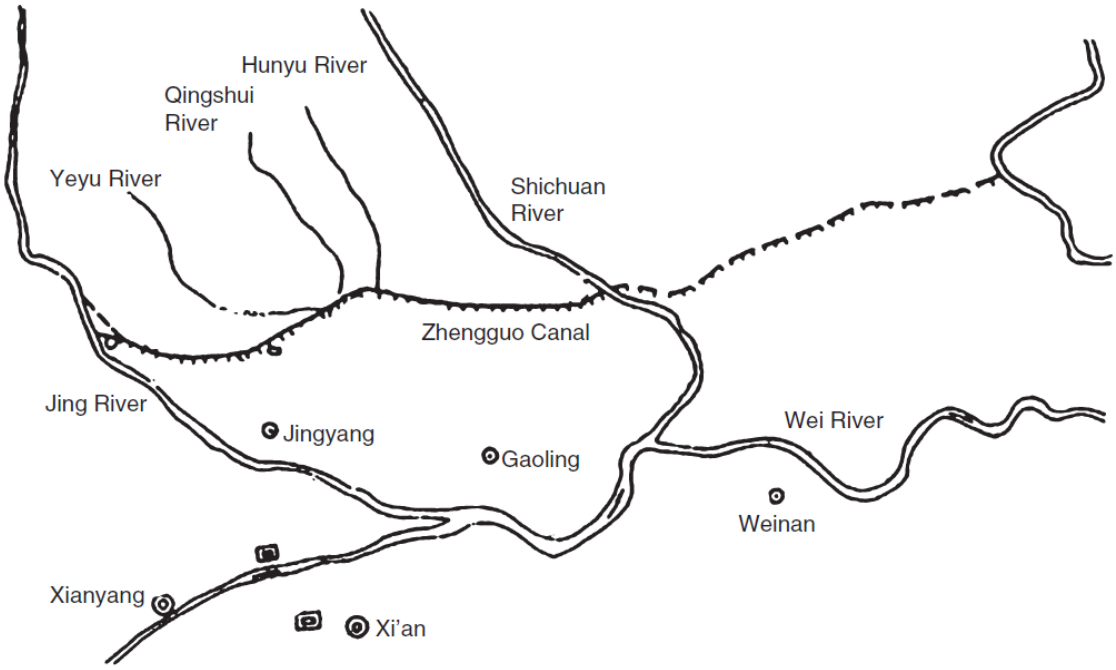

Figure 7.2 Diagram of the Zhengguo canal, with locations of major and secondary rivers and cities it flows through (Zhuang 2017)

7.2.2 Military use of iron

In terms of the use of iron for weapon production, current evidence appears to indicate uneven development stages among the vassal states. On the one hand, there is archaeological and historical evidence suggesting the wide use of iron in weapon production during the Warring States period. For instance, in the fallen soldiers' tomb in M44 in the Yan state capital, the majority of the weapons (51 out of 53 in total) were made of iron, including swords, spears, halberds and armours etc., while only one sword and one dagger-axe were made of bronze (Liu 1975). Unlike other regular burials, M44 is special in the sense that the purpose of building such a burial was to

demonstrate the military triumph over the deceased, namely 22 soldiers who were all violently killed and randomly thrown together; therefore, the weapon findings directly reflect the technological choice in real life. According to the typology of the weapons and the inscriptions on them, the excavators believe these soldiers were from the Yan state during the late Warring States period, indicating iron weapons were commonly used in the Yan state army during this time.

In the southern part of central China, the Chu state was also leading in iron weapon production based on the archaeological and historical evidence. Among the Changsha Chu tombs, a total number of 39 iron swords dated to the Warring States period, including several types of iron swords and halberd were unearthed, which is more than all the iron swords currently found in the Qin burials dated to Warring States period combined. According to the *Shi Chi*, the Duke *Zhao* of Qin, who was in position during 306 BC - 251 BC, publicly expressed his concern over the high-quality iron swords produced in the Chu state to his chancellor, *Fan Ju*, worrying the advantage of the weapons may constitute a threat to the Qin state. This indicates that the Duke of the Qin state acknowledges the importance of iron weapons in warfare, and there is a high level of iron weapon usage in the Chu state during the late Warring States period, whose manufacturing technique were much better than the Qin state.

On the other hand, based on the archaeological evidence in the Qin state, iron weapons were much less common in Qin burials comparing to its counterpart states. To begin with, weapons in the terracotta army, which were mostly manufactured in the late Warring States period and early Qin dynasty, were exclusively made of bronze, with only six iron ones, including a spear, an arrowhead, and four bronze arrowheads with iron tang being found (Shaanxi Provincial Institute of Archaeology and Emperor Qinshihuang's Mausoleum Site Museum 2000). Such a phenomenon seems to be

suggesting that even during the early Qin dynasty, bronze was still the main material for weapon production in the Qin army. However, in recent years, with the on-going excavation work, iron weapons, including swords, spears, arrowheads etc. has been found in Qin burials (see section 3.3.2). Analytical work carried out on these weapons in this thesis has shown that their manufacturing techniques in the Qin state is well developed, with all the essential technologies developed and applied. In the meantime, with the innovation of the liquid decarburisation techniques, iron weapons could conceivably have been produced at a relatively low cost in the Qin state, therefore mass production of iron weapons will be achievable. While the overall quantity of iron weapons findings in the Qin state is still relatively low comparing to other vassal states, such a contrast is more likely to be the result of different mortuary traditions. For instance, in the Changsha Chu cemetery in Hunan province, more than 1200 weapons (excluding 309 bronze arrowheads), including 39 iron ones dated to Warring States period were excavated from 2048 burials. As for comparison, in Xinfeng cemetery, only 12 weapons, including 10 bronze ones and 2 iron swords were excavated from 596 burials. This clearly suggests that the burial tradition between these two states were different, where the Qin people are less likely to use weapons as funerary objects comparing to the Chu people.

Regarding the bronze weapons buried with the terracotta army, it is more reasonable to believe that such weapons were specifically produced to be buried with the emperor rather than reflecting the actual choice of weapon usage in the Qin army. While previous study has demonstrated that the production of such weapons was well organised, and the final products were finely alloyed and sharpened, which seems to be suggesting a utilitarian purpose (Martinón-Torres et al. 2014; Li et al. 2014; Li et al. 2011; Li et al. 2016; Bevan et al. 2018). However, it needs to be born in mind that the

terracotta army is a special case since it is designed to serve the emperor's afterlife, and the cost of production will be less relevant. In this sense, bronze is aesthetically more pleasing than iron, more resistant to corrosion, and easy to be manufactured in batch with a high level of standardisation. Additionally, bronze has always been considered as a more suitable material for ritual purposes and often found in high-ranking burials, while iron is much more utilitarian and less likely to be used for ritual purpose. More importantly, the mechanical strength of bronze weapons is considerably lower than iron ones with a steel microstructure. Typical bronze weapon contains 15 - 20 wt.% of tin, which has the optimum performance. Analysis carried out on four bronze swords from the pit 1 in the terracotta army have shown the tin content is between 17.9 - 19.8 wt.%, which gives such an alloy a golden colour as well as favourable mechanical strength (hardness and tensile strength) (Emperor Qinshihuang's Mausoleum Site Museum 2018: 282-292). However, compared to the iron sword found in the Xinfeng cemetery, which consisted of a Widmannstätten structure, and many other craft tools analysed in this research which have fine grained pearlite or layered microstructure, the bronze weapons in the terracotta army would be considerably inferior.

While the quality of the bronze and iron weapons cannot be directly compared from a theoretical perspective due to many affecting factors such as grain size, heat treatments as well as overall design etc., it is clear that iron weapons were desired in the Qin state, while the essential technologies were also developed and adopted. In this sense, I would argue that the actual level of iron usage in the Qin army should be much higher than what the current archaeological evidence suggests.

To sum up, based on the analytical results and the archaeological findings, I propose that during the late Warring States period and Qin dynasty, iron weapons should have

been used widely in the Qin army – or at least, more frequently than the current archaeological evidence might suggest. The absence of iron weapons from the terracotta army should be seen as a conscious technological choice, where bronze was intentionally chosen to be used for weapon production to serve the emperor's afterlife. This assumption is based on two grounds: first, analysis of iron weapon samples in this thesis have shown all essential technologies for iron weapon production were developed and adopted in the Qin state, which allows the mass production of iron weapons at reasonable cost, while historical evidence also suggest a demand of iron weapons in the Qin state during the Warring States period; second, from a practical point of view, bronze weapons are inferior in terms of their overall quality compared to its iron counterparts, while the mass production based on cast iron smelting also made the cost of production for iron lower than bronze, therefore the iron weapons must have been widely produced in the Qin state, and its contribution to the unification war should not be underestimated. However, such argument is still largely hypothetic, and more work on the archaeological findings from non-burial contexts in the Qin state needs to be done to further verify/falsify this conclusion.

8. Conclusion and future work

8.1 How was iron produced in the State of Qin during Warring States period?

Based on the analytical results of the archaeological samples, it has been demonstrated that from the later stage of the middle Warring States period onward, cast iron smelting had been adopted in the Qin state for iron production, with no concrete evidence of bloomery iron smelting being practiced in this area. In comparison with bloomery iron smelting, cast iron smelting was carried out in a blast furnace with higher temperature and more reducing atmosphere, consequently an iron-carbon alloy with a higher carbon content (usually between 3 - 5 wt.%) and lower melting temperature was produced. Aiming to cost-effectively produce various types of iron objects using cast iron, a well-developed technological system was established in the Qin state during the late Warring States period. In this system, mould casting and forging were the two fundamental shape formation techniques for making iron products. The mould casting technique involved pouring liquid cast iron into casting moulds and subsequent solidification, therefore allowing mass-production of iron objects with well-designed shapes. Based on the analytical results, it appears that when practicing the mould casting process, different solidification control mechanisms were applied for different product categories. When the primary casting product needed to be further decarburised or malleablised, a faster cooling rate was applied to facilitate the crystallisation of the metal into white cast iron; when producing some types of daily use objects such as tripods, cooking pots and lamps, mottled or grey cast iron were more common material, indicating a slower cooling rate was ensured through pre-heating the mould before casting, and hence favouring the crystallisation of various amount of flake graphite.

Since cast iron is hard and brittle, various types of decarburisation or malleablisation techniques were adopted to improve the mechanical strength of cast iron in the Qin state. For most of the farming implements and craft tools, the analytical results have shown an annealing process was applied after casting. This technique involved heating the finished cast in the annealing kiln to above 700˚C. Depending on the actual engineering parameter settings, cast iron will be either decarburised by removing the excessive carbon in an oxidising condition, or malleablised by transforming the carbon atoms into graphite (temper carbon) in a neutral or reducing condition. Based on the analytical results, the craftspeople were able to finely control the annealing process to achieve different microstructures.

For making weapons and certain types of craft tools which need high mechanical strength, forging instead of mould casting was adopted. The forging process requires soft iron or steel as raw material. The production of such materials was achieved through the decarburisation of cast iron. The results presented in this thesis indicate that both solid and liquid state decarburisation of cast iron were adopted in the Qin state. The solid-state decarburisation involved annealing cast iron in the kiln for an extended period of time, where the cast iron will be thoroughly decarburised into soft iron or steel, and then further forged into final product. The liquid state decarburisation of cast iron was documented in the form of the traditional *chaogang* process, or as the so-called fining process. In the *chaogang* process, cast iron was first smelted/melted, then the melted cast iron was induced into fining hearth, where it was stirred and decarburised through contact with oxygen from the air. In the fining process, solid cast iron was directly heated up in the fining hearth to a semi-molten state, then further stirred and decarburised. Additionally, this thesis has also found a special type of slag inclusions, as illustrated in samples NJG-6 and NJG-7, which could be representing a

decarburisation technique different from both the annealing and *chaogang*/fining process. However, there is currently no archaeological or historical evidence to suggest the details of such a process.

In addition, the metallographic study showed that multiple heat-treatment techniques were employed for iron production in the Qin state. These include quenching from different temperatures, annealing, tempering, and normalising for recrystallisation; these techniques variously aimed to further increase the mechanical strength of the finished products.

8.2 How was such a production system developed and shaped throughout history?

Due to the limited analytical work carried out on the iron production in the Qin state prior to this research, the iron production technologies before the middle stage of the Warring States period remain unclear. Although it has been demonstrated that bloomery iron was used in the Qin state since early Spring and Autumn period as a valuable material, owing to the limited quantity of such findings and the lack of production sites, this thesis cannot ascertain whether these iron findings were locally produced or imported.

Based on the analytical results obtained from this research, the iron smelting technique in the Qin state become fully based on cast iron smelting since the later stages of the middle Warring States period. Such a technological transition most likely took place from the early stage of the Warring States period, as a result of a combination of technological and social choices.

From a technological perspective, cast iron smelting is more efficient in terms of ore utilisation rate compared to the bloomery smelting process, which will allow more

options when selecting the ore; it can be carried out continuously, therefore it is suitable for large scale production. Additionally, the primary product of the smelting process, cast iron, has a low melting temperature, hence can be used for mould casting production, which fits the technological tradition established since the Bronze Age, where the majority of bronzewares were cast into shape. From a social perspective, due to the restricted occurrence of ore deposit and political control over the mining and smelting, bronze was not always available for the common people, therefore a replacement cheap metal was in dire need for utilitarian purposes. In the meantime, the agricultural development during the Warring States period demanded large quantities of affordable farming tools, which bloomery smelting would struggle to deliver. In this sense, the cast iron smelting technique, whether locally developed or introduced from the eastern part of central China, perfectly met the technological condition and social demand, therefore it was quickly adopted in the Qin state during the Warring States period.

Regarding the utilisation of cast iron, a complicated technological system was also developed and adopted in the Qin state. As discussed in detail in previous sections, this system was based on series of technological choices made by the craftspeople, who aimed to produce different categories of iron products using the using the most cost-beneficial techniques.

To begin with, when making daily use artefacts including vessels, lamps and small ornaments, the most common method in the Qin state was the mould casting technique. Compared to the forging technique, mould casting is relatively straightforward, where the smelted or melted cast iron can be poured into casting moulds with pre-designed shape and size. The casting process can be carried out in

batches; therefore, the final product will have a higher standardisation rate and lower cost.

In addition to the daily use artefacts, most of the farming implements were also shaped using this method. However, the mould casting technique used for making farming implements were different from the daily use artefacts. When making large daily use artefacts, a slower cooling rate was often applied to improve the overall quality of the casting and extend the service life of the artefacts with a relatively lower cost compared to other methods such as annealing. For those farming implements, a higher cooling rate was applied during casting to allow the liquid cast iron to crystallise into white cast iron, where it could be further annealed for decarburisation or malleablisation.

In order to make iron products which required higher mechanical strength, such as craft tools and weapons, the forging technique was more commonly applied for production in the Qin state. Through the forging process, metal could be further consolidated, and the grain size reduced, therefore the final product would have a higher toughness. However, forging required repeated heating and hammering, which cannot be carried out in batches, therefore being more costly in terms of fuel and labour consumption. More importantly, forging required malleable soft iron or steel as raw material, hence a decarburisation process will be needed to convert the cast iron into soft iron or steel prior to the manufacturing process, with additional material and labour costs.

The conversion of cast iron into soft iron or steel in the Qin state was achieved through two technological pathways, namely the solid state annealing and liquid state fining/*chaogang* process. The annealing process usually took several days to complete the decarburisation of cast iron, whereas the liquid state fining/*chaogang*

usually only took less than an hour. In the meantime, maintaining a high temperature for a long duration in the annealing kiln would also require a significant amount of fuel, whereas the fuel consumption for the fining/*chaogang* is much less. However, annealing decarburisation could create soft iron or steel with a clean metal matrix, which theoretically had better mechanical strength compared to the liquid state decarburisation products, where more slag inclusions would be formed and trapped in the metal matrix. In this sense, the annealing process was a more costly technique yet with better product qualities, whereas the fining/*chaogang* process was a technological choice involving compromises between the product quality and the overall production cost.

8.3 The social impact of iron production in the Qin state

Based on the synthesis of current research results, this thesis argued that the agricultural production in the Qin state benefited greatly from the iron production industry in three main spheres: the application of iron farming implements significantly increased the arable land in the Qin state; higher tool efficiency increased the productivity of peasants, allowing more yield per capita; the building of irrigation systems further increased the yield per unit area.

Considering iron weapon production in the Qin state, based on the analytical work along with the archaeological findings in recent years, this thesis has put forward the proposition that iron weapon production and usage in the Qin state was much more developed than the current archaeological finding suggests. The bronze weapons in the terracotta army as well as in civilian burials were mostly like to be chosen especially for ritual purposes rather reflecting the technological choice in real life. Given the highly developed iron manufacturing techniques and new iron weapon

findings in the Qin state, it seems reasonable to argue that iron weapons were widely produced and used in the Qin army during the late Warring States period.

8.4 Future work

While it is hoped that this research has provided a substantial body of new data and a renewed understanding of iron production in the Qin state during the Warring States period, this thesis has also highlighted several research questions that still need to be addressed with additional research.

To begin with, owing to the lack of mining, smelting, and manufacturing sites being located and excavated within the Qin state, some key information regarding the primary smelting and manufacturing of iron, such as the type of ore exploited, furnace design, organisation of production etc. is still largely missing from the picture.

Additionally, more scientific study of archaeological iron dated to the Spring and Autumn and early to middle Warring States period will be necessary to show the technological transformation and development of iron production in the Qin state prior to the onset of large-scale cast iron smelting based iron production system.

Some technical issues also need to be further investigated through more analytical and experimental work. For instance, while it has been established that the production of white cast iron and grey/mottled cast iron involved different forms of mould casting technique, the actual operational differences remain unclear. These will need to be explored through experimental work to gain a better understanding of the factors affecting the technological choice. Furthermore, whether the carbon content of the cast iron used to produce different types of cast iron products was intentionally controlled also needs to be investigated by analysing more archaeological samples.

The annealing process, especially annealing for malleablisation, is still poorly understood. Owing to this, the evaluation of engineering parameters, including the annealing duration, temperature, and atmosphere should be investigated in further

detail. In this sense, experimental work with fine grained parameter settings will provide a valuable reference dataset for understanding the production technique of specific archaeological samples, and further help to qualitatively evaluate the cost-benefit of the various forms of techniques and understanding the technological choices.

Additionally, due to the lack of archaeological evidence, our understanding of the fining/*chaogang* process adopted in early China is largely based on the study of compositional data of slag inclusions with reference to a theoretical understanding of the technique. In future work, the replication of the fining and *chaogang* process and the comparison between experimental and archaeological results will be key to test the validity of current research methods and results. Meanwhile, while the compositional data analysis of the slag inclusions carried out in this thesis were able to differentiate the production techniques of the analysed samples, it will be of great importance to further develop a discriminative approach specially optimised for indirect iron products from early China.

Finally, due to the lack of reliable proxies, the discussion of the social impact of iron production on early agricultural development is largely speculation of correlation rather than causations. In the future, with more archaeobotanical work revealing the scale and intensity of agricultural production in the Guanzhong Plain during different periods in reference to controlled area, it is possible that a better understanding could be gained toward the direct impact of iron production on the farming industry.

References

Aitchison, J. (1986). *The statistical analysis of compositional data*. London, Chapman and Hall.

Atlas Foundry Company (2001), *Mechanical Properties of Gray Iron*. http://www.atlasfdry.com/grayiron-hardness.htm, 2001.

Bai, C. (1994). Analytical report on the fragment of an iron sword unearthed from the tomb no.2 in Yimen, Baoji, dated to Spring and Autumn period 宝鸡市益门村 M2 出土春秋铁剑残块分析鉴定报告. *Cultural Relics 文物*(9), 82-85.

Bai, Y. (1985). Discussion on whether bronze farming tools were used during the Shang and Western Zhou dynasty 殷代西周是否大量使用青铜农具的考古学观察. *Agricultural Archaeology 农业考古* (1): 70-82.

Bai, Y. (1989). Discussion again on whether bronze farming tools were used during the Shang and Western Zhou dynasty 殷代西周是否大量使用青铜农具之考古学再观察. *Agricultural Archaeology 农业考古*(1): 194-204.

Bai, Y. (2004). *Archaeological study on the iron objects dated to Pre-Qin and Han dynasty 先秦两汉铁器的考古学研究* (Doctoral Dissertation, Shandong University)

Baoji Municipal Institute of Archaeology. (2016). *Cultural Relics in a Qin burial: the No.2 tomb in Yimen, Baoji dated to Spring and Autumn period 秦墓遗珍: 宝鸡益门二号春秋墓*. Beijing, Science press 科学出版社.

Beijing University of Iron and Steel Technology. (1975). Metallographic examination of iron objects unearthed from tomb no. 44 in Yanxiadu site, Yi county 易县燕下都 44 号墓葬铁器金相考察初步报告. *Archaeology 考古*(4), 241-243.

Beijing University of Iron and Steel Technology. (1976). Scientific study of iron objects from the hoard in Mianchi, Henan province 河南渑池窖藏铁器检验报告. *Cultural Relics 文物*(8), 52-58.

Bevan, A., Li, X., Zhao, Z., Huang, J., Laidlaw, S., Xi, N., ... & Martinon-Torres, M. (2018). Ink marks, bronze crossbows and their implications for the Qin Terracotta Army. *Heritage Science*, 6(1), 1-10.

Birch, T. (2006). Abandoned or unused? Ultra-high carbon steel and cast iron lumps from Semlach/Eisner. *The production of ferrum Noricum at the Hüttenberger Erzberg. The results of interdisciplinary research at Semlach/Eisner between 2009.*

Boserup, E. (1965). *The conditions of agricultural growth: The economics of agrarin change under population pressure*. London, George Allen & Unwin LTD

Bowman, M. D. , Munse, W. H. , & Will, W. . (1984). Fatigue behavior of butt welds with slag inclusions. *Journal of Structural Engineering*, 110(12), 2825-2842.

Bronson, B. (1999). The transition to iron in ancient China. *The archaeometallurgy of the Asian Old World*. 16: 177-198.

Chang Kuang-Chih. (2013) *Bronze Age in China 中国青铜时代*, Beijing, Sanlian Press 三联出版社.

Charlton, M. (2007). Ironworking in northwest Wales: An evolutionary analysis (Doctoral dissertation, University College London).

Charlton, M. F., Crew, P., Rehren, T., & Shennan, S. J. (2010). Explaining the evolution of ironmaking recipes–An example from northwest Wales. *Journal of Anthropological Archaeology*, 29(3), 352-367.

Chen, G. (1990). Bronze Age cultures and earlu Iron Age cultures in Xinjiang Area 关于新疆地区的青铜时代和早期铁器时代文化. *Kaogu 考古*(4), 366-374.

Chen, H. (2017). Discussion on the production and management of iron farming implements in the Qin state based on archaeological findings 从出土实物看秦国铁农具的生产制造及管理. *Agricultural Archaeology 农业考古* (4): 117-122.

Chen, J. (2014). *New investigation into the metal production in ancient China 中国古代金属冶铸文明新探*. Beijing, Science Press 科学出版社.

Chen, J. and R. Han (1999). *Metallographic study on the iron objects unearthed from the tomb of Marquis Chu in Shizishan, Xuzhou 徐州狮子山西汉楚王陵出土铁器的金相实验研究*. *Cultural Relics 文物*(7): 84-91.

Chen, J., & Zhang, Z. (2016). Discussion on the chaogang technique in early China based on the slag analysis 基于炉渣分析的古代炒钢技术判定问题. *Cultural Relics in Southern China 南方文物* (1), 115-121.

Chen, J., Mao, R., Wang, H., Chen, H., Xie, Y., & Qian, Y. (2012). Iron objects unearthed from Siwa culture burial in Mogou, Lintan, Gansu province and the origin of iron smelting in early China 甘肃临潭磨沟寺洼文化墓葬出土铁器与中国冶铁技术起源. *Cultural Relics 文物*(8), 45-53.

Chen, J., Yang, J., Sun, B. & Pan, Y. (2009). Manufacturing techniques of the bimetallic product unearthed from M27 in Liangdai Village 梁带村遗址 M27 出土铜铁复合器的制作技术. *China Science 中国科学* 39(9): 1574-1581.

Chen, K., Wang, Y., Liu, Y., Mei, J., & Jiang, T. (2018). Meteoritic origin and manufacturing process of iron blades in two Bronze Age bimetallic objects from China. *Journal of Cultural Heritage*, 30, 45-50.

Chen, M. (2013). *An overview of the oracle inscriptions of the Shang Dynasty 殷墟卜辞综述*, Beijing, Zhonghua Book Company 中华书局.

Chen, W. (2012). *Readings of the Liye Qin bamboo text 里耶秦简牍校释*. Wuhan, Wuhan University Press 武汉大学出版社.

Wan, C. (1976). A Comparative Study of the Casting of Bronze Ting-cauldrons from Anyang and Hui-hsien. Proceedings of a Symposium on Scientific Methods of Research in the Study of Ancient Chinese Bronzes and Southeast Asian Metal and Other Archaeological Artifacts, edited by N. Barnard, pp17-46, National Gallery of Victoria, Melbourne.

Childe, V. G. (1944). Archaeological ages as technological stages. *The Journal of the Royal Anthropological Institute of Great Britain and Ireland* 74(1/2): 7-24.

Collini, L. , Nicoletto, G. , & R. Koneˇcná. (2008). Microstructure and mechanical properties of pearlitic gray cast iron. Materials Science & Engineering A, 488(1-2), 529-539.

Comelli, D., et al. (2016). The meteoritic origin of Tutankhamun's iron dagger blade. *Meteoritics & Planetary Science* 51(7): 1301-1309.

Craddock, P. T. (1995). *Early metal mining and production*, Edinburgh, Edinburgh University Press.

Craddock, P. T., Wayman, M. L., Wang, H., & Michaelson, C. (2003). Chinese cast iron through twenty-five hundred years. In Proceedings of the 1st Forbes symposium on scientific research in the field of Asian art at the Freer Gallery of Art, London.

Crew, P., Charlton, M., Dillmann, P., Fluzin, P., Salter, C., & Truffaut, E. (2011). Cast iron from a bloomery furnace. *The Archaeometallurgy of Iron*, 239-262.

Cui, Z., and Tan, Y. (2000). *Metallurgy and Heat Treatment 金属学与热处理*. Beijing: Mechanical Industry Publishing House 机械工业出版社.

Dai, C. (2000). Qin cemetery in Dabaozishan, Li county 礼县大堡子山秦公墓地及有关问题. *Cultural Relics 文物* (5): 74-80.

Dai, W. (2012). The Qin iron officials based on written records 出土文字材料所见秦铁官. *Hunan Provincial Museum Collection of Papers 湖南省博物馆馆刊*(0): 35.

Di, N. (2012). Primary study on the iron objects unearthed from Qin cemeteries in Guanzhong Plain 关中地区秦墓出土铁器初步研究. Journal of Zhengzhou University: *Philosophy and Social Science 郑州大学学报: 哲学社会科学版* 45(6): 146-150.

Dillmann, P., & L'Héritier, M. (2007). Slag inclusion analyses for studying ferrous alloys employed in French medieval buildings: supply of materials and diffusion of smelting processes. *Journal of Archaeological Science*, 34(11), 1810-1823.

Dillmann, P., Schwab, R., Bauvais, S., Brauns, M., Disser, A., Leroy, S. & Fluzin, P. (2017). Circulation of iron products in the North-Alpine area during the end of the first Iron Age (6 th-5 th c. BC): A combination of chemical and isotopic approaches. *Journal of Archaeological Science*, 87, 108-124.

Disser, A., Dillmann, P., Bourgain, C., l'Héritier, M., Vega, E., Bauvais, S., & Leroy, M. (2014). Iron reinforcements in Beauvais and Metz Cathedrals: from bloomery or finery? The use of logistic regression for differentiating smelting processes. *Journal of archaeological science*, 42, 315-333.

Dong, L. (1993) *Annotations and analysis of Guo Yu 国语译注辨析*. Guangzhou, Jinan University Press 暨南大学出版社

Du, N., Li, J., Zhang, G., Wang, X., & Li, Y. (2011). Investiagtion and study of the iron production site in the capital city of the Qi state in Linzi, Shandong province 山东临淄齐国故城东北部冶铁遗址的调查与研究. *Journal of jiangxi university of technology 江西理工大学学报, 32*(6), 12-15.

Duan, H. (2001). *Investigation and study of the iron objects unearthed from the three-Jin area: a discussion on the first major development of iron production in early China 三晋地区出土战国铁器的调查与研究: 兼论中国钢铁技术第一次大发展* (Doctoral Dissertation, University of Science and Technology Beijing).

Emperor Qinshihuang's Mausoleum Site Museum. (2018). *Excavation report of the sacrifice pit no.1 of Emperor Qinshihuang's Mausoleum (2009-2011) 秦始皇帝陵一号兵马俑陪葬坑发掘报告(2009-2011)*. Beijing: Cultural Relics Press 文物出版社.

Engels, F. (1972). The Origin of the Family, Private Property and the State. 1884. New York, International.

Erb-Satullo, N. L. (2018). The Innovation and Adoption of Iron in the Ancient Near East. *Journal of Archaeological Research*: 1-51.

Fillery-Travis, R. (2016). *Iron production in the Western Roman Empire: A diachronic study of technology and society based on two archaeological sites* (Doctoral dissertation, University College London).

Fleming, S. J. and H. R. Schenck (1989). *History of technology: The role of metals*, UPenn Museum of Archaeology.

Forbes R.J. (1964). *Studies in ancient technology vol. 9*. Leiden, E.J. Brill.

Franklin U.M. (1983). On bronze and other metals in early China. In Keightly, D. (ed.) *The origins of Chinese civilisation*. Berkeley, University of California Press.

Gao, X.(2010).Burial tradition of beaking artefacts and use Ming vessels in Shang Tombs 商墓中的毁器习俗与明器化现象. *Archaeology and Cultural Relics 考古与文物* (01),42-49.

Gettens, R. J., Clarke, R. S., & Chase, W. T.. (1971). *Two early Chinese bronze weapons with meteoritic iron blades*. Freer Gallery of Art.

Goldstein, J. I., et al. (2017). Ion microprobe analyses of carbon in Fe–Ni metal in iron meteorites and mesosiderites. *Geochimica et Cosmochimica Acta* 200: 367-407.

Gordon, R. B., & Van der Merwe, N. J. (1984). Metallographic study of iron artefacts from the eastern Transvaal, South Africa. *Archaeometry*, *26*(1), 108-127.

Gordon, R. B., & Killick, D. J. (1993). Adaptation of technology to culture and environment: bloomery iron smelting in America and Africa. *Technology and Culture*, 34(2), 243-270.

Gordon, R. B. (1997). Process deduced from ironmaking wastes and artefacts. *Journal of Archaeological Science*, 24(1), 9-18.

Guo, W. (2009). From western Asia to the Tianshan Mountains: on the early iron artefacts found in Xinjiang. *Metallurgy and civilisation: Eurasia and beyond*: 107-115.

Han, J. (2018). Early iron objects and early Iron Age in Xinjiang Area 新疆地区的早期铁器和早期铁器时代. *Social Science 社会科学战线*(7), 130-137.

Han, R. (1998). Metallographic study of iron objects in early China before the 5th century BC 中国早期铁器(公元前 5 世纪以前)的金相学研究. *Cultural Relics(文物)*(2): 87-96.

Han, R. & Chen, J. (2013). Discussion on the transition from bronze to iron in ancient China 中国古代冶铁替代冶铜制品的探讨. *Journal of Guangxi University for Nationalities: Natural science edition 广西民族大学学报:自然科学版* 19(3): 9-16.

Han, R. & T. Ko (2007). *History of Science and Technology in China: Mining and Metallurgy 中国科学技术史:矿冶卷*, Beijing, Science Press.

Han, R., Jiang, T. & Wang, B. (1999). Examination of the iron blades in bronzes unearthed from the Guo State Cemetery. *The Guo State Cemetery in Sanmenxia*. Beijing, Cultural Relics Press: 539-573.

Han, R., Sun, S., & Li, X. (2015). *Metallography of metallic objects from early China 中国古代金属材料显微组织图谱*. Science Press 科学出版社.

Han, W. (1986). Oppinions on the ethnic origin of Qin people 关于秦人族属及文化渊源管见. *Cultural Relics 文物*(4): 25-30.

Han, W. & Jiao, N. (1988). Overview on the excavation of the Yong capital city of Qin state 秦都雍城考古发掘研究综述. *Archaeology and Cultural Relics 考古与文物* 5(6): 121.

Han, W., Shang, Z., Ma, Z., Zhao, C. & Jiao, N. (1985). Excavation report of the No.1 architectural complex in Majiazhuang, Fengxiang 凤翔马家庄一号建筑群遗址发掘简报. *Cultural Relics 文物*(2): 1-29.

Hebei Provincial Institute of Cultural Heritage. (1996). *Yan Xia Du 燕下都*, Beijing, Cultural Relics Press 文物出版社.

Henan Provincial Institute of Cultural Heritage & Archaeological Department of National Museum. (1992). *Dengfeng Wangchenggang and Yangcheng 登封王城岗与阳城*. Beijing, Cultural Relics Press 文物出版社.

Henan Provincial Instute of Cultural Heritage and Archaeology. (1998). Excavation report of the iron production site in Jiudian, Xiping, Henan province 河南省西平县酒店冶铁遗址试掘简报.*Huaxia Archaeology 华夏考古*(4): 27-33.

Hua, J. (1982). Discussion on the high toughness cast iron during Han and Wei dynasties 汉魏高强度铸铁的探讨. *Studies In The History of Natural Sciences 自然科学史研究* (1): 1-20.

Hua, J., Yang, G., & Liu, E. (1960). Metallographic study of iron objects dated to Warring States period and Han dynasty 战国两汉铁器的金相学考查初步报告. *Acta Archaeologica Sinica 考古学报*(1), 73-88.

Huang, Q., Li, Y., Chen, J., & Tie, F. (2016). A summary of ancient iron smelting technology based on iron slag analysis 以炉渣分析为主揭示古代炼铁技术的研究与探索. *Journal of National Museum of China 中国国家博物馆馆刊*, 000(011), 145-153.

Hubei Provincial Institute of Cultural Relics and Archaeology, Laohekou Municipal Museum (2003). Excavation report of the Yangying site in Laohekou, Hubei province, dated to Spring and Autumn period 湖北老河口杨营春秋遗址发掘简报. *Jianghan Archaeology 江汉考古* 000(003): 16-35.

Hwang, M. (2014). Entering the Heavy Casting Era: the introduction of bronze casting technology and the formation of Chinese bronze technology 迈向重器时代-铸铜技术的输入与中国青铜技术的形成. *Institute of History and Linguistics, Academia Sinica 中央研究院历史语言研究所集刊*, 575-678.

International Standard Organisation. (2008). *Microstructure of cast irons—Part 1: Graphite classification by visual analysis (945-1)*. Retrieved from https://www.iso.org/standard/41501.html

Iles, L. (2014). The exploitation of manganese-rich 'ore'to smelt iron in Mwenge, western Uganda, from the mid second millennium AD. *Journal of archaeological science*, *49*, 423-441.

Iles, L., & Martinón-Torres, M. (2009). Pastoralist iron production on the Laikipia Plateau, Kenya: wider implications for archaeometallurgical studies. *Journal of Archaeological Science*, *36*(10), 2314-2326.

Jambon, A. (2017). Bronze Age iron: Meteoritic or not? A chemical strategy. *Journal of Archaeological Science* 88: 47-53.

Jockenhövel, A., C. Willms, T. Abdinghoff & M. Overbeck (1997). Archaeological Investigations on the Beginning of Blast Furnace-Technology in Central Europe. *Early Ironworking in Europe, archaeology and experiment*.

Kang, S. (2013). *Pottery vessels imitating bronze ritual vessels in Yin ruin 殷墟仿铜陶礼器研究*. Master dissertation, Shaanxi Normal University.

Keightley, D. N. . (1976). Where have all the swords gone? reflections on the unification of china. *Early China*, 2, 31-34.

Killick, D.(2014) From Ores to Metal. in Roberts, B. W. & Thornton, C. P.(ED.) *Archaeometallurgy in global perspective (pp. 11-46)*, Springer.

Ko, T., Wu, K. Han, R. & Miao, C. (1993). Preliminary study on a batch of early iron objects unearthed from Henan province 河南古代一批铁器的初步研究. *Cultural Relics in Central Plain 中原文物*(1): 99-107.

Kunming Institute of Technology. (1988). Research on a new process of low-temperature annealing of malleable cast iron and the theory of graphitisation 可锻铸铁低温退火的新工艺及其石墨化理论的探讨. *Casting 铸造* (2) 17-22

Lam, W. (2014). Everything Old is New Again? Rethinking the Transition to Cast Iron Production in the Central Plains of China. *Journal of Anthropological Research* 70(4): 511-542.

Lam, W., Chen, J., Chong, J., Lei, X., & Tam, W. L. (2018). An iron production and exchange system at the center of the Western Han Empire: Scientific study of iron products and manufacturing remains from the Taicheng site complex. *Journal of Archaeological Science*, 100, 88-101.

Larreina-Garcia, D. (2017). *Copper and bloomery iron smelting in Central China: Technological traditions in the Daye County (Hubei)* (Doctoral dissertation, University College London).

Larreina-Garcia, D. , Li, Y. , Liu, Y. , & Martinón-Torres, M. (2018). Bloomery iron smelting in the daye county (hubei): technological traditions in qing china. *Archaeological Research in Asia*, 16, 148-165.

Lei, C. (1980). Discovery and its meaning of farming implements dated to Warring States period 战国铁农具的考古发现及其意义. *Archaeology 考古*(3): 259-265.

Lei, C. (1986). Agricultural developments during the Warring States period: symbol, reason and impact 战国时期农业发展的标志、原因与作用浅析. *Agricultural Archaeology 农业考古*(2): 55-65.

Lemonnier, P. (1993). *Technological choices: transformation in material cultures since the Neolithic*. London: Routledge.

Li, C. (2004). Microstructure of grey cast iron and the effect of some alloy elements 灰铸铁的组织和几种合金元素的影响(一). *Foundry Panorama 铸铁纵横* 000(012), 10-17.

Li, C. (2005a). Microstructure of grey cast iron and the effect of some alloy elements 灰铸铁的组织和几种合金元素的影响(二). *Foundry Panorama 铸铁纵横* 000(001), 15-17.

Li, J. (1984). *Geography of Shaanxi 陕西地理*. Xi'an, Shaanxi Peoples' Publishing House 陕西人民出版社

Li, J. (2005b). Archaeological findings and study of iron farming implements dated to Warring States period 战国时期铁农具的考古发现与研究. *Agricultural Archaeology 农业考古*(1): 194-196.

Li, K., & Xu, Z. (2006). Overview of the Dujiangyan irrigation scheme of ancient China with current theory. *Irrigation and Drainage: The journal of the International Commision on Irrigation and Drainage*, 55(3), 291-298

Li, S., Qian, H. & Li, J. (1983). On the formation process of spheroidal graphite and its matrixin early Han iron objects 关于汉代铁器中球状石墨和基体组织成因的研究. *Journal of Chongqing University (Natural Science)重庆大学学报 (自然科学版)* 1: 007.

Li, X. J., Bevan, A., Martinón-Torres, M., Rehren, T., Cao, W., Xia, Y., & Zhao, K. (2014). Crossbows and imperial craft organisation: the bronze triggers of China's Terracotta Army. *Antiquity*, 88(339), 126-140.

Li, X. J., Martinón-Torres, M., Meeks, N. D., Xia, Y., & Zhao, K. (2011). Inscriptions, filing, grinding and polishing marks on the bronze weapons from the Qin Terracotta Army in China. *Journal of Archaeological Science*, 38(3), 492-501.

Li, X., Bevan, A., Martinón-Torres, M., Xia, Y., & Zhao, K. (2016). Marking practices and the making of the Qin Terracotta Army. *Journal of Anthropological Archaeology*, 42, 169-183.

Li, Z. (1975). The development of iron and steel technology in early feudalism China 中国封建社会前期钢铁冶炼技术发展的探讨. *Acta Archaeologica Sinica 考古学报*(2): 1-22.

Li, Z. (1976)a. Scientific study of the bronze battle-axe with iron blade unearthed from Gaocheng dated to Shang dynasty 关于藁城商代铜钺铁刃的分析. *Acta Archaeologica Sinica 考古学报* (2): 17-34.

Li, Z. (1976)b. The metallurgical acievements in early China based on the iron products unearthed from Mianchi 从渑池铁器看我国古代冶金技术的成就. *文物 Cultural Relics* (08), 59-61.

Li, Z. (1982). Metallographic study of iron objects unearted from Zhenping, Henan province, dated to Han dynasty 河南镇平出土的汉代铁器金相分析. *Archaeology 考古*(3), 320-321.

Liang, Y. (2008). On the formation of the Qin culture based on the burial tradition of the Qin tombs 从秦墓葬俗看秦文化的形成. *Archaeology and Cultural Relics 考古与文物* 000(001): 54-61.

Liang, Y. (2017)a. Journey of the exploration of the early Qin culture 早期秦文化的探索历程. *Journal of Tianshui Normal University 天水师范学院学报*(1): 39-46.

Liang, Y. (2017)b. On the origin and formation process of the early Qin culture 论早期秦文化的来源与形成. *Acta Archaeologica Sinica 考古学报*(2): 149-174.

Lide, D. R. (2005). Abundance of elements in the Earth's crust and in the sea. *CRC handbook of chemistry and physics, Internet Version*, 14-17.

Lin, J. (1978). Exploration of early history of the Qin people 秦人早期历史探索. *Journal of Northwest University: philosophy and social science 西北大学学报: 哲学社会科学版*(1): 20-25.

Liu, D. & Zhu, Y. (1981). A tomb dated to Spring and Autumn period in Jingjiazhuang, Lingtai, Gandu province 甘肃灵台县景家庄春秋墓. *Archaeology 考古*(4): 298-301.

Liu, D. (1962). Findings of pottery casting molds in Cangcheng, Xinzheng, Henan province 河南新郑仓城发现战国铸铁器泥范. *Archaeology 考古*(3): 165-166.

Liu, P. (2019). Production and circulation of iron farming implements produced from the state owned workshops in the Qin state 秦官营铁农具的生产管理及民间供给. *Ancient Civilisation 古代文明*(2): 7.

Liu, Z. (1983). The study of the Agricultural-Military principle and legal system from “the book of Lord Shang” 论《商君书》的耕战与法治思想. *Journal of Shandong Normal University (Social Science) 山东师大学报(哲学社会科学版)*(4), 1-9.

Liu, Q. & Li, Y. (1985). Investigation and excavation of the Yueyang city dated to Qin and Han dynasties 秦汉栎阳城遗址的勘探和试掘. *Acta Archaeologica Sinica 考古学报*(03): 353-381.

Liu, S. (1975). Excavation report of the tomb no.44 in Yi county, Hebei province 河北易县燕下都 44 号墓发掘报告. *Archaeology 考古*(04): 228-240.

Marks, R. B. (2011). *China: its environment and history*. Rowman & Littlefield Publishers.

Martinón-Torres, M. (2002). Chaîne Opératoire: The concept and its applications within the study of technology. *Gallaecia: revista de arqueoloxía e antigüidade*, (21), 29-44.

Martinón‐Torres, M. (2018). Ore and Smelting Slag. *The Encyclopedia of Archaeological Sciences*, 1-4.

Martinón-Torres, M., & Killick, D. (2015). Archaeological theories and archaeological sciences. *The Oxford Handbook of Archaeological Theory*. Oxford University Press

Martinón-Torres, M., Li, X. J., Bevan, A., Xia, Y., Zhao, K., & Rehren, T. (2014). Forty thousand arms for a single emperor: from chemical data to the labor organization behind the bronze arrows of the Terracotta Army. *Journal of Archaeological Method and Theory*, 21(3), 534-562.

Mei, J., Wang, P., Chen, K., Wang, L., Wang, Y., & Liu, Y. (2015). Archaeometallurgical studies in China: some recent developments and challenging issues. *Journal of Archaeological Science*, 56, 221-232.

Nanjing Museum (1974). Tomb no.2 date to eastern Zhou period in Liuhe, Jiangsu province 江苏六合程桥二号东周墓. *Archaeology 考古*(2): 116-120.

Navasaitis, J. & Selskienė, A. (2007). Metallographic examination of cast iron lump produced in the bloomery iron making process. *Materials Science* 13(2): 167-173.

Peng, H. (2002). *Qin bamboo text in Shuihudi 睡虎地秦墓竹简*. Hubei, Hubei Fine Arts Publishing House 湖北美术出版社.

Piaskowski, J. (1976). Classification of the structures of slag inclusions in early objects made of bloomery iron. *Archaeologia Polona Wroc aw*, 17, 139-149.

Piaskowski, J. (1992). Distinguishing between directly and indirectly smelted iron and steel. *Archeomaterials*, 6(2), 169-173.

Pines, Y. (2013). *Birth of an empire: the state of qin revisited*. Global Area & International Archive.

Pleiner, R. (2000). *Iron in archaeology: the European bloomery smelters*, Archeologický Ustav AV ČR.

Pleiner, R. (2001). Cast Iron in the European Bloomery Period*. Acta Metallurgica Slovaca* 7: 97-101.

Pleiner, R. (2006). *Iron in archaeology: early European blacksmiths*, Archeologický ústav AV Čr.

Portal, J. (2007). *The First Emperor*. London. British Museum Press.

Qian, H. & Li, S. (1985). Prelimary study on the formation of spheroidal graphite in early iron objects 古汉铁器中球墨成因初探. *Exploration of the great nature 大自然探索* (1): 171-179.

Rapp, G. (2009). *Archaeomineralogy*. Berlin, Springer.

Rehder, J. E. (2000). *The mastery and uses of fire in antiquity*. Quebec: McGill-Queen's University Press.

Rehder, J. E. (2000). *The mastery and uses of fire in antiquity*. Quebec: McGill-Queen's University Press.

Rehren, T., Charlton, M., Chirikure, S., Humphris, J., Ige, A., & Veldhuijzen, H. A. (2007). Decisions set in slag: the human factor in African iron smelting. *Metals and mines: studies in archaeometallurgy*, 211-218.

Rehren, T., T. Belgya, A. Jambon, G. Káli, Z. Kasztovszky, Z. Kis, I. Kovács, B. Maróti, M. Martinón-Torres and G. Miniaci (2013). "5,000 years old Egyptian iron beads made from hammered meteoritic iron." Journal of Archaeological Science 40(12): 4785-4792.

Rong, Y., Luo, W., Wei, G., Song, G. & Wang, C. (2013). Production techniques of iron objects unearthed from Shenmingpu site 申明铺遗址出土铁器的工艺考察. *Sciences of Conservation and Archaeology 文物保护与科技考古* 25(3): 64-70.

Rostoker, W. & Bronson, B. (1990). *Pre-industrial iron: its technology and ethnology*, Archaeomaterials.

Rostoker, W., Bronson, B., Dvorak, J., & Shen, G. (1983). Casting farm implements, comparable tools and hardware in ancient China. *World archaeology*, 15(2), 196-210.

Schiffer, M. B. (2004) Studying technological change: A behavioral perspective, *World Archaeology*, 36:4

Scott, D. A. (1992). *Metallography and microstructure in ancient and historic metals*. Getty publications.

Sellet, F. (1993). Chaîne opératoire; the concept and its applications. *Lithic technology*, 18(1-2), 106-112.

Serneels, V., & Perret, S. (2003). Quantification of smithing activities based on the investigation of slag and other material remains. *Archaeometallurgy in Europe*, 1, 469-478.

Shaanxi Provincial Insitute of Archaeology. (2019). Excavation of the bone workshop in Niejiagou, Xianyang, Shaanxi province 陕西咸阳聂家沟秦代制骨作坊清理简报. *考古与文物Archaeology and Cultural Relics*(3): 50-62

Shaanxi Provincial Institute of Archaeology & Emperor Qinshihuang's Mausoleum Site Museum (2000). *Excavation report of the Emperor Qinshihuang's Mausoleum* 秦始皇帝陵园考古报告. Beijing, Science Press 科学出版社.

Shaanxi Provincial Institute of Archaeology. (1998). *Dianzi Qin cemetery in Long county* 陇县店子秦墓 Sanqin Publishing House 三秦出版社.

Shaanxi Provincial Institute of Archaeology. (2017). *Lintong, Xinfeng – archaeological report of the burials dated to Warring States period and Han dynasty 临潼新丰——战国秦汉墓葬考古发掘报告*. Science Press 科学出版社.

Shaanxi Provincial Institute of Archaeology. (2018)a. Excavation report of the Qin sites and burials in Yanjiazhai, Xianyang, dated to Warring States period 西咸阳闫家寨战国秦遗址, 墓葬发掘简报. *Archaeology and Cultural Relics 考古与文物* (4): 18-41.

Shaanxi Provincial Institute of Archaeology. (2018)b. Overview of archaeological work on the Qin and Han dynasties in Shaanxi during 2008-2017 2008～2017 年陕西秦汉考古综述. *Archaeology and Cultural Relics 考古与文物* 229(05): 68-112.

Shaanxi Provincial Institute of Archaeology. (2019). Excavation report of the bone workshop in Niejiagou, Xianyang, Shaanxi province 陕西咸阳聂家沟秦代制骨作坊清理简报. *Archaeology and Cultural Relics 考古与文物* 000 (003): 50-62

Sillar, B., & Tite, M. (2000). The challenge of 'technological choices' for material science approaches in archaeology. *Archaeometry*, 42, 2-20.

Sima, Q. (2010) *Shi Chi (with translation and annotion)*史记. Beijing: Zhonghua Book Company 中华书局.

Song,Y. (1997) *Tiangong Kaiwu 天工开物*, Beijing, China Art Net 中国艺术网.

Starley, D. (1999). Determining the technological origins of iron and steel. *Journal of Archaeological Science*, 26(8), 1127-1133.

Tang, C. (2019). New knowlwdge on the iron official system in the Qin state 秦铁官体系与冶铁业新识. Jianghan Archaeology 江汉考古 161(02): 75-80.

Taylor, S. & Shell, C. (1986). Social and historical implications of early Chinese iron technology. *The beginning of the use of metals and alloys*: 205-221.

Taylor, S. (1988). Early chinese iron technology: some social and historical implications. *Cina*(21): 319-338.

Tian, J. (2014). Production techniques of the pottery vessels imitating bronze ritual vessels in Yicheng 宜城跑马堤墓地战国仿铜陶礼器制作工艺研究. *Jianghan Archaeology 江汉考古*(3): 76-84.

Tian, Y. (2013). Study of the layout of the Yong capital city of the Qin state 秦都雍城布局研究 *Archaeology and Cultural Relics 考古与文物*(5): 65-73.

Tylecote, R. F. (1981). Comparison between Western and Eastern metallurgical technologies as deduced from traditional Japanese and Chinese illustrations. *Bulletin of the Metals Museum*, 6, 1-14.

Tylecote, R. F. (1992). *A history of metallurgy* (2nd ed). London: Institute of Metals.

Tylecote, R. F., Austen, J. N., & Wrath, A. E. (1971). The mechanism of the bloomery process in shaft furnaces. *Journal of the Iron and Steel Institute*, 209, 342-263.

Van Der Merwe, N. J. & Avery, D. H. (1982). Pathways to Steel: Three different methods of making steel from iron were developed by ancient peoples of the Mediterranean, China, and Africa. *American Scientist* 70(2): 146-155.

Veldhuijzen, H. A., & Rehren, T. (2007). Slags and the city: early iron production at Tell Hammeh, Jordan, and Tel Beth-Shemesh, Israel. *Metals and mines: studies in archaeometallurgy*, 189-201.

Wagner, D. B. (1985). *Dabieshan : traditional Chinese iron-production techniques practised in southern Henan in the twentieth century*. Curzon press

Wagner, D. B. (1989). Toward the reconstruction of ancient Chinese techniques for the production of malleable cast iron. *East Asian Institute occasional papers*, 4, 3-72.

Wagner, D. B. (2001). *The state and the iron industry in Han China*, NIAS Press.

Wagner, D. B. (1996). *Iron and steel in ancient China*. Leiden: E.J. Brill (2nd edition with corrections).

Wagner, D. B. (2008). *Science and Civilisation in China: Science and Civilisation in China: Vol. 5, Chemistry and Chemical Technology. Ferrous Metallurgy*, Cambridge University Press.

Wang, B. (2004). Iron farming implements: its origin, development and impact 铁农具的产生、发展及其影响分析. *Journal of Nanjing Agricultural University 南京农业大学学报* 4(3): 83-86.

Wang, M. (1960) Check and Annote of the *Taipingjing* 太平经校注 Beijing: Zhonghua Book Company

Wang, X. (1991) *Ferrous Metallurgy part1: Iron Smelting 钢铁冶金学: 炼铁卷*. Beijing, Metallurgical Industry Press

Wang, X. (2005) *Ferrous Metallurgy part2: Steel Making 钢铁冶金学: 炼钢卷*. Beijing, Metallurgical Industry Press

Wang, Y. (1991). Ethnic origin and migration route of the Qin people 秦人的族源及迁徙路线. *Historical Study 历史研究*(3): 32-39.

Wei, S. (2017). Overview of the early iron findings in Xinjiang—discussion on the origin of early iron objects in Xinjiang and the transmission of iron smelting techniques 新疆早铁器时代铁器考古发

现概述——兼论新疆的铁器来源与冶铁术的传播问题. *Western China Archaeology 西部考古* (03)3-20.

Wertime, T. A. & Muhly, J. D. (1980). *The coming of the age of iron*, Yale University Press New Haven.

Trousdale, W. (1977). Where All the Swords Have Gone. *Early China,* 3, 65-66.

Williams, R. (2013). A Question of Grey or White: Why Abraham Darby Chose to Smelt Iron with Coke. *Historical Metallurgy*, 47, 125-137.

Wood, J. R., & Hsu, Y. T. (2020). Recycling Roman glass to glaze Parthian pottery. *Iraq*, 82, 259-270.

Wu, Z. & Shang, Z. (1981). Excavation report of the Gaozhuang Qin cemetery in Fengxiang, Shaanxi province 陕西凤翔高庄秦墓地发掘简报. Archaeology And Cultural Relics 考古与文物(1): 12-35.

Xinxiang Municipal Institute of Cultural Heritage. (1996). Excavation report of the iron casting site in Huixian, Henan province, dated to the Warring States period 河南辉县市古共城战国铸铁遗址发掘简报. *Huaxi Archaeology 华夏考古*(1): 1-9.

Yalçin, Ü. (1999). Early iron metallurgy in Anatolia. *Anatolian Studies*, 49, 177-187.

Yan, G. & Wu, B. (1985). *Production technology of malleable cast iron 可锻铸铁生产技术*. Shanghai, Shanghai Scientific and Technical Literature Publishing House 上海科技人文出版社.

Yang, G. (1960). Scientific study of the iron casting moulds found in Xinlong 兴隆铁范的科学考查. *Cultural Relics 文物*(2), 20-21.

Yang, K. (1973). *The Shangyang Reform 商鞅变法*. Shanghai: Shanghai people's publishing house 上海人民出版社.

Yang, K. (1960). *The development history of traditional steel making techniques 中国土法炼铁炼钢技术发展简史*. Shanghai: Shanghai people's publishing house 上海人民出版社.

Yang, K. (1980). Innovation of the iron farming implements and its social impact in history of China 我国历史上铁农具的改革及其作用. *Historical Research 历史研究* (5): 89-98.

Yang, K. (2014). *Development history of iron metallurgy in ancient China 中国古代冶铁技术发展史*. Shanghai: Shanghai people's publishing house 上海人民出版社.

Ye, J. (1975). Characterisation of iron and bronze mining tools unearthed from the Tonglushan mining site 铜绿山古矿井遗址出土铁制及铜制工具的初步鉴定. *Cultural Relics 文物* (2): 19-25.

Ye, X. (1999). The study of the Shangyang Reform and its institutional innovation 论商鞅变法与制度创新. *Financial Research 财经研究*, 02, 58-62.

Yu, M. & Qian, W. (2010). Discussion on the development of iron weapons during the Qin and Han dynasty based on archaeological findings 从出土数量的变化看我国秦汉时期铁兵器的发展状况. *Silk Road* (18),11-14.

Yu, X. (1957). Study of the social nature of Shang dynasty based on oracle inscriptions 从甲骨文看商代社会性质. *Journal of Northeast Renmin University: Social Science 东北人民大学学报社会科学版* Z1: 197-136.

Yuan, Z. (1990). Developments and main achievements of the Qin culture based on archaeological materials 从考古资料看秦文化的发展和主要成就. *Museology 文博*(05): 9-20+113.

Yue, Z., Li, Y. & Shen, M. (2017). Discussion on the two development trajectories of bronze ritual vessels in Yinxu 试论殷墟晚期青铜礼器的两个发展方向[J]. *Jianghan Archaeology* (003):89-108.

Zhang, B. (2017).简牍所见战国时期秦国官农具的管理. *Agricultural History of China 中国农史*(01),56-62+120.

Zhang, H. (2017). Study of the burials with pottery ritual vessles during western Zhou period 西周仿铜陶礼器墓研究. MA dissertation, Shanxi University

Zhang, P. , Li, S. X. , & Zhang, Z. F. . (2011). General relationship between strength and hardness. *Materials Science & Engineering A*, 529, 62-73.

Zhang, T. (1993). Discussion on the tomb in Yimen, dated to Spring and Autumn period 秦器三论——益门春秋墓几个问题浅谈. *Cultural Relics 文物*(10): 20-27.

Zhang, X. & Zhang, X. (1990). Scientific study on the bronze battle-axe with an iron blade unearthed from pinggu, Beijing, dated to Shang dynasty 北京平谷刘家河商代铜钺铁刃的分析鉴定. *Cultural relics 文物*(7): 66-71.

Zhang, Y. (2002). Discussion on the origin of funerary wares 明器起源及相关问题探讨. *Huaxia Archaeology 华夏考古*, (3), 24-30.

Zhang, Z. (2015a). *Archaeometallurgical study on the iron production site in Dongpingling, Zhangqiu, Shandong province 山东章丘东平陵故城冶铁遗址冶金考古研究.* (MSc dissertation, Peking University)

Zhang, Z. (2015b). *Comparative study on the burial traditions of the Qin tombs near Xi'an 西安地区周秦墓葬文化比较研究*, MA dissertation, Shaanxi Normal University.

Zhao, H. (1987). Exploring new leads on the origin of Qin culture 寻找秦文化渊源的新线索. *Museology 文博*(1): 1-7

Zhao, H. (1997). Oppinions on the ethnic origin of the tomb no.2 in Yimen, Baoji city 宝鸡市益门村二号春秋墓族属管见. *Archaeologyu and Cultural Relics 考古与文物*(1): 31-34.

Zhao, Q., Li, J., Han, R., Qiu, L. & Tsun, K. (1985). New discussion on the Tieshenggou iron smelting site in Gong county 巩县铁生沟汉代冶铸遗址再探讨. *Acta Archaeologica Sinica 考古学报*(2): 157-183.

Zheng, S. (1956). Casting moulds dated to Warring States period found in Xinglong, Rehe 热河兴隆发现的战国生产工具铸范. *Archaeology 考古*(1): 29-35.

Zhuang, Y. (2017). State and irrigation: archeological and textual evidence of water management in late Bronze Age China. *Wiley Interdisciplinary Reviews: Water*, 4(4), e1217.

Zhuang, Y., Bao, W., & French, C. (2016). Loess and early land use: Geoarchaeological investigation at the early Neolithic site of Guobei, Southern Chinese Loess Plateau. *Catena*, 144, 151-162.

Zou, H. (2000). *Tianma-Qucun 天马-曲村*. Beijing, Science Press 科学出版社

Appendices

Appendix-1 Timeline of Chinese Dynasties in Bronze Age and early Iron Age

<table>
<tr><td colspan="2">The Shang dynasty</td><td></td><td>16th -11th century BC</td></tr>
<tr><td rowspan="3">The Zhou dynasty</td><td>Western Zhou</td><td></td><td>11th century BC-771 BC</td></tr>
<tr><td rowspan="2">Eastern Zhou*</td><td>The Spring and Autumn period</td><td>770-475 BC</td></tr>
<tr><td>The Warring States period</td><td>475-221 BC</td></tr>
<tr><td colspan="2">The Qin dynasty</td><td></td><td>221-207 BC</td></tr>
<tr><td colspan="2" rowspan="2">The Han dynasty</td><td>Western Han</td><td>202 BC- 9 AD</td></tr>
<tr><td>Eastern Han</td><td>25 – 220 AD</td></tr>
</table>

*The ruling of Zhou royalty ended in 256 BC.

Appendix-2 Detailed information of final sample collection

City	Site	Typology	Category	Arch No.	Dating	Lab No.	Note
Xi'an	Xinfeng	Tripod	Artefacts for daily use	M312:6	Stage 3	XF-1	4 samples taken
Xi'an	Xinfeng	Tripod	Artefacts for daily use	M135:10	Stage 3	XF-2	3 samples taken
Xi'an	Xinfeng	Tripod	Artefacts for daily use	M423:6	Stage 3	XF-3	2 samples taken
Xi'an	Xinfeng	Tripod	Artefacts for daily use	M156:4	Stage 3	XF-4	
Xi'an	Xinfeng	Mou	Artefacts for daily use	M391:43	Stage 4	XF-5	2 samples taken
Xi'an	Xinfeng	Pot	Artefacts for daily use	M691:13	Stage 4	XF-7	
Xi'an	Xinfeng	Pot	Artefacts for daily use	M691:11	Stage 4	XF-8	2 samples taken
Xi'an	Xinfeng	Pot	Artefacts for daily use	M423:8	Stage 3	XF-9	2 samples taken
Xi'an	Xinfeng	Pot	Artefacts for daily use	M415:5	Stage 4	XF-10	2 samples taken
Xi'an	Xinfeng	Pot	Artefacts for daily use	M125:7	Stage 2	XF-11	
Xi'an	Xinfeng	Pot	Artefacts for daily use	M668:		XF-12	
Xi'an	Xinfeng	Pot	Artefacts for daily use	M160:10	Stage 4	XF-14	2 samples taken
Xi'an	Xinfeng	Pot	Artefacts for daily use	M150:7	Stage 2	XF-15	2 samples taken
Xi'an	Xinfeng	Pot	Artefacts for daily use	M213:9	Stage 3	XF-16	2 samples taken
Xi'an	Xinfeng	Pot	Artefacts for daily use	M630:9	Stage 4	XF-17	2 samples taken
Xi'an	Xinfeng	Pot	Artefacts for daily use	M700:7	Stage 4	XF-18	
Xi'an	Xinfeng	Belt-hook	Artefacts for daily use	M225:2	Stage 3	XF-20	
Xi'an	Xinfeng	Belt-hook	Artefacts for daily use	M564:1		XF-21	
Xi'an	Xinfeng	Belt-hook	Artefacts for daily use	M355:1	Stage 4	XF-22	
Xi'an	Xinfeng	Lamp	Artefacts for daily use	M388:21	Stage 3	XF-24	
Xi'an	Xinfeng	Adze(Ben)	Farming implements	M398:8	Stage 3	XF-25	
Xi'an	Xinfeng	Adze(Ben)	Farming implements	M651:11	Stage 2	XF-27	

Xi'an	Xinfeng	Adze(Ben)	Farming implements	M402:9	Stage 3	XF-28	
Xi'an	Xinfeng	Adze(Ben)	Farming implements	M62:17	Stage 3	XF-29	
Xi'an	Xinfeng	Shovel(Chan)	Farming implements	M7:10	Stage 3	XF-30	
Xi'an	Xinfeng	Shovel(Chan)	Farming implements	M651:12	Stage 3	XF-31	
Xi'an	Xinfeng	Spade(Cha)	Farming implements	M128:11	Stage 3	XF-33	
Xi'an	Xinfeng	Spade(Cha)	Farming implements	M107:3	Stage 2	XF-34	
Xi'an	Xinfeng	Spade(Cha)	Farming implements	M266:3	Stage 4	XF-35	
Xi'an	Xinfeng	Knife	Craft tools	M295:6		XF-36	
Xi'an	Xinfeng	Knife	Craft tools	M390:13	Stage 3	XF-37	
Xi'an	Xinfeng	Awl	Craft tools	M48:6	Stage 4	XF-F17	
Xi'an	Xinfeng	Chisel	Craft tools	M402:10	Stage 3	XF-F19	
Xi'an	Xinfeng	Spoon	Artefacts for daily use	M423:7	Stage 3	XF-F26	
Xi'an	Xinfeng	Lamp	Artefacts for daily use	M212:1	Stage 4	XF-F27	
Xi'an	Xinfeng	Sword	Weapon	M256:16	Stage 2	XF-F29	
Xi'an	Xiekou	Ploughshare	Farming implement	M63:4		XK-Pl1	
Xi'an	Xiekou	Pot	Artefacts for daily use	M31:18		XK-Pot7	
Xi'an	Xiekou	Pot	Artefacts for daily use	M52:27		XK-Pot8	
Xi'an	Xiekou	Pot	Artefacts for daily use	M49:26		XK-Pot9	
Xi'an	Xiekou	Lamp	Artefacts for daily use	M30:7		XK-La13	
Xi'an	Xiekou	Lamp	Artefacts for daily use	M52:24		XK-La14	
Xi'an	Xiekou	Lamp	Artefacts for daily use	M52:25		XK-La15	
Xi'an	Xiekou	Lamp	Artefacts for daily use	M52:26		XK-La16	
Xi'an	Xiekou	Lamp	Artefacts for daily use	M51:15		XK-La17	
Xi'an	Xiekou	Spear	Weapon	M49:13		XK-Sp1	
Xi'an	Xiekou	Saw	Craft tools	M49:19		XK-Saw1	

Xi'an	Xiekou	Sword	Weapon	M19:11		XK-Sw14	Corroded
Xi'an	Xiekou	Sword	Weapon	M33:9		XK-Sw15	
Xi'an	Xiekou	Knife	Craft tools	M49:11		XK-Kn10	
Xi'an	Xiekou	Knife	Craft tools	M38:2		XK-Kn11	
Xian Yang	Niejiagou	Chisel	Craft tools	T3:20		NJG-1	
Xian Yang	Niejiagou	Chisel	Craft tools	T1:14		NJG-2	
Xian Yang	Niejiagou	Chisel	Craft tools	T3:22		NJG-3	
Xian Yang	Niejiagou	Chisel	Craft tools	T2:28		NJG-4	
Xian Yang	Niejiagou	Chisel	Craft tools	T1:05		NJG-5	
Xian Yang	Niejiagou	Chisel	Craft tools	T3:27		NJG-6	
Xian Yang	Niejiagou	Chisel	Craft tools	T2:12		NJG-7	
Xian Yang	Niejiagou	Chisel	Craft tools	T1:03		NJG-8	
Xian Yang	Niejiagou	Chisel	Craft tools	T3:22		NJG-9	
Xian Yang	Niejiagou	Chisel	Craft tools	T4:14		NJG-11	
Xian Yang	Niejiagou	Chisel	Craft tools	T1:7		NJG-12	
Xian Yang	Niejiagou	Knife	Craft tools	T3:25		NJG-13	
Xian Yang	Niejiagou	Knife	Craft tools	T3:10		NJG-14	
Xian Yang	Niejiagou	Knife	Craft tools	T4:06		NJG-16	
Xian Yang	Niejiagou	Knife	Craft tools	T1:08		NJG-17	
Xian Yang	Niejiagou	Knife	Craft tools	T3:28		NJG-18	
Xian Yang	Niejiagou	Knife	Craft tools	T3:19		NJG-19	
Xian Yang	Niejiagou	Shovel(Chan)	Artefacts for daily use	T3:24		NJG-20	
Xian Yang	Niejiagou	Shovel(Chan)	Artefacts for daily use	T2:21		NJG-21	
Xian Yang	Niejiagou	Shovel(Chan)	Artefacts for daily use	T4:12		NJG-22	
Xian Yang	Niejiagou	Adze(Ben)	Artefacts for daily use	T2:25		NJG-23	

Xian Yang	Niejiagou	Bar	Unknown	T4:10		NJG-24	
Xian Yang	Niejiagou	Fragment	Unknown	T1:1		NJG-31	
Xian Yang	Niejiagou	Fragment	Unknown	T2:27		NJG-32	
Xian Yang	Niejiagou	Fragment	Unknown	T1:4		NJG-33	Rectangular shaped
Xian Yang	Niejiagou	Fragment	Unknown	T4:7		NJG-34	Belt shaped
Xian Yang	Niejiagou	Fragment	Unknown	T2:24		NJG-35	
Xian Yang	Niejiagou	Fragment	Unknown	T2:4		NJG-36	
Xian Yang	Yancun	Spade(Cha)	Farming implements	M61:1		YC-1	
Xian Yang	Yancun	Spade(Cha)	Farming implements	M52		YC-2	Item located in the tomb passage
Xian Yang	Yancun	Spade(Cha)	Farming implements	M81		YC-3	Item located in the tomb passage
Xian Yang	Yancun	Belt-hook	Artefacts for daily use	M53:1		YC-4	
Xian Yang	Yancun	Belt-hook	Artefacts for daily use	M66:4		YC-5	
Xian Yang	Changxingcun	Sickle	Farming implements	T2lower:1		CXC-1	
Xian Yang	Airport	Arrowhead	Weapon	M352:4		JC-1	
Xian Yang	Airport	Arrowhead	Weapon	M352:4		JC-2	
Xian Yang	Airport	Arrowhead	Weapon	M352:4		JC-3	
Xian Yang	Airport	Arrowhead	Weapon	M352:4		JC-4	
Xian Yang	Airport	Vessel	Artefacts for daily use	M363:4		JC-5	
Xian Yang	Airport	Vessel	Artefacts for daily use	M369:2		JC-6	
Xian Yang	Lüdi	Arrowhead	Weapon	M8:4		LD-1	
Xian Yang	Lüdi	Arrowhead	Weapon	M8:3		LD-2	
Xian Yang	Lüdi	Spade(Cha)	Farming implements	M8:1		LD-3	
Xian Yang	Lüdi	Adze(Ben)	Farming implements	M48:1		LD-4	
Xian Yang	Ningyuan	Spade(Cha)	Farming implements	M82:2		NY-1	
Xian Yang	Ningyuan	Shovel(Chan)	Farming implements	M67:4		NY-2	

Xian Yang	Ningyuan	Adze(Ben)	Farming implements	M6:4		NY-3	
Xian Yang	Ningyuan	Belt-hook	Artefacts for daily use	M61:5		NY-4	
Xian Yang	Ningyuan	Knife	Craft tools	M28:1		NY-6	
Xian Yang	Ningyuan	Fragment	Unknown	M67:7		NY-8	
Xian Yang	Ningyuan	Pot	Artefacts for daily use	M36:13		NY-9	
Xian Yang	Hejia	Belt-hook	Artefacts for daily use	M71:6		HJ-1	
Xian Yang	Hejia	Belt-hook	Artefacts for daily use	M24:1		HJ-2	
Xian Yang	Hejia	Belt-hook	Artefacts for daily use	M30:1		HJ-4	
Xian Yang	Hejia	Belt-hook	Artefacts for daily use	M52:1		HJ-5	
Xian Yang	Hejia	Belt-hook	Artefacts for daily use	M45:1		HJ-6	
Xian Yang	Hejia	Belt-hook	Artefacts for daily use	M15:5		HJ-7	
Xian Yang	Hejia	Belt-hook	Artefacts for daily use	M46:1		HJ-8	
Xian Yang	Hejia	Belt-hook	Artefacts for daily use	M61:5		HJ-9	
Xian Yang	Hejia	Belt-hook	Artefacts for daily use	M41:2		HJ-10	
Xian Yang	Hejia	Ring	Artefacts for daily use	M3:1		HJ-11	
Baoji	Gaoxin	Knife	Craft tools	M17:1		GX-2	
Baoji	Gaoxin	Spade(Cha)	Farming implements	M26:1		GX-3	Item located in the tomb passage

Appendix-3 Metallography images of analysed samples

Xinfeng Cemetery

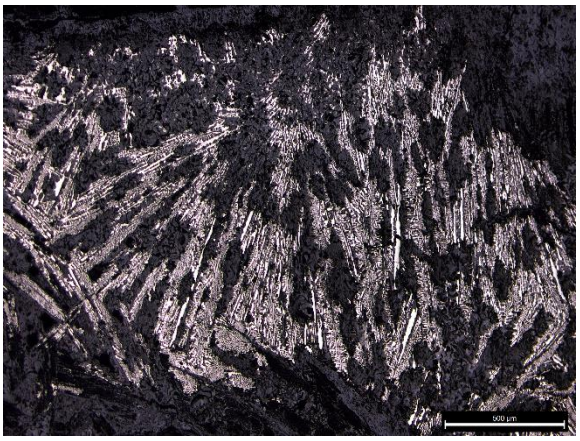

XF-1-BODY, tripod, mottled cast iron, graphite flakes (type A) on mixed matrix of ledeburite and pearlite.

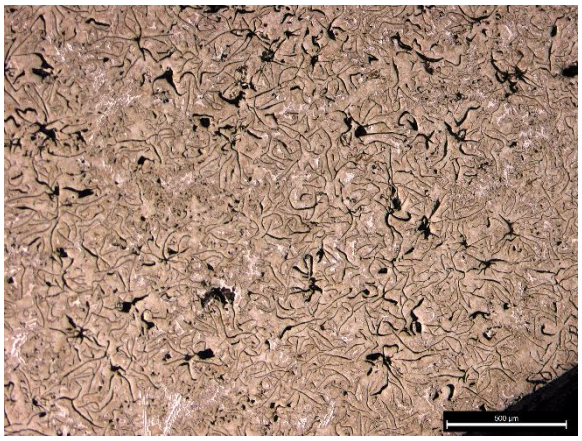

XF-1-EAR, tripod, grey cast iron, graphite flakes (type A) on a pearlite matrix (small amount of cementite remains).

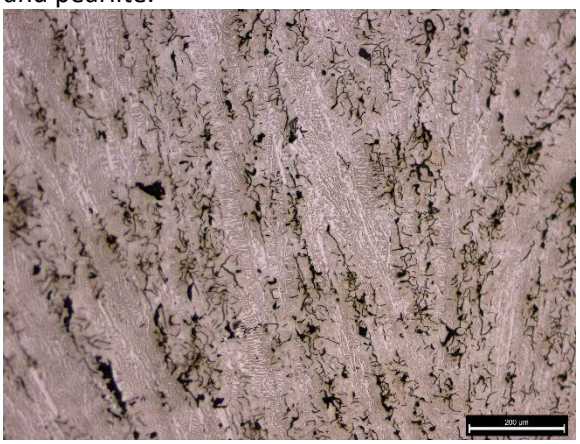

XF-1-LEG, tripod, mottled cast iron, graphite flakes (type A) on mixed matrix of ledeburite and pearlite.

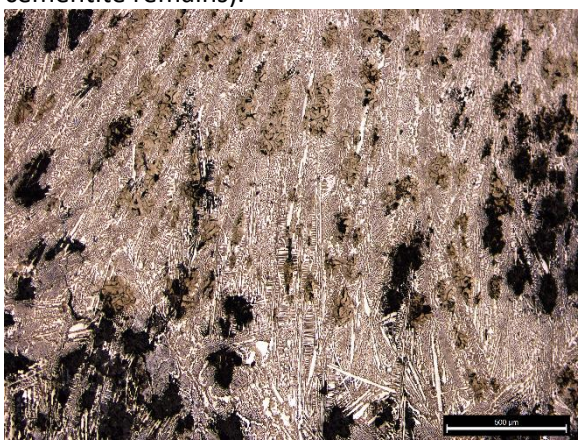

XF-1-LIP, tripod, mottled cast iron, graphite flakes (type A) on mixed matrix of ledeburite and pearlite.

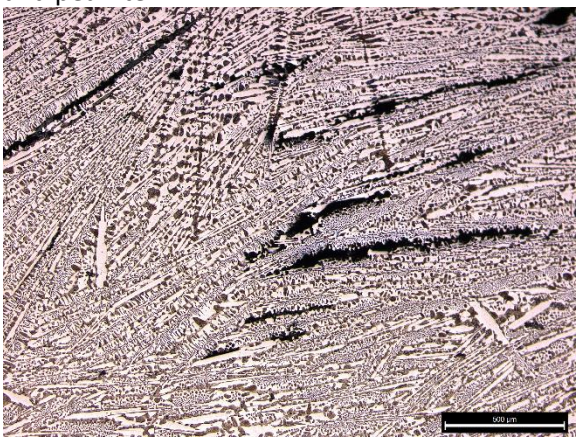

XF-2-BODY, tripod, white cast iron, modified ledeburite.

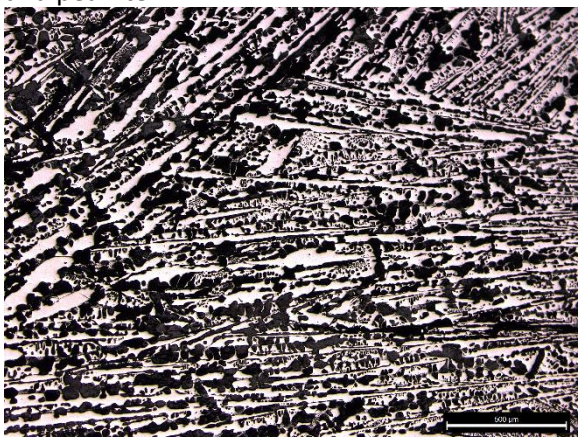

XF-2-LEG, tripod, white cast iron, ledeburite structure

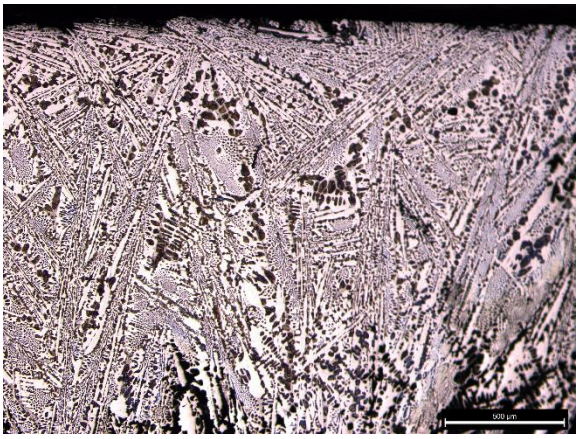

XF-2-LIP, tripod, white cast iron, modified ledeburite.

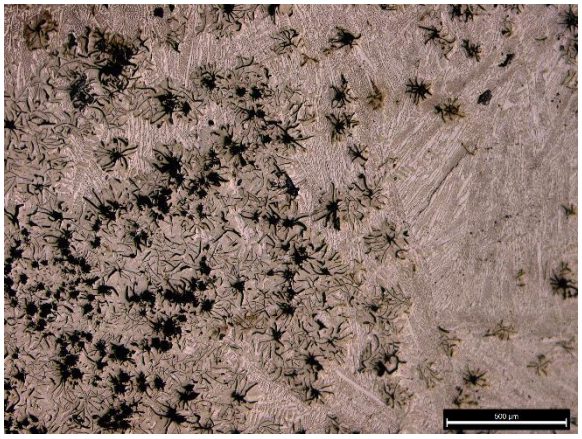

XF-3-LID, tripod, mottled cast iron, graphite flakes (type-F) on mixed matrix of ledeburite and pearlite.

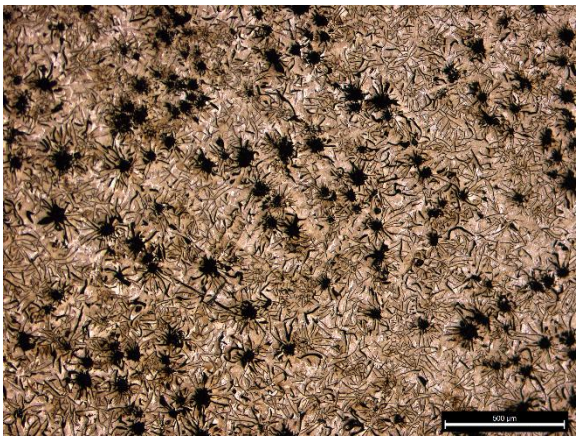

XF-3-LIP, tripod, grey cast iron, graphite flakes(type-F) on a pearlite matrix.

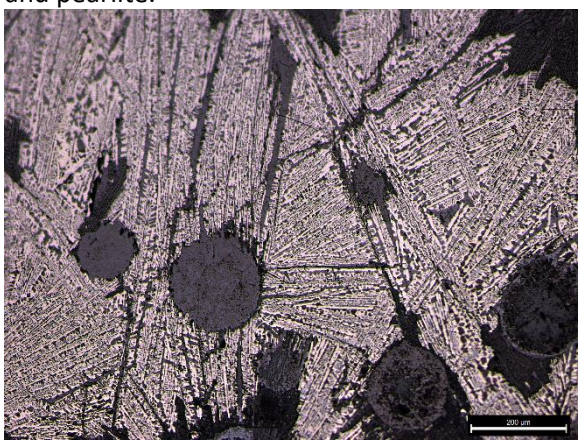

XF-4, tripod, white cast iron, ledeburite structure.

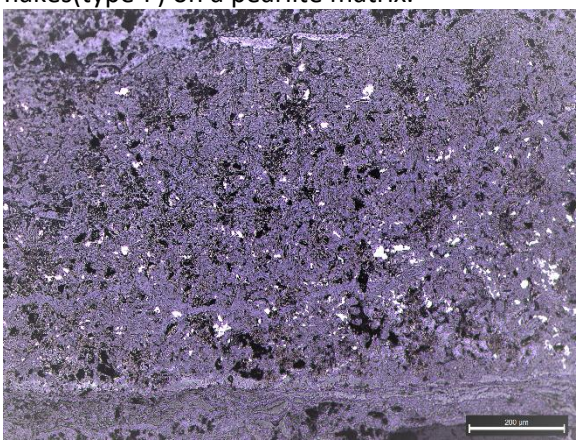

XF-5-BODY, mou(鏊), corroded, graphite flakes distributed on the corroded matrix, possibly mottled cast iron

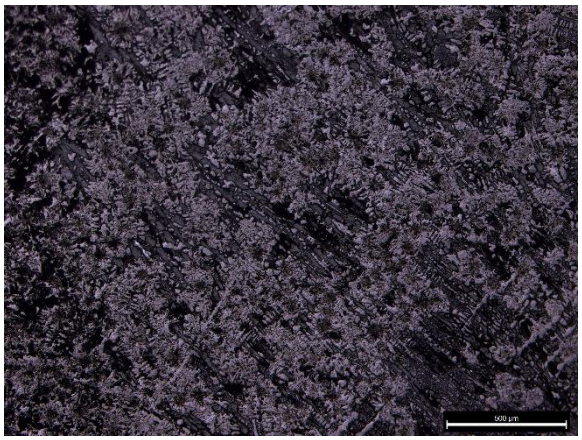

XF-5-LIP, mou(鏊), corroded, mottled cast iron, graphite flakes distributed in the corroded matrix, with ledeburite ghost microstructure

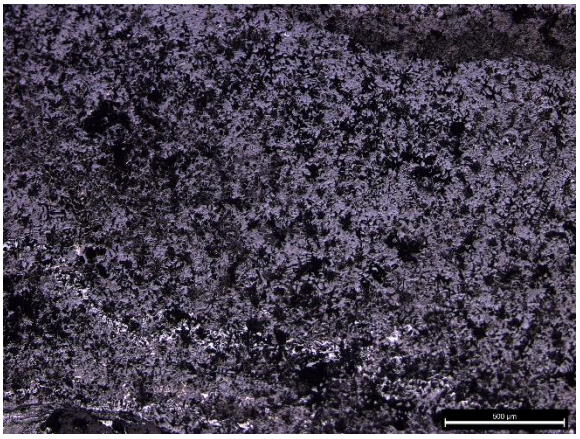

XF-7-BODY, pot, grey cast iron, graphite flakes (type-F) on corroded matrix.

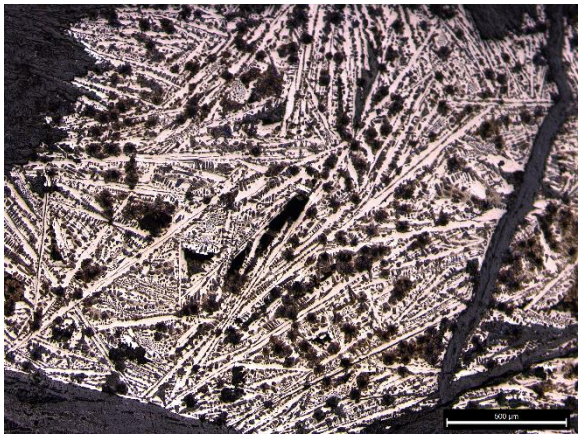

XF-8-BODY, pot, mottled cast iron, graphite flakes (type-F) on mixed matrix of ledeburite and pearlite.

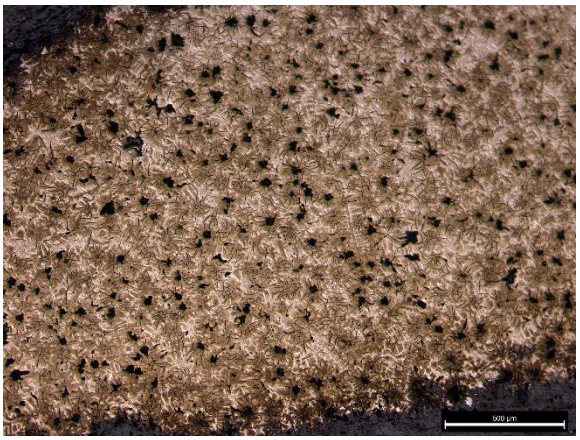

XF-8-LIP, pot, grey cast iron, graphite flakes (type-F) on pearlite matrix.

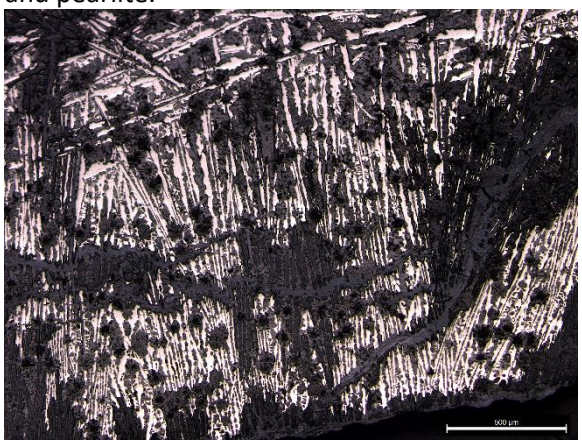

XF-9-BODY, pot, grey cast iron, graphite flakes (type-F) on mixed matrix of ledeburite and pearlite.

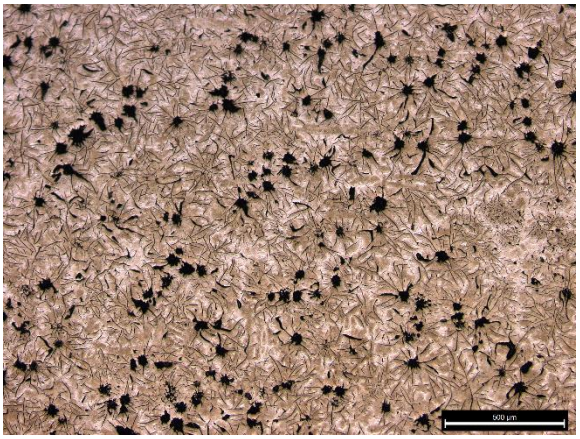

XF-9-LIP, pot, grey cast iron, graphite flakes (type-F) on pearlite matrix.

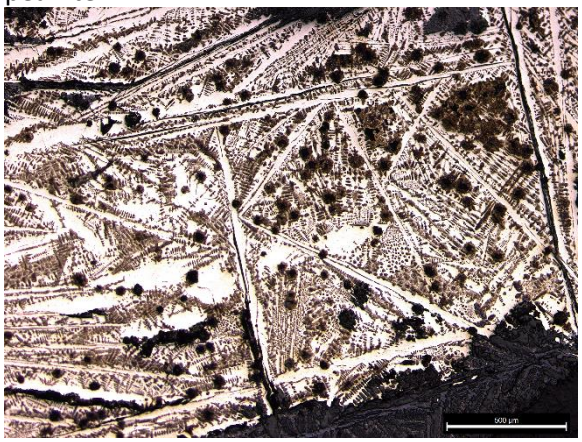

XF-10-BODY, pot, grey cast iron, graphite flakes (type-F) on mixed matrix of pearlite, ledeburite and primary cementite.

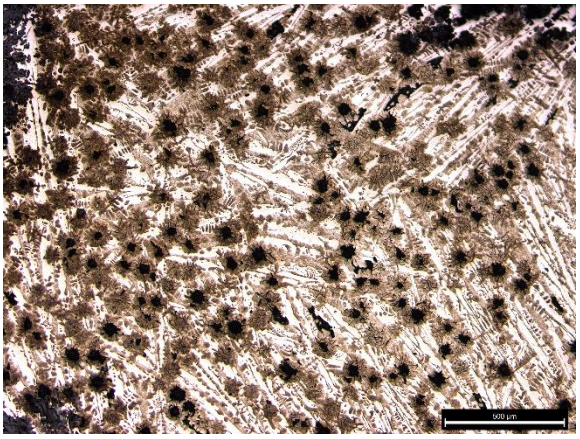

XF-10-LIP, pot, grey cast iron, graphite flakes (type-F) on mixed matrix of pearlite, ledeburite and primary cementite.

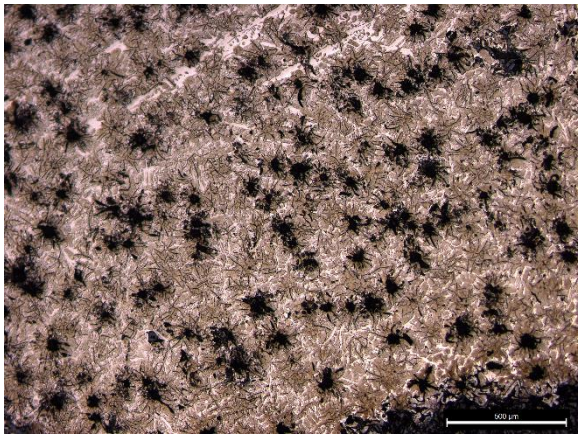

XF-11-BODY, pot, grey cast iron, graphite flakes (type-F) on pearlite matrix.

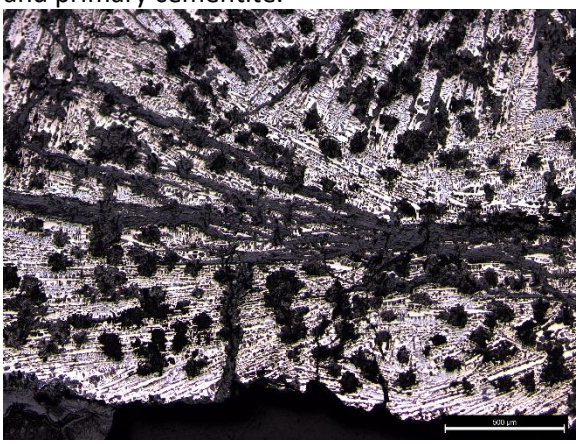

XF-12-BODY, pot, grey cast iron, graphite flakes (type-F) on mixed matrix of pearlite and ledeburite.

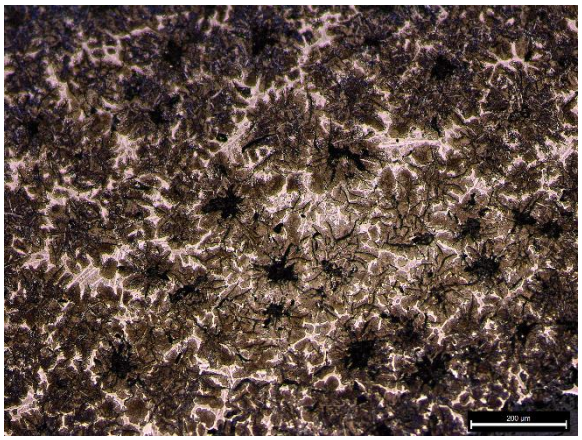

XF-14-BODY, pot, mottled cast iron, graphite flakes (type-F) on mixed matrix of pearlite and few cementite.

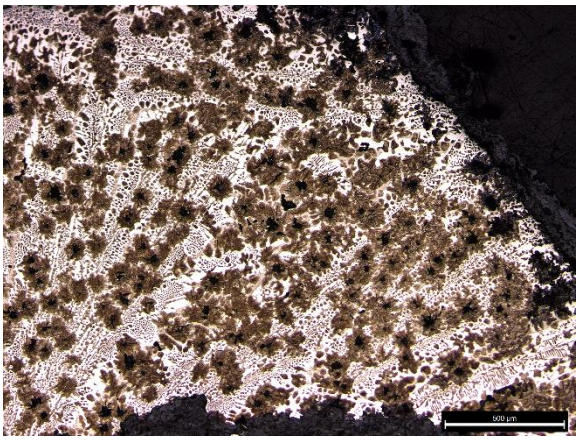

XF-14-LIP, pot, mottled cast iron, graphite flakes (type-F) on mixed matrix of pearlite and ledeburite.

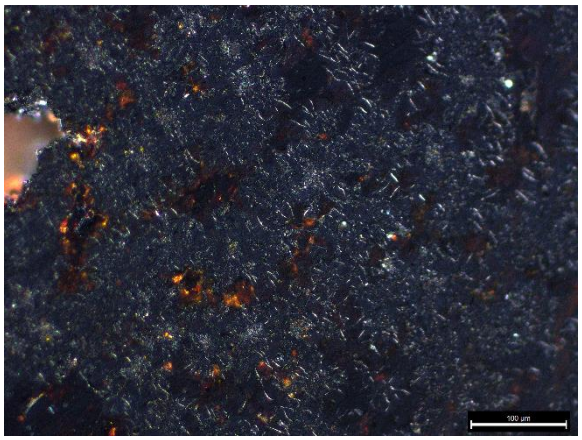

XF-15-BODY, pot, grey cast iron, corroded, graphite flakes (type-F) can be seen under polarized light.

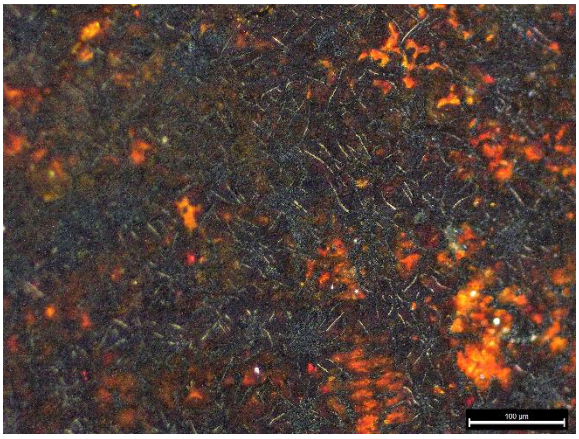

XF-15-LIP, pot, grey cast iron, corroded, graphite flakes (type-F) can be seen under polarized light.

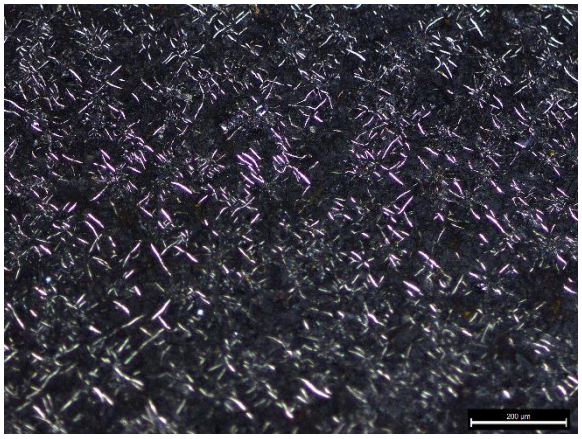

XF-16-BODY, pot, grey cast iron, corroded, graphite flakes (type-F) can be seen under polarized light.

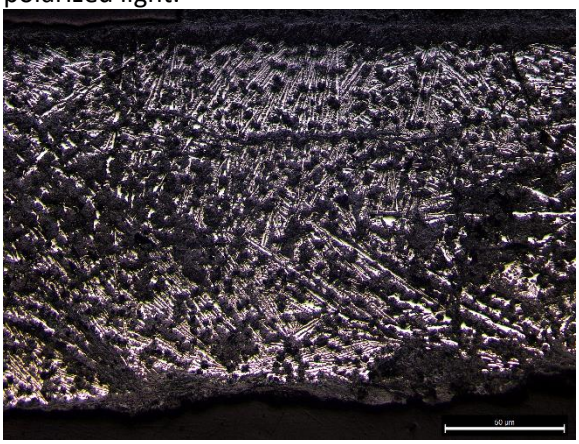

XF-16-LIP, pot, mottled cast iron, graphite flakes (type-F) on mixed matrix of ledeburite and pearlite.

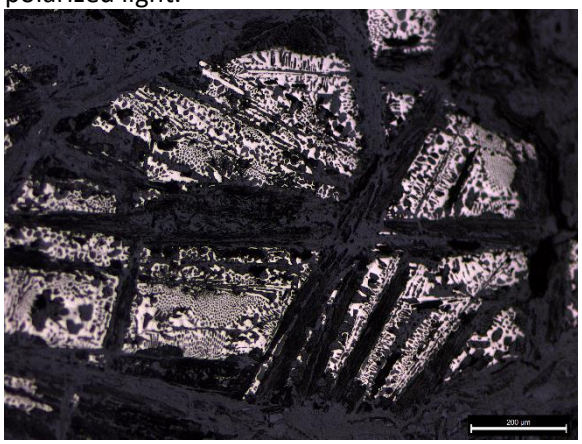

XF-17-BODY, pot, white cast iron, ledeburite structure.

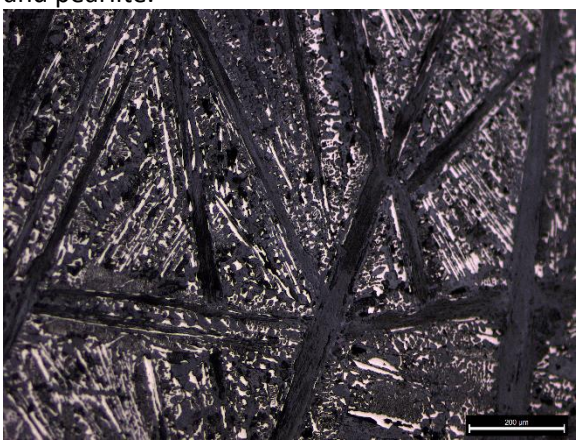

XF-17-LIP, pot, white cast iron, ledeburite structure.

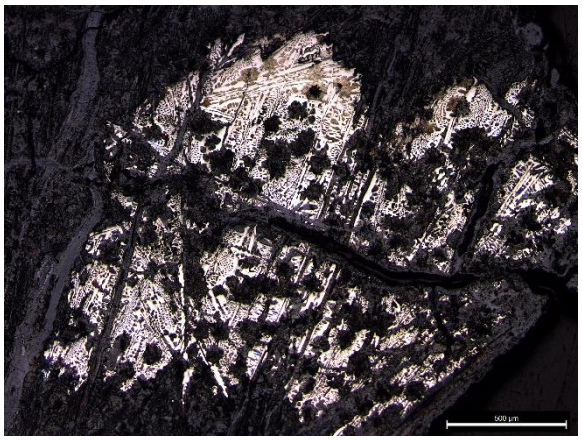

XF-18-BODY, pot, mottled cast iron, graphite flakes (type-F) on mixed matrix of ledeburite and pearlite.

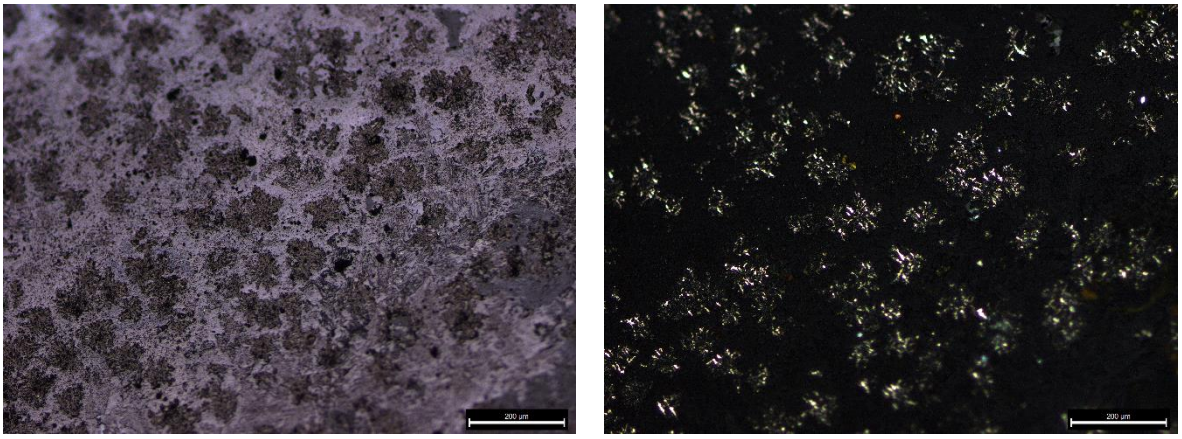

XF-20, belt-hook, malleable cast iron, corroded, ghost structure of pearlite can be seen on the left, and graphite nodules can be seen under unpolarized light on the right.

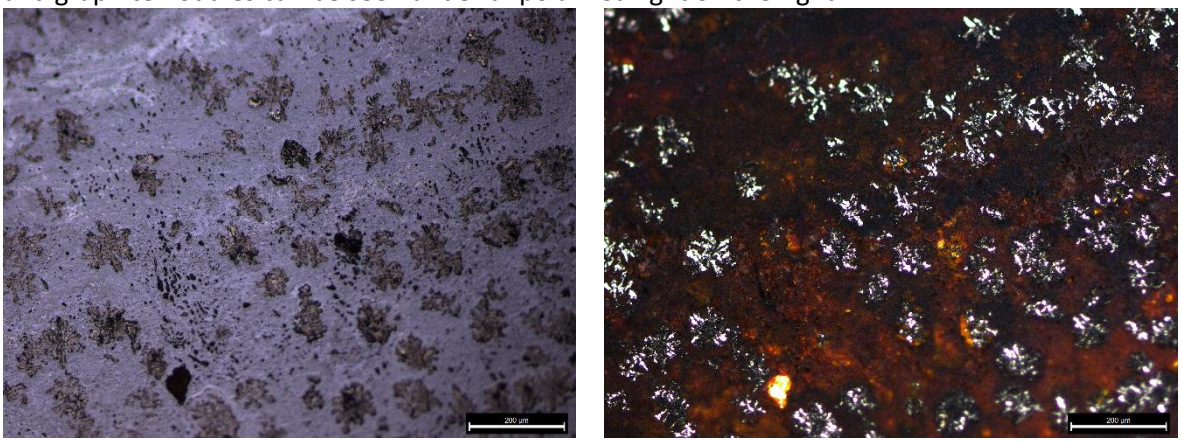

XF-21, belt-hook, malleable cast iron, corroded, ghost structure of pearlite can be seen on the left, and graphite nodules can be seen under unpolarized light on the right.

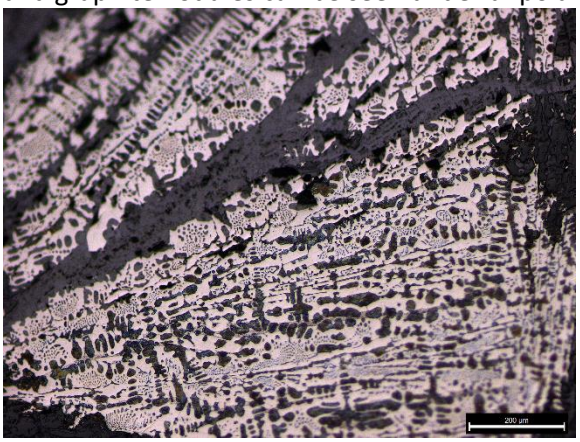

XF-22, belt-hook, white cast iron, ledeburite microstructure with modified ledeburite.

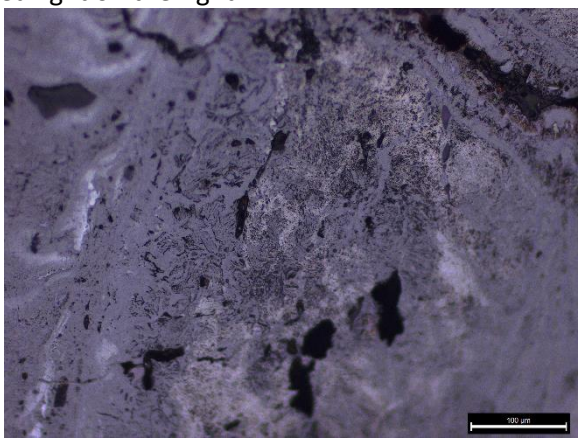

XF-23, belt-hook, corroded, ghost structure of pearlite can be seen.

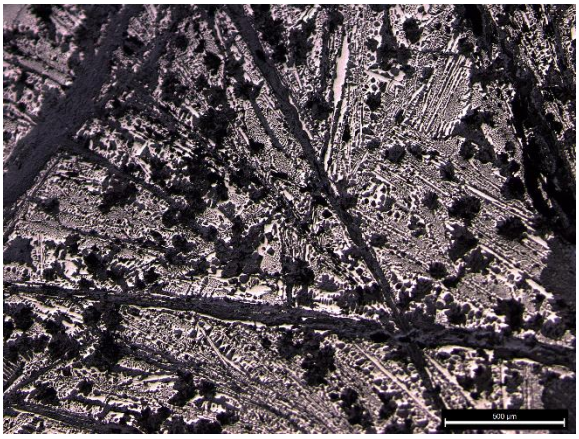

XF-24, lamp, mottled cast iron, graphite flakes (type-F) on mixed matrix of ledeburite and pearlite.

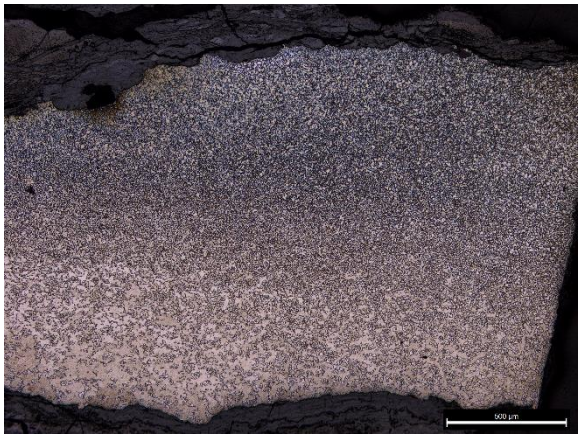

XF-25, adze(ben), steel, granular pearlite on ferrite matrix.

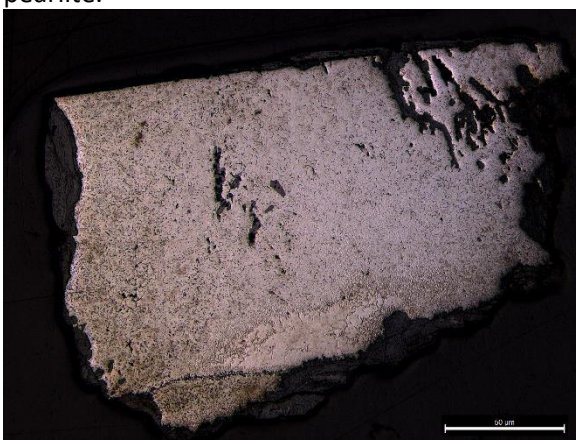

XF-27, adze(ben), Widmannstätten structure on the left and ferrite on the right.

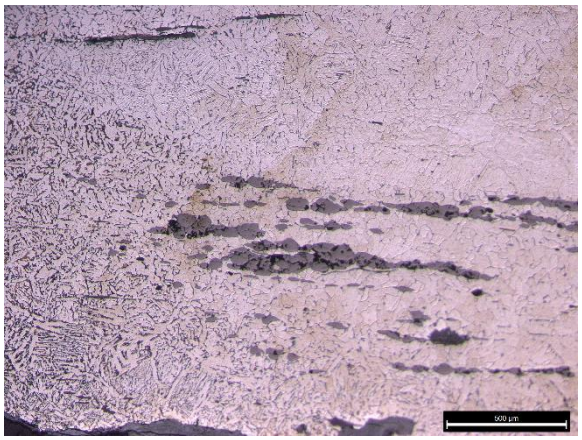

XF-28, adze(ben), Widmannstätten structure on the left and ferrite on the right. Slag inclusions lined up in the matrix.

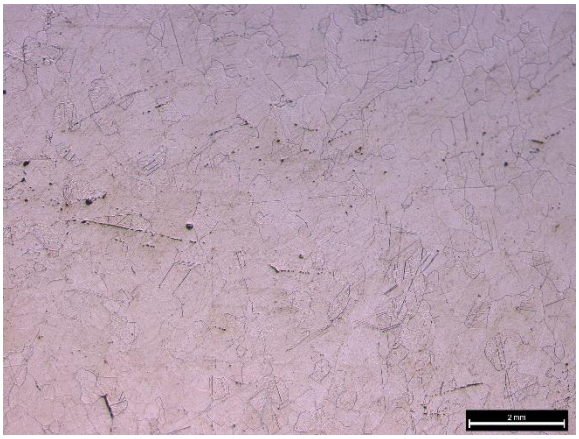

XF-29, adze(ben), ferrite grains.

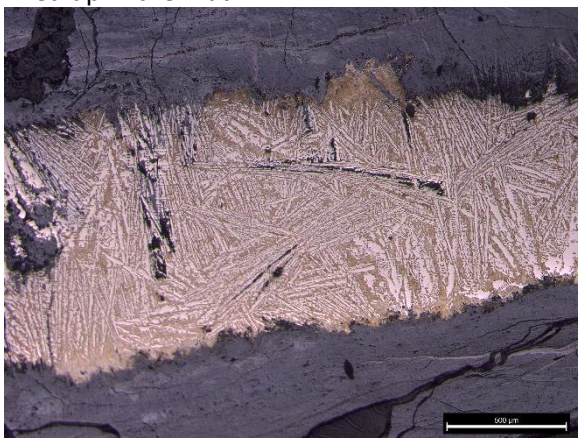

XF-30, shovel (Chan), decarburised white cast iron core with pearlite structure on the surface.

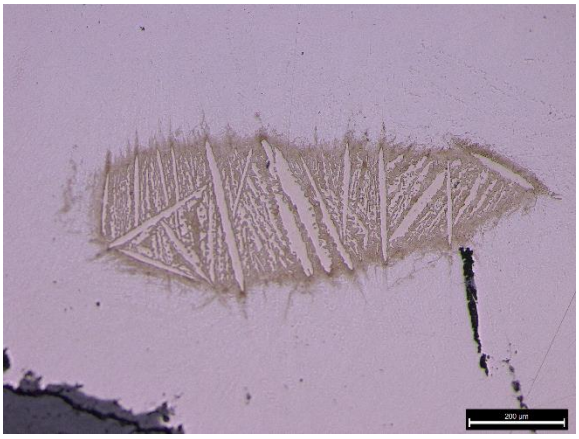

XF-31, shovel (Chan), decarburised white cast iron core surrounded by ferrite.

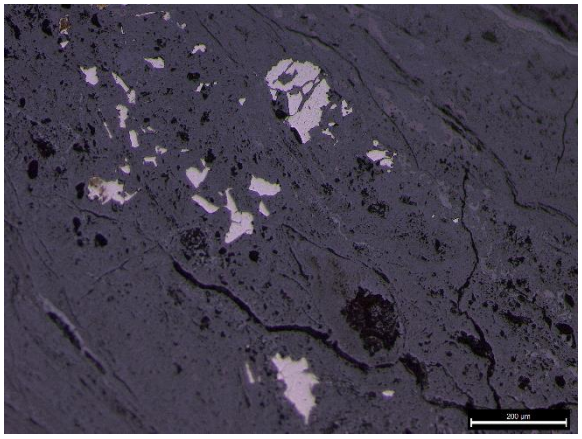

XF-32, shovel (Chan), corroded, with few ferrite grains left.

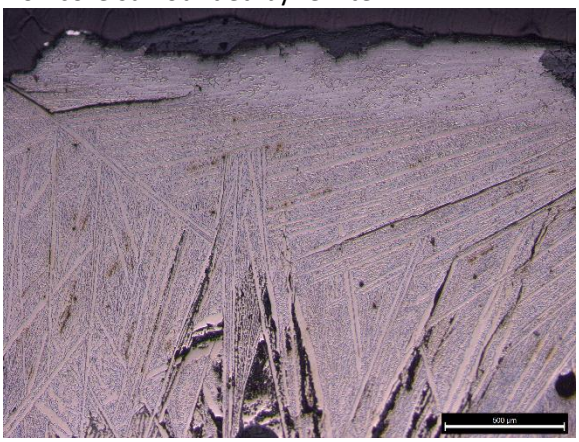

XF-33, spade (Cha), decarburised white cast iron core, with ferrite grains on the surface.

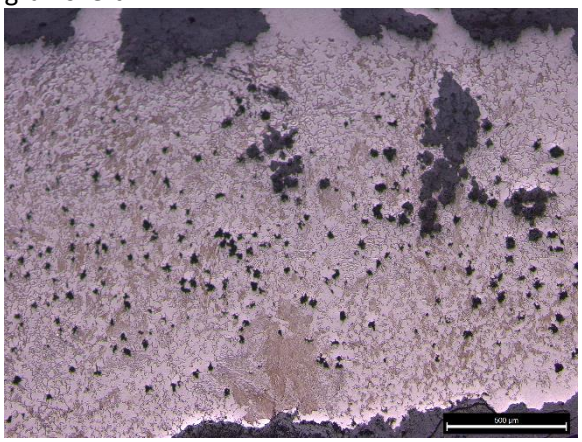

XF-34, spade (Cha), tempered carbon in the center on a mixed matrix of ferrite and pearlite, with ferrite grains on the surface.

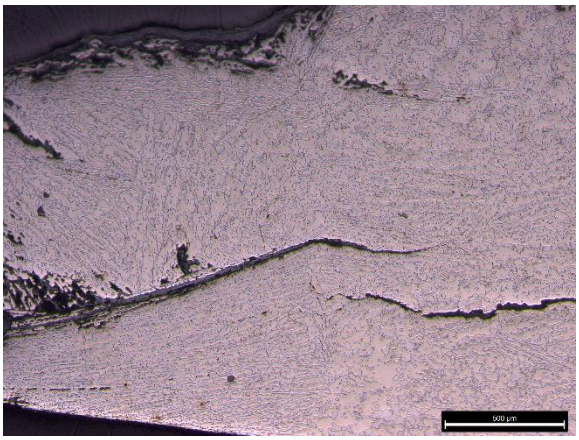

XF-35, spade (Cha), decarburised white cast iron.

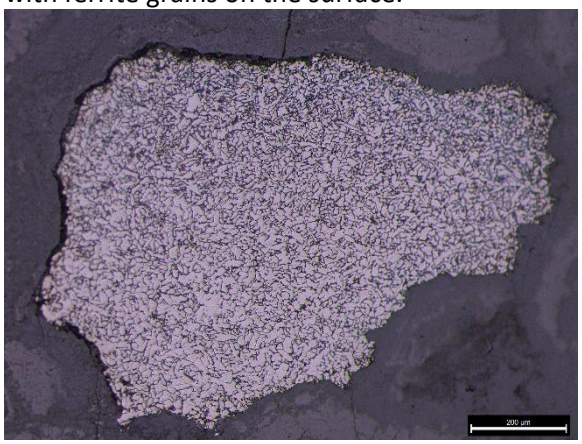

XF-36, knife, corroded, a small piece of iron in the core, with ferrite and pearlite structure.

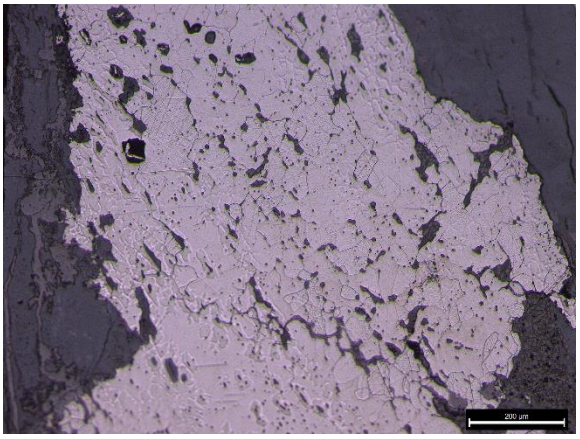

XF-37, knife, ferrite grains with slag inclusions.

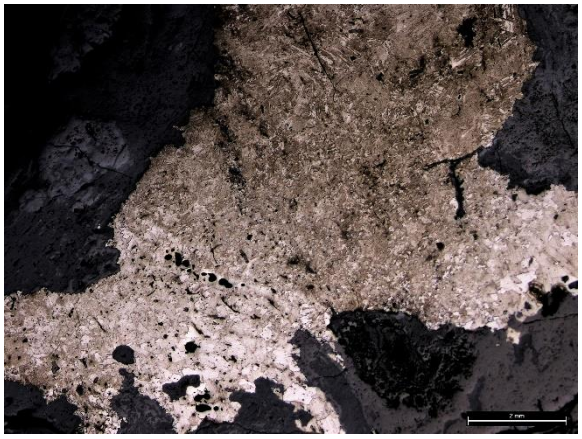

XF-F17, awl, bottom left corner, ferrite grains, top-right corner, martensite structure.

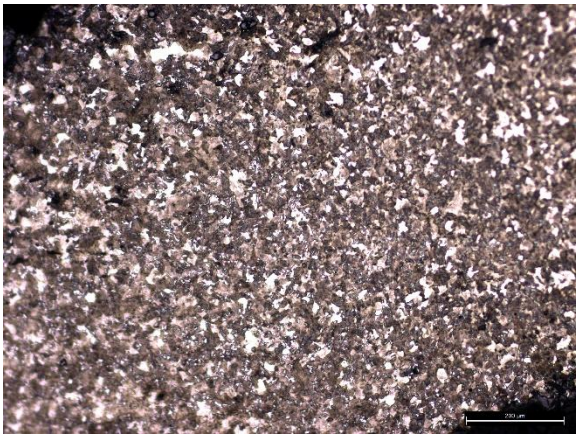

XF-F19, chisel, ferrite and pearlite structure.

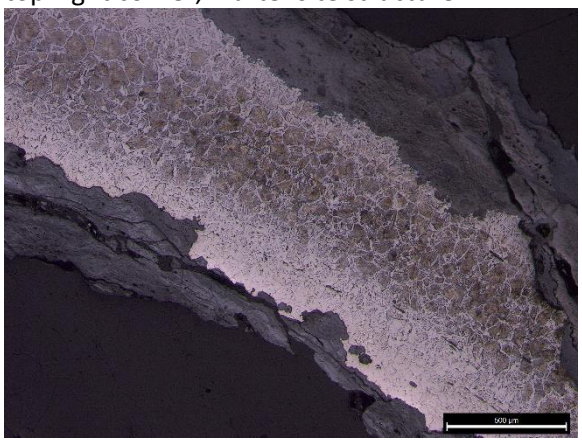

XF-F26, spoon, widmannstätten structure in the center with ferrite grains on the surface.

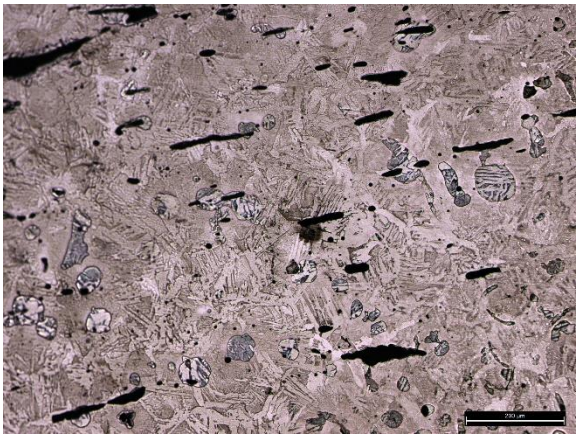

XF-F29, sword, widmannstätten structure with slag inclusions in the matrix.

Xiekou cemetery

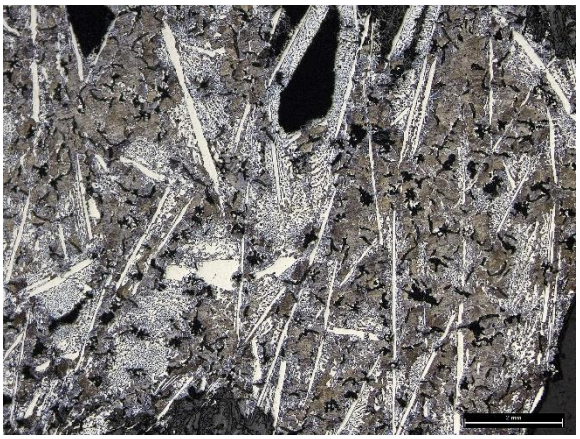

XK-Pl1, ploughshare, vermicular graphite on mixed matrix of pearlite, primary cementite and ledeburite.

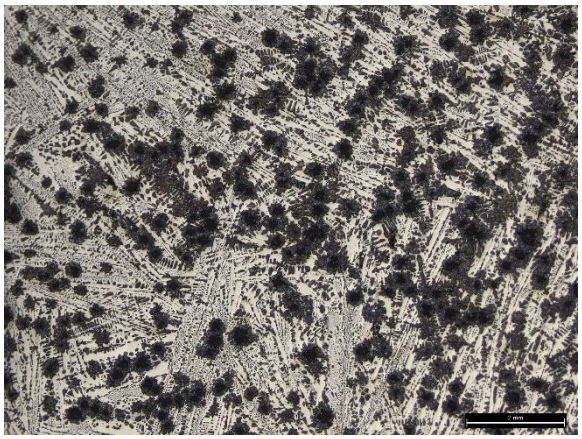

XK-Pot7, pot, mottled cast iron, graphite flakes (type-F) on mixed matrix of ledeburite and pearlite.

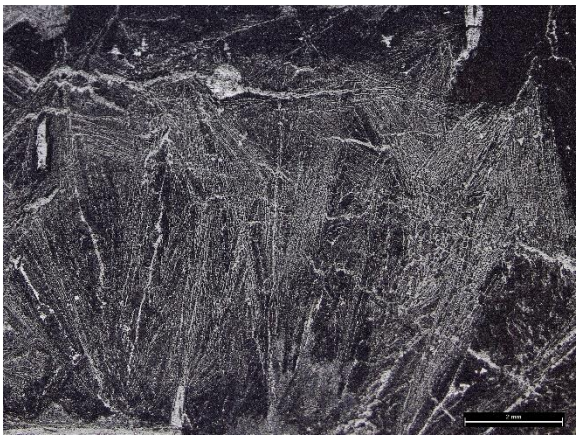

XK-Pot8, pot, corroded, ghost structure of white cast iron.

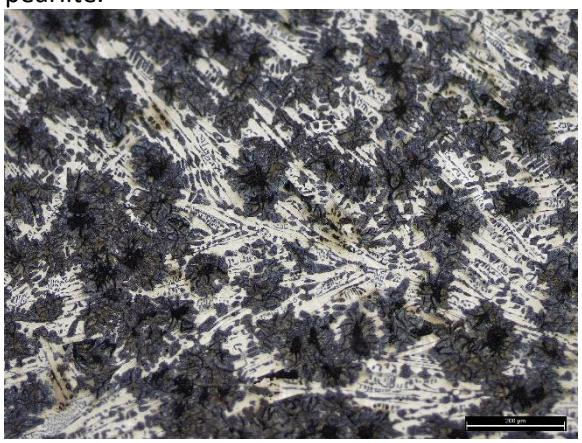

XK-Pot9, pot, mottled cast iron, graphite flakes (type-F) on mixed matrix of ledeburite and pearlite.

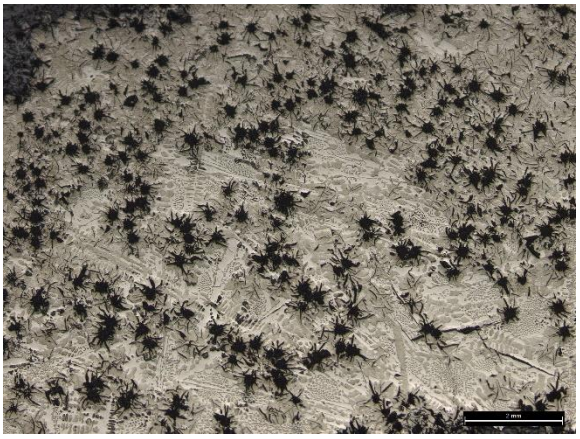

XK-La13, lamp, mottled cast iron, graphite flakes (type-F) on mixed matrix of ledeburite and pearlite.

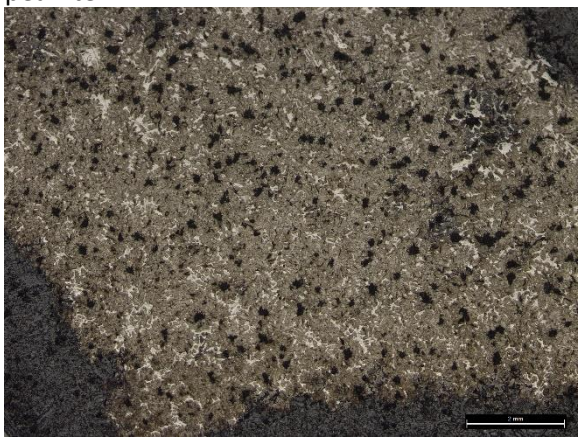

XK-La14, lamp, grey cast iron, graphite flakes (type-F) on pearlite matrix.

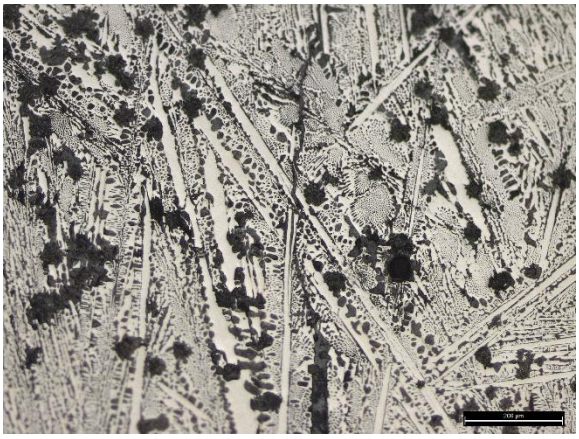

XK-La15, lamp, mottled cast iron, few graphite flakes (type-F) on a hyper-eutectic white cast iron matrix, with ledeburite and primary cementite.

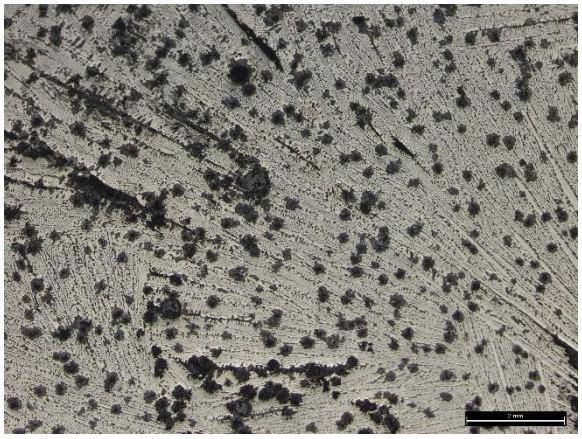

XK-La16, lamp, mottled cast iron, graphite flakes (type-F) on mixed matrix of ledeburite and pearlite.

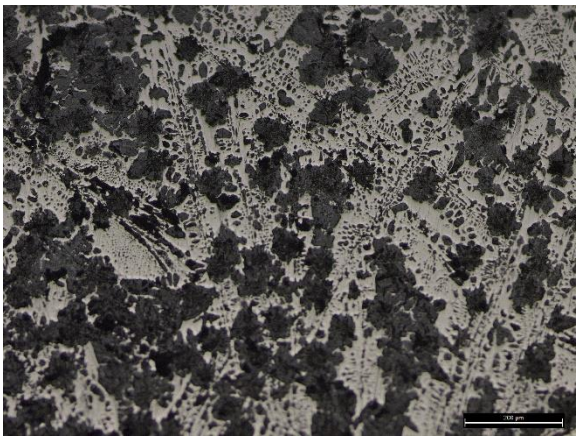

XK-La17, lamp, mottled cast iron, graphite flakes (type-F) on mixed matrix of ledeburite and pearlite.

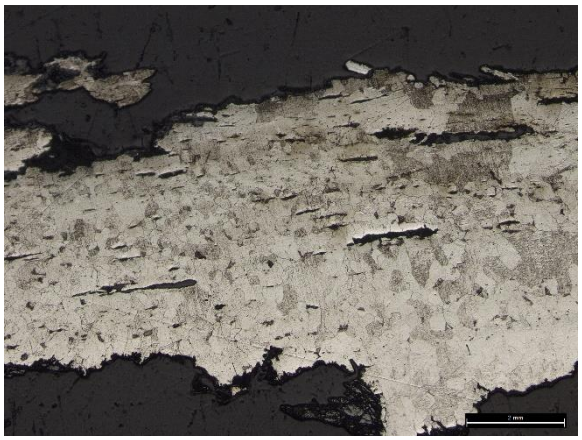

XK-Sp1, spear, ferrite grains with slag inclusions on the matrix.

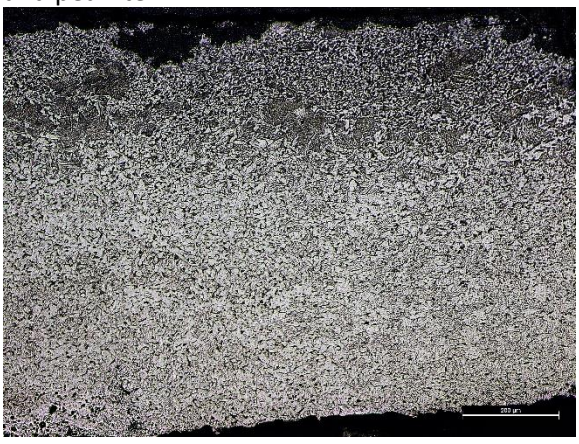

Saw-1, saw, ferrite and pearlite structure.

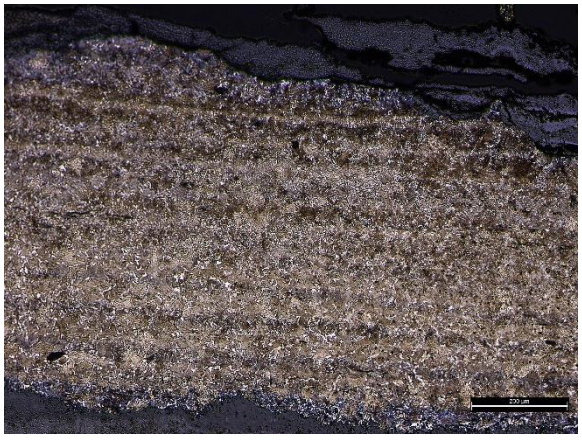

Kn-10, knife, layered structure of ferrite and pearlite.

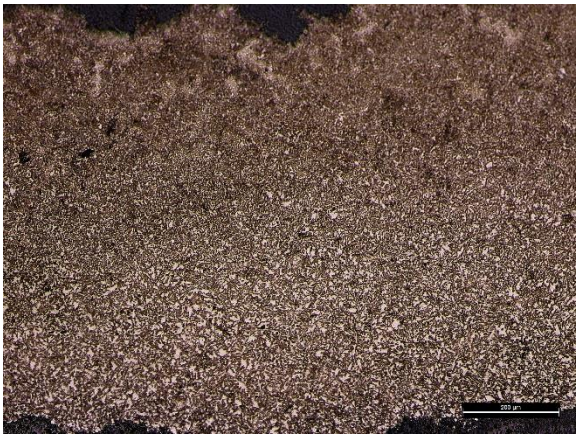

Kn-11, knife, ferrite and pearlite.

Niejiagou bone workshop

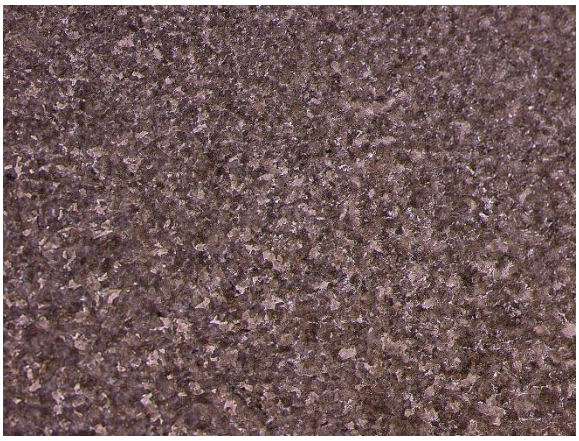

NJG-1, chisel, pearlite grains.

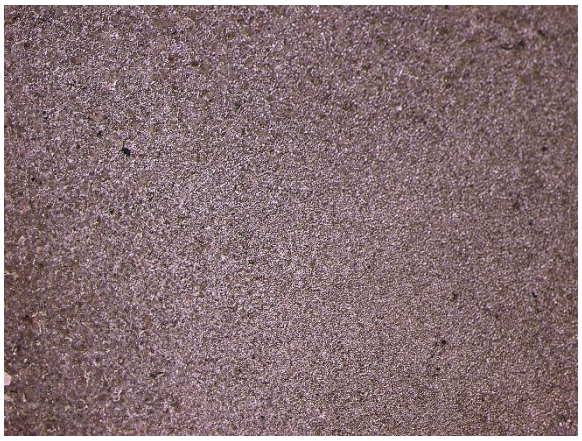

NJG-2, chisel, granular pearlite.

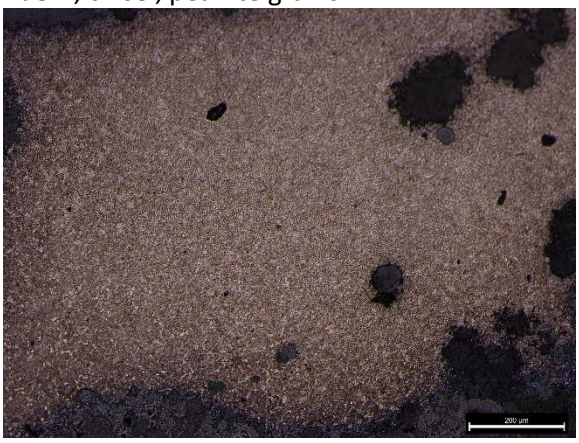

NJG-3, chisel, granular pearlite.

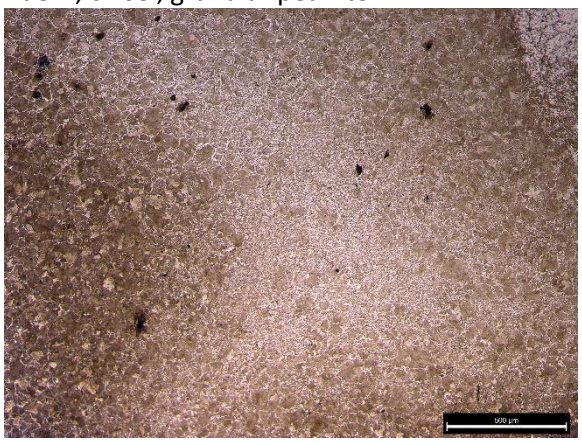

NJG-4, chisel, Widmannstätten structure.

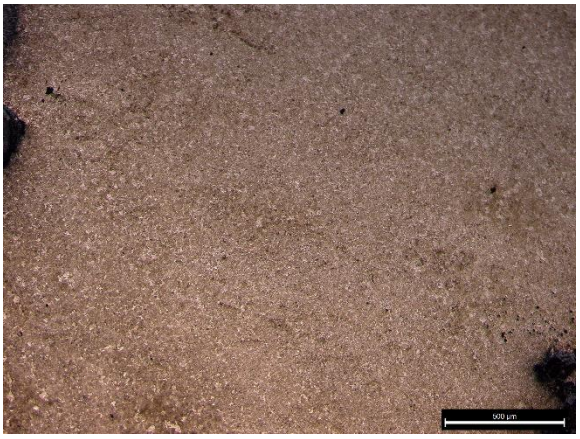

NJG-5, chisel, pearlite.

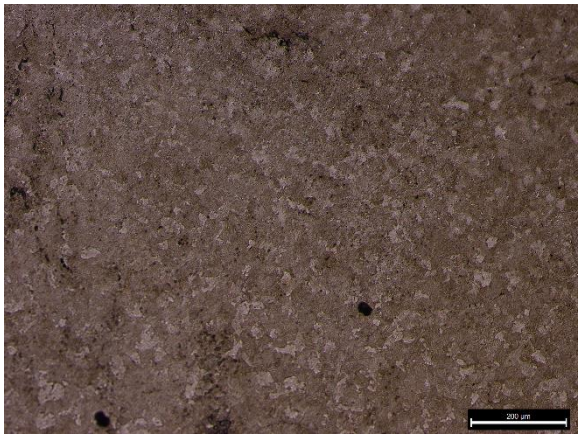

NJG-6, chisel, pearlite and ferrite.

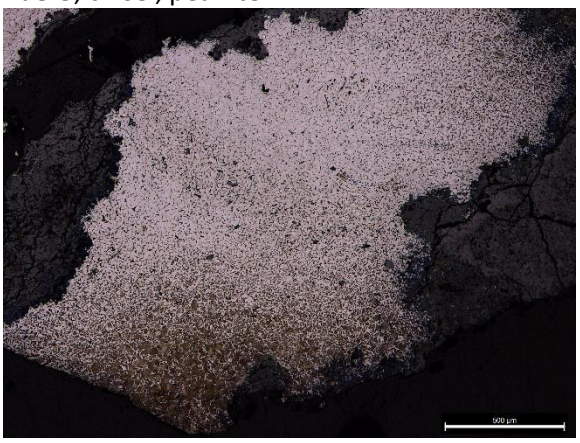

NJG-7, chisel, Widmannstätten structure on the surface with ferrite and pearlite in the center.

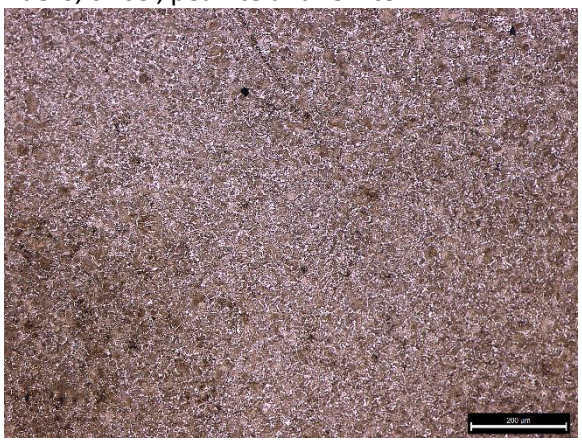

NJG-8, chisel, ferrite and pearlite.

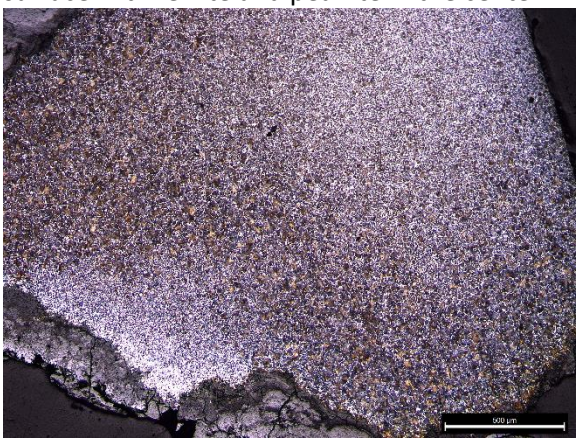

NJG-9, chisel, ferrite and pearlite.

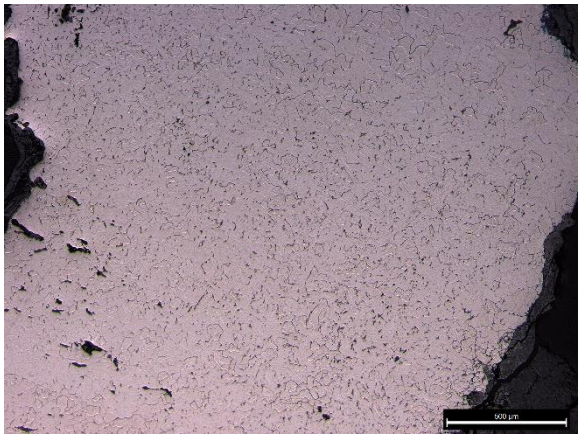

NJG-11, chisel, ferrite grains with pearlite in the grain boundaries.

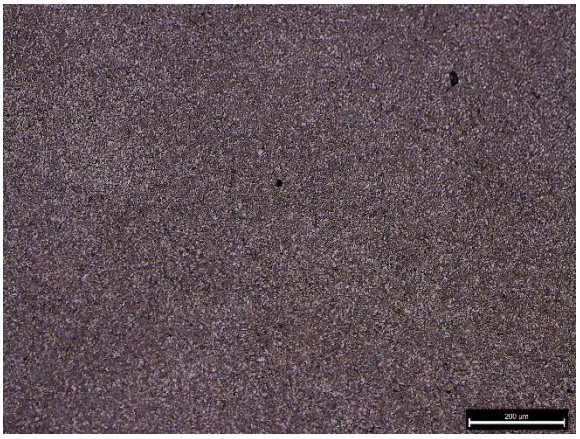

NJG-12, chisel, granular ferrite and pearlite.

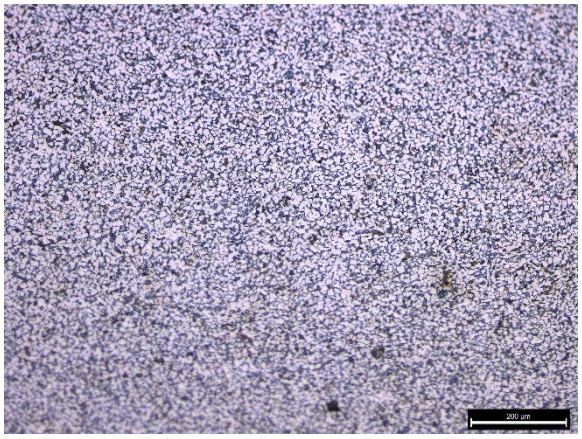

NJG-13, ferrite and pearlite

NJG-14, knife, ferrite with small amount of nodular pearlite

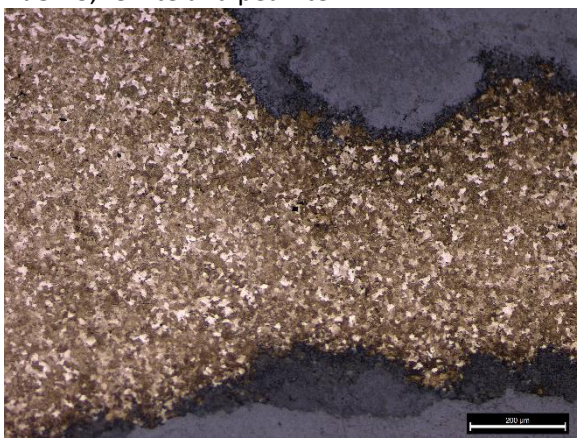

NJG-16, knife, ferrite and pearlite

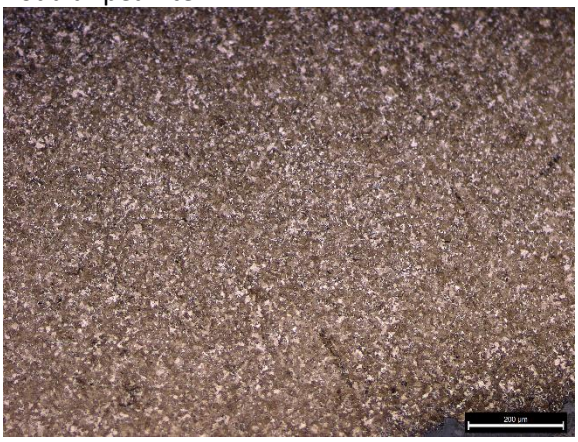

NJG-17, knife, ferrite and pearlite

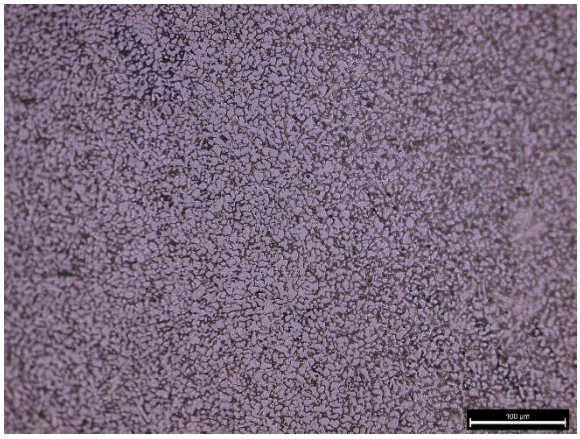

NJG-18, knife, ferrite and pearlite

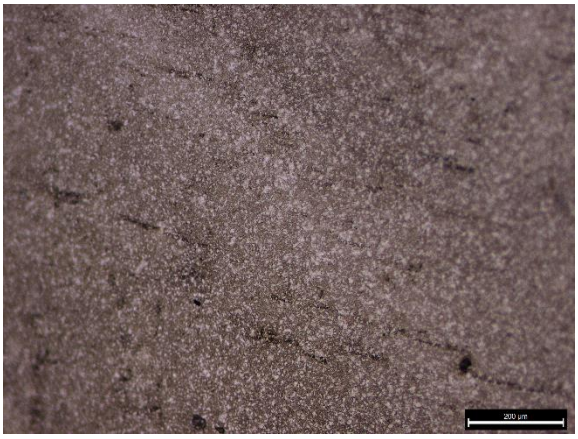

NJG-19, knife, ferrite and pearlite

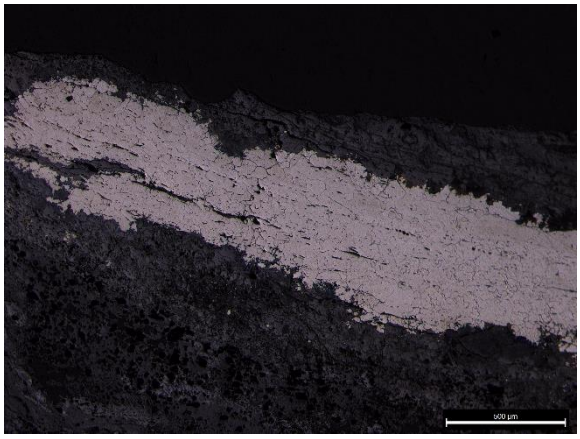

NJG-20, shovel (*chan*), ferrite grains with slag inclusions linearly distributed

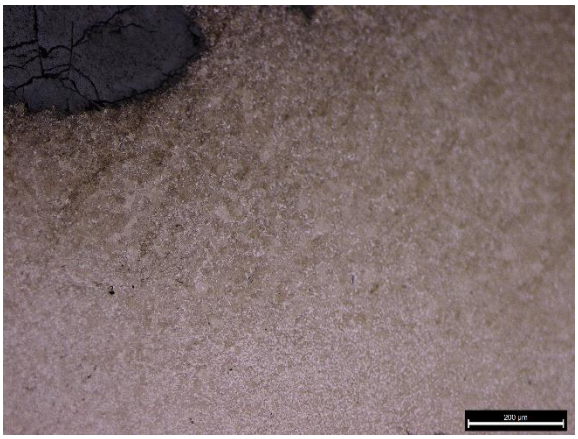

NJG-21, shovel (*chan*), ferrite and pearlite

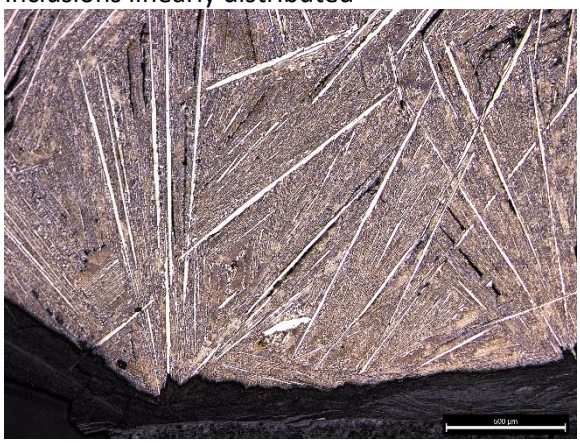

NJG-22, shovel(*chan*), primary cementite and ledeburite

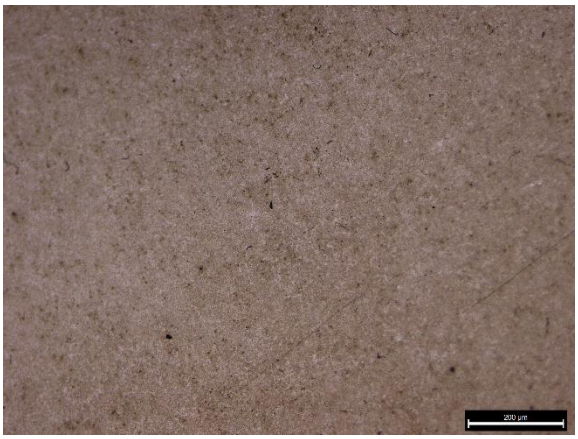

NJG-23, Adze (*Ben*), pearlite

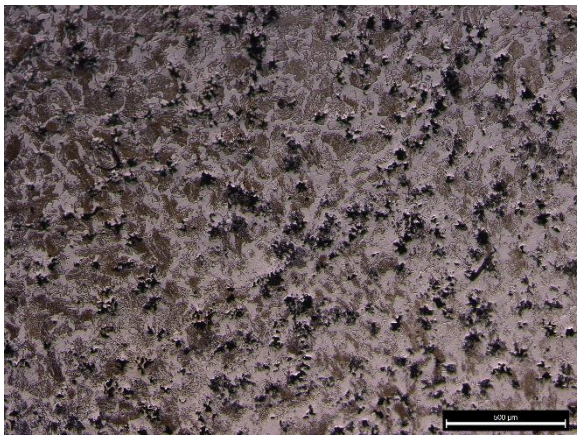

NJG-24, iron bar, malleable cast iron

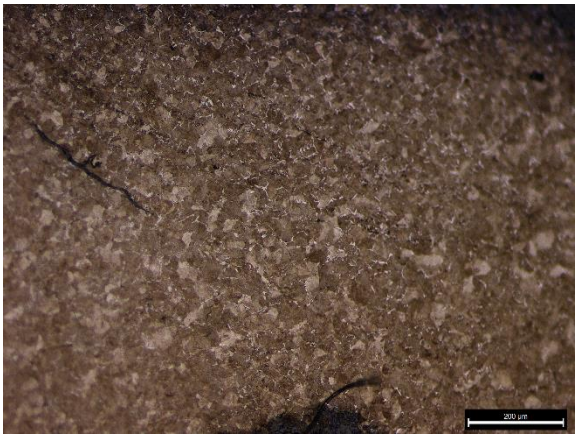

NJG-31, fragment, ferrite and pearlite

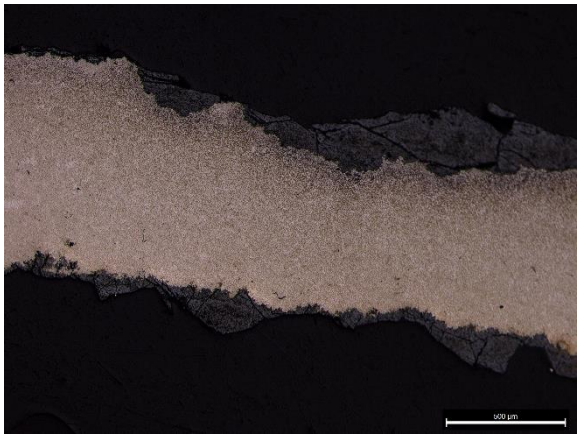

NJG-32, fragment, ferrite and pearlite

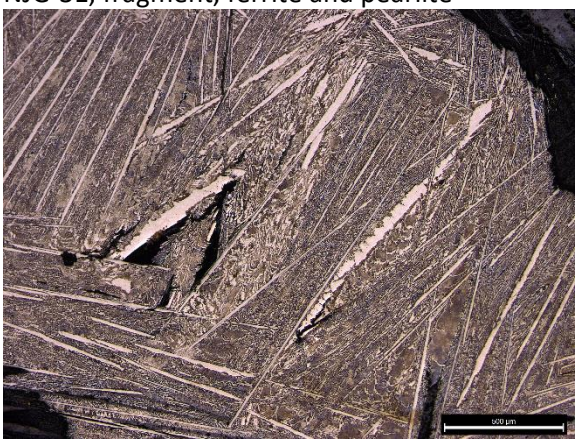

NJG-33, fragment, primary cementite and ledeburite

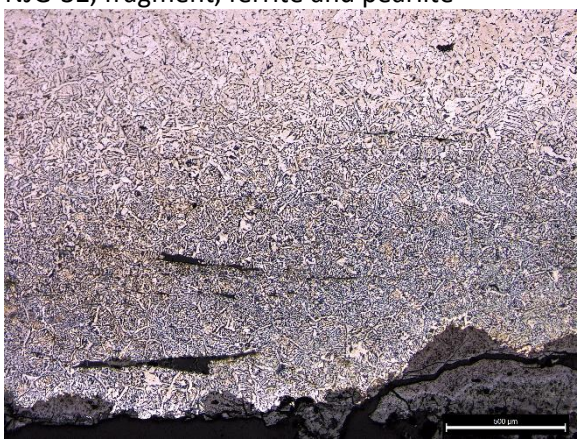

NJG-34, fragment, Widmannstatten microstructure

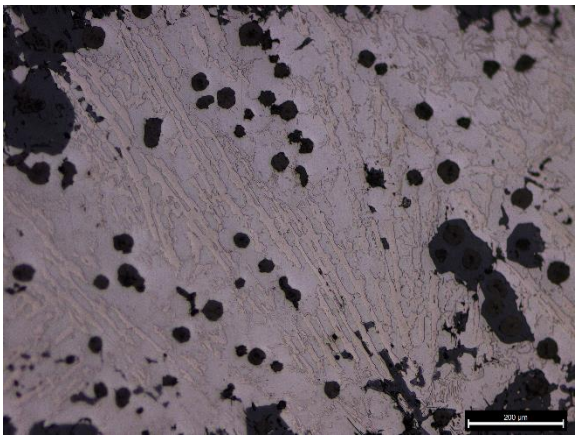

NJG-35, fragment, nodular graphite and ferrite

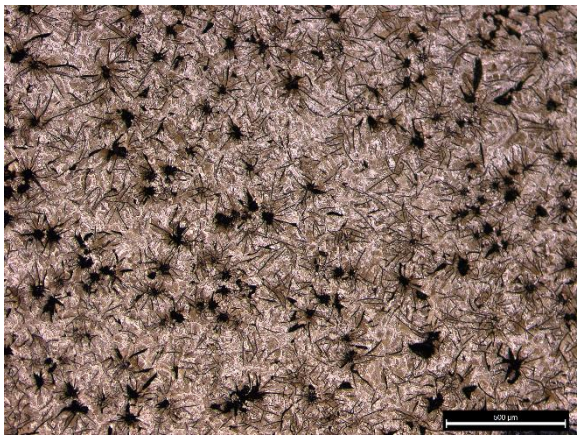

NJG-36, fragment, flake graphite on pearlite matrix

Yancun

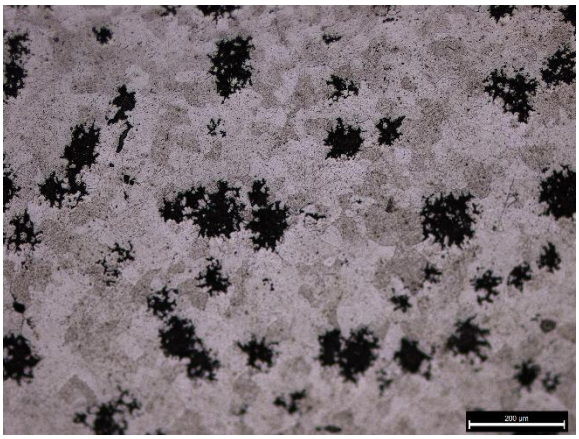

YC-1, Spade (*Cha*), flocculant graphite on ferrite matrix

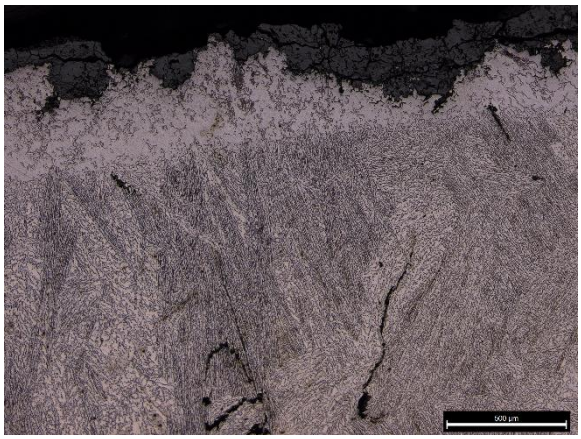

YC-2, Spade (*Cha*), ledeburite microstructure in center, with a layer of ferrite on the surface

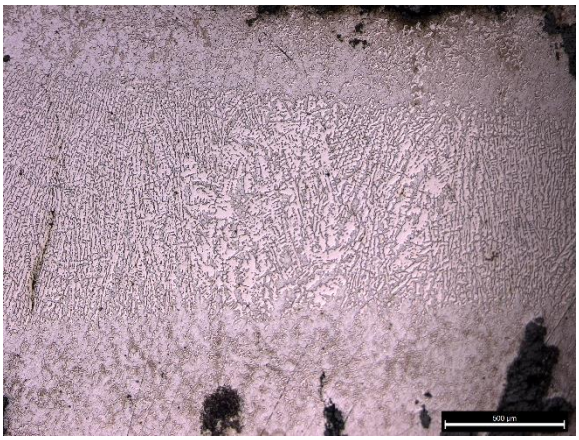

YC-3, Spade (*Cha*), ghost microstructure of ledeburite in the center with layer of ferrite and pearlite on the surfac

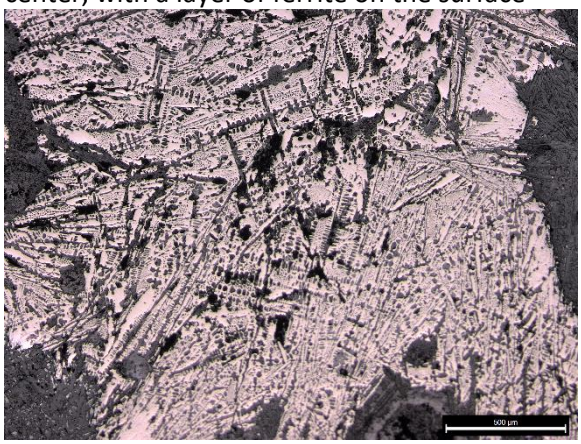

YC-4, belt-hook, pearlite and ledeburite

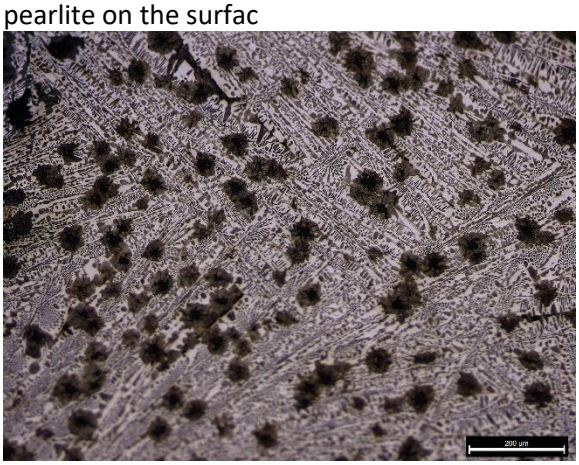

YC-5, belt-hook, flake graphite on ledeburite matrix

Changxingcun

CXC-1, sickle, ferrite grains in the center and pearlite & ferrite on both surface

Xianyang Airport

JC-1, arrowhead, ferrite grains

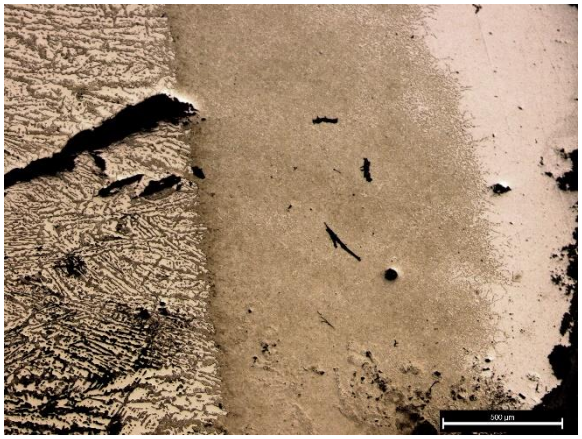

JC-2, arrowhead, from center toward surface, ledeburite, pearlite and ferrite

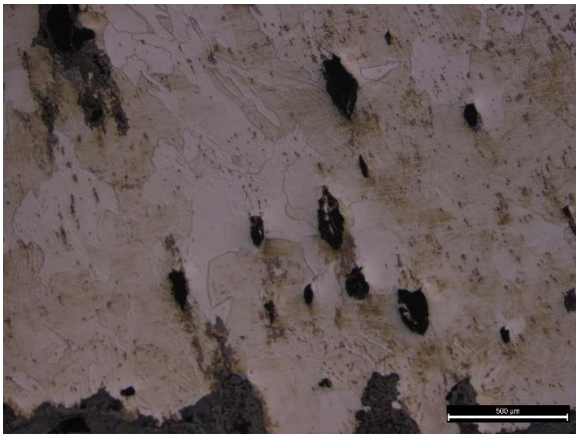

JC-3, arrowhead, ferrite

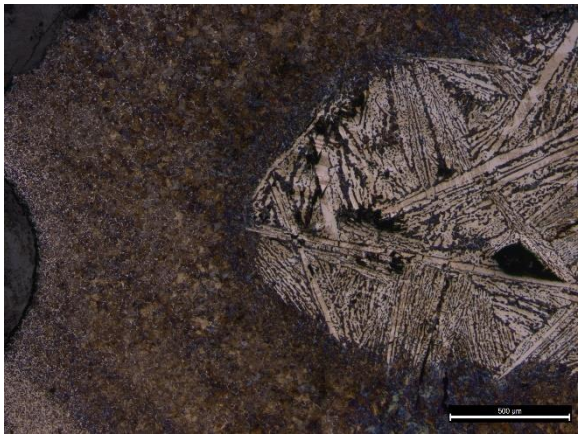

JC-4, arrowhead, primary cementite and ledeburite in the center, pearlite on the surface

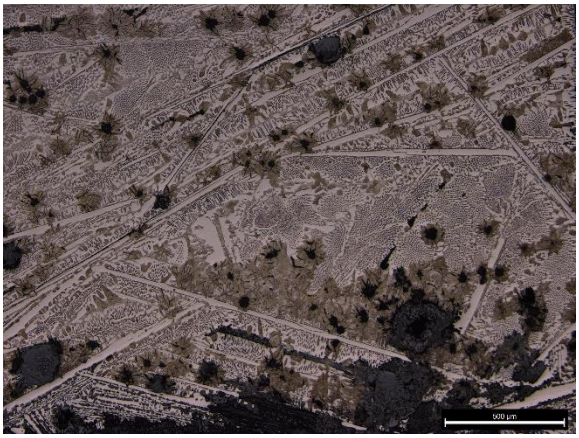

JC-5, vessel fragment, flake graphite on ledeburite matrix

Lüdi

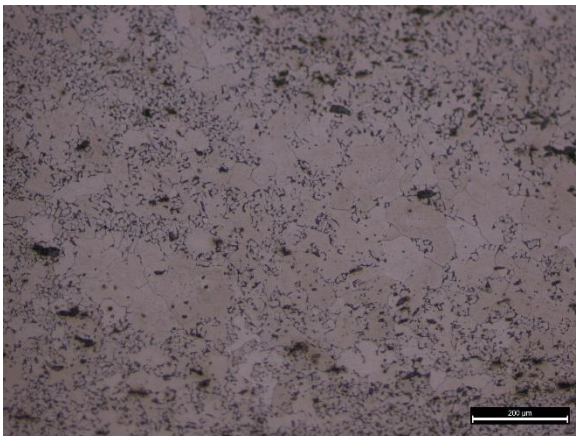

LD-1, arrowhead, mixture of ferrite and ferrite & pearlite

LD-2, arrowhead, mixture of ferrite and ferrite & pearlite

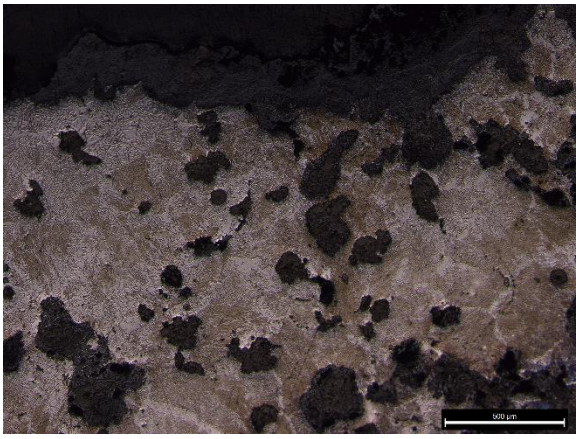

LD-3, Spade (*Cha*), nodular graphite on pearlite matrix

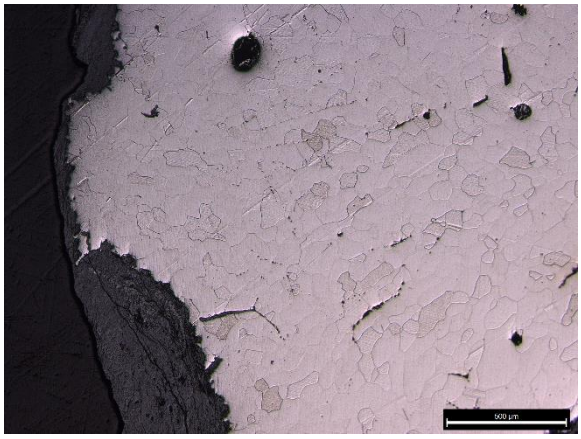

LD-4, Shovel (*Chan*), ferrite grain

Ningyuan

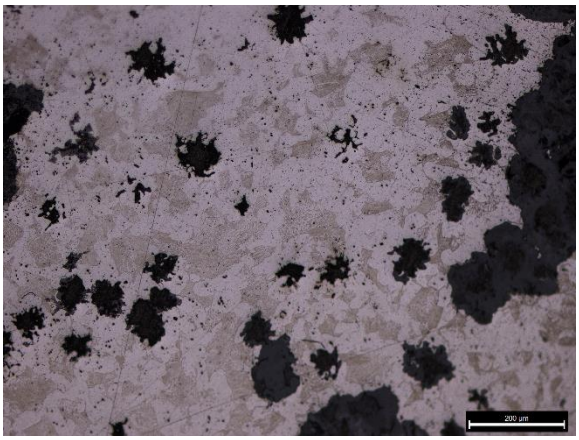

NY-1, Spade (*Cha*), flocculant graphite on pearlite and ferrite matrix

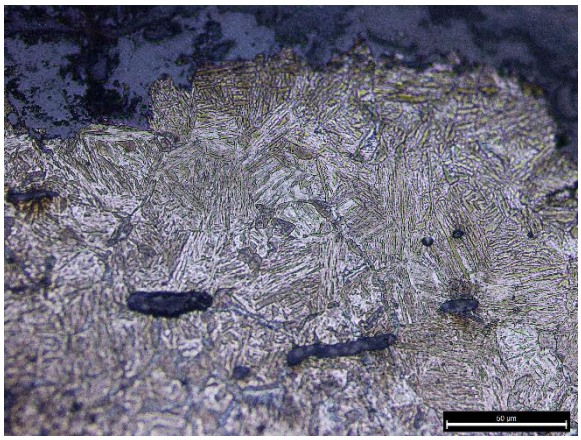

NY-2, Shovel (*Chan*), martensite

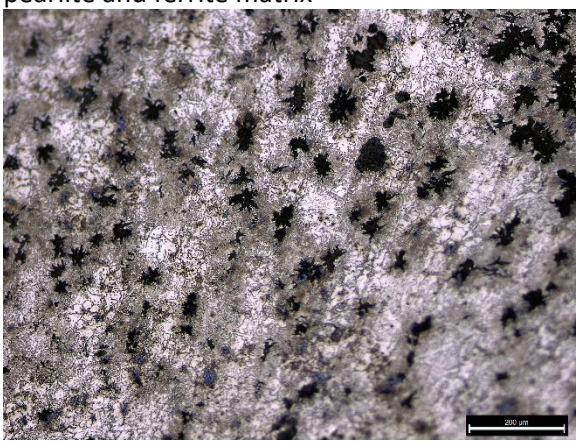

NY-3, Adze (*Ben*), flocculant graphite on pearlite and ferrite matrix

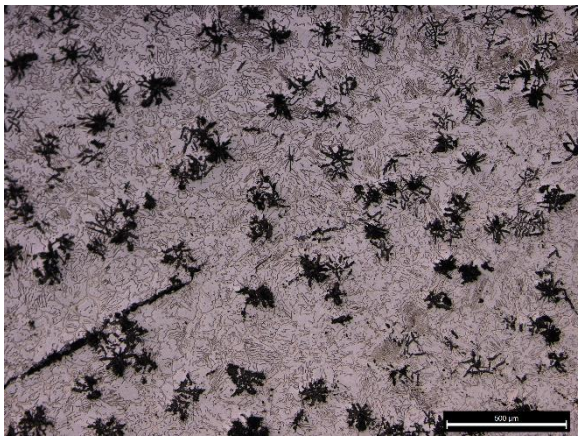

NY-4, belt-hook, flocculant graphite on pearlite matrix

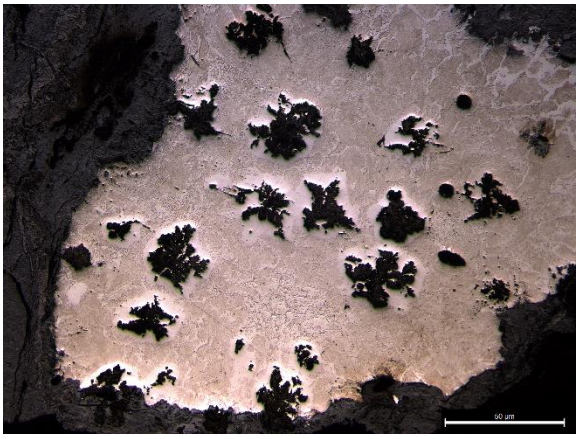

NY-6, knife, flocculant graphite on pearlite and ferrite matrix

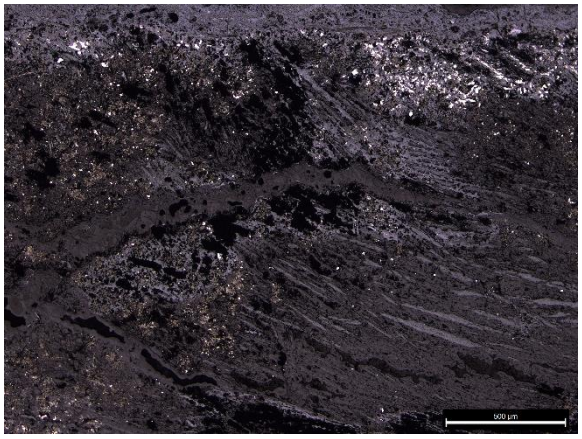

NY-8, fragment, ghost microstructure of ledeburite and flake graphite

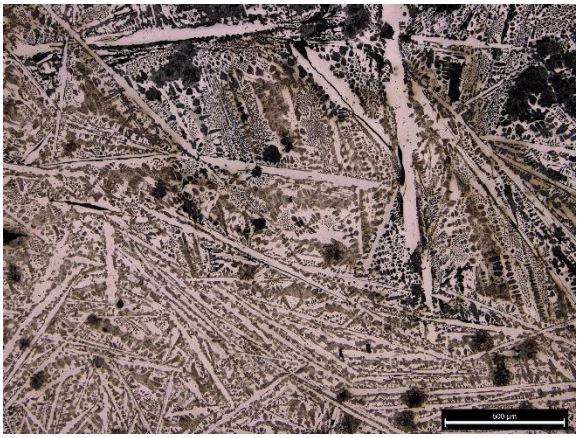

NY-9, pot, primary cementite and ledeburite. Small amount of flake graphite precipitated

Hejia

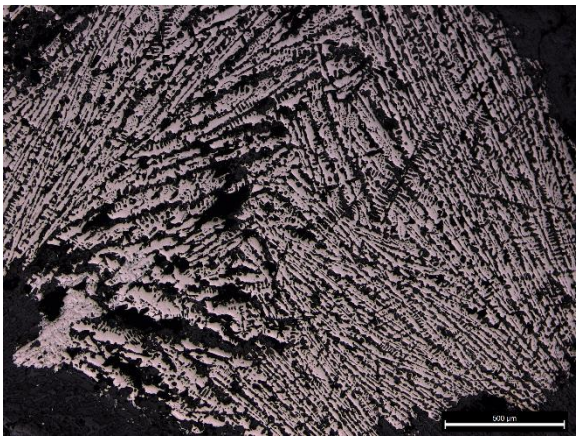

HJ-1, belt-hook, ledeburite

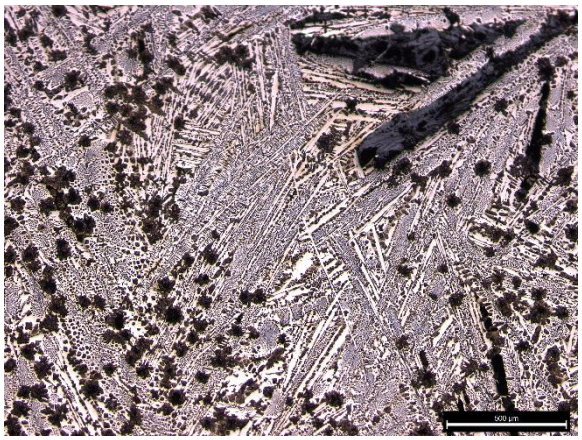

HJ-2, belt-hook, flake graphite on ledeburite matrix

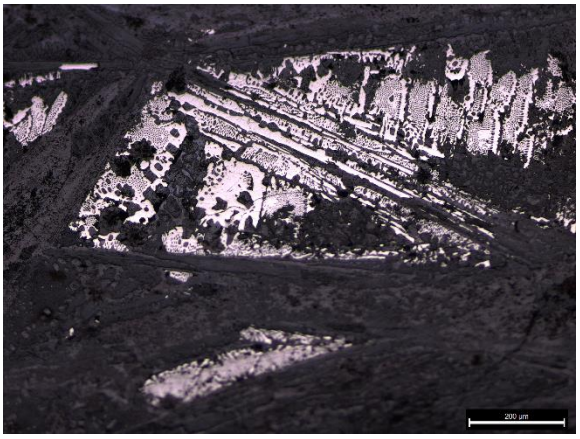

HJ-4, belt-hook, flake graphite on ledeburite matrix

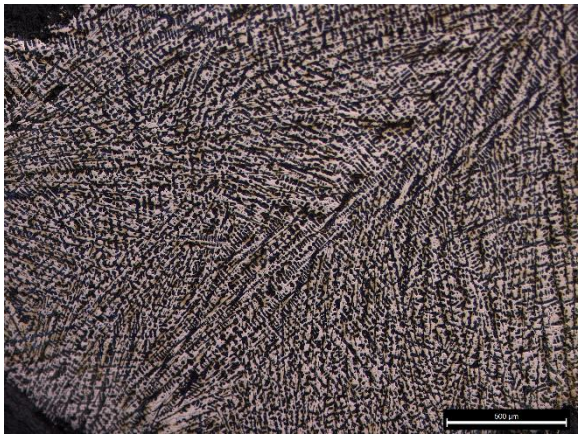

HJ-5, belt-hook, ledeburite

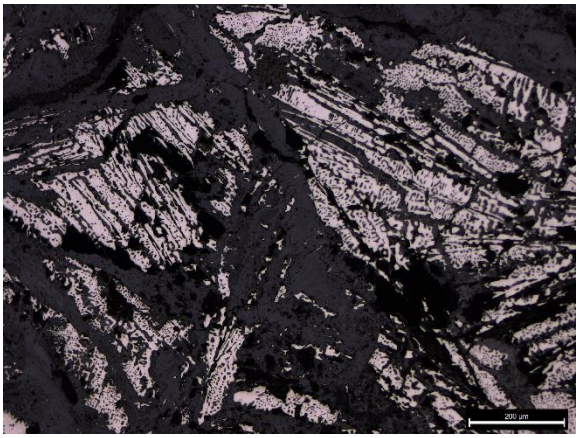

HJ-6, belt-hook, ledeburite

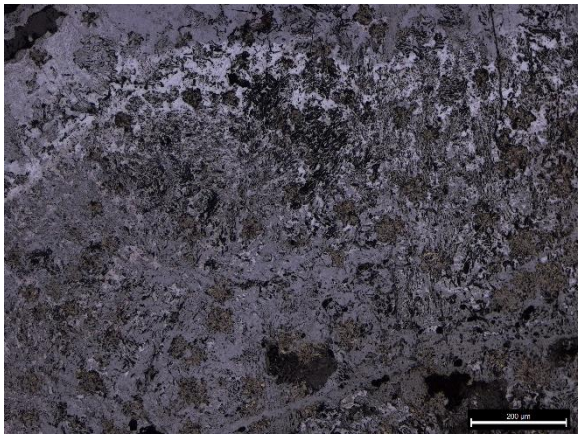

HJ-7, belt-hook, ghost structure of flocculant graphite on pearlite matrix

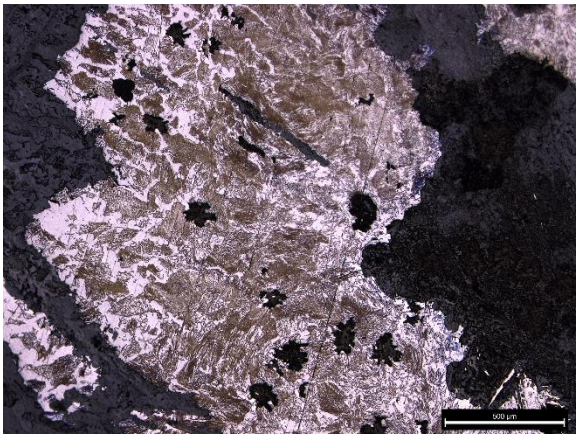

HJ-8, belt-hook, flocculant

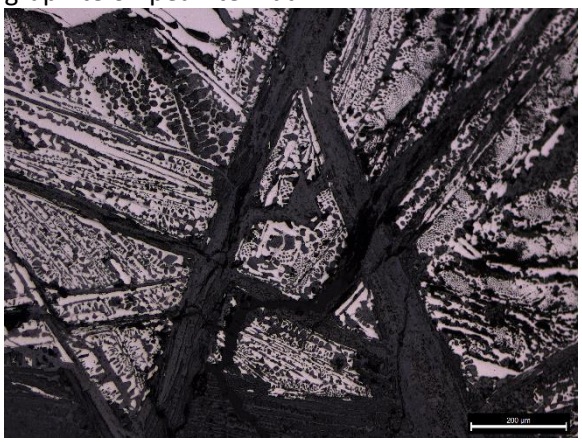

HJ-9, belt-hook, ledeburite

Gaoxin primary school

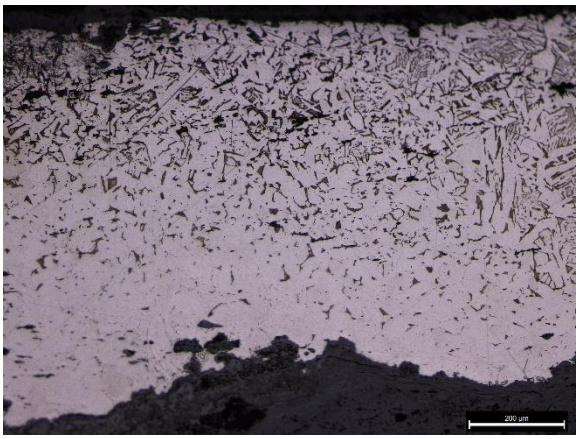

GX-2, knife, ferrite and pearlite

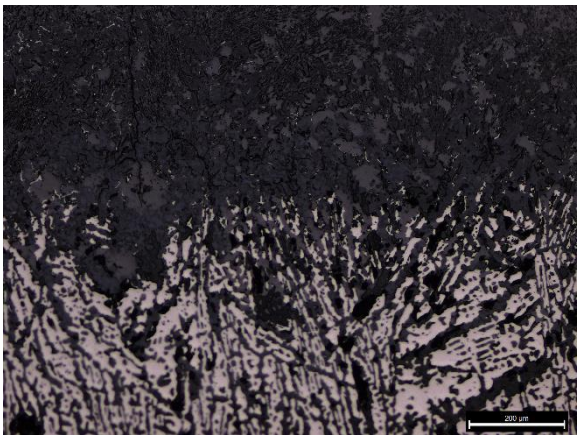

GX-3, Spade (*Cha*), ledeburite in the center, with ghost structure of pearlite on the surface

Appendix-4 SEM-EDS analysis of CRMs

BHVO-2 Basalt, Hawaiian Volcanic Observatory

		Na_2O	MgO	Al_2O_3	SiO_2	P_2O_5	K_2O	CaO	TiO_2	MnO	FeO
Philips	*Measurement-1*	2.1	7.1	13.4	50.1	n.d.	0.5	12.1	2.9	0.2	11.5
	Measurement-2	2.1	7.1	13.4	50.0	n.d.	0.6	12.3	3.0	0.3	11.3
	Measurement-3	2.1	7.1	13.5	50.1	n.d.	0.5	11.9	3.0	n.d.	11.6
	Measurement-4	2.1	7.0	13.5	50.4	n.d.	0.6	12.0	3.0	n.d.	11.4
	Measurement-5	2.3	7.0	13.4	49.9	n.d.	0.5	12.2	2.9	0.2	11.6
	Average	2.1	7.1	13.4	50.1	n.d.	0.6	12.1	3.0	0.3	11.5
	Given value	2.2	7.3	13.6	50.4	0.3	0.5	11.5	2.8	0.2	11.2
	Std.	0.07	0.04	0.07	0.16		0.03	0.12	0.04	0.04	0.13
	CV%	3.31	0.57	0.51	0.31		5.85	0.98	1.17	16.95	1.10
	Absolute error	-0.1	-0.2	-0.2	-0.3		0.0	0.6	0.2	0.1	0.3
	Relative error	-5.0	-3.0	-1.5	-0.6		5.3	5.1	8.2	50.3	2.4
Oxford	*Measurement-1*	2.1	7.2	13.6	50.3	0.3	0.5	11.7	2.9	0.2	11.2
	Measurement-2	2.2	7.2	13.7	50.4	n.d.	0.5	11.6	3.0	n.d.	11.3
	Measurement-3	2.2	7.3	13.2	50.4	n.d.	0.5	11.8	2.9	0.2	11.5
	Measurement-4	2.1	7.4	13.6	50.5	n.d.	0.5	11.6	2.8	0.2	11.2
	Average	2.2	7.3	13.5	50.4	0.3	0.5	11.7	2.9	0.2	11.3
	Given value	2.2	7.3	13.6	50.4	0.3	0.5	11.5	2.8	0.2	11.2
	Std.	0.03	0.06	0.19	0.06	0.00	0.01	0.08	0.06	0.01	0.12
	CV%	1.24	0.79	1.41	0.13	0.00	1.16	0.71	2.07	7.94	1.09
	Absolute error	-0.1	0.0	-0.1	0.0	0.0	0.0	0.2	0.1	0.0	0.1
	Relative error	-3.2	-0.3	-0.9	0.0	-0.1	1.8	1.6	5.0	-3.4	1.0

United States Geological Survey (USGS), 1998. Certificate of Analysis: Basalt, Hawaiian Volcanic Observatory, BHVO-2.

http://crustal.usgs.gov/geochemical_reference_standards/basaltbhvo2.html#bibliography

BCR-2

		Na_2O	MgO	Al_2O_3	SiO_2	P_2O_5	K_2O	CaO	TiO_2	FeO
Philips	*Measurement-1*	3.0	3.5	13.3	54.8	0.5	1.9	7.6	2.6	12.8
	Measurement-2	2.9	3.5	13.3	54.8	0.5	1.9	7.7	2.6	12.8
	Measurement-3	3.2	3.5	13.4	54.6	0.5	1.9	7.6	2.5	12.9
	Measurement-4	3.0	3.5	13.3	54.9	0.3	2.0	7.5	2.4	13.0
	Measurement-5	2.9	3.5	13.5	55.0	n.d.	1.9	7.6	2.4	13.2
	Average	3.0	3.5	13.4	54.8	0.5	1.9	7.6	2.5	12.9
	Given value	3.2	3.6	13.7	55.0	0.4	1.8	7.2	2.3	12.6
	Std.	0.12	0.03	0.08	0.13	0.07	0.05	0.06	0.05	0.14
	CV%	3.85	0.88	0.58	0.24	15.78	2.43	0.84	2.20	1.09
	Absolute arror	-0.2	-0.1	-0.4	-0.2	0.1	0.1	0.3	0.2	0.3
	Relative error	-6.6	-4.1	-2.7	-0.4	27.6	5.3	4.8	8.6	2.4
Oxford	*Measurement-1*	3.1	3.6	13.6	54.9	0.3	1.9	7.3	2.5	12.8
	Measurement-2	3.1	3.6	13.7	55.3	n.d.	1.9	7.3	2.5	12.5
	Measurement-3	3.2	3.6	12.7	55.8	n.d.	1.9	7.5	2.5	12.9
	Measurement-4	3.2	3.6	13.8	54.9	n.d.	1.9	7.3	2.5	12.9
	Average	3.1	3.6	13.5	55.2	0.3	1.9	7.4	2.5	12.8
	Given value	3.2	3.6	13.7	55.0	0.4	1.8	7.2	2.3	12.6
	Std.	0.04	0.02	0.45	0.35	0.00	0.02	0.08	0.01	0.14
	CV%	1.29	0.63	3.32	0.64	0.00	0.88	1.14	0.50	1.07
	Absolute arror	-0.1	-0.1	-0.3	0.2	0.0	0.1	0.1	0.2	0.1
	Relative error	-3.0	-1.9	-2.1	0.4	-8.4	3.3	1.5	7.8	1.1

United States Geological Survey (USGS), 1998. Certificate of Analysis: Basalt, Columbia River, BCR-2.

http://crustal.usgs.gov/geochemical_reference_standards/pdfs/basaltbcr2.pdf

Appendix-5 Raw compositional data of slag inclusions

Sample XF-25

Na_2O	MgO	Al_2O_3	SiO_2	P_2O_5	SO_3	K_2O	CaO	TiO_2	MnO	FeO
0.7	1.7	12.1	41.9	2.4	0.2	2.2	14.8	0.6	1.0	22.6
0.6	1.7	13.7	46.1	1.6	0.3	2.6	13.9	0.6	1.0	18.0
0.6	1.8	12.5	44.1	2.7	0.4	2.4	15.3	0.6	1.0	18.8
0.6	1.7	13.0	44.6	1.7	0.3	2.5	13.8	0.6	1.0	20.1
0.7	1.7	13.6	47.4	1.7	0.2	2.6	14.9	0.6	1.0	15.6
0.6	1.8	13.5	46.5	1.8	0.3	2.5	15.4	0.6	1.1	15.9
0.7	1.6	12.6	42.5	1.3	0.4	2.3	12.9	0.5	0.9	24.4
0.7	1.7	13.3	46.5	1.9	0.2	2.4	14.2	0.6	1.1	17.4
0.7	1.6	13.4	46.7	1.3	0.3	2.7	14.9	0.6	1.1	16.8
0.7	1.6	13.1	45.5	1.4	0.4	2.5	14.1	0.6	1.0	19.1

Sample XF-27

Na_2O	MgO	Al_2O_3	SiO_2	P_2O_5	SO_3	K_2O	CaO	TiO_2	V_2O_5	MnO	FeO
n.d.	0.7	4.6	27.9	8.0	0.8	1.5	29.4	0.3	n.d.	0.3	26.6
0.8	0.9	2.4	14.2	23.0	0.5	1.1	27.2	n.d.	n.d.	0.2	29.7
0.6	0.6	4.8	27.9	9.1	0.8	1.6	28.7	0.3	n.d.	0.3	25.4
1.3	3.0	8.1	43.8	2.2	n.d.	2.7	13.9	0.6	2.0	1.0	21.4
1.4	2.4	8.4	42.5	2.5	0.1	3.1	12.8	0.5	1.4	0.9	24.0
1.2	2.7	8.2	41.9	2.5	n.d.	2.5	13.8	0.5	1.7	0.9	24.1
1.2	2.4	8.4	44.0	2.9	n.d.	2.6	13.9	0.5	1.4	1.0	21.7
n.d.	3.0	6.7	29.8	1.4	0.3	n.d.	11.1	0.5	1.5	0.4	45.3
1.1	1.9	9.0	44.2	3.1	0.2	2.6	14.0	0.6	1.1	1.1	21.1
1.2	2.4	8.6	43.2	3.0	0.2	2.9	13.7	0.5	1.0	0.7	22.9
0.5	1.5	7.1	42.6	2.3	0.4	1.5	37.9	0.5	0.2	0.6	4.9
7.1	0.5	2.8	38.6	1.6	0.8	2.2	40.0	0.4	n.d.	0.3	5.8
0.4	1.4	5.2	44.2	2.1	0.6	1.1	39.3	0.4	n.d.	0.6	4.6
0.7	1.4	6.6	39.9	4.1	0.3	2.3	31.9	0.5	0.2	0.9	11.4
0.4	0.9	4.4	45.4	2.2	0.3	1.1	40.7	n.d.	n.d.	0.5	4.1
0.7	1.7	7.3	39.7	2.7	0.4	2.0	32.9	0.5	0.2	0.8	11.2
0.6	1.6	7.1	39.2	3.4	0.4	1.9	34.5	0.6	0.2	1.1	9.4
0.6	1.5	5.9	38.7	4.3	0.4	1.6	34.8	0.5	0.4	0.9	10.5

0.6	1.3	5.5	37.4	6.0	0.4	1.9	34.4	0.4	0.3	0.9	11.0
0.6	1.7	6.9	39.6	4.7	0.3	1.8	32.7	0.5	0.3	1.0	10.0
n.d.	0.4	1.6	47.0	2.0	0.2	n.d.	45.3	n.d.	0.2	0.3	3.1
0.6	1.5	6.8	37.6	7.9	0.2	2.0	34.4	0.5	0.3	0.9	7.5
0.6	1.7	5.5	31.4	7.2	0.3	1.4	28.2	0.4	0.3	1.1	21.9
1.0	1.3	3.1	45.0	3.7	0.3	6.3	25.1	1.6	3.3	2.3	7.0
1.2	1.1	2.5	46.1	3.8	0.2	8.3	21.1	2.0	3.9	2.9	6.9
1.2	1.1	2.3	44.5	4.0	n.d.	8.1	20.4	1.9	2.9	2.8	10.9
0.4	3.9	2.6	17.5	18.2	n.d.	1.5	34.7	n.d.	0.7	n.d.	20.6
0.3	2.1	1.8	15.0	24.9	n.d.	1.2	48.0	n.d.	0.2	n.d.	6.5
0.3	1.3	0.4	11.2	29.6	n.d.	0.7	52.0	n.d.	0.3	n.d.	4.3
0.3	0.7	0.4	12.1	28.0	n.d.	0.4	51.0	n.d.	n.d.	0.1	7.1
0.3	1.9	3.9	22.5	14.5	n.d.	1.4	41.4	n.d.	n.d.	n.d.	14.2
0.5	2.2	1.0	12.2	26.2	n.d.	1.2	45.8	n.d.	0.2	n.d.	10.7
0.5	0.8	n.d.	n.d.	44.3	n.d.	0.6	46.1	n.d.	n.d.	n.d.	7.7
0.3	1.0	0.7	3.6	41.3	n.d.	0.8	44.3	n.d.	n.d.	n.d.	7.9
0.6	1.0	n.d.	1.8	42.0	n.d.	1.4	46.0	n.d.	n.d.	n.d.	7.2
n.d.	n.d.	3.3	33.1	2.0	n.d.	1.9	1.0	0.1	n.d.	n.d.	58.7
n.d.	n.d.	3.0	34.7	1.8	n.d.	2.2	0.9	0.2	n.d.	n.d.	57.4
n.d.	n.d.	3.1	30.2	1.8	n.d.	1.6	0.9	n.d.	n.d.	n.d.	62.5
n.d.	n.d.	3.3	35.3	1.9	n.d.	2.4	1.0	0.1	n.d.	n.d.	56.0
n.d.	n.d.	2.3	26.9	1.8	0.2	1.3	1.0	n.d.	n.d.	n.d.	66.6
n.d.	n.d.	3.4	35.1	2.0	n.d.	2.2	1.1	0.1	n.d.	n.d.	56.1
n.d.	n.d.	3.4	34.6	2.0	n.d.	2.2	0.9	n.d.	n.d.	n.d.	57.1
n.d.	n.d.	3.3	35.9	1.5	n.d.	2.4	0.8	n.d.	n.d.	n.d.	56.2
n.d.	n.d.	3.3	34.6	1.7	n.d.	2.1	0.7	0.1	n.d.	n.d.	57.6
n.d.	n.d.	3.3	35.3	1.4	n.d.	2.4	0.7	n.d.	n.d.	n.d.	57.0
n.d.	n.d.	3.6	35.7	1.7	n.d.	2.4	0.9	n.d.	n.d.	n.d.	55.7
n.d.	n.d.	2.9	30.0	1.6	n.d.	1.6	1.0	n.d.	n.d.	n.d.	63.0

Sample XF-28

Na_2O	MgO	Al_2O_3	SiO_2	P_2O_5	SO_3	K_2O	CaO	TiO_2	V_2O_5	MnO	FeO
1.2	2.4	12.1	56.6	n.d.	n.d.	2.0	13.2	0.7	n.d.	0.3	11.4
0.9	2.1	9.9	46.0	1.2	n.d.	2.0	18.8	0.4	n.d.	n.d.	18.7
1.1	2.1	9.2	45.2	1.5	n.d.	2.0	19.2	0.4	n.d.	n.d.	19.3
1.2	1.8	9.8	46.4	2.3	0.2	2.8	15.7	0.5	n.d.	n.d.	19.5

1.2	1.8	9.5	45.9	2.3	n.d.	2.4	16.7	0.5	n.d.	0.1	19.6
1.1	2.1	10.6	51.7	0.4	n.d.	1.9	10.9	0.6	n.d.	0.3	20.4
1.0	2.2	10.5	50.8	0.6	0.1	1.8	11.5	0.6	n.d.	0.3	20.6
1.0	2.2	10.1	48.4	0.7	n.d.	1.7	10.9	0.6	n.d.	0.3	24.3
1.2	2.5	10.0	46.5	0.7	n.d.	1.6	11.5	0.6	n.d.	0.3	25.1
1.3	2.0	9.2	43.0	2.4	0.2	1.8	12.6	0.5	n.d.	0.2	26.9
1.0	1.6	8.7	42.5	2.6	0.2	2.3	13.7	0.4	n.d.	n.d.	27.0
1.1	1.8	8.1	42.1	2.5	n.d.	2.1	14.4	0.4	n.d.	0.1	27.5
1.3	2.0	9.2	42.0	2.2	0.3	1.8	12.5	0.4	n.d.	0.2	28.2
0.9	2.0	9.1	43.6	1.7	0.1	1.5	10.3	0.5	n.d.	0.3	30.0
n.d.	8.9	4.0	22.9	14.1	n.d.	1.4	15.3	0.4	n.d.	1.6	31.5
n.d.	6.9	5.5	22.3	13.3	n.d.	1.3	16.4	0.5	0.4	1.7	31.8
1.1	1.6	8.3	39.6	2.1	0.2	2.2	12.3	0.3	n.d.	0.1	32.3
n.d.	6.3	4.2	21.5	14.5	0.2	1.2	16.2	0.4	n.d.	1.5	34.1
n.d.	n.d.	2.8	21.2	18.6	0.2	1.3	19.9	n.d.	n.d.	n.d.	36.0
n.d.	n.d.	6.6	32.8	5.1	0.2	1.2	14.8	0.2	n.d.	n.d.	39.3
n.d.	0.9	4.3	24.8	8.1	n.d.	1.7	20.8	n.d.	n.d.	0.2	39.3
n.d.	n.d.	2.6	22.8	15.7	0.2	1.3	17.6	n.d.	n.d.	n.d.	39.7
n.d.	n.d.	5.5	32.1	4.9	0.2	1.1	13.3	0.2	n.d.	n.d.	42.8
n.d.	0.9	3.9	21.6	7.8	0.2	1.3	18.3	0.2	n.d.	0.2	45.7
n.d.	2.0	2.3	12.1	19.4	0.3	0.6	9.8	n.d.	n.d.	0.5	53.1
n.d.	0.9	4.7	22.7	5.6	n.d.	1.3	10.2	0.2	n.d.	0.2	54.2
n.d.	1.6	3.5	10.0	18.0	0.1	0.4	6.1	0.3	0.5	0.4	59.2
n.d.	0.9	3.7	18.9	5.1	n.d.	1.0	8.9	0.2	n.d.	n.d.	61.2
n.d.	n.d.	1.2	17.9	7.5	0.3	0.5	3.3	0.3	0.9	1.5	66.8
n.d.	n.d.	0.6	3.8	24.9	0.3	0.1	2.8	n.d.	n.d.	0.2	67.3
n.d.	n.d.	n.d.	19.8	6.9	0.7	n.d.	0.2	0.5	0.3	2.1	69.4
n.d.	n.d.	3.1	15.5	3.7	n.d.	0.8	6.7	0.2	n.d.	n.d.	70.0
n.d.	n.d.	1.2	12.5	9.6	0.3	0.2	2.3	n.d.	n.d.	1.3	72.6
n.d.	0.9	2.4	10.6	3.9	n.d.	0.7	5.5	0.2	n.d.	n.d.	75.9
n.d.	1.4	1.5	5.2	7.3	n.d.	0.3	3.3	0.2	0.5	0.3	80.0

Sample XF-37

Al_2O_3	SiO_2	P_2O_5	SO_3	K_2O	CaO	TiO_2	V_2O_5	MnO	FeO
1.3	9.7	26.7	1.1	0.7	4.1	n.d.	0.3	0.9	55.4
1.8	8.7	22.7	0.7	0.3	2.8	0.3	4.0	0.8	58.0

2.0	9.9	24.0	0.3	0.7	4.4	n.d.	n.d.	0.3	58.5
1.7	13.7	14.7	n.d.	1.1	5.0	n.d.	n.d.	0.3	63.6
1.9	11.6	12.7	0.4	1.2	4.7	n.d.	n.d.	n.d.	67.6
2.0	14.4	19.9	1.3	0.8	4.0	0.4	1.4	0.8	55.1
2.6	19.1	17.0	1.4	0.9	4.6	0.3	1.7	1.0	51.3
2.1	16.5	19.9	1.7	0.8	4.3	0.1	0.3	1.1	53.3
1.7	17.1	17.4	1.0	0.8	3.6	n.d.	0.2	0.9	57.4
1.9	13.4	19.8	1.5	0.7	4.7	0.1	0.2	0.6	57.1
1.6	11.8	21.9	1.4	0.8	5.3	n.d.	n.d.	0.7	56.6
1.4	10.8	14.9	1.1	0.4	3.1	0.2	0.5	0.5	67.1
1.3	14.2	16.1	0.8	0.4	2.9	0.1	0.2	0.6	63.4
0.9	10.4	11.5	0.6	0.3	2.4	0.1	0.5	0.5	72.9
1.5	11.1	14.2	1.2	0.4	3.1	0.2	0.5	0.5	67.3
1.3	13.4	10.4	1.3	0.4	2.7	n.d.	0.2	0.7	69.8
n.d.	16.2	16.7	0.8	0.3	1.6	n.d.	n.d.	0.9	63.6

Sample XF-F17

Na_2O	MgO	Al_2O_3	SiO_2	P_2O_5	SO_3	K_2O	CaO	TiO_2	V_2O_5	MnO	FeO
n.d.	0.9	1.2	4.8	1.7	n.d.	0.5	3.3	n.d.	0.5	n.d.	87.2
n.d.	0.4	1.4	7.0	4.8	n.d.	0.3	3.6	n.d.	0.3	n.d.	82.1
n.d.	0.7	1.6	8.4	11.1	n.d.	0.9	8.2	n.d.	n.d.	n.d.	69.1
n.d.	0.6	1.6	9.3	9.5	n.d.	0.5	5.9	n.d.	n.d.	n.d.	72.6
0.4	0.6	1.4	9.5	16.5	n.d.	0.9	7.4	n.d.	n.d.	n.d.	63.4
n.d.	0.7	1.5	9.6	18.1	n.d.	0.5	6.2	n.d.	0.4	0.3	62.8
0.4	0.6	1.9	10.2	14.1	n.d.	0.9	7.9	n.d.	n.d.	n.d.	64.1
0.4	0.4	1.9	10.2	9.1	n.d.	0.7	5.8	n.d.	0.3	n.d.	71.0
0.4	0.6	1.8	10.6	14.0	n.d.	1.0	8.7	n.d.	0.3	n.d.	62.6
n.d.	0.7	1.7	10.6	14.2	n.d.	1.2	8.6	n.d.	0.3	n.d.	62.7
0.3	0.5	1.9	10.9	12.1	n.d.	0.2	9.1	n.d.	n.d.	n.d.	64.9
0.3	0.7	2.4	11.0	17.1	n.d.	0.5	6.3	n.d.	n.d.	n.d.	61.6
n.d.	0.4	2.0	11.2	12.0	n.d.	1.0	7.3	n.d.	n.d.	n.d.	66.1
n.d.	0.6	2.3	11.9	19.5	0.6	1.0	7.8	n.d.	n.d.	0.3	56.0
0.5	0.6	2.1	12.0	11.4	n.d.	1.1	8.6	n.d.	n.d.	n.d.	63.8
0.4	0.7	2.2	12.1	10.3	n.d.	0.8	6.8	n.d.	0.3	n.d.	66.4
0.3	0.7	2.1	12.9	16.1	n.d.	1.2	11.2	n.d.	n.d.	n.d.	55.4
n.d.	0.9	2.3	13.1	14.1	0.6	0.8	7.7	n.d.	n.d.	n.d.	60.5

n.d.	0.7	2.2	13.8	16.4	n.d.	1.2	10.9	n.d.	n.d.	n.d.	53.5
0.4	0.7	2.0	14.2	15.2	n.d.	1.3	11.1	n.d.	n.d.	n.d.	55.2
0.4	1.1	3.2	15.2	17.5	n.d.	1.0	10.9	n.d.	n.d.	0.3	50.5
0.5	0.7	2.5	15.4	16.0	n.d.	1.2	11.5	n.d.	n.d.	0.3	52.0
0.4	0.9	2.4	15.5	15.7	n.d.	1.2	11.3	n.d.	n.d.	n.d.	52.7
0.4	0.7	2.5	15.5	16.0	n.d.	1.1	12.4	n.d.	n.d.	n.d.	51.4
0.4	0.7	2.6	15.8	12.5	n.d.	1.4	9.7	n.d.	n.d.	n.d.	56.9
0.3	0.6	2.6	16.1	13.8	n.d.	1.1	9.8	n.d.	n.d.	n.d.	55.6
n.d.	1.2	3.5	16.2	14.3	n.d.	0.7	10.5	0.3	n.d.	n.d.	53.2
0.5	0.7	2.6	16.5	12.9	n.d.	1.2	10.1	n.d.	n.d.	n.d.	55.6
0.3	0.7	3.1	17.2	14.1	n.d.	1.4	10.1	n.d.	n.d.	n.d.	53.1
0.4	0.7	3.3	18.0	10.3	n.d.	1.3	10.3	n.d.	n.d.	n.d.	55.6
0.4	0.7	3.4	18.6	11.7	n.d.	1.3	11.6	n.d.	n.d.	n.d.	52.5
0.5	1.5	4.4	19.5	6.2	n.d.	1.7	11.9	0.3	0.4	0.3	53.2
0.6	1.5	4.1	19.6	8.5	n.d.	1.9	12.5	n.d.	0.6	0.3	50.4
0.5	0.7	3.5	20.3	10.3	n.d.	1.3	11.0	n.d.	n.d.	0.3	52.0
0.4	0.9	3.0	21.1	15.0	n.d.	1.1	12.0	n.d.	n.d.	0.3	46.2
0.7	1.8	5.8	23.5	1.6	n.d.	1.8	15.3	0.3	n.d.	n.d.	48.5
0.6	1.8	6.2	23.6	2.3	0.7	1.6	12.9	0.3	n.d.	n.d.	50.0
0.6	1.6	5.5	23.8	1.4	n.d.	2.6	14.9	0.4	n.d.	n.d.	49.2
0.7	2.1	5.6	25.1	4.4	n.d.	2.2	16.3	0.3	0.8	0.3	42.2
0.7	0.7	4.0	25.2	11.7	0.4	1.6	17.9	n.d.	n.d.	n.d.	37.8
0.5	2.1	6.0	25.6	1.5	n.d.	1.8	16.0	0.4	0.6	0.3	44.9
0.7	2.6	6.7	26.5	0.5	n.d.	1.9	16.7	0.4	n.d.	n.d.	44.0
0.5	2.0	5.4	26.7	0.8	n.d.	1.8	14.7	0.4	n.d.	0.4	47.4
0.6	1.7	5.6	27.3	3.6	n.d.	3.3	13.5	0.4	n.d.	n.d.	44.1
0.5	2.3	6.1	27.4	2.9	n.d.	2.0	18.5	0.4	0.6	0.2	39.2
n.d.	2.5	7.0	27.4	n.d.	n.d.	2.0	17.1	n.d.	n.d.	n.d.	43.9
0.7	1.8	6.3	29.0	1.9	n.d.	2.7	17.2	0.4	0.4	0.2	39.2
0.6	2.1	7.0	29.5	1.9	n.d.	2.3	15.7	0.3	0.3	n.d.	40.2
0.7	1.8	6.7	29.5	2.1	n.d.	2.9	18.0	0.3	0.3	n.d.	37.7
0.6	2.0	7.0	30.3	1.9	n.d.	2.6	16.6	0.4	0.3	n.d.	38.1
0.7	1.7	6.6	30.5	2.1	n.d.	3.0	18.2	0.6	0.4	0.3	36.0
0.8	2.1	6.2	30.8	0.7	n.d.	2.8	18.0	0.4	0.5	0.5	37.3
0.7	2.3	6.7	31.1	2.2	n.d.	2.7	19.3	0.4	0.5	0.3	33.9
0.7	2.3	7.9	32.8	1.0	n.d.	3.1	20.0	0.6	n.d.	n.d.	31.8
0.7	2.9	8.1	33.1	1.1	n.d.	2.5	21.2	0.5	n.d.	n.d.	29.9
0.7	2.6	7.5	34.2	3.6	n.d.	2.5	23.8	0.5	0.5	0.3	23.7
0.9	2.5	8.1	34.3	0.6	n.d.	2.9	21.9	0.6	n.d.	0.3	27.7

0.8	2.5	7.7	34.7	6.3	n.d.	3.2	23.7	0.5	1.2	0.4	19.1
0.9	2.5	6.9	34.8	0.7	n.d.	3.3	21.2	0.4	0.5	0.5	28.4
0.8	2.8	8.3	34.8	0.6	n.d.	2.8	22.5	0.5	n.d.	n.d.	26.9
0.7	3.1	8.3	35.2	0.6	n.d.	2.8	22.7	0.6	n.d.	0.3	25.9

Sample XF-F19

Na_2O	MgO	Al_2O_3	SiO_2	P_2O_5	K_2O	CaO	TiO_2	V_2O_5	MnO	FeO
n.d.	0.5	0.7	3.1	2.7	0.7	2.2	n.d.	n.d.	n.d.	90.1
0.8	0.6	0.9	3.6	16.5	1.0	14.3	n.d.	0.3	n.d.	62.0
n.d.	0.4	1.1	4.0	1.0	0.4	1.1	n.d.	0.4	n.d.	91.7
0.5	0.4	1.3	5.2	7.0	0.8	6.2	n.d.	0.5	n.d.	78.0
n.d.	0.5	0.9	5.8	0.6	0.3	2.5	n.d.	n.d.	n.d.	89.3
n.d.	0.6	1.4	5.9	2.0	0.7	2.1	n.d.	n.d.	n.d.	87.3
n.d.	1.1	1.5	6.8	5.8	0.6	8.6	n.d.	n.d.	n.d.	75.6
n.d.	0.4	1.4	6.9	1.2	0.4	3.3	n.d.	n.d.	n.d.	86.4
0.4	0.6	1.1	7.0	4.1	0.5	5.3	n.d.	n.d.	n.d.	81.1
n.d.	0.9	1.6	7.2	4.0	0.7	5.8	n.d.	n.d.	n.d.	79.8
0.6	0.7	1.6	7.4	22.4	1.8	22.0	n.d.	n.d.	n.d.	43.6
0.6	0.7	1.7	7.5	4.6	1.0	4.4	n.d.	0.3	n.d.	79.2
0.4	0.5	1.7	8.4	2.0	0.6	3.6	n.d.	n.d.	n.d.	82.8
0.4	1.3	1.5	8.7	19.3	1.0	21.7	n.d.	n.d.	n.d.	45.0
0.5	1.5	3.0	9.1	15.4	1.3	15.7	n.d.	n.d.	n.d.	53.7
n.d.	1.2	2.1	9.3	2.6	0.6	6.5	n.d.	0.3	n.d.	77.3
n.d.	1.0	2.0	9.9	6.5	0.8	9.3	n.d.	0.4	n.d.	70.1
n.d.	1.1	2.4	10.0	6.7	0.5	10.6	n.d.	0.2	n.d.	68.5
0.7	1.2	2.0	10.3	20.5	1.2	27.5	n.d.	n.d.	n.d.	35.3
0.5	1.2	1.9	10.6	11.9	1.1	15.2	n.d.	n.d.	n.d.	57.7
0.6	1.3	2.3	10.8	11.3	0.8	15.5	n.d.	0.3	n.d.	57.2
0.3	1.3	2.4	11.2	5.7	0.8	10.0	n.d.	0.3	n.d.	67.9
n.d.	0.8	2.3	12.1	8.7	1.0	5.7	n.d.	n.d.	n.d.	69.4
0.4	1.3	2.5	12.2	12.5	1.1	18.1	n.d.	n.d.	n.d.	52.1
0.5	1.1	2.5	12.3	11.4	1.0	13.6	n.d.	n.d.	n.d.	57.5
0.5	1.2	2.5	12.5	10.1	1.0	14.7	n.d.	n.d.	n.d.	57.5
n.d.	0.9	2.8	12.7	1.4	0.6	4.0	n.d.	n.d.	n.d.	77.6
n.d.	0.9	2.7	12.7	2.4	0.5	6.7	n.d.	n.d.	n.d.	74.0
0.6	0.6	2.5	12.9	7.5	1.6	6.5	n.d.	0.7	0.3	66.9

0.4	1.2	2.6	13.1	7.8	0.8	12.8	n.d.	n.d.	n.d.	61.2
0.3	1.2	2.7	13.6	11.3	0.8	14.9	n.d.	0.3	n.d.	54.8
n.d.	1.4	2.6	13.6	4.6	0.7	8.0	n.d.	n.d.	n.d.	69.1
0.4	1.0	2.7	13.8	7.4	1.0	11.1	n.d.	n.d.	n.d.	62.5
0.4	0.7	2.8	13.9	15.7	1.9	13.7	n.d.	0.8	0.3	49.7
0.6	1.1	3.0	14.2	5.1	1.1	10.4	n.d.	n.d.	n.d.	64.6
0.4	1.0	2.9	14.7	7.3	1.4	6.6	n.d.	0.3	n.d.	65.4
0.4	1.5	3.0	14.7	8.0	1.3	15.9	n.d.	n.d.	n.d.	55.1
0.4	1.1	2.8	14.7	3.8	1.1	11.9	n.d.	n.d.	n.d.	64.2
0.4	1.6	2.9	14.8	6.7	0.8	15.1	n.d.	n.d.	n.d.	57.5
0.4	1.3	2.7	14.9	7.0	1.2	12.7	n.d.	n.d.	n.d.	59.8
0.4	1.3	3.3	15.1	1.4	1.0	6.4	n.d.	0.5	n.d.	70.7
0.4	0.9	3.0	15.2	4.0	1.3	9.2	n.d.	n.d.	n.d.	66.0
0.5	1.4	3.0	15.4	8.3	1.5	14.3	0.3	n.d.	n.d.	55.5
n.d.	1.3	3.1	16.0	13.0	0.9	16.7	n.d.	0.4	n.d.	48.6
0.4	1.3	2.9	16.2	2.9	1.0	12.8	n.d.	n.d.	n.d.	62.2
n.d.	1.7	3.1	16.3	16.2	0.9	21.9	n.d.	0.6	n.d.	39.4
0.3	1.5	3.3	16.6	12.2	1.0	20.2	0.3	n.d.	n.d.	44.6
0.4	1.8	3.3	16.8	3.2	1.1	13.4	n.d.	n.d.	n.d.	60.0
0.3	1.8	3.4	16.9	15.8	1.7	22.1	0.3	n.d.	0.3	37.5
n.d.	1.7	3.4	18.1	16.0	1.2	24.2	0.2	0.4	n.d.	34.8
0.4	1.8	3.4	18.6	5.9	1.4	14.1	0.3	n.d.	n.d.	54.2
0.6	1.8	3.8	18.7	16.6	2.0	25.8	n.d.	0.9	n.d.	29.8
0.6	1.3	3.6	18.9	5.1	1.2	13.1	n.d.	n.d.	0.3	55.9
0.5	1.2	3.8	19.0	2.1	1.5	13.1	n.d.	n.d.	n.d.	58.9
n.d.	1.1	3.9	19.5	4.4	1.2	12.9	n.d.	n.d.	n.d.	57.0
0.6	1.7	4.0	19.8	5.4	1.6	17.0	n.d.	n.d.	n.d.	49.8
0.4	1.7	3.6	20.2	3.7	1.2	15.9	n.d.	n.d.	n.d.	53.2
0.5	1.9	3.8	20.4	3.5	0.9	14.7	n.d.	0.3	n.d.	54.0
0.5	1.5	4.0	21.1	2.3	1.6	11.0	n.d.	n.d.	n.d.	57.6
0.6	1.8	4.1	22.3	11.7	2.1	19.2	0.2	0.5	0.3	37.1
0.4	1.8	3.9	23.0	9.7	1.4	20.8	n.d.	0.6	n.d.	38.4
0.7	1.3	5.1	25.2	2.1	1.4	9.1	0.3	n.d.	0.3	54.5
0.5	2.0	4.6	25.6	2.0	1.7	19.3	0.3	n.d.	n.d.	44.0
0.4	1.6	5.4	27.0	6.0	1.5	18.8	n.d.	0.3	n.d.	39.0
1.1	1.5	7.0	31.6	1.1	1.2	6.5	0.5	n.d.	n.d.	49.6

Sample XF-F26

Na_2O	MgO	Al_2O_3	SiO_2	P_2O_5	SO_3	K_2O	CaO	TiO_2	V_2O_5	MnO	FeO
0.9	2.7	5.8	48.1	n.d.	n.d.	2.5	23.6	0.7	n.d.	2.3	13.6
0.8	1.8	5.0	36.9	n.d.	0.2	2.4	18.2	0.3	n.d.	1.7	32.9
0.8	1.2	3.7	31.6	1.3	0.2	2.1	14.6	0.2	n.d.	1.0	43.3
0.8	2.3	4.9	36.7	n.d.	n.d.	2.1	19.4	0.5	n.d.	1.9	31.5
0.7	2.3	5.1	38.9	0.2	0.3	2.4	22.8	0.6	n.d.	2.3	24.6
0.6	2.1	4.0	29.5	n.d.	n.d.	1.7	18.8	0.4	n.d.	1.6	41.3
0.7	1.8	4.1	32.4	n.d.	n.d.	2.1	16.1	0.4	n.d.	1.6	40.9
n.d.	1.2	4.2	33.1	4.7	0.4	1.8	15.5	0.3	n.d.	1.1	37.7
0.5	1.1	2.9	24.2	8.1	0.4	1.3	17.3	0.3	n.d.	1.0	43.0
0.7	1.2	4.4	27.6	5.9	0.8	2.4	14.6	0.2	n.d.	0.5	41.8
0.9	2.7	5.7	27.6	3.3	0.3	2.7	11.9	0.3	n.d.	0.6	44.0
0.9	2.4	5.8	45.6	n.d.	n.d.	2.8	21.4	0.7	0.2	3.1	17.2
0.8	2.5	5.9	43.8	n.d.	0.2	2.7	20.8	0.6	0.2	3.1	19.5
0.9	2.4	5.6	43.3	n.d.	n.d.	2.8	20.3	0.7	n.d.	3.1	21.1
0.7	2.0	4.8	35.2	n.d.	0.2	2.3	17.3	0.6	n.d.	2.8	34.2
0.8	2.4	5.9	42.2	n.d.	0.1	2.6	19.4	0.6	0.1	3.0	22.9
0.8	2.4	5.5	40.3	n.d.	0.2	2.5	18.8	0.6	n.d.	2.9	25.9
0.8	2.5	5.5	41.8	n.d.	n.d.	2.7	19.4	0.6	0.1	3.1	23.4
0.7	2.0	4.7	37.8	2.5	0.3	2.4	14.9	0.5	0.4	2.3	31.5
0.7	1.7	3.9	29.5	2.2	0.3	2.1	12.7	0.4	0.3	2.1	44.2
0.8	2.3	5.3	43.5	0.7	0.2	2.4	15.7	0.5	0.2	2.6	25.8
0.8	2.3	5.3	42.9	0.7	0.2	2.4	15.4	0.6	0.2	2.7	26.6
0.8	2.3	5.2	45.9	0.7	0.3	2.7	18.1	0.6	0.2	2.9	20.4
0.7	2.0	5.0	37.5	0.8	0.2	2.3	15.0	0.5	0.3	2.4	33.3
n.d.	n.d.	1.4	23.0	10.7	0.4	1.2	4.1	0.2	n.d.	3.6	55.3
n.d.	n.d.	1.1	19.5	8.7	0.2	1.0	3.2	0.2	0.3	3.2	62.7
n.d.	n.d.	0.1	19.9	12.3	0.3	2.1	1.1	0.2	0.3	6.0	57.8
n.d.	n.d.	n.d.	20.8	12.9	n.d.	1.9	n.d.	0.1	0.2	9.0	55.0
n.d.	n.d.	0.7	17.1	8.2	0.3	1.5	2.2	0.3	0.3	3.4	66.1
n.d.	n.d.	0.7	22.4	9.1	0.4	2.0	2.8	0.2	0.2	4.3	58.0
n.d.	n.d.	n.d.	14.7	11.6	n.d.	0.7	n.d.	0.3	0.6	5.9	66.3
n.d.	n.d.	0.4	14.5	8.4	0.2	1.5	1.0	0.3	0.5	3.8	69.4
n.d.	n.d.	0.7	19.3	11.3	0.4	2.0	1.8	0.2	n.d.	4.3	60.0
n.d.	n.d.	0.5	11.8	6.5	0.3	2.2	1.6	0.2	0.6	3.1	73.2
n.d.	n.d.	1.0	21.7	10.5	0.6	2.5	3.6	0.2	n.d.	4.1	55.9
n.d.	n.d.	0.1	18.7	10.3	0.3	0.4	0.2	0.3	0.5	6.0	63.4

n.d.	n.d.	n.d.	19.4	7.9	n.d.	n.d.	n.d.	0.2	0.5	5.8	66.2
n.d.	n.d.	n.d.	25.6	4.2	n.d.	n.d.	n.d.	n.d.	0.5	5.9	63.9
n.d.	n.d.	n.d.	18.4	12.4	0.5	1.2	0.2	0.2	0.2	6.0	60.8
n.d.	n.d.	0.9	19.7	11.3	0.3	1.1	0.5	0.2	0.2	5.2	60.5
n.d.	n.d.	n.d.	26.2	3.4	n.d.	n.d.	n.d.	0.1	0.2	6.6	63.5
n.d.	n.d.	0.4	15.1	8.6	0.2	1.6	1.0	0.3	0.4	3.9	68.6
n.d.	n.d.	n.d.	18.1	13.5	0.4	2.6	0.8	n.d.	n.d.	5.0	59.6
n.d.	n.d.	n.d.	17.0	14.6	0.3	3.2	n.d.	n.d.	0.2	5.7	59.0
1.0	n.d.	n.d.	18.4	15.6	0.6	5.0	0.5	0.1	n.d.	6.2	52.7
n.d.	n.d.	n.d.	17.0	13.0	n.d.	2.1	0.3	0.3	0.9	5.8	60.8
n.d.	n.d.	n.d.	15.2	13.1	0.4	2.5	n.d.	0.3	0.4	5.3	62.8
n.d.	n.d.	n.d.	19.4	13.8	0.2	2.1	0.3	n.d.	n.d.	6.0	58.3
n.d.	1.0	1.2	8.5	22.3	0.8	0.4	6.3	0.1	0.2	0.9	58.3
n.d.	0.9	1.2	8.0	25.0	1.6	0.4	5.6	n.d.	n.d.	1.0	56.4
n.d.	n.d.	0.8	11.2	16.8	1.4	0.6	7.2	0.1	0.2	0.8	60.9
n.d.	1.0	1.3	10.0	14.0	1.5	0.5	5.9	0.2	0.4	0.7	64.6
n.d.	n.d.	2.9	18.7	14.2	1.1	1.0	4.9	n.d.	n.d.	0.3	57.0
n.d.	n.d.	3.0	19.6	15.7	1.3	1.2	6.6	0.1	n.d.	0.3	52.3
n.d.	1.1	1.4	11.7	22.5	2.0	0.7	8.4	n.d.	n.d.	0.9	51.5
0.7	1.1	4.3	27.4	5.9	0.8	2.4	14.7	0.3	n.d.	0.5	41.9
1.0	2.7	5.5	27.5	3.2	0.4	2.6	12.1	0.3	n.d.	0.6	44.3
n.d.	n.d.	2.3	15.9	18.0	1.2	1.1	5.3	0.2	n.d.	0.4	55.6
n.d.	n.d.	1.9	14.9	17.9	1.3	0.9	5.0	n.d.	n.d.	n.d..4	57.6

Sample XF-F29

Na_2O	MgO	Al_2O_3	SiO_2	P_2O_5	SO_3	K_2O	CaO	TiO_2	V_2O_5	MnO	FeO
0.8	1.9	5.2	29.1	11.0	0.6	0.8	16.8	0.4	0.4	1.3	31.6
0.7	2.3	5.5	30.5	9.9	0.6	0.8	15.8	0.4	0.4	1.3	31.9
n.d.	1.8	5.1	29.0	12.0	n.d.	0.7	17.3	n.d.	n.d.	1.3	32.8
0.6	1.9	4.0	24.6	12.3	0.6	0.7	18.4	0.4	0.4	1.6	33.3
0.6	1.9	5.1	29.0	9.1	0.9	0.7	14.7	0.4	0.5	1.3	35.7
0.7	1.8	4.8	27.2	10.6	0.7	0.7	15.1	0.4	0.4	1.2	36.5
0.6	2.0	4.0	27.0	10.6	0.7	0.6	15.2	0.4	0.5	1.5	36.5
0.7	2.3	5.1	27.2	9.8	0.5	0.7	14.6	0.5	0.5	1.1	37.3
0.6	1.7	3.5	18.8	16.5	0.5	0.4	19.3	0.3	n.d.	0.9	37.6
0.6	2.2	5.1	27.1	9.8	0.6	0.7	14.5	0.4	0.3	1.1	37.6

0.7	1.9	4.4	24.1	13.9	0.8	0.9	12.7	0.5	0.3	1.9	37.8
0.8	1.9	4.6	26.2	10.2	0.8	0.9	14.5	0.3	0.3	1.3	38.1
0.8	2.0	4.2	23.6	13.9	1.0	1.0	12.7	0.4	0.4	1.8	38.1
0.8	2.0	5.0	28.8	7.0	0.6	0.7	13.7	0.5	0.8	1.4	38.4
0.5	1.9	4.4	25.6	11.1	0.7	0.6	14.8	0.3	0.3	1.2	38.6
0.8	1.9	4.5	25.7	10.7	0.8	0.9	13.8	0.3	0.5	1.0	39.0
0.7	2.0	4.7	25.0	11.9	0.5	0.7	13.2	0.3	0.3	1.2	39.6
0.7	2.0	4.2	23.5	13.5	0.7	0.9	12.2	0.3	0.4	1.7	39.8
0.6	1.8	4.6	27.2	8.6	0.7	0.6	13.4	0.4	0.3	1.4	40.4
0.5	1.7	4.3	26.0	9.8	1.0	0.5	13.1	0.3	0.5	1.5	40.5
0.5	1.8	4.5	25.9	9.1	0.6	0.5	13.7	0.4	0.3	1.3	41.4
0.7	1.8	4.9	27.8	7.0	0.9	0.6	12.5	0.5	0.4	1.2	41.8
0.6	1.8	3.9	22.6	13.0	0.7	0.8	11.9	0.3	0.4	1.7	42.3
0.7	1.6	4.2	25.0	10.0	1.0	0.6	12.7	0.4	0.3	1.1	42.4
0.4	1.8	3.2	20.6	14.7	1.5	0.6	11.2	0.4	0.4	2.1	43.0
0.7	1.4	3.4	23.7	10.8	1.0	0.6	12.3	0.3	0.3	1.3	44.3
0.6	1.7	3.4	24.9	9.2	1.0	0.5	11.7	0.4	0.2	1.8	44.5
0.5	1.5	3.5	23.4	10.9	1.0	0.7	12.1	0.3	0.3	1.3	44.5
0.7	1.4	3.3	23.1	11.9	1.0	0.6	11.3	0.4	n.d.	1.6	44.6
0.5	1.5	3.1	20.3	12.9	0.8	0.3	13.6	0.3	0.5	1.3	44.9
0.7	1.9	4.5	24.4	8.1	0.7	0.5	12.4	0.3	0.3	1.0	45.2
0.4	1.6	3.8	25.1	8.1	1.0	0.5	10.8	0.4	0.3	1.7	46.5
0.5	1.8	4.2	24.6	8.1	0.7	0.4	11.5	n.d.	0.4	1.1	46.7
0.6	1.7	3.6	24.5	8.0	0.8	0.5	10.6	0.3	0.3	1.7	47.6
0.3	1.4	3.2	21.8	10.6	1.2	0.4	10.8	0.4	0.4	1.4	47.9
0.5	1.5	3.1	22.0	10.3	1.0	0.5	11.3	0.3	0.3	1.3	47.9
0.4	1.2	2.6	16.2	18.8	1.2	0.6	9.0	0.3	n.d.	1.7	48.0
0.4	1.6	3.0	19.7	13.6	1.8	0.5	8.6	0.4	0.3	1.7	48.4
0.4	1.5	2.8	18.8	13.3	1.2	0.5	9.8	0.5	0.8	1.9	48.7
0.6	1.7	3.5	23.4	7.9	0.9	0.4	10.0	0.3	0.3	1.5	49.4
0.5	1.6	3.4	23.0	8.1	0.9	0.4	9.8	0.3	0.2	1.7	50.0
n.d.	1.8	3.1	19.7	11.8	1.5	0.2	8.5	0.3	0.3	1.8	50.9
0.3	1.6	2.8	18.6	13.0	1.5	0.4	8.2	0.3	0.4	1.6	51.5
0.3	1.3	3.0	16.3	15.1	1.5	0.5	8.5	0.3	n.d.	1.6	51.6
n.d.	1.4	2.6	17.3	13.9	1.7	0.4	9.0	0.3	n.d.	1.5	51.8
0.3	1.3	2.8	18.6	13.0	2.0	0.4	7.7	0.3	n.d.	1.5	51.9
0.3	1.5	2.8	18.5	12.5	1.4	0.5	8.3	0.4	0.3	1.5	52.1
0.4	1.5	3.0	21.5	8.2	1.0	0.5	7.8	n.d.	n.d.	1.5	54.6
0.4	1.3	2.9	20.7	6.9	1.3	0.2	6.5	0.3	n.d.	1.1	58.3

Sample XK-Kn10

Na_2O	MgO	Al_2O_3	SiO_2	K_2O	CaO	TiO_2	MnO	FeO
1.6	2.2	10.0	47.8	1.6	13.9	0.6	2.5	19.8
1.6	2.8	10.4	47.7	1.6	13.5	0.7	0.9	20.8
1.5	2.5	10.2	46.9	1.6	13.7	0.6	1.9	21.1
1.4	2.2	9.8	50.2	1.2	11.1	0.7	2.1	21.3
1.6	2.3	9.3	44.3	1.5	13.6	0.6	2.7	23.8
1.4	2.8	9.9	45.5	1.3	12.7	0.8	1.1	24.5
1.2	2.0	9.7	47.4	1.3	10.8	0.6	2.1	24.8
1.0	2.2	8.4	47.9	0.9	10.2	0.7	2.7	25.5
1.3	2.1	9.3	42.3	1.5	15.0	0.6	0.6	27.4
1.5	2.2	9.5	40.2	1.5	13.5	0.7	2.0	28.8
1.6	2.2	9.1	38.0	1.5	13.3	0.6	2.1	31.6
1.7	2.2	8.9	39.9	1.5	11.7	0.4	2.1	31.6
1.2	2.2	9.4	39.5	1.2	13.8	0.6	0.4	31.6
1.4	2.6	9.0	40.5	1.1	11.5	0.6	1.0	32.4
1.8	2.4	13.5	35.0	1.6	10.3	0.8	1.3	33.3
1.4	2.1	8.3	41.7	1.2	9.3	0.6	1.7	33.7
1.3	2.0	8.6	38.4	1.3	11.9	0.6	2.1	33.7
1.2	2.5	7.8	37.4	1.4	10.9	0.6	2.2	36.0
1.4	1.8	10.4	41.6	1.5	5.1	0.6	0.3	37.4
1.4	2.0	8.3	36.8	1.3	10.3	0.6	1.9	37.4
1.2	2.2	8.8	35.4	1.2	12.4	0.6	0.5	37.8
1.4	2.2	8.6	34.4	1.3	12.2	0.5	1.6	37.9
1.2	1.8	7.9	38.0	1.0	9.2	0.5	1.8	38.6
1.3	2.0	7.3	32.3	1.1	9.4	0.5	1.4	44.8

Sample XK-Sp1

Na_2O	MgO	Al_2O_3	SiO_2	P_2O_5	SO_3	K_2O	CaO	MnO	FeO
0.5	1.2	3.6	24.2	9.2	n.d.	0.7	8.6	0.7	51.1
0.5	0.7	3.2	19.3	7.7	0.8	0.6	8.0	0.3	58.8
0.4	0.6	3.0	17.4	5.4	0.7	0.7	7.0	0.3	64.6
0.4	1.0	3.0	20.3	8.6	0.6	0.5	7.5	0.4	57.5

n.d.	0.4	1.1	7.6	2.4	n.d.	0.3	4.9	0.2	83.0
n.d.	n.d.	1.0	5.3	2.2	n.d.	0.2	3.3	n.d.	88.1
n.d.	0.5	1.5	9.4	1.6	0.6	n.d.	3.4	n.d.	82.8
n.d.	n.d.	1.7	4.8	1.2	n.d.	n.d.	2.3	n.d.	90.0
n.d.	n.d.	2.6	6.7	4.7	n.d.	1.5	7.6	n.d.	77.0
n.d.	n.d.	0.7	4.3	1.3	n.d.	n.d.	3.0	n.d.	90.7

Sample XK-Sw14

Na_2O	MgO	Al_2O_3	SiO_2	P_2O_5	K_2O	CaO	TiO_2	MnO	FeO
1.3	2.7	11.0	57.3	n.d.	3.1	19.2	0.9	0.8	3.7
1.6	2.9	11.4	58.6	n.d.	3.0	16.7	0.7	0.2	4.7
1.4	2.7	11.0	55.5	n.d.	3.0	19.5	1.0	0.8	4.8
1.4	2.4	10.2	57.8	n.d.	2.8	16.6	0.9	0.5	7.6
1.4	2.3	10.2	58.0	n.d.	2.9	15.4	1.0	0.5	8.5
1.0	3.5	8.4	47.2	n.d.	2.3	25.7	0.7	1.1	10.1
1.3	2.0	9.9	50.2	n.d.	4.2	21.5	0.6	n.d.	10.4
1.0	4.3	12.1	41.5	n.d.	2.4	21.3	0.8	0.4	16.1
0.8	4.3	11.1	40.5	0.8	1.9	21.1	0.9	n.d.	18.5
1.2	2.5	8.1	44.5	n.d.	2.3	14.4	0.7	1.1	25.1
1.1	2.3	10.1	39.6	0.9	3.0	15.6	0.7	n.d.	26.6
0.9	3.7	11.0	33.4	n.d.	1.8	15.6	0.8	0.3	32.7

Sample NJG-6

SiO_2	P_2O_5	MnO	FeO
7.9	16.8	8.5	66.8
8.8	13.7	7.6	69.8
10.4	13.9	7.9	67.8
5.7	11.2	6.0	76.8
5.6	8.8	5.6	79.7
6.3	11.7	6.1	75.7
8.1	13.1	7.1	71.7
5.8	10.2	5.5	78.3
3.8	6.8	6.0	83.1
12.1	14.7	10.4	62.7

13.8	14.8	11.0	60.3
11.1	17.1	10.4	61.2
7.3	26.9	30.1	35.2
7.9	25.9	29.0	37.0
9.9	20.5	23.5	45.6
17.9	11.2	10.8	60.1
17.0	13.0	11.4	58.4
9.7	18.4	11.4	60.4
8.8	10.2	8.6	72.1
10.1	16.7	10.1	63.1
14.4	11.7	9.5	64.5
11.9	18.3	14.6	55.1
10.2	25.8	13.9	49.7
10.0	26.4	14.2	49.1
9.8	26.1	14.9	48.7
10.7	25.1	14.2	49.5

Sample NJG-7

MgO	Al_2O_3	SiO_2	P_2O_5	SO_3	K_2O	CaO	TiO_2	V_2O_5	MnO	FeO
n.d.	n.d.	10.8	23.6	n.d.	n.d.	3.2	0.2	0.2	2.3	59.8
n.d.	n.d.	6.6	26.1	n.d.	0.2	7.9	n.d.	n.d.	2.2	57.1
1.0	0.3	17.0	17.1	0.2	n.d.	4.5	0.2	n.d.	2.9	56.8
0.9	0.5	13.4	20.7	1.9	0.2	5.6	0.2	0.2	2.5	53.9
n.d.	n.d.	7.8	24.0	0.3	n.d.	2.3	0.2	0.2	1.8	63.5
0.9	0.2	10.1	23.9	n.d.	n.d.	4.6	n.d.	n.d.	1.7	58.6
n.d.	n.d.	5.6	14.9	0.7	n.d.	3.0	n.d.	n.d.	0.8	74.9
1.1	1.1	26.1	9.6	0.6	n.d.	10.3	1.0	0.3	10.9	39.2
n.d.	n.d.	4.2	31.3	1.0	0.1	1.6	n.d.	n.d.	0.7	61.1
n.d.	n.d.	8.6	20.0	0.8	n.d.	n.d.	n.d.	n.d.	1.9	68.7
n.d.	n.d.	2.2	6.1	0.3	n.d.	0.2	n.d.	0.2	0.6	90.5
n.d.	n.d.	7.6	20.2	0.8	n.d.	n.d.	0.2	0.2	1.0	70.0
n.d.	n.d.	13.6	17.7	2.2	n.d.	0.3	0.4	0.2	2.0	63.6
n.d.	n.d.	1.8	31.2	1.1	n.d.	1.8	n.d.	n.d.	0.5	63.7
n.d.	n.d.	3.7	29.6	1.9	0.2	1.7	n.d.	n.d.	0.2	62.8
n.d.	n.d.	5.0	30.2	1.5	n.d.	3.1	n.d.	n.d.	1.1	59.1
n.d.	n.d.	3.7	14.1	0.3	n.d.	3.0	0.1	0.2	0.8	77.7

n.d.	n.d.	5.4	26.5	0.5	n.d.	2.9	n.d.	n.d.	1.1	63.7
n.d.	n.d.	4.2	31.0	1.9	0.1	5.6	n.d.	n.d.	1.1	56.1
n.d.	n.d.	2.1	32.7	1.4	n.d.	1.8	n.d.	n.d.	0.5	61.6
n.d.	n.d.	2.1	32.1	1.2	0.1	1.9	n.d.	n.d.	0.6	62.1
n.d.	n.d.	2.1	31.6	1.1	n.d.	1.9	n.d.	n.d.	0.5	62.7
n.d.	n.d.	1.4	24.6	0.7	n.d.	2.6	n.d.	n.d.	n.d.	70.7
n.d.	n.d.	2.7	9.8	n.d.	n.d.	1.7	n.d.	n.d.	n.d.	85.8
n.d.	n.d.	0.9	31.8	1.0	n.d.	1.7	n.d.	n.d.	n.d.	64.6
0.8	2.2	24.6	12.9	1.4	0.2	8.4	0.4	0.4	5.0	43.8
n.d.	2.6	17.3	11.7	1.2	0.3	4.4	1.4	7.0	3.2	50.9
n.d.	n.d.	10.6	23.8	n.d.	n.d.	3.1	0.2	0.2	2.4	59.8
n.d.	n.d.	14.3	20.9	2.0	0.1	5.6	0.3	0.2	2.6	54.0
n.d.	n.d.	13.2	17.1	n.d.	n.d.	1.6	n.d.	n.d.	1.8	66.4
n.d.	n.d.	27.5	1.1	n.d.	n.d.	n.d.	n.d.	0.1	6.1	65.1
n.d.	n.d.	20.9	4.0	n.d.	n.d.	n.d.	1.0	0.2	5.4	68.6
n.d.	n.d.	12.1	20.4	n.d.	n.d.	n.d.	n.d.	n.d.	3.5	64.0
n.d.	n.d.	21.2	8.7	1.2	n.d.	0.3	1.0	n.d.	6.6	61.0

Sample NJG-11

Na_2O	MgO	Al_2O_3	SiO_2	P_2O_5	SO_3	K_2O	CaO	TiO_2	V_2O_5	MnO	FeO
0.8	4.7	8.0	39.7	3.1	0.4	1.9	32.1	0.6	0.7	0.6	7.4
0.2	3.9	4.1	27.5	14.6	n.d.	0.6	39.5	0.5	0.9	0.5	7.7
1.1	3.9	7.3	38.7	6.6	0.4	2.4	27.0	0.5	0.7	0.7	11.0
1.1	3.7	7.4	38.1	6.8	0.4	2.4	26.4	0.5	0.8	0.7	11.8
n.d.	3.4	3.3	20.9	21.9	n.d.	0.4	36.5	0.4	0.6	0.3	12.4
0.9	3.9	7.2	36.0	6.7	0.4	1.9	28.1	0.5	0.9	0.7	12.8
0.9	3.9	7.5	38.5	5.3	0.3	2.1	26.5	0.5	0.7	0.7	13.1
0.8	4.0	7.5	37.7	5.5	0.4	1.8	27.1	0.5	0.7	0.6	13.4
n.d.	3.6	4.3	29.7	12.0	0.1	0.6	33.3	0.6	0.8	0.5	14.5
0.9	4.2	7.1	37.5	2.8	0.3	1.9	28.8	0.5	0.5	0.5	15.0
0.8	2.6	6.0	29.7	12.3	0.6	1.8	22.6	0.4	0.6	0.5	22.5
0.8	3.0	4.9	22.7	17.3	0.6	1.7	22.6	0.3	0.4	0.6	25.2
0.8	3.4	5.8	26.4	13.4	0.6	1.6	20.3	0.4	1.2	0.6	25.5
0.8	2.4	5.5	27.8	13.0	0.6	1.7	20.7	0.4	0.7	0.5	26.0
0.8	2.8	4.5	21.9	14.8	1.0	1.6	17.7	0.3	0.2	0.5	34.1
n.d.	2.4	4.2	19.6	15.9	1.4	1.3	13.1	0.2	0.1	0.4	41.4

n.d.	1.5	3.5	18.6	15.1	0.3	1.1	15.6	0.2	0.2	0.2	43.7
n.d.	1.6	2.1	14.1	23.2	0.2	1.7	9.4	n.d.	n.d.	0.2	47.6
n.d.	1.4	3.5	18.5	16.6	1.0	1.0	8.7	0.2	0.3	0.3	48.6
n.d.	1.3	3.7	18.5	15.4	0.7	0.7	9.2	n.d.	n.d.	0.2	50.5
n.d.	1.5	3.6	18.5	13.3	0.7	0.8	9.2	0.2	n.d.	0.2	52.3
n.d.	1.9	4.2	20.8	7.5	0.4	0.8	10.3	0.2	0.4	0.3	53.3
n.d.	n.d.	3.8	20.3	10.7	0.4	0.8	8.9	0.1	n.d.	0.2	54.8
n.d.	1.5	3.3	16.6	11.0	0.6	0.6	7.7	0.2	0.2	0.2	58.0
n.d.	1.5	4.0	18.1	6.2	0.3	0.9	7.1	0.3	0.3	0.3	61.2
n.d.	1.5	3.4	15.3	9.7	0.5	0.6	6.6	0.2	0.3	0.2	61.8
n.d.	1.0	3.1	14.0	3.3	0.3	0.6	3.7	0.2	0.1	n.d.	73.9
n.d.	1.7	2.8	11.0	4.3	0.2	0.6	4.6	0.2	0.5	0.3	73.9
n.d.	0.9	2.1	6.8	4.1	0.3	0.3	2.8	0.3	0.9	0.2	81.3

Sample NJG-20

Na_2O	MgO	Al_2O_3	SiO_2	P_2O_5	SO_3	K_2O	CaO	TiO_2	V_2O_5	MnO	FeO
n.d.	0.9	2.3	9.6	25.7	n.d.	0.9	26.8	n.d.	n.d.	n.d.	33.8
0.5	0.7	0.9	11.3	24.0	n.d.	0.5	25.7	n.d.	0.5	1.6	34.2
0.5	0.5	0.6	6.3	25.1	n.d.	0.5	26.9	n.d.	n.d.	0.1	39.5
n.d.	1.2	4.6	20.0	10.6	0.4	1.6	20.0	0.1	n.d.	0.3	41.3
n.d.	1.1	1.6	7.8	21.4	0.2	0.5	22.8	n.d.	n.d.	0.4	44.4
n.d.	1.3	4.7	19.8	8.4	0.4	1.9	18.5	n.d.	n.d.	0.3	44.9
n.d.	1.3	2.8	15.0	16.5	0.8	1.3	13.8	n.d.	n.d.	0.9	47.7
n.d.	n.d.	2.5	11.4	19.1	1.0	0.3	17.2	n.d.	n.d.	0.7	47.8
0.7	1.6	6.4	26.0	2.9	0.4	1.8	11.8	0.2	n.d.	0.2	47.9
0.8	0.5	0.8	7.4	20.3	0.2	0.9	20.8	n.d.	n.d.	0.3	47.9
n.d.	1.3	2.1	11.6	19.6	0.7	1.3	14.2	0.1	n.d.	0.8	48.4
n.d.	1.3	2.2	12.0	18.4	0.5	1.3	14.6	n.d.	n.d.	0.9	48.7
0.5	0.7	0.7	8.0	17.9	n.d.	0.5	19.7	n.d.	0.4	1.4	50.3
0.5	1.5	5.0	20.5	4.3	0.3	1.4	14.0	0.2	n.d.	0.3	52.0
n.d.	1.3	3.6	15.6	9.4	0.3	1.3	15.8	0.1	n.d.	0.4	52.2
n.d.	0.9	2.8	12.8	10.4	0.3	1.0	12.2	n.d.	n.d.	0.4	59.2
n.d.	1.0	2.8	12.4	10.6	0.5	1.1	11.6	0.2	n.d.	0.5	59.4
n.d.	0.9	2.3	10.9	12.0	0.8	0.9	9.6	0.2	0.2	0.7	61.4
n.d.	1.4	4.2	16.0	3.9	0.2	1.3	10.8	0.3	n.d.	0.2	61.7
n.d.	1.3	3.5	13.4	5.4	0.2	1.0	12.4	0.2	n.d.	0.3	62.2

n.d.	1.1	3.7	14.5	4.4	0.2	1.0	12.3	n.d.	n.d.	0.2	62.6
n.d.	0.9	2.8	12.1	8.2	0.4	0.9	10.2	n.d.	n.d.	0.5	64.0
n.d.	n.d.	0.7	4.4	13.1	n.d.	0.5	13.6	n.d.	n.d.	n.d.	67.7
n.d.	1.2	3.5	12.8	4.4	0.2	0.6	5.6	0.2	n.d.	0.3	71.3
n.d.	n.d.	2.3	8.4	2.1	0.3	0.2	4.5	n.d.	0.2	0.4	81.6
n.d.	n.d.	1.3	7.3	4.6	0.4	0.2	3.9	n.d.	0.2	0.5	81.7
n.d.	n.d.	1.5	7.4	2.5	0.2	0.2	5.2	n.d.	n.d.	0.2	83.0
n.d.	n.d.	0.9	3.7	4.7	0.2	n.d.	5.8	n.d.	n.d.	0.1	84.6

Sample NJG-34

Na_2O	MgO	Al_2O_3	SiO_2	P_2O_5	SO_3	K_2O	CaO	TiO_2	MnO	FeO
0.8	3.3	9.5	45.1	n.d.	n.d.	2.4	34.1	0.5	0.4	3.8
1.2	2.9	11.9	54.9	n.d.	n.d.	3.2	19.8	0.7	0.3	5.0
1.2	2.8	11.1	51.3	n.d.	n.d.	3.3	20.4	0.7	0.3	9.0
1.2	2.4	9.2	39.8	n.d.	n.d.	1.9	10.9	0.4	0.2	34.0
1.3	2.9	11.6	52.7	n.d.	n.d.	2.7	17.8	0.7	0.2	10.1
1.3	2.9	12.5	57.9	n.d.	n.d.	2.9	16.2	0.7	0.2	5.4
1.4	2.6	11.8	55.3	n.d.	n.d.	2.8	14.0	0.7	0.2	11.1
1.3	3.0	12.2	55.4	n.d.	n.d.	3.2	20.8	0.8	0.3	3.1
1.1	3.0	12.1	55.9	n.d.	n.d.	3.2	21.1	0.7	0.3	2.7
0.6	3.4	8.4	41.6	0.9	n.d.	1.8	36.1	0.5	0.4	6.3
0.9	3.8	10.4	42.5	n.d.	0.3	2.6	33.1	0.6	0.3	5.5
0.8	3.4	9.7	44.1	n.d.	0.2	2.4	35.7	0.5	0.2	3.0
0.9	3.4	9.5	46.2	n.d.	n.d.	2.8	34.0	0.6	0.2	2.5
0.9	3.6	9.6	44.3	n.d.	0.2	2.5	33.2	0.6	0.2	5.1

Sample CXC-1

Na_2O	MgO	Al_2O_3	SiO_2	P_2O_5	SO_3	K_2O	CaO	TiO_2	MnO	FeO
n.d.	n.d.	1.4	14.6	6.3	0.4	0.7	1.7	n.d.	1.3	73.7
n.d.	n.d.	1.2	10.1	3.7	0.6	0.1	1.0	n.d.	0.9	82.4
n.d.	n.d.	2.2	13.5	4.7	0.7	0.2	1.7	n.d.	1.0	76.0
n.d.	n.d.	1.9	13.8	5.1	0.8	0.4	1.8	0.2	1.1	75.0
n.d.	n.d.	2.4	19.1	7.9	0.9	0.5	2.6	n.d.	1.4	65.3
n.d.	n.d.	2.0	12.9	3.6	0.3	0.1	1.5	n.d.	1.1	78.6

n.d.	n.d.	1.6	9.4	3.0	0.6	0.1	1.0	0.2	0.9	83.4
n.d.	n.d.	1.1	8.0	2.3	0.8	0.2	0.8	n.d.	0.7	86.1
n.d.	n.d.	1.8	11.6	4.0	1.3	0.2	1.4	0.2	0.9	78.5
n.d.	n.d.	0.9	8.5	2.9	1.3	0.3	1.1	n.d.	0.8	84.3
n.d.	n.d.	1.8	14.7	5.6	0.5	0.8	1.9	n.d.	1.1	73.7
n.d.	n.d.	1.4	9.5	3.4	0.7	0.5	1.2	n.d.	0.8	82.5
n.d.	n.d.	1.9	17.0	4.6	0.8	0.4	1.7	n.d.	1.2	72.3
n.d.	n.d.	1.9	14.0	3.8	0.7	0.5	1.6	n.d.	1.1	76.5
n.d.	n.d.	1.8	13.6	4.6	0.6	0.1	1.5	n.d.	1.0	76.9
n.d.	n.d.	2.3	16.5	5.2	0.7	0.2	1.9	n.d.	1.1	72.1
n.d.	n.d.	1.3	10.2	3.4	1.5	n.d.	1.2	n.d.	0.7	81.8
n.d.	n.d.	1.9	16.0	4.8	0.8	0.5	2.0	n.d.	1.2	72.9
n.d.	n.d.	2.0	12.3	3.7	0.6	0.3	1.5	n.d.	1.1	78.6
n.d.	n.d.	1.5	10.2	3.0	0.4	0.3	1.2	n.d.	0.9	82.4
n.d.	n.d.	2.5	19.8	5.8	0.8	0.7	2.3	n.d.	1.4	66.7
n.d.	n.d.	1.2	12.2	3.2	0.5	0.2	1.5	n.d.	1.0	80.2
n.d.	n.d.	0.7	6.9	2.0	0.4	0.2	0.7	n.d.	0.7	88.5
n.d.	n.d.	1.4	10.2	2.8	0.5	0.2	1.3	n.d.	1.0	82.6
n.d.	n.d.	1.8	13.7	3.7	0.6	0.2	1.8	n.d.	1.1	77.3
n.d.	n.d.	1.4	12.8	3.1	0.5	0.1	1.3	0.2	1.2	79.4
n.d.	n.d.	2.2	20.0	11.3	0.3	0.9	2.9	n.d.	1.6	60.8
n.d.	n.d.	2.4	17.9	5.9	0.7	0.6	2.1	n.d.	1.3	69.1
n.d.	n.d.	2.1	15.0	5.5	1.6	0.3	2.0	n.d.	1.2	72.2
n.d.	n.d.	2.4	15.7	10.2	0.7	0.9	2.4	n.d.	1.3	66.4
n.d.	n.d.	2.1	17.9	6.4	0.9	0.6	2.4	n.d.	1.4	68.2
n.d.	n.d.	2.9	20.4	8.0	1.0	1.2	2.7	n.d.	1.7	62.1
n.d.	n.d.	2.7	20.3	7.2	1.0	0.9	2.7	n.d.	1.7	63.5
n.d.	n.d.	2.6	15.8	5.2	1.5	0.3	2.5	n.d.	1.2	70.9
n.d.	n.d.	2.4	18.2	7.3	0.9	0.9	2.4	n.d.	1.4	66.4
n.d.	n.d.	2.2	17.2	5.6	0.9	0.7	2.2	n.d.	1.3	69.9
n.d.	n.d.	2.2	18.7	6.8	1.2	0.6	2.4	n.d.	1.5	66.6
n.d.	n.d.	3.2	22.7	8.9	1.6	1.4	3.6	n.d.	1.6	57.1
n.d.	n.d.	n.d.	0.2	0.4	16.0	n.d.	0.2	n.d.	n.d.	83.3
n.d.	n.d.	1.8	20.9	9.8	0.5	0.5	2.5	n.d.	1.6	62.6
n.d.	n.d.	2.2	17.1	4.8	0.8	0.7	2.1	n.d.	1.3	71.0
n.d.	n.d.	1.3	10.3	2.8	1.0	0.3	1.5	n.d.	0.8	82.1
0.7	1.3	7.1	60.9	n.d.	n.d.	4.3	13.8	0.5	4.3	7.2
0.8	1.2	7.3	59.3	n.d.	n.d.	4.6	13.5	0.4	4.3	8.7
0.5	1.2	7.3	61.5	n.d.	n.d.	4.8	12.8	0.4	4.2	7.3

0.5	1.2	7.6	59.6	n.d.	n.d.	4.0	12.4	0.5	4.0	10.3
n.d.	1.2	6.6	52.2	n.d.	n.d.	2.4	11.0	0.3	3.4	22.9
0.7	1.2	8.2	62.9	n.d.	n.d.	5.5	13.5	0.4	4.1	3.7
0.6	1.2	7.2	60.8	n.d.	n.d.	4.1	13.1	0.4	4.3	8.4
0.5	1.2	7.4	59.4	n.d.	n.d.	4.3	12.7	0.5	4.2	9.9
0.6	1.2	7.2	61.0	n.d.	n.d.	5.0	13.4	0.4	4.1	7.1
0.5	1.2	7.6	58.8	n.d.	0.2	4.6	13.6	0.4	4.2	8.8
0.6	1.1	7.3	58.4	n.d.	n.d.	4.5	12.6	0.4	4.0	11.1
0.6	1.2	7.2	58.0	n.d.	n.d.	4.5	12.5	0.3	3.9	11.9
n.d.	0.9	6.2	49.4	n.d.	n.d.	1.9	9.3	0.4	3.2	28.7
0.7	1.1	7.8	63.4	n.d.	n.d.	4.5	12.4	0.4	5.0	4.8
0.6	1.2	7.4	59.9	n.d.	n.d.	4.7	13.5	0.4	4.3	8.0
0.5	1.2	7.5	61.6	n.d.	n.d.	4.8	14.2	0.4	4.4	5.6
0.6	1.3	7.6	57.4	n.d.	0.2	4.2	12.6	0.4	4.0	11.7
0.7	1.2	7.2	57.9	n.d.	n.d.	4.8	13.3	0.4	4.3	10.2
0.6	1.3	7.4	60.0	n.d.	n.d.	5.1	12.6	0.5	4.4	8.1
0.7	1.3	7.3	59.5	n.d.	n.d.	5.1	13.5	0.4	4.2	8.1
0.7	1.2	7.6	61.7	n.d.	n.d.	5.3	14.0	0.4	4.4	4.7
0.6	1.2	7.8	60.7	n.d.	n.d.	5.0	14.2	0.5	4.3	5.8
0.7	1.3	7.7	61.9	n.d.	n.d.	5.2	13.7	0.4	4.5	4.6
0.5	1.2	7.3	54.4	n.d.	n.d.	3.6	11.9	0.4	4.0	16.7
0.8	1.3	7.5	62.2	n.d.	n.d.	5.4	14.3	0.4	4.5	3.8
0.8	1.3	7.2	61.2	n.d.	n.d.	5.2	14.0	0.4	4.5	5.5
0.8	1.2	7.3	57.3	n.d.	n.d.	4.6	11.7	0.4	5.5	11.3
0.7	1.1	6.7	54.9	n.d.	0.2	3.9	11.5	0.4	5.5	15.0
0.6	1.1	7.6	59.6	n.d.	n.d.	5.2	13.0	0.4	5.1	7.5
0.6	1.2	7.7	57.0	n.d.	n.d.	4.4	13.1	0.5	4.3	11.3
0.7	1.3	7.7	59.6	n.d.	n.d.	4.9	14.1	0.4	4.3	6.9
0.7	1.3	7.7	61.5	n.d.	n.d.	4.9	13.7	0.4	4.4	5.4
0.6	1.2	7.5	58.6	n.d.	n.d.	4.4	12.9	0.4	4.2	10.3
0.6	1.2	7.6	62.0	n.d.	n.d.	4.9	14.3	0.5	4.4	4.4
0.6	1.2	7.6	60.7	n.d.	n.d.	5.1	13.3	0.4	4.4	6.8
0.6	1.3	7.5	61.1	n.d.	n.d.	5.1	13.7	0.4	4.5	5.9
0.7	1.2	7.6	60.3	n.d.	n.d.	4.7	13.7	0.4	4.4	6.9
0.8	1.3	7.4	63.2	n.d.	n.d.	5.1	14.2	0.4	4.5	3.2
0.6	1.3	7.9	62.4	n.d.	n.d.	5.1	14.2	0.5	4.6	3.4
0.8	1.2	7.5	61.5	n.d.	n.d.	5.1	14.2	0.5	4.4	4.8
0.7	1.3	7.6	62.4	n.d.	n.d.	4.9	14.5	0.4	4.6	3.5
0.6	1.2	7.3	58.9	n.d.	0.2	4.5	14.0	0.5	4.6	8.3

Sample NY-2

MgO	Al_2O_3	SiO_2	P_2O_5	SO_3	K_2O	CaO	TiO_2	V_2O_5	MnO	FeO
1.0	1.1	7.7	18.8	0.2	0.8	7.3	n.d.	1.0	0.7	61.5
0.8	1.2	8.2	16.0	n.d.	0.4	6.4	n.d.	1.0	0.7	65.5
0.8	1.7	7.6	13.9	n.d.	0.6	5.6	0.2	1.1	0.8	67.8
1.3	1.2	4.5	8.6	0.2	0.4	2.5	0.2	2.1	0.7	78.4
1.2	1.8	9.0	4.2	n.d.	1.0	2.2	0.2	0.8	n.d.	79.8
n.d.	0.9	7.1	1.6	n.d.	0.5	2.8	n.d.	0.2	n.d.	87.0
n.d.	1.5	7.2	0.8	n.d.	0.6	2.6	n.d.	n.d.	n.d.	87.3
n.d.	0.8	6.6	0.8	n.d.	0.5	2.6	n.d.	0.7	n.d.	88.1
n.d.	1.4	6.0	1.1	n.d.	0.7	1.9	n.d.	0.6	n.d.	88.3
n.d.	1.2	5.1	0.5	n.d.	0.4	2.0	n.d.	n.d.	n.d.	90.8
n.d.	0.8	5.1	0.7	n.d.	0.4	2.0	n.d.	0.2	n.d.	90.8

Sample JC-1

Al_2O_3	SiO_2	P_2O_5	SO_3	K_2O	CaO	V_2O_5	MnO	FeO
1.2	10.9	9.0	0.4	0.5	11.8	n.d.	0.2	44.5
1.1	9.5	6.0	0.3	0.4	8.9	n.d.	0.2	46.3
1.1	8.6	4.4	0.4	0.3	7.1	n.d.	n.d.	51.0
0.8	6.3	4.5	n.d.	0.2	6.1	n.d.	n.d.	52.1
1.1	11.8	10.3	0.6	0.6	13.9	n.d.	n.d.	53.6
1.3	12.7	7.5	0.5	0.7	10.3	n.d.	n.d.	56.7
1.2	11.2	4.7	0.5	0.5	8.5	n.d.	n.d.	57.1
1.3	14.4	9.3	n.d.	0.7	13.7	n.d.	n.d.	60.6
1.2	12.1	15.1	0.6	0.8	18.2	n.d.	n.d.	61.3
1.8	18.7	14.1	0.6	0.9	17.4	n.d.	n.d.	66.2
0.8	9.1	10.9	n.d.	0.3	12.6	n.d.	n.d.	66.4
1.0	12.4	14.1	n.d.	0.4	15.5	n.d.	n.d.	67.0
1.9	18.7	13.9	0.7	0.6	13.1	n.d.	n.d.	73.5
1.6	16.8	11.7	0.7	0.9	14.7	n.d.	n.d.	73.9
1.3	14.3	11.0	0.4	0.9	14.6	n.d.	n.d.	78.3
0.4	1.9	2.9	0.5	n.d.	1.2	n.d.	n.d.	82.1
n.d.	2.2	4.6	0.7	n.d.	1.1	n.d.	1.3	86.1
0.3	2.3	7.3	0.5	n.d.	2.2	0.3	1.2	90.0

Sample LD-1

Na_2O	MgO	Al_2O_3	SiO_2	P_2O_5	SO_3	K_2O	CaO	TiO_2	V_2O_5	MnO	FeO
n.d.	1.6	12.3	38.6	4.9	0.3	1.3	21.2	0.5	n.d.	0.7	18.4
n.d.	1.6	12.6	38.0	5.3	0.2	1.3	21.8	0.5	n.d.	0.8	18.0
n.d.	1.5	11.9	42.0	2.7	0.3	1.8	20.4	0.4	n.d.	0.7	18.5
0.4	1.4	11.4	42.9	2.6	n.d.	2.1	20.7	0.4	n.d.	0.7	17.4
n.d.	1.5	10.4	38.5	3.6	0.2	1.8	18.5	0.4	n.d.	0.8	24.3
n.d.	1.6	12.9	36.2	4.4	n.d.	1.0	18.6	0.5	n.d.	0.6	24.3
0.4	1.4	14.7	42.1	1.9	n.d.	2.3	17.4	0.6	n.d.	0.5	18.8
n.d.	1.4	14.6	42.3	2.2	n.d.	2.2	17.7	0.6	n.d.	0.5	18.6
n.d.	1.4	14.2	41.6	2.1	0.2	2.1	17.6	0.7	n.d.	0.7	19.5
n.d.	1.2	13.9	40.1	2.2	0.2	2.0	16.9	0.5	n.d.	0.6	22.3
0.5	1.4	16.6	57.3	n.d.	n.d.	2.2	15.8	0.7	n.d.	0.7	4.9
0.4	1.4	17.0	58.3	n.d.	n.d.	2.4	16.4	0.7	n.d.	0.7	2.8
0.3	1.4	15.9	70.1	n.d.	n.d.	2.4	4.3	0.9	n.d.	0.8	3.9
0.2	1.4	10.0	41.3	1.3	0.2	1.0	19.8	0.4	0.3	1.7	22.4
0.3	1.3	10.3	42.7	1.2	0.3	1.1	20.0	0.5	0.3	1.7	20.5
0.2	1.5	11.5	48.4	0.8	0.3	1.2	24.6	0.6	0.2	2.1	8.5
0.2	1.4	10.9	45.6	0.5	0.5	1.2	23.3	0.4	0.3	2.0	13.8
0.3	1.3	9.2	35.5	1.0	0.2	0.9	15.2	0.2	0.2	1.2	34.9
0.4	1.4	10.6	42.1	0.8	n.d.	1.0	19.9	0.4	0.3	1.6	21.5
0.5	1.8	22.3	50.5	n.d.	n.d.	3.0	15.4	0.9	n.d.	0.4	5.4
0.5	1.9	25.7	49.5	n.d.	n.d.	2.9	16.1	0.8	n.d.	0.3	2.4
0.5	1.8	22.3	50.5	n.d.	n.d.	2.8	15.1	0.8	n.d.	0.3	5.9
0.6	1.8	22.1	50.3	n.d.	n.d.	2.8	15.3	0.8	n.d.	0.4	5.9
0.4	n.d.	10.9	76.0	n.d.	n.d.	4.9	1.3	1.3	n.d.	n.d.	5.2
0.6	1.1	25.2	48.0	n.d.	n.d.	2.1	11.9	0.6	n.d.	n.d.	10.6
0.4	2.0	23.1	51.3	n.d.	n.d.	3.2	16.5	0.9	n.d.	0.5	2.2
0.4	2.0	23.0	51.1	n.d.	n.d.	3.1	16.3	0.8	n.d.	0.4	2.9
0.4	2.0	23.3	51.4	n.d.	n.d.	3.1	16.6	0.8	n.d.	0.5	1.9
0.4	1.9	23.3	51.0	n.d.	n.d.	3.1	16.2	0.8	n.d.	0.4	2.8
0.6	1.2	27.2	50.7	n.d.	n.d.	2.5	14.3	0.6	n.d.	0.2	2.8
0.4	1.9	26.9	50.0	n.d.	n.d.	2.9	14.2	0.7	n.d.	0.3	2.7
0.5	2.2	25.5	50.2	n.d.	n.d.	3.1	15.5	0.8	n.d.	0.4	1.9
0.4	1.5	25.7	55.1	n.d.	n.d.	3.5	9.1	0.8	n.d.	1.0	3.0
0.4	1.8	27.7	52.6	n.d.	n.d.	3.1	9.5	0.8	n.d.	1.0	3.2
0.4	1.6	27.8	52.4	n.d.	n.d.	3.3	8.7	0.8	n.d.	0.8	4.2
n.d.	1.5	27.1	51.1	n.d.	n.d.	3.2	8.4	0.7	n.d.	0.7	7.4

0.4	1.8	27.4	52.4	n.d.	n.d.	3.3	8.7	0.9	n.d.	0.9	4.4
0.4	1.6	27.7	53.2	n.d.	n.d.	3.5	8.8	0.8	n.d.	0.7	3.3
0.3	1.6	28.0	53.2	n.d.	n.d.	3.3	8.8	0.9	n.d.	0.8	3.0
0.4	1.8	29.3	52.6	n.d.	n.d.	3.1	9.2	0.9	n.d.	1.0	1.9
0.3	1.6	24.3	54.6	n.d.	n.d.	2.9	7.8	0.8	n.d.	0.9	6.9
0.3	1.6	27.9	50.2	n.d.	n.d.	3.1	8.5	0.7	n.d.	0.7	7.1
n.d.	0.8	8.0	24.0	3.4	0.5	1.6	15.1	0.2	n.d.	0.2	46.2
n.d.	0.9	8.0	23.1	2.2	0.4	1.5	11.2	0.3	n.d.	0.3	52.1
n.d.	n.d.	6.6	16.8	1.7	0.5	0.8	8.0	0.3	n.d.	n.d.	65.3
n.d.	n.d.	3.2	8.6	2.4	0.6	0.6	3.6	0.2	n.d.	n.d.	80.7
n.d.	n.d.	6.6	13.0	1.3	n.d.	0.5	5.4	0.2	n.d.	0.2	72.8
n.d.	n.d.	8.6	16.4	2.7	0.5	0.9	6.7	0.2	n.d.	0.3	63.8
n.d.	1.0	9.1	22.0	2.5	0.1	1.4	8.8	0.3	n.d.	0.3	54.5
n.d.	0.8	5.7	17.6	2.7	n.d.	0.7	6.1	0.2	n.d.	0.2	66.0
n.d.	n.d.	9.9	15.0	1.4	0.5	1.0	5.3	0.3	n.d.	n.d.	66.7
n.d.	0.9	7.6	21.5	1.9	0.3	1.0	8.7	0.2	n.d.	0.2	57.8
n.d.	n.d.	10.6	16.1	1.6	0.5	0.9	7.8	n.d.	n.d.	0.2	62.4
n.d.	n.d.	6.7	19.3	1.7	0.4	1.4	8.5	0.2	n.d.	n.d.	61.7
n.d.	n.d.	7.8	23.4	1.5	n.d.	1.3	10.6	0.2	n.d.	n.d.	55.3
n.d.	n.d.	6.4	17.2	1.4	n.d.	1.1	8.6	0.2	n.d.	n.d.	65.1
n.d.	n.d.	4.3	13.2	1.2	n.d.	0.7	7.1	n.d.	n.d.	n.d.	73.6
n.d.	n.d.	5.8	15.5	1.4	0.3	0.8	8.7	n.d.	n.d.	n.d.	67.5
n.d.	n.d.	6.5	20.9	0.5	n.d.	0.8	5.3	0.2	n.d.	0.3	65.5
n.d.	n.d.	3.8	11.5	0.8	n.d.	0.6	5.9	n.d.	n.d.	n.d.	77.5
n.d.	n.d.	3.2	9.5	0.7	n.d.	0.6	5.7	0.2	n.d.	0.2	80.0
n.d.	n.d.	4.3	13.8	0.9	n.d.	0.9	8.0	n.d.	n.d.	0.2	71.9
n.d.	n.d.	4.2	11.5	0.7	n.d.	0.7	6.4	n.d.	n.d.	n.d.	76.6
n.d.	n.d.	5.4	13.3	1.0	n.d.	0.4	5.6	n.d.	n.d.	n.d.	74.4
n.d.	n.d.	3.9	9.4	1.0	n.d.	n.d.	4.7	0.2	n.d.	n.d.	80.8
n.d.	n.d.	1.4	3.6	0.5	0.2	0.1	1.7	n.d.	n.d.	n.d.	92.6

Sample LD-2

Na_2O	MgO	Al_2O_3	SiO_2	P_2O_5	SO_3	K_2O	CaO	TiO_2	V_2O_5	MnO	FeO
0.7	2.2	7.9	34.9	2.5	n.d.	2.1	28.4	0.5	0.5	0.4	19.9
n.d.	3.2	3.2	14.2	25.2	n.d.	0.8	31.6	0.2	0.3	0.3	21.1
0.7	2.4	7.7	33.9	2.2	n.d.	2.0	28.0	0.5	0.7	0.4	21.6

n.d.	3.1	2.8	12.8	26.5	n.d.	0.8	29.6	n.d.	n.d.	0.3	24.1
n.d.	2.3	7.8	33.5	3.2	n.d.	1.3	25.4	0.5	0.4	0.3	25.3
n.d.	2.2	3.8	15.8	20.3	n.d.	0.6	30.2	0.3	0.3	n.d.	26.6
n.d.	2.1	3.9	16.2	18.8	n.d.	0.6	29.0	0.3	0.3	0.2	28.7
0.6	1.9	6.4	30.2	4.3	n.d.	1.7	24.5	0.3	0.5	0.4	29.3
0.6	2.0	7.5	31.6	3.8	n.d.	1.6	22.7	0.4	0.2	0.3	29.5
n.d.	2.0	7.7	31.9	3.5	n.d.	1.5	22.5	0.4	0.4	0.3	29.8
n.d.	1.9	7.3	30.4	5.4	n.d.	1.3	22.6	0.4	0.3	0.2	30.3
n.d.	2.0	7.4	31.4	3.7	n.d.	1.5	22.2	0.4	0.2	0.3	30.9
n.d.	2.0	3.8	15.1	20.5	n.d.	0.5	26.9	n.d.	n.d.	0.2	31.0
n.d.	2.0	7.9	32.2	2.9	n.d.	2.1	20.6	0.4	0.3	0.3	31.4
n.d.	1.9	5.2	28.5	3.3	n.d.	0.4	28.5	0.3	0.3	0.3	31.4
n.d.	2.3	4.5	24.0	9.1	0.2	0.6	26.4	0.3	0.7	0.3	31.6
n.d.	2.1	7.3	28.9	4.1	n.d.	0.8	23.0	0.4	0.5	0.5	32.5
n.d.	1.9	7.3	30.2	4.0	n.d.	1.5	21.9	0.3	0.2	0.3	32.5
n.d.	1.6	5.4	26.8	9.2	0.2	1.9	21.4	0.3	0.4	0.3	32.5
0.6	1.8	6.2	27.0	4.8	n.d.	1.6	22.0	0.3	0.6	0.4	34.9
n.d.	2.0	6.7	25.9	6.3	n.d.	1.0	22.2	0.4	0.2	0.4	35.2
n.d.	1.5	4.7	26.7	6.3	n.d.	1.5	22.4	n.d.	0.9	0.6	35.3
n.d.	2.8	5.5	25.2	6.2	n.d.	0.5	23.0	0.5	0.6	0.3	35.5
n.d.	1.8	6.0	26.6	8.8	n.d.	1.7	18.2	0.3	0.2	0.4	36.1
0.6	1.8	6.8	28.7	4.7	n.d.	1.6	19.0	0.3	n.d.	0.2	36.2
n.d.	1.7	5.9	26.4	10.2	n.d.	1.8	17.2	n.d.	n.d.	0.4	36.4
n.d.	3.6	2.4	15.0	23.0	n.d.	1.3	17.4	n.d.	0.2	0.2	36.9
n.d.	1.9	5.6	25.4	10.3	n.d.	1.8	16.6	0.2	n.d.	0.3	37.9
n.d.	0.9	4.0	23.5	7.8	0.4	1.5	20.9	0.2	0.6	0.6	39.7
n.d.	1.4	5.6	22.2	9.1	n.d.	0.9	20.0	0.2	n.d.	0.2	40.5
n.d.	1.6	6.1	23.3	5.3	n.d.	0.9	19.1	0.4	0.3	0.2	42.8
n.d.	1.6	5.5	21.3	8.1	n.d.	0.9	17.9	0.3	0.2	0.2	44.0
n.d.	1.6	5.6	24.7	6.2	n.d.	1.6	15.8	0.3	n.d.	0.2	44.2
n.d.	2.5	5.1	19.2	7.9	0.2	0.8	17.3	0.4	0.6	0.3	45.9
n.d.	1.6	5.5	21.0	5.4	n.d.	0.8	17.2	0.3	0.4	n.d.	47.8
n.d.	1.5	4.8	18.2	8.4	n.d.	0.7	16.5	0.2	0.4	0.2	49.2
n.d.	0.7	4.4	20.3	4.0	n.d.	0.8	14.0	n.d.	n.d.	n.d.	55.7
n.d.	0.8	4.2	19.8	4.4	n.d.	0.8	13.9	n.d.	n.d.	n.d.	56.1
n.d.	1.5	4.7	16.9	4.2	n.d.	0.6	12.8	0.2	0.5	0.2	58.3
n.d.	n.d.	2.6	13.8	4.6	n.d.	0.8	11.4	n.d.	n.d.	n.d.	66.8
n.d.	n.d.	3.1	13.6	2.3	n.d.	0.7	9.0	n.d.	n.d.	n.d.	71.4
n.d.	n.d.	3.0	11.9	2.3	n.d.	0.4	8.3	n.d.	n.d.	n.d.	74.1

n.d.	n.d.	2.7	11.1	2.1	n.d.	0.5	7.0	n.d.	n.d.	n.d.	76.6
n.d.	n.d.	2.6	10.7	1.7	n.d.	0.5	6.6	n.d.	n.d.	n.d.	78.0
n.d.	0.8	2.0	7.3	4.7	0.4	0.1	5.6	n.d.	0.4	0.3	78.4
n.d.	n.d.	2.4	9.6	2.8	n.d.	0.3	6.1	n.d.	n.d.	n.d.	78.8
n.d.	n.d.	2.3	9.8	1.6	n.d.	0.5	6.5	n.d.	n.d.	n.d.	79.3
n.d.	n.d.	2.3	8.5	1.6	n.d.	0.4	5.3	n.d.	n.d.	n.d.	81.9
n.d.	n.d.	2.0	7.8	1.4	n.d.	0.3	5.0	n.d.	n.d.	n.d.	83.5
n.d.	n.d.	1.6	6.3	1.2	n.d.	0.3	4.3	n.d.	n.d.	n.d.	86.3

Sample GX-2

Na_2O	MgO	Al_2O_3	SiO_2	P_2O_5	SO_3	K_2O	CaO	TiO_2	MnO	FeO
0.6	5.1	7.0	35.1	0.8	n.d.	1.1	38.4	0.4	0.4	11.2
0.5	4.5	6.9	37.6	1.0	n.d.	1.2	43.8	0.4	0.5	3.6
0.6	5.3	6.7	36.6	1.0	n.d.	1.0	40.2	n.d.	0.5	8.2
0.5	4.4	6.6	37.4	0.8	0.3	1.2	42.6	0.5	0.5	5.1
0.4	4.4	7.2	38.5	0.9	n.d.	1.2	43.8	0.5	0.4	2.8
0.4	5.6	4.5	34.0	1.0	0.2	0.9	40.5	0.4	0.4	12.2
0.6	5.4	6.4	34.6	1.0	n.d.	0.9	38.3	0.3	0.4	12.0
0.4	4.6	6.3	37.6	1.3	n.d.	1.2	43.8	0.5	0.5	3.8
0.5	4.4	6.8	38.5	0.8	n.d.	1.2	44.4	0.5	0.5	2.5
0.4	5.6	5.0	36.9	1.2	n.d.	1.0	45.7	0.6	0.4	3.4
0.5	4.3	7.2	39.0	0.8	0.2	1.3	44.1	0.5	0.5	1.7
0.4	4.7	6.3	36.5	0.9	n.d.	1.0	41.9	0.5	0.4	7.4
0.4	4.8	6.1	37.0	1.0	n.d.	1.2	43.8	0.6	0.5	4.6
0.3	3.9	6.6	38.9	1.1	0.3	1.0	43.8	0.5	0.4	3.2
0.4	4.1	6.9	38.7	0.8	0.3	1.1	44.5	0.4	0.4	2.4
0.5	4.8	6.4	38.1	0.7	0.3	1.1	44.9	0.5	0.4	2.3
0.5	5.3	5.9	38.1	0.7	0.2	0.9	43.7	0.5	0.3	3.9
0.3	4.3	6.5	39.0	0.7	0.3	0.9	44.7	0.5	0.3	2.5
0.5	5.0	6.9	39.1	0.6	0.2	1.1	44.1	0.5	0.3	1.7